NASA Contractor Report 4009

Aeroelastic Effects in Multirotor Vehicles

Part II: Methods of Solution and Results Illustrating Coupled Rotor/Body Aeromechanical Stability

C. Venkatesan and P. P. Friedmann

GRANT NAG2-116
FEBRUARY 1987

NASA

NASA Contractor Report 4009

Aeroelastic Effects in Multirotor Vehicles

Part II: Methods of Solution and Results Illustrating Coupled Rotor/Body Aeromechanical Stability

C. Venkatesan and P. P. Friedmann
University of California
Los Angeles, California

Prepared for
Ames Research Center
under Grant NAG2-116

National Aeronautics
and Space Administration

Scientific and Technical Information Branch

1987

PREFACE

This report is a sequel to an earlier report titled "Aeroelastic Effects in Multirotor Vehicles with Application to a Hybrid Heavy Lift System, Part I: Formulation of Equations of Motion", (NASA CR-3822, August 1984).

The research effort reported herein was carried out in the Mechanical, Aerospace and Nuclear Engineering Department at UCLA by Dr. C. Venkatesan and Professor P. Friedmann who served as the principal investigator.

The authors want to take this opportunity to express their gratitude to the grant monitor Dr. H. Miura for his numerous constructive comments and suggestions, as well as for much of the numerical data used in Section 4.2.1.

TABLE OF CONTENTS

LIST OF FIGURES

LIST OF TABLES

NOMENCLATURE

a	:	Lift curve slope
BR	:	Buoyancy ratio (Buoyancy of the envelope/Total weight)
$c=2b$	:	Blade chord
$[c]$	:	Damping matrix
c_{d0}	:	Profile drag coefficient for the blade
C_T	:	Thrust coefficient
e	:	Hinge offset
$\hat{e}_x, \hat{e}_y, \hat{e}_z$	:	Unit vectors along X,Y,Z directions of the body axes
$F_{x,y,z}$	:	Forces along X,Y,Z directions acting on the vehicle
g_{SF}, g_{SL}, g_{ST}	:	Damping coefficients in flap, lag and torsional degrees of freedom of the blade respectively, in rotating system
$\bar{g}_{SF}, \bar{g}_{SL}, \bar{g}_{ST}$	:	Damping nondimensionalized with respect to $m\Omega R^3$
h_1	:	Distance between origin 0_s and underslung load
h_2	:	Distance between centerline and rotor hub
h_3	:	Distance between centerline and center volume of the envelope
h_4	:	Distance between centerline and c.g. of the envelope
h_5	:	Distance between the origin 0_s and c.g. of the structure
I_{MB3}, I_{MB2}	:	Principal moments of inertia per unit length of the blade about the cross-sectional axes
$I_{xx}, I_{xy}, I_{yx}, I_{yy}$	:	Inertion of the complete vehicles about X,Y,Z axes
$[K]$	:	Stiffness matrix
K_{SBXY}, K_{SBXZ}	:	Supporting structure bending stiffness in X-Y plane and in X-Z plane respectively (in fundamental mode)
K_{ST}	:	Supporting structure torsional stiffness (in fundamental mode)
$K_{\beta_B}, K_{\zeta_B}, K_{\phi_B}$	:	Root spring stiffnesses in flap, lag and torsional respectively, simulating blade stiffness
K_{ϕ_c}	:	Control system stiffness
ℓ_{F1}, ℓ_{F2}	:	Distance between origin 0_s and c.g. of the fuselages F_1 and F_2

m : Mass per unit length of the blade

$[M]$: Mass matrix

M_{SBXY}, M_{SBXZ} : Generalized mass associated with supporting structure bending in X-Y and X-Z planes respectively (in fundamental mode)

M_{ST} : Generalized mass associated with supporting structure torsion (in fundamental mode)

M_x, M_y, M_z : Moments about X,Y,Z axes acting on the vehicle

M_β, M_ζ, M_ϕ : Blade root moments in flap, lag and torsion respectively

N : Number of blades in one rotor

O_s : Origin of the axes system located at the centerline of the supporting structure

P_Z^S : Buoyancy on the envelope

$\{q\}$: Generalized coordinate vector

R : Rotor radius

R_{xs}, R_{ys}, R_{zs} : Perturbational translational motion of the origin O_s

S_k : k^{th} eigenvalue

t : Time

T_1, T_2 : Thrust developed by rotor systems R_1 and R_2 respectively

W_{EN} : Weight of the envelope

W_{F1}, W_{F2} : Weight of the fuselages F_1 and F_2

W_s : Weight of the supporting structure

W_{UN} : Weight of the underslung load

β_k, ζ_k, ϕ_k : Flap, lead-lag and torsion angles of the k^{th} blade

$\beta_{k0}^i, \zeta_{k0}^i, \phi_{k0}^i$: Equilibrium trim angles in flap, lag and torsion of the k^{th} blade respectively for the i^{th} rotor system, i = 1,2

β_0, ζ_0, ϕ_0 : Equilibrium trim angles in flap, lag and torsion respectively

$\Delta\beta_k, \Delta\zeta_k, \Delta\phi_k$: Perturbational quantities in flap, lag and torsion respectively

β_p : Blade precone angle

β_M, ζ_M, ϕ_M : Generalized coordinates for collective flap, lag and torsion modes

$\beta_{-M}, \zeta_{-M}, \phi_{-M}$: Generalized coordinates for alternating flap, lag and torsion modes

$\beta_{nc}, \zeta_{nc}, \phi_{nc}$: Generalized coordinates for n-cosine flap, lag and torsion modes

$\beta_{ns}, \zeta_{ns}, \phi_{ns}$: Generalized coordinates for n-sine flap, lag and torsion modes

β_p : Progressing flap mode (high frequency)

β_R : Regressing or progressing flap mode (low frequency)

ζ_p : Progressing lag mode (high frequency)

ζ_R : Regressing or progressing flap mode (low frequency)

ϕ_p : Progressing torsion mode (high frequency)

ϕ_R : Regressing torsion mode (low frequency)

ε : Order of magnitude used for ordering various quantities

η_1, η_2 : Free - free fundamental modes for bending of the supporting structure in X,Y plane (horizontal)and X,Z plane (vertical) respectively

η_3 : Free - free fundamental torsion mode of the supporting structure

θ_c : Collective pitch setting of the blade

θ_0^i : Collective pitch for i^{th} rotor

θ_0 : Effective angle of attack

θ, θ_y : Perturbational rotational motion of the vehicle in pitch

θ_x, ϕ : Perturbational rotational motion of a vehicle in roll

θ_{ZL} : Zero lift angle of attack of the blade

λ : Inflow ratio

ξ_1, ξ_2 : Generalized coordinates for the fundamental mode bending of the supporting structure in X-Y plane (horizontal) and X-Z plane (vertical) respectively

ξ_3 : Generalized coordinate for the fundamental torsion mode of the supporting structure

ρ_A : Density of air

σ : Solidity ratio

σ_k : Real part of the k^{th} eigenvalue

ψ : Nondimensional time (Ωt)

ψ_k : Azimuth angle for the k^{th} blade

Ω : Rotor R.P.M.

Ω_i : i^{th} rotor R.P.M,

$\bar{\omega}_F, \bar{\omega}_L, \bar{\omega}_{T1}, \bar{\omega}_{T2}$: Nondimensional frequency parameters of the nonrotating blade in flap, lag and torsion respectively

$\bar{\omega}_{SBXY}, \bar{\omega}_{SBXZ}$: Nondimensional bending frequencies of the supporting structure in X-Y plane and X-Z plane respectively

$\bar{\omega}_{ST}$: Nondimensional torsional frequency of the supporting structure

$\bar{\omega}_\beta, \bar{\omega}_\zeta, \bar{\omega}_\phi$: Nondimensional rotating natural frequencies of the blade in flap, lag and torsion respectively

ω_k : Imaginary part of the k^{th} eigenvalue

$(\ )_x$: Derivative with respect to x

$(\dot{\ })$: Derivative with respect to nondimensional time $\psi = \Omega t$

$(\bar{\ })$: Nondimensional quantities

SUMMARY

This report is a sequel to the earlier report titled "Aeroelastic Effects in Multi-Rotor Vehicles with Application to Hybrid Heavy Lift System, Part I: Formulation of Equations of Motion". The trim and stability equations are presented for a twin rotor system with a buoyant envelope and an underslung load attached to a flexible supporting structure. These equations are specialized for the case of hovering flight. The stability equations are written in multi-blade coordinates. The total number of degrees of freedom for hybrid heavy lift vehicle consisting of two four bladed rotors is 31. Hence the stability analysis yields a total of 62 eigenvalues corresponding to these 31 degrees of freedom. A careful parametric study is performed, and used subsequently to identify the various blade and vehicle modes. The eigenvalues are identified by relating them to the physical degrees of freedom present in the system. This identification is based on a parametric study in which the fundamental parameters governing the system are varied. The coupling between various blade modes and vehicle modes is identified. Finally, it is shown that the coupled rotor/vehicle stability analysis provides information on both the aeroelastic stability as well as complete vehicle dynamic stability in the longitudinal and lateral planes. Also presented, in this report, are the results of an analytical study aimed at predicting the aeromechanical stability of a single rotor helicopter in ground resonance. The theoretical results are found to be in good agreement with the experimental results available in the literature, thereby validating the analytical model for the dynamics of the coupled rotor/support system.

1. INTRODUCTION

This report is a sequel to the previous report entitled "Aeroelastic Effects in Multi-Rotor Vehicles with Application to Hybrid Heavy Lift System, Part I: Formulation of Equations of Motion" [Ref. 1], in which the equations of motion governing the aeroelastic behavior of an approximate model representing an Hybrid Heavy Lift Airship (HHLA) (Fig. 1) were derived. The equations derived in Ref. 1 were representative of a somewhat simplified model shown in Fig. 2. The model consists of two rotors, a buoyant envelope and an underslung load, attached to a flexible supporting structure.* The various degrees of freedom, considered in deriving the equations of motion, are flap, lag, torsion for each blade, rigid body translation and rotation of the complete vehicle and the degrees of freedom representing the normal modes of vibration of the flexible supporting structure. It is useful to review some of the more important assumptions used in deriving the equations of motion, namely:

1) The rotor consists of three or more blades.
2) The rotors are lightly loaded.
3) The rotors are in uniform inflow.
4) There is no aerodynamic interference between the rotor and the buoyant envelope. The aerodynamic model used for the rotor blade is the quasi-steady aerodynamic model with apparent mass terms.
5) The rotor blade is modeled as a rigid blade with orthogonal springs located at the root of the blade (Fig. 3). This model enables one to represent simultaneously configurations employing either hingeless or articulated rotor system. The hinge sequence is given in Ref. 1.
6) Since the geometrical nonlinearities due to moderate deflections of the blade are known to have significant role in rotary wing aeroelasticity

*The flexible portion consists of the elements having a length ℓ_{F1} and ℓ_{F2} shown in Fig. 2 .

[Ref. 2], these nonlinearities are included in the analysis. Retention of the nonlinear terms is based upon an ordering scheme [Refs. 1 and 2]. The blade degrees of freedom, representing the blade slopes, are assigned an order $0(\varepsilon)$, where $0.1 < \varepsilon < 0.15$. The rigid body degrees of freedom of the vehicle are assumed to be of a slightly smaller magnitude $0(\varepsilon^{3/2})$ and the elastic deformations of the supporting structure are of the order magnitude $0(\varepsilon^2)$. This assumption is quite important for obtaining equations which are manageable from an algebraic point of view. The ordering scheme consists of neglecting terms of the order $0(\varepsilon^2)$ when compared to unity, thus $1 + 0(\varepsilon^2) \simeq 1$.

The equations of motion for the model vehicle (Fig. 2) are nonlinear coupled differential equations and they represent the coupled rotors/vehicle dynamics in forward flight. These coupled equations are classified in three groups, each group representing an appropriate sub-system equations. They are:

1) rotor blade equations of motion in flap, lead-lag and torsion,

2) rigid body equations of motion of the complete vehicle,

3) equations of motion of the flexible supporting structure.

The main advantage, due to separating the equations into various groups, consists of the ability to deal with various types of problems, such as isolated rotor aeroelastic stability or coupled single rotor/fuselage stability, etc., in a convenient manner. The coupled equations have considerable versatility and they can be used to study a number of diverse problems which are listed below:

1. Isolated rotor aeroelastic stability.
2. Coupled single rotor/fuselage dynamics.
3. Response to cyclic and collective pitch inputs.
4. Response to higher harmonic control inputs.

5. Stability analysis of twin rotor system connected by a flexible structure.

6. Dynamics of a Hybrid Heavy Lift Airship.

Depending on the type of analysis desired, the equations are simplified and modified to obtain an appropriate solution.

Because of the unique nature of the multirotor model (Fig. 2), the results of the stability analysis could not be compared with any other results available in the literature. But on the other hand, experimental results are available, in the literature, for the aeromechanical stability of a single rotor helicopter in ground resonance. Hence, solving this problem analytically will provide an opportunity to validate both the equations of motion for the coupled rotor/vehicle system and also the method of solution. Therefore, two different types of problems are solved using the analytical model, for the coupled rotor/vehicle dynamics, presented in Ref. 1. In the first case, the equations of motion are used to predict the aeromechanical stability of a single rotor helicopter in ground resonance. It was found that the analytical results are in good agreement with the experimental results indicating that both the equations of motion for coupled rotor/vehicle system and the method of solution are valid.

In the second case, the stability of a model vehicle (Fig. 2) representing an HHLA in hover is analyzed. The total number of degrees of freedom for the model HHLA consisting of two four bladed rotors is 31 . Hence, the stability analysis yields a total of 62 eigenvalues corresponding to these 31 degrees of freedom. Based on a careful parametric study, various blade and vehicle modes have been identified. A physical interpretation of the eigenvalues is obtained from a systematic study of the eigenvalue variations as a consequence of the variations of the vehicle system parameters. Finally the coupling between various

blade modes and vehicle modes is identified.

In this report, the method of solution, the relevant trim (equilibrium) and linearized stability equations for the two applications mentioned above are considered and explored in detail.

2. METHOD OF SOLUTION

The equations of motion representing the dynamics of the coupled rotor/vehicle system, presented in Ref. 1, can be used to obtain either the response or the stability of the vehicle. The method of solution depends on the type of problem being considered, i.e. whether a response or stability analysis is required. For a stability analysis, one must distinguish between the case of hover which is relatively simple and the case of forward flight which is much more complicated. In this section, the method of solution used for the aeroelastic stability of a multirotor vehicle in hover is presented.

The equations of motion, for coupled rotor/vehicle problem, are usually nonlinear coupled differential equations with periodic coefficients. These differential equations can be either ordinary or partial depending on the type of model used for the representation of the blade. If the blade is modelled as a rigid blade with root springs, the resulting equations will be nonlinear ordinary differential equations. On the other hand, if the blade is modelled as a flexible beam, the final equations will be nonlinear partial differential equations. In this case, the partial differential equations are first transformed into ordinary differential equations using Galerkin's method. Thereafter, the method of solution is the same, irrespective of the modelling of the blade. In the present case, because the blade is modelled as a rigid blade with root springs (Fig. 3), the equations of motion are nonlinear coupled ordinary differential equations with periodic coefficients. To obtain the stability of the vehicle the following procedure is used:

1. Evaluation of the trim or equilibrium state.
2. Linearization of the nonlinear ordinary differential equations about the equilibrium position (linearized equations will have periodic coefficients).

3. Transformation of the linearized equations with periodic coefficients to linearized equations with constant coefficients, by applying multi-blade coordinate transformation.

4. Evaluation of the eigenvalues of the linearized equations with constant coefficients to obtain the information on the stability of the system.

These four steps can be separated into two stages of analysis, namely, (i) a trim analysis intended to establish the nonlinear equilibrium position of the blade, and (ii) a stability analysis of the linearized perturbation equations about the equilbrium state. A description of these two analyses are provided in the following sections.

2.1 Trim or Equilibrium State Solution

In the trim analysis, the force and moment equilibrium of the complete vehicle together with the moment equilibrium of the individual blade about its root in flap, lead-lag and torsion are satisfied respectively. It is important to recognize that only the generalized coordinates representing the blade degrees of freedom will have a steady state value representing the equilibrium position. The generalized coordinates associated with the rigid body motions of the vehicle are essentially perturbational quantities and hence their equilibrium, or trim, values are identically zero. In deriving the equations of motion for the flexible supporting structure, it was assumed that the vibrations of the structure occur about a deflected equilibrium position. The determination of the equilibrium position of the supporting structure is unimportant in the case considered here, for the following reasons: (a) this equilibrium position is not going to affect the equilibrium values of the blade degrees of freedom, since the blade equations contain only the time derivatives of the degrees of freedom representing the elastic modes of the supporting structure. The physical reason for this

mathematical dependence is due to the fact that blade inertia and aerodynamic loads depend on the hub motion and not on the hub equilibrium position. The hub motion is related to the fuselage motion and the vibration of the supporting structure, and (b) the final linearized differential equations used for the stability analysis do not contain any term dependent on the static equilibrium of the supporting structure because only the perturbational blade inertia and aerodynamic loads excite the vehicle rigid body motion and the vibration of the supporting structure. Hence, the generalized coordinates for the vibration modes of the supporting structure are again perturbational quantities.

The k^{th} blade degrees of freedom can be written as

$$\begin{aligned} \beta_k &= \beta_{k0} + \Delta\beta_k\ (\psi) && \text{Flap} \\ \zeta_k &= \zeta_{k0} + \Delta\zeta_k\ (\psi) && \text{Lead Lag} \\ \phi_k &= \phi_{k0} + \Delta\phi_k\ (\psi) && \text{Torsion} \end{aligned} \qquad (2.1)$$

where β_{k0}, ζ_{k0}, ϕ_{k0} are the steady state values and $\Delta\beta_k$, $\Delta\zeta_k$, $\Delta\phi_k$ are the perturbational quantities.

Linearization of the equations is accomplished by substituting these expressions into the nonlinear coupled differential equations and neglecting terms containing the products or squares of the perturbational quantities. The remaining terms will have either the steady state quantities as coefficients or the time dependent perturbational quantities, multiplied by the steady state values or some appropriate constants. Separation of these terms yields two groups: one group of terms contains only the steady state quantities and constants (i.e., time independent quantities). These represent the trim or equilibrium equations. These are nonlinear algebraic equations which represent force and moment equilibrium equations determining the steady state. The second group contains the time dependent perturbational quantities and represents the linearized

equations of motion about the equilibrium position. These linearized dynamic equations of equilibrium are used for the stability analysis. The steady state equilibrium equations can be written symbolically as

for the complete vehicle

$$F_x = F_y = F_z = 0 \tag{2.2}$$

$$M_x = M_y = M_z = 0 \tag{2.3}$$

and for the individual blade

$$M_\beta = M_\zeta = M_\phi = 0 \tag{2.4}$$

where F_x, F_y and F_z represent the forces of the vehicle in X,Y,Z directions, respectively; M_x, M_y, M_z represent the moments on the vehicle about X,Y,Z axes respectively; and M_β, M_ζ, M_ϕ represent the moments of the blade forces about the root; respectively.

In these equations, F_x, F_y and M_x are identically zero. The remaining equations for the vehicle can be written as

$$F_z = T_1 + T_2 + P_Z^S - W = 0 \tag{2.5}$$

$$M_y = 0 \tag{2.6}$$

$$M_z = 0 \tag{2.7}$$

where T_1 and T_2 are the magnitude of the thrust developed by the two rotor systems R_1 and R_2, P_Z^S is the static buoyancy on the envelope, and W is the weight of the complete vehicle.

The quantities T_1 and T_2 are functions of the steady state flap, lag and torsion angles, collective pitch angles and the operating conditions of the rotors. Equation (2.7) for M_z represents the torques developed by the two rotor systems. These torques can be either balanced by having a tail rotor for each main rotor or by having two counter-rotating main rotors. For the case where the rotors are assumed to be counter-rotating, the blade loads are to be evaluated for the two rotor system with angular velocities $+\Omega\hat{e}_z$ and $-\Omega\hat{e}_z$ respectively.

In Ref. 1, the rotor loads are derived for a typical rotor with angular velocity $+ \Omega\hat{e}_z$ and the same expressions for loads are used both rotors. Thus we assume that the torque developed by each main rotor is compensated by a tail rotor.

Equation (2.6) for M_y consists of the pitching moments developed by the thrust of the rotors and gravity loads on the various components.

The steady state moment equilibrium equations for the individual blade will have the following symbolic form

$$M_\beta = f_1^i (\beta_{k0}^i, \zeta_{k0}^i, \phi_{k0}^i, \theta_0^i) = 0 \tag{2.8}$$

$$M_\zeta = f_2^i (\beta_{k0}^i, \zeta_{k0}^i, \phi_{k0}^i, \theta_0^i) = 0 \tag{2.9}$$

$$M_\phi = f_3^i (\beta_{k0}^i, \zeta_{k0}^i, \phi_{k0}^i, \theta_0^i) = 0 \tag{2.10}$$

where i = 1,2 refers to the two rotor systems R_1 and R_2 respectively and k refers to the k^{th} blade in the i^{th} system. For the case of steady state, all the blades in each rotor system will have the same steady state values (or equilibrium quantities) and thus the subscript 'k' can be deleted.

Equations (2.5), (2.6), (2.8) - (2.10) are nonlinear algebraic equations. There is a total of 8 equations and 8 variables (β_0^i, ζ_0^i, ϕ_0^i, θ_0^i ; i = 1,2). These eight equations can be solved iteratively by the Newton-Raphson method, to obtain the steady state values. Failure to converge during iteration can be attributed to the divergence or static instability of the blade. (These equilibrium equations are given in the next chapter.)

In deriving the equations of motion, the inflow ratio λ is assumed to be constant over the disc. The typical value chosen for the inflow ratio is its value at 75% of the blade span. It is given as [Ref. 3]

$$\lambda = \frac{\sigma a}{16} \left(-1 + \sqrt{1 + \frac{24\ \theta_0}{\sigma a}} \right) \tag{2.11}$$

where θ_0 is the collective pitch of the blade.

2.2 Iterative Procedure for the Trim Solution

The equilibrium equations of the blade (Eq. 2.8 - 2.10) and the equations of the complete vehicle (Eq. 2.5 and 2.6) have to be solved numerically to obtain the steady state values of the blade deflections in flap, lag and torsion (β_0^i, ζ_0^i, ϕ_0^i ; i = 1,2) and the collective pitch angles (θ_0^i, i = 1,2) of the rotor systems R_1 and R_2. Blade equilibrium is obtained by an iterative procedure. It can be seen from the equilibrium equations of the blade (Eq. 2.8-2.10) that the equations for the blade in i^{th} rotor system consists only the variables corresponding to that rotor system. Hence these equations can be solved separately for each rotor. By assuming a collective pitch angle of θ_0^1, the equations (2.8) - (2.10) are solved to obtain the equilibrium angles (β_0^1, ζ_0^1, ϕ_0^1) of the blade in rotor system R_1. Then by assuming a collective pitch angle θ_0^2, the equilibrium equations are solved again for the equilibrium angles (β_0^2, ζ_0^2, ϕ_0^2) of the blade in rotor system R_2. It is important to recognize that these equilibrium angles of the blades can be different for the two rotor systems R_1 and R_2, because these angles depend upon the operating conditions and the blade parameters which can be different for the two rotor systems. However all the blades in each rotor system will have the same equilibrium angles. After obtaining β_0^1, ζ_0^1, ϕ_0^1 and β_0^2, ζ_0^2, ϕ_0^2, these quantities are substituted in the vehicle equilibrium equations (Eq. 2.5 and 2.6) and these two equations are solved simultaneously to get the updated values for the collective pitch angles (θ_0^1 and θ_0^2) for the two rotor systems. With these updated collective pitch angles, the blade equilibrium equations, for the two rotor systems, are solved again to obtain a new set of equilibrium angles for the blade (β_0^i, ζ_0^i, ϕ_0^i ; i = 1,2). These equilibrium angles of the blades are again substituted in the vehicle equilibrium equations to get the second stage updated values for the collective pitch angles θ_0^1 and θ_0^2. These

steps are repeated until convergence is achieved. This procedure is also illustrated by the following flow chart. A computer program implementing this calculation for the trim (or equilibrium) position of the blade was developed. A check on the number of iterations is provided in the computer program to avoid excessive use of computer time in case of divergence.

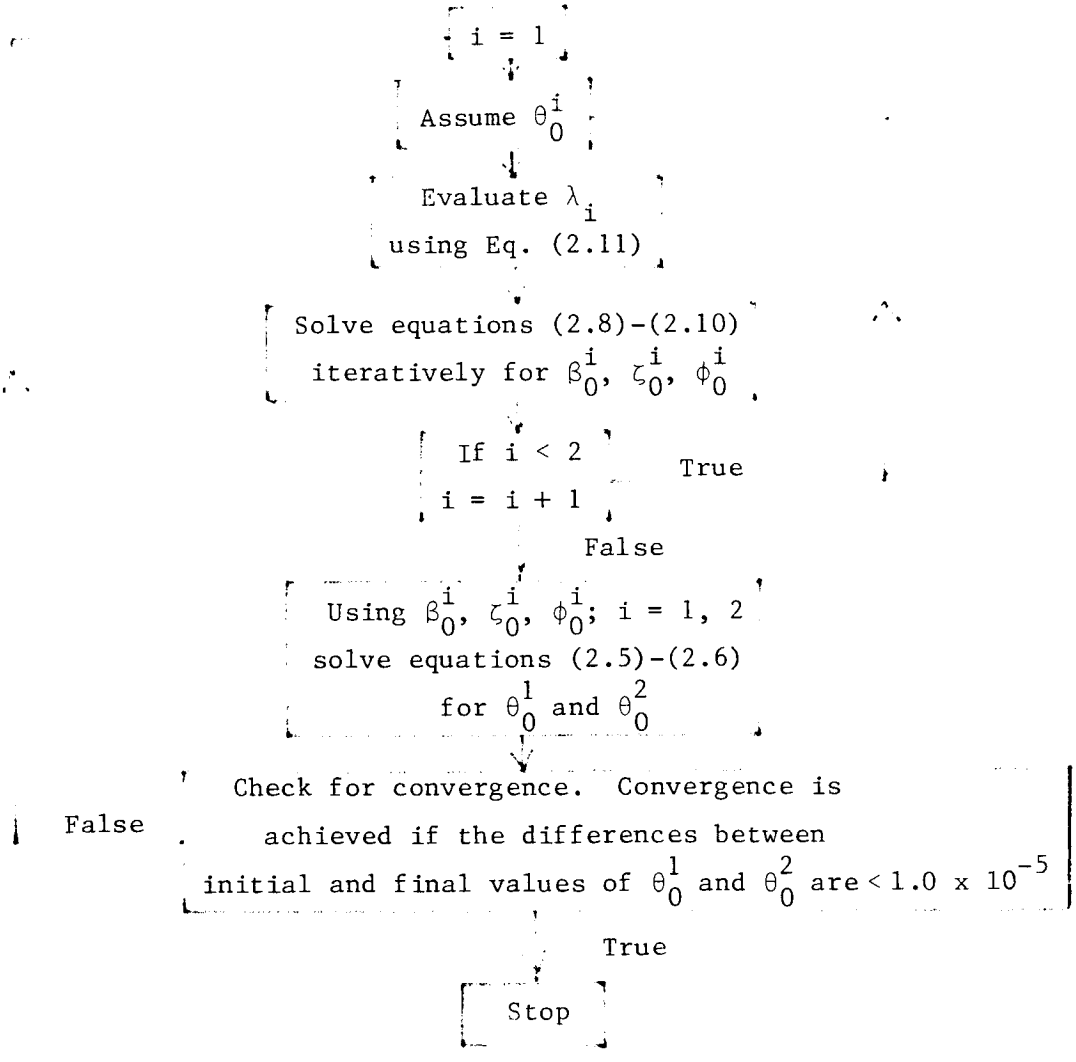

Flow Chart Illustrating the Solution Procedure for the Blade Equilibrium Position

The procedure described above is restricted to the case of hover where the coordinates describing blade equilibrium are not time dependent. For the case of forward flight, the equilibrium values will be time dependent and a more complicated procedure, described in Ref. 4, is required to determine the trim quantities. The basic difference is that, for the case of hover the trim values can be obtained by solving a system of nonlinear algebraic equations, while for forward flight the solution of a system of nonlinear coupled ordinary differential equations is required.

2.3 Description of the Stability Analysis

The perturbational equations of motion, linearized about the equilibrium position, can be written in the following form

$$[M]\{\ddot{q}\} + [C]\{\dot{q}\} + [K]\{q\} = 0 \tag{2.12}$$

where $\{q\}$ contains all the degrees of freedom representing the blade motion, the rigid body motions of the vehicle and the flexible modes of the supporting structure.

The matrices [M], [C], [K] can be identified as mass, damping and stiffness matrices respectively and the elements of these matrices are functions of the equilibrium values.

The stability of the vehicle about the trim condition is obtained by solving the eigenvalue problem represented by Equation (2.12). For convenience Equation (2.12) is written in state variable form

$$\{\dot{y}\} = [F]\{y\} \tag{2.13}$$

where $\{y\}^T = \left\lfloor \{y_1\}^T, \{y_2\}^T \right\rfloor$

and $\{y_1\} = \{\dot{q}\}$; $\{y_2\} = \{q\}$

and

$$[F] = \begin{bmatrix} -[M]^{-1}[C] & -[M]^{-1}[K] \\ \hline [I] & 0 \end{bmatrix}$$

Assuming a solution of the form $\{y\} = \{y\} e^{S\psi}$, Equation (2.13) reduces to a standard eigenvalue problem

$$[F] \{y\} = S\{y\} \tag{2.14}$$

The eigenvalues of Eq. (2.14) can be either real or complex conjugate pairs.

$$S_k = \sigma_k \pm i\omega_k \tag{2.15}$$

The complex part of the eigenvalue (ω_k) represents the modal frequency and the real part (σ_k) represents the modal damping. The system is stable when $\sigma_k < 0$ and the stability boundary is given by $\sigma_k = 0$.

This relatively simple procedure can become complicated depending on the form of the matrices [M], [C] and [K]. In the aeroelastic stability analysis of isolated rotor in hover, these matrices contain constant elements. Thus solution of this eigenvalue problem is straight-forward. However, in the case of coupled rotor/body system stability analysis in hover or for stability of isolated rotors in forward flight, these matrices will have elements which are time dependent. The reason for the appearance of time dependent or periodic coefficients, for these two cases, is different. For coupled rotor/body problem, these matrices become time dependent due to the fuselage perturbational motion. This fuselage perturbational motion introduces, through the hub motion, periodic terms in inertia and aerodynamic loads of the blade. In the case of isolated rotor in forward flight, these matrices become time dependent due to the periodic aerodynamic excitation associated with forward flight.

When the coefficient matrices of the linearized perturbational equations are periodic the stability analysis can be performed by applying

one of two possible techniques. One can use either Floquet theory or introduce a multiblade coordinate transformation [Refs. 3,5]. For the coupled rotor/body type of analysis in hover, which is the main objective of this study, the multiblade coordinate transformation is successful in eliminating the time dependent coefficients from the equations of motion. During this coordinate transformation, the blade degrees of freedom in the rotating coordinate system are transformed into a nonrotating hub fixed coordinate system. It is worthwhile mentioning that this transformation is also frequently denoted by the term Fourier coordinate transformation, Coleman transformation and more recently rotor plane coordinate transformation.

The multiblade coordinate transformation is implemented by applying the operators, given below, to the blade equations.

$$\begin{aligned}
&\frac{1}{N}\sum_{k=1}^{N}(\ldots) && \text{collective operator}\\
&\frac{1}{N}\sum_{k=1}^{N}(-1)^{k}(\ldots) && \text{alternating operator}\\
&\frac{1}{N}\sum_{k=1}^{N}\cos n\psi_k(\ldots) && \text{n-cosine operator}\\
&\frac{1}{N}\sum_{k=1}^{N}\sin n\psi_k(\ldots) && \text{n-sine operator}
\end{aligned} \tag{2.16}$$

where N is the number of blades

and $n = 1,\ldots.L$ $\quad L = \frac{N-1}{2}$ for odd N

$\quad L = \frac{N-2}{2}$ for even N

The resulting equations are identified according to the operator used in the transformation. These operators are applied only to the blade equations because

only the blade equations are written in the rotating coordinate system. The vehicle equations are written in the nonrotating frame and in these equations, rotor loads appear as a sum of various loads due to the individual blade. A clear description of the theory of this transformation is presented in Refs. 3 and 5. A brief summary of this transformation is also given in Appendix A.

During the derivation of the final trim and linearized perturbation equations, two items are noteworthy. First, in Ref. 1, the blade loads are derived for typical rotor blade rotating with angular speed Ω. During nondimensionalization of various quantities, the time is nondimensionalized as $\psi = \Omega t$. When the general expressions for the blade loads are applied to two different rotors operating at different values of Ω, then the nondimensional time ψ will be different for the two rotor systems. Consider the two rotor systems R_1 and R_2 to be operating at angular speeds Ω_1 and Ω_2 respectively. Then $\Omega_1 t$ is the nondimensional time used in the rotor load expressions for the rotor system R_1 and $\Omega_2 t$ is the corresponding nondimensional time for rotor system R_2. For the sake of consistency, the nondimensional time should be made the same for all rotor systems. Assuming that Ω_1 is the reference R.P.M. for the nondimensionalization of time. Then the time derivative termswhich appear in the blade loads of rotor system R_2 must be multiplied by a factor $\left(\frac{\Omega_1}{\Omega_2}\right)$. The power of this factor depends on the order of the time derivative.

A similar problem is also encountered when multiblade coordinate transformation is applied to a multirotor system. In the n-cosine and n-sine transformation Eq. (2.16), ψ_k refers to the azimuth angle of the k^{th} blade

$$\psi_k = \Omega t + 2\pi k/N \tag{2.17}$$

where it is understood that Ω is the angular speed or R.P.M. corresponding to

the particular rotor, and N is the number of blades in the rotor system. In the case of multiple rotor systems, this equation can be written for the k^{th} blade in the i^{th} rotor system as

$$\psi_k^i = \Omega_i t + \frac{2\pi k}{N} \tag{2.18}$$

Note that the above equation contains the R.P.M. or angular speed of the i^{th} rotor system. This value of ψ_k^i, Eq. (2.18), must be used in the n-cosine and n-sine transformation operators for the i^{th} rotor system, and care should be exercised when applying these operators in transforming the time derivatives of the blade degrees of freedom. For consistency in nondimensionalization, the time derivative terms in the i^{th} rotor system are nondimensionalized with respect to the reference angular speed Ω_1 of the rotor R_1. These statements imply that for multirotor systems the expressions provided in Ref. 3 and 5, for transforming the time derivatives of the rotating blade degrees of freedom to the nonrotating system, should not be used directly. The correct form for implementing this transformation for a multirotor vehicle where each rotor is operating at different angular speeds, i.e. Ω_1 and Ω_2, is provided in Appendix B. Consistency in nondimensionalization of time and the multiblade coordinate transformation for multiple rotor systems can be both achieved by multiplying the first and second time derivative terms, in the transformed multiblade coordinates for the i^{th} rotor system by $\left(\frac{\Omega_1}{\Omega_i}\right)$ and $\left(\frac{\Omega_1}{\Omega_i}\right)^2$ respectively, where Ω_i is the i^{th} rotor R.P.M. and Ω_1 is the reference angular speed.

(2) The second noteworthy item is related to the rotor hub loads. When deriving the equations of motion of the vehicle, the rotor hub loads have to be evaluated. The rotor hub loads are obtained by summing up the contributions from the individual blade loads. The expression for the individual blade load will have the centrifugal term as the leading term, the order of magnitude of this

term is 0(1). After summing up the individual blade loads, the resulting hub load expressions will have a leading term of order of magnitude $0(\varepsilon)$ only, because the centrifugal contributions from the blades cancel each other and thus the net contribution due to these terms is zero. Therefore, care must be taken to retain terms up to order $0(\varepsilon^{5/2})$ in the individual blade load expressions, so that the resulting coupled rotor/vehicle equations of motion will represent a consistent nonlinear mathematical model.

The two items, discussed above, have been carefully implemented in the equations which have been derived in this report. Next these equations are specialized to study air resonance type problems. For this class of problems, it is common practice to suppress the vertical motion motion and the yaw degree of freedom, thus in the final equations

$$R_{zs} = 0 \ , \ \dot{R}_{zs} = 0 \ , \ \ddot{R}_{zs} = 0 \tag{2.19}$$

and

$$\theta_{zs} = 0 \ , \ \dot{\theta}_{zs} = 0 \ , \ \ddot{\theta}_{zs} = 0 \tag{2.20}$$

have been substituted. The final equations for the equilibrium position (trim) and for the stability analysis are given in the next chapter.

3. EQUATIONS FOR TRIM AND STABILITY ANALYSIS

In this chapter, the complete set of equations, used for the equilibrium position and stability analysis, are presented. The linearized stability equations are given in multiblade or rotor-plane coordinate system. This chapter is divided into two major sections. In the first section, the equations pertaining to the twin rotor model (Fig. 2) representing an HHLA, are presented. Two sets of equations are provided for the HHLA model: one for articulated rotors and the other for hingeless rotors. The second section presents the equations used for predicting the aeromechanical stability of a single rotor helicopter in ground resonance, including the effect of the aerodynamic loads.

3.1 Equations for Twin Rotor Model of an HHLA

The degrees of freedom included in the analysis of twin rotor model of an HHLA are listed below.

Blade degrees of freedom

Flap	β_M^i , β_{-M}^i , β_{nc}^i , β_{ns}^i	
Lead-lag	ζ_M^i , ζ_{-M}^i , ζ_{nc}^i , ζ_{ns}^i	i = 1,2 refers to the two rotor systems R_1 and R_2
Torsion	ϕ_M^i , ϕ_{-M}^i , ϕ_{nc}^i , ϕ_{ns}^i	

The subscript M refers to the collective mode, -M refers to the alternating mode (only for rotors with even number of blades), nc refers to the n-cosine mode, ns refers to the n-sine mode.

Rigid body degrees of freedom of the vehicle

X - Translation	$\bar{R}_{xs}$
Y - Translation	$\bar{R}_{ys}$
Roll	θ_x
Pitch	θ_y

Degrees of freedom for the flexible supporting structure

Bending in X-Y plane (Horizontal plane)	$\frac{\xi_1}{R}$
Bending in X-Z plane (Vertical plane)	$\frac{\xi_2}{R}$
Torsion	ξ_3

These degrees of freedom represent the three normal modes of vibration of the supporting structure, two for bending in two orthogonal planes and one for torsion.

Thus the total number of degrees of freedom for a vehicle consisting of two four bladed rotor systems is 31.

3.1.1 Static Equilibrium Equations (Trim Equations)

In the following, the nonlinear algebraic equations required for the calculation of the trim quantities, for a hovering vehicle, are presented. These equations are solved to obtain β_{k0}^i , ζ_{k0}^i , ϕ_{k0}^i , θ_0^i and λ_i, where i=1,2, refers to the two rotor systems. Since the form of the equations are the same for the blades in both rotor systems R_1 and R_2, only one set of blade equations is needed. It should be noted that these blade equations are solved separately for each rotor system with its own parameters. Furthermore for convenience in writing these equations the superscript, i, is deleted from the equilibrium quantities only.

Flap Equation

$$\beta_{k0}\, F_T(1,i) + \zeta_{k0}\, F_T(2,i) + \phi_{k0}\, F_T(3,i)$$

$$+ \beta_{k0}\, \zeta_{k0}\, F_T(4,i) + \phi_{k0}\, \zeta_{k0}\, F_T(5,i) + \phi_{k0}\, \beta_{k0}\, F_T(6,i) + F_T(7,i) = 0 \qquad (3.1)$$

$i = 1,2$, refers to the two rotor systems R_1 and R_2

$$F_T(1,i) = \bar{\omega}_F^2 + (\bar{\omega}_L^2 - \bar{\omega}_F^2)\sin^2\theta_0 + \frac{\bar{\ell}^3}{3} + \bar{e}\,\frac{\bar{\ell}^2}{2}$$

$$F_T(2,i) = (\bar{\omega}_L^2 - \bar{\omega}_F^2)\sin\theta_0\cos\theta_0 + \nu\,\frac{\bar{\ell}^4}{4}\,\beta_p$$

$$F_T(3,i) = -\nu \left(\frac{\bar{\ell}^4}{4} + \frac{\bar{\ell}^3}{3} \quad 2\bar{e} \right)$$

$$F_T(4,i) = \nu \frac{\bar{\ell}^4}{4}$$

$$F_T(5,i) = -\bar{\omega}_F^2 - (\bar{\omega}_L^2 - \bar{\omega}_F^2) \sin^2\theta_0$$

$$F_T(6,i) = (\bar{\omega}_L^2 - \bar{\omega}_F^2) \sin\theta_0 \cos\theta_0$$

$$F_T(7,i) = \beta_p \left(\frac{\bar{\ell}^3}{3} + \frac{\bar{\ell}^2}{2} \bar{e} \right) - \nu \left[\frac{\bar{\ell}^4}{4} \theta_0 + \frac{\bar{\ell}^3}{3} (-\lambda + 2 \bar{e} \theta_0) - \frac{\bar{\ell}^2}{2} \bar{e} \lambda \right]$$

where

$$\bar{\omega}_F^2 = \frac{K_{\beta_B}}{m\Omega^2 R^3}$$

$$\bar{\omega}_L^2 = \frac{K_{\zeta_B}}{m\Omega^2 R^3}$$

$$\bar{\ell} = 1 - \bar{e}$$

$$\bar{e} = \frac{e}{R}$$

$$\nu = \frac{\rho_A abR}{m}$$

Lead-Lag Equation

$$\zeta_{k0} L_T(1,i) + \beta_{k0} L_T(2,i) + \phi_{k0} L_T(3,i)$$

$$+ \phi_{k0} \beta_{k0} L_T(4,i) + \phi_{k0} \zeta_{k0} L_T(5,i) + \beta_{k0} \zeta_{k0} L_T(6,i) + L_T(7,i) = 0 \tag{3.2}$$

$$L_T(1,i) = -\bar{\omega}_L^2 + (\bar{\omega}_L^2 - \bar{\omega}_F^2) \sin^2\theta_0 - \frac{\bar{\ell}^2}{2} \bar{e} + \nu \left(-\frac{\bar{\ell}^4}{4} \beta_p \theta_0 - \frac{\bar{\ell}^3}{3} \quad 2\lambda\beta_p \right)$$

$$L_T(2,i) = -(\bar{\omega}_L^2 - \bar{\omega}_F^2) \sin\theta_0 \cos\theta_0$$

$$L_T(3,i) = \nu \left(-\frac{\bar{\ell}^3}{3} \lambda - \frac{\bar{\ell}^2}{2} \lambda \bar{e} \right)$$

$$L_T(4,i) = -\bar{\omega}_L^2 + (\bar{\omega}_L^2 - \bar{\omega}_F^2)\sin^2\theta_0$$

$$L_T(5,i) = (\bar{\omega}_L^2 - \bar{\omega}_F^2)\sin\theta_0\cos\theta_0 - \nu\frac{\bar{\ell}^4}{4}\beta_p$$

$$L_T(6,i) = \nu\frac{\bar{\ell}^3}{3}\lambda$$

$$L_T(7,i) = \nu\{-\frac{c_{d0}}{a}(\frac{\bar{\ell}^4}{4} + 2\frac{\bar{\ell}^3}{3}\bar{e}) - \frac{\bar{\ell}^3}{3}\lambda\theta_0 + \frac{\bar{\ell}^2}{2}\lambda(\lambda-\bar{e}\theta_0)\}$$

Torsion Equation

$$\phi_{k0}T_T(1,i) + \zeta_{k0}T_T(2,i) + \beta_{k0}T_T(3,i)$$

$$+ \beta_{k0}\zeta_{k0}T_T(4,i) + \zeta_{k0}\phi_{k0}T_T(5,i) + \zeta_{k0}^2T_T(6,i)$$

$$+ \beta_{k0}\zeta_{k0}^2T_T(7,i) + \beta_{k0}^2\zeta_{k0}^3T_T(8,i) + \beta_{k0}\zeta_{k0}^3T_T(9,i)$$

$$+ \beta_{k0}^2\zeta_{k0}T_T(10,i) + \beta_{k0}^2\zeta_{k0}\phi_{k0}T_T(11,i) + \beta_{k0}^2\zeta_{k0}^3\phi_{k0}T_T(12,i)$$

$$+ \beta_{k0}\zeta_{k0}\phi_{k0}T_T(13,i) + \beta_{k0}\zeta_{k0}^3\phi_{k0}T_T(14,i) + \beta_{k0}\phi_{k0}T_T(15,i)$$

$$+ \beta_{k0}\zeta_{k0}^2\phi_{k0}T_T(16,i) + T_T(17,i) = 0 \qquad (3.3)$$

$$T_T(1,i) = -\bar{\omega}_{T_1}^2 - \bar{\omega}_{T_2}^2 + \bar{\ell}(\sin^2\theta_0 - \cos^2\theta_0)(\frac{I_{MB3}}{mR^2} - \frac{I_{MB2}}{mR^2})$$

$$+ \bar{x}_I\sin\theta_0\frac{\bar{\ell}^2}{2}\beta_p + \nu\bar{x}_A(\frac{\bar{\ell}^3}{3} + \frac{\bar{\ell}^2}{2}2\bar{e})$$

$$T_T(2,i) = -\beta_p(\frac{\bar{\ell}^3}{3} + \frac{\bar{\ell}^2}{2}\bar{e}) - \bar{x}_I\sin\theta_0\frac{\bar{\ell}^2}{2} + \nu(\frac{\bar{\ell}^4}{4}\theta_0 + \frac{\bar{\ell}^3}{3}(-\lambda+2\bar{e}\theta_0) - \frac{\bar{\ell}^2}{2}\bar{e}\lambda)$$

$$+ \nu\bar{x}_A(-\frac{\bar{\ell}^3}{3}\beta_p) + \bar{\ell}(\frac{I_{MB3}}{mR^2}\cos^2\theta_0 + \frac{I_{MB2}}{mR^2}\sin^2\theta_0)\beta_p$$

$$T_T(3,i) = -\nu[-\frac{c_{d0}}{a}(\frac{\bar{\ell}^4}{4} + 2\frac{\bar{\ell}^3}{3}\bar{e}) - \frac{\bar{\ell}^3}{3}\lambda\theta_0 - \frac{\bar{\ell}^2}{2}\lambda(-\lambda+\bar{e}\theta_0)] - \bar{x}_I\frac{\bar{\ell}^2}{2}\cos\theta_0$$

$$T_T(4,i) = \bar{\omega}_{T_1}^2 - \frac{\bar{\ell}^3}{3} + \bar{\ell}(\frac{I_{MB3}}{mR^2}\cos^2\theta_0 + \frac{I_{MB2}}{mR^2}\sin^2\theta_0) + \nu\frac{\bar{\ell}^4}{4}\beta_p\theta_0$$

$$- \nu \frac{\bar{\ell}^3}{3} \; 2\lambda\beta_p - \nu \bar{x}_A \frac{\bar{\ell}^3}{3}$$

$$T_T(5,i) = - \bar{x}_I \cos\theta_0 \; \frac{\bar{\ell}^2}{2} + \nu \left(\frac{\bar{\ell}^4}{4} + \frac{\bar{\ell}^3}{3} \; 2\bar{e} \right)$$

$$T_T(6,i) = - \nu\beta_p \frac{\bar{\ell}^4}{4}$$

$$T_T(7,i) = -\nu\frac{\bar{\ell}^4}{4} - \nu\left[- \frac{c_{d0}}{a} \left(\frac{\bar{\ell}^4}{4} + 2\frac{\bar{\ell}^3}{3}\bar{e} \right) - \frac{\bar{\ell}^3}{3}\lambda\theta_0 - \frac{\bar{\ell}^2}{2}\lambda(-\lambda+\bar{e}\theta_0) \right]$$

$$T_T(8,i) = - \nu\left(- \frac{\bar{\ell}^4}{4} \theta_0 + 2\frac{\bar{\ell}^3}{3}\lambda \right)$$

$$T_T(9,i) = \nu\frac{\bar{\ell}^4}{4} \beta_p\theta_0 - \nu\frac{\bar{\ell}^3}{3} \; 2\lambda\beta_p$$

$$T_T(10,i) = - \nu \left(- \frac{\bar{\ell}^4}{4} \theta_0 + 2\frac{\bar{\ell}^3}{3} \lambda\right)$$

$$T_T(11,i) = \nu\frac{\bar{\ell}^4}{4}$$

$$T_T(12,i) = \nu\frac{\bar{\ell}^4}{4}$$

$$T_T(13,i) = \nu\frac{\bar{\ell}^4}{4} \beta_p$$

$$T_T(14,i) = \nu\frac{\bar{\ell}^4}{4} \beta_p$$

$$T_T(15,i) = \nu \left(\frac{\bar{\ell}^3}{3}\lambda + \frac{\bar{\ell}^2}{2}\lambda\bar{e} \right)$$

$$T_T(16,i) = \nu \left(\frac{\bar{\ell}^3}{3}\lambda + \frac{\bar{\ell}^2}{2}\lambda\bar{e} \right)$$

$$T_T(17,i) = \bar{x}_I \cos\theta_0 \left[- \beta_p \left(\frac{\bar{\ell}^2}{2} + \bar{\ell}\bar{e} \right) \right] + \bar{\ell} \left[-\left(\frac{I_{MB3}}{mR^2} - \frac{I_{MB2}}{mR^2} \right) \sin\theta_0 \cos\theta_0 \right]$$
$$+ \nu\bar{x}_A \left(\frac{\bar{\ell}^3}{3} \theta_0 + \frac{\bar{\ell}^2}{2} (-\lambda + 2\bar{e}\theta_0) - \bar{e}\bar{\ell}\lambda \right)$$

Equations (3.1)-(3.3) are valid for both articulated as well as hingeless blades.

For articulated rotors $\bar{\omega}_F = 0$

$\bar{\omega}_L = 0$

$$\bar{\omega}_{T_1} = 0$$

and $$\bar{\omega}_{T_2}^2 = \frac{K_\phi}{m\Omega^2 R^3} \quad ; \quad K_\phi = \frac{K_{\phi_B} K_{\phi_C}}{K_{\phi_B} + K_{\phi_C}}$$

For hingeless rotors $$\bar{\omega}_{T_1}^2 = \frac{K_\phi}{m\Omega^2 R^3}$$

and $$\bar{\omega}_{T_2} = 0$$

In the above blade equilibrium equations, the inflow ratio λ is [Ref. 3]

$$\lambda = \frac{\sigma a}{16} \left(-1 + \sqrt{1 + \frac{1.5\theta_0}{(\sigma a/16)}} \right) \tag{3.4}$$

Force Equilibrium Relation

For hover, the thrust developed by the two rotors and the buoyancy force on the envelope must balance the weight of the complete vehicle. Also, the pitching moment due to the various forces about Y-axis (Fig. 2) must be zero.

$$\sum_{i=1}^{2} \left[\sum_{k=1}^{N} m\Omega^2 R^2 \left\{ \nu \left[\frac{\bar{\ell}^3}{3} \left(\theta_0 + \phi_{k0} - \zeta_{k0}\beta_p - \zeta_{k0}\beta_{k0} \right) + \frac{\bar{\ell}^2}{2} \left(-\lambda + 2\bar{e}\theta_0 + 2\bar{e}\phi_{k0} \right) - \bar{\ell}\bar{e}\lambda \right] \right\} \right]_i + P_Z^S - \left(W_{F1} + W_{F2} + W_{UN} + W_{EN} + W_S \right) = 0 \tag{3.5}$$

Moment Equilibrium Relation

$$\sum_{i=1}^{2} \left[-\bar{\ell}_{Fi} \left\{ \sum_{k=1}^{N} m\Omega^2 R^3 < \nu \left[\frac{\bar{\ell}^3}{3} \left(\theta_0 + \phi_{k0} - \zeta_{k0}\beta_p - \zeta_{k0}\beta_{k0} \right) + \frac{\bar{\ell}^2}{2} \left(-\lambda + 2\bar{e}\theta_0 + 2\bar{e}\phi_{k0} \right) - \bar{\ell}\bar{e}\lambda \right] > \right\} \right]_i + \ell_{F1} W_{F1} + \ell_{F2} W_{F2} + h_5 W_s = 0 \tag{3.6}$$

In equations (3.5) and (3.6) the symbol 'i' outside the brackets indicates that all the quantities within the bracket refer to the i^{th} rotor. The quantities within the bracket can be different for different rotor systems.

In total, these are eight equations, three blade equilibrium equations for each rotor (total 6) and two vehicle equilibrium equations. As explained in the previous chapter, these equations are solved iteratively to obtain the equilibrium state. The solution consists of β_{k0}^{i}, ζ_{k0}^{i}, ϕ_{k0}^{i}, θ_{0}^{i} ; 1 = 1,2, these equilbrium quantities are the same for all the blades in one rotor system.

3.1.2 Stability Equations

The equations of motion for the blade as well as for the vehicle are linearized about the equilibrium state. These linearized equations are then transformed into multiblade or rotor plane coordinates. The final linearized equations, written in the multiblade coordinates are given below.

Collective Flap Equation

$$\begin{aligned}
&\beta_M^i F_c(1,i) + \zeta_M^i F_c(2,i) + \phi_M^i F_c(3,i) \\
&+ \dot{\beta}_M^i F_c(4,i) + \dot{\zeta}_M^i F_c(5,i) + \dot{\phi}_M^i F_c(6,i) \\
&+ \ddot{\beta}_M^i F_c(7,i) + \dot{\theta}_y F_c(8,i) + \frac{\dot{\xi}_2}{R} F_c(9,i) \\
&+ \ddot{\theta}_y F_c(10,i) + \frac{\ddot{\xi}_2}{R} F_c(11,i) = 0
\end{aligned} \tag{3.7}$$

i = 1,2 refers to the i^{th} rotor

$$\begin{aligned}
F_c(1,i) &= \bar{\omega}_F^2 + (\bar{\omega}_L^2 - \bar{\omega}_F^2) \sin^2\theta_0 + \phi_{k0} (\bar{\omega}_L^2 - \bar{\omega}_F^2) \sin\theta_0 \cos\theta_0 \\
&\quad + \nu \frac{\bar{\ell}^4}{4} \zeta_{k0} + \frac{\bar{\ell}^3}{3} + \frac{\bar{\ell}^2}{2} \bar{e}
\end{aligned}$$

$$F_c(2,i) = -\phi_{k0} \{ \bar{\omega}_F^2 + (\bar{\omega}_L^2 - \bar{\omega}_F^2) \sin^2\theta_0 \} + (\bar{\omega}_L^2 - \bar{\omega}_F^2) \sin\theta_0 \cos\theta_0$$

$$+ \nu \frac{\bar{\ell}^4}{4} \quad (\beta_p + \beta_{k0})$$

$$F_c(3,i) = - \zeta_{k0} \{ \bar{\omega}_F^2 + (\bar{\omega}_L^2 - \bar{\omega}_F^2) \sin^2\theta_0 \} + \beta_{k0} (\bar{\omega}_L^2 - \bar{\omega}_F^2) \sin\theta_0 \cos\theta_0$$
$$- \nu \frac{\bar{\ell}^3}{3} \quad 2 \bar{e} - \nu \frac{\bar{\ell}^4}{4}$$

$$F_c(4,i) = (\bar{g}_{SF} + \nu \frac{\bar{\ell}^4}{4} + \nu \frac{\bar{\ell}^3}{3} \quad \bar{e}) \quad \frac{\Omega_1}{\Omega_i}$$

$$F_c(5,i) = [2 \frac{\bar{\ell}^3}{3} \quad (\beta_{k0} + \beta_p) - 2 \nu \frac{\bar{\ell}^4}{4} (\theta_0 + \phi_{k0}) + \nu \frac{\bar{\ell}^3}{3} \lambda] \quad \frac{\Omega_1}{\Omega_i}$$

$$F_c(6,i) = [- \nu \frac{\bar{\ell}^3}{3} \bar{b} - \frac{1}{2} \nu \bar{b} \quad \frac{\bar{\ell}^3}{3} \quad \cos\theta_0] \quad \frac{\Omega_1}{\Omega_i}$$

$$F_e(7,i) = [\frac{\bar{\ell}^3}{3} + \frac{1}{2} \nu \frac{\bar{\ell}^3}{3} \quad \bar{b} \cos\theta_0] \quad (\frac{\Omega_1}{\Omega_i})^2$$

$$F_c(8,i) = - \bar{\ell}_{Fi} \nu \frac{\bar{\ell}^3}{3} \quad (\frac{\Omega_1}{\Omega_i})$$

$$F_c(9,i) = \eta_2 \quad (\ell_{Fi}) \quad \nu \frac{\bar{\ell}^3}{3} \quad \frac{\Omega_1}{\Omega_i}$$

$$F_c(10,i) = - \bar{\ell}_{Fi} \quad \frac{\bar{\ell}^2}{2} \quad (\frac{\Omega_1}{\Omega_i})^2$$

$$F_c(11,i) = \eta_2(\ell_{Fi}) \frac{\bar{\ell}^2}{2} \quad (\frac{\Omega_1}{\Omega_i})^2$$

It should be mentioned that the angular speed Ω can be different for the two rotors, and thus the blade static equilibrium represented by β_{k0}, ζ_{k0}, ϕ_{k0}, θ_0, λ can differ from one rotor to another. Thus the coefficients F_c can be different for the two rotors, Actually Eq. (3.7) represents two equations, one for each rotor system.

Alternating Flap Equation (For even N only)

$$\beta_{-M}^{i} F_A(1,i) + \zeta_{-M}^{i} F_A(2,i) + \phi_{-M}^{i} F_A(3,i)$$
$$+ \dot{\beta}_{-M}^{i} F_A(4,i) + \dot{\zeta}_{-M}^{i} F_A(5,i) + \dot{\phi}_{-M}^{i} F_A(6,i)$$
$$+ \ddot{\beta}_{-M}^{i} F_A(7,i) = 0 \qquad (3.8)$$

$$F_A(1,i) = \bar{\omega}_F^2 + (\bar{\omega}_L^2 - \bar{\omega}_F^2)\sin^2\theta_0 + \phi_{k0}(\bar{\omega}_L^2 - \bar{\omega}_F^2)\sin\theta_0\cos\theta_0 + \nu\frac{\bar{\ell}^4}{4}\zeta_{k0} + \frac{\bar{\ell}^3}{3} + \frac{\bar{\ell}^2}{2}\bar{e}$$

$$F_A(2,i) = -\phi_{k0}\{\bar{\omega}_F^2 + (\bar{\omega}_L^2 - \bar{\omega}_F^2)\sin^2\theta_0\} + (\bar{\omega}_L^2 - \bar{\omega}_F^2)\sin\theta_0\cos\theta_0 + \nu\frac{\bar{\ell}^4}{4}(\beta_p + \beta_{k0})$$

$$F_A(3,i) = -\zeta_{k0}\{\bar{\omega}_F^2 + (\bar{\omega}_L^2 - \bar{\omega}_F^2)\sin^2\theta_0\} + \beta_{k0}(\bar{\omega}_L^2 - \bar{\omega}_F^2)\sin\theta_0\cos\theta_0 - \nu\frac{\bar{\ell}^3}{3}2\bar{e} - \nu\frac{\bar{\ell}^4}{4}$$

$$F_A(4,i) = (\bar{g}_{SF} + \nu\frac{\bar{\ell}^4}{4} + \nu\frac{\bar{\ell}^3}{3}\bar{e})\frac{\Omega_1}{\Omega_i}$$

$$F_A(5,i) = \{2\frac{\bar{\ell}^3}{3}(\beta_{k0} + \beta_p) - 2\nu\frac{\bar{\ell}^4}{4}(\theta_0 + \phi_{k0}) + \nu\frac{\bar{\ell}^3}{3}\lambda\}\frac{\Omega_1}{\Omega_i}$$

$$F_A(6,i) = \{-\nu\frac{\bar{\ell}^3}{3}\bar{b} - \frac{1}{2}\nu\bar{b}\frac{\bar{\ell}^3}{3}\cos\theta_0\}\frac{\Omega_1}{\Omega_i}$$

$$F_A(7,i) = \{\frac{\bar{\ell}^3}{3} + \frac{1}{2}\nu\bar{b}\frac{\bar{\ell}^3}{3}\cos\theta_0\}\left(\frac{\Omega_1}{\Omega_i}\right)^2$$

n-Cosine Flap Equation

$$\beta_{nc}^i F_{nc}(1,i) + \beta_{ns}^i F_{nc}(2,i) + \zeta_{nc}^i F_{nc}(3,i) + \zeta_{ns}^i F_{nc}(4,i) + \phi_{nc}^i F_{nc}(5,i) + \phi_{ns}^i F_{nc}(6,i) + \dot{\beta}_{nc}^i F_{nc}(7,i) + \dot{\beta}_{ns}^i F_{nc}(8,i) + \dot{\zeta}_{nc}^i F_{nc}(9,i) + \dot{\phi}_{nc}^i F_{nc}(10,i) + \ddot{\beta}_{nc}^i F_{nc}(11,i) + \ddot{\theta}_y F_{nc}(12,i) + \dot{\theta}_y F_{nc}(13,i) + \dot{\theta}_x F_{nc}(14,i) + \dot{\bar{R}}_{ys} F_{nc}(15,i) + \frac{\dot{\xi}_1}{R} F_{nc}(16,i) + \dot{\xi}_3 F_{nc}(17,i) = 0 \qquad (3.9)$$

$$F_{nc}(1,i) = \bar{\omega}_F^2 + (\bar{\omega}_L^2 - \bar{\omega}_F^2)\sin^2\theta_0 + \phi_{k0}(\bar{\omega}_L^2 - \bar{\omega}_F^2)\sin\theta_0\cos\theta_0 + \nu\frac{\bar{\ell}^4}{4}\zeta_{k0} + \frac{\bar{\ell}^3}{3} + \frac{\bar{\ell}^2}{2}\bar{e} - n^2\frac{\bar{\ell}^3}{3} - n^2\frac{1}{2}\nu\bar{b}\frac{\bar{\ell}^3}{3}\cos\theta_0$$

$$F_{nc}(2,i) = n\left(\nu \frac{\bar{\ell}^4}{4} + \nu \frac{\bar{\ell}^3}{3} \bar{e} + \bar{g}_{SF} \right)$$

$$F_{nc}(3,i) = -\phi_{k0}\left\{ \bar{\omega}_F^2 + (\bar{\omega}_L^2 - \bar{\omega}_F^2) \sin^2\theta_0 \right\} + (\bar{\omega}_L^2 - \bar{\omega}_F^2) \sin\theta_0 \cos\theta_0 + \nu \frac{\bar{\ell}^4}{4} (\beta_p + \beta_{k0})$$

$$F_{nc}(4,i) = n\left\{ 2 \frac{\bar{\ell}^3}{3} (\beta_{k0} + \beta_p) - 2 \nu \frac{\bar{\ell}^4}{4} (\theta_0 + \phi_{k0}) + \nu \frac{\bar{\ell}^3}{3} \lambda \right\}$$

$$F_{nc}(5,i) = -\zeta_{k0}\left\{ \bar{\omega}_F^2 + (\bar{\omega}_L^2 - \bar{\omega}_F^2) \sin^2\theta_0 \right\} + \beta_{k0} (\bar{\omega}_L^2 - \bar{\omega}_F^2) \sin\theta_0 \cos\theta_0 - \nu \frac{\bar{\ell}^4}{4} - \nu \frac{\bar{\ell}^3}{3} 2 \bar{e}$$

$$F_{nc}(6,i) = n\left\{ -\nu \frac{\bar{\ell}^3}{3} \bar{b} - \frac{1}{2} \nu \bar{b} \frac{\bar{\ell}^3}{3} \cos\theta_0 \right\}$$

$$F_{nc}(7,i) = \left\{ \nu \frac{\bar{\ell}^4}{4} + \nu \frac{\bar{\ell}^3}{3} \bar{e} + \bar{g}_{SF} \right\} \frac{\Omega_1}{\Omega_i}$$

$$F_{nc}(8,i) = n\left\{ 2 \frac{\bar{\ell}^3}{3} + \frac{1}{2} 2 \nu \frac{\bar{\ell}^3}{3} \bar{b} \cos\theta_0 \right\} \frac{\Omega_1}{\Omega_i}$$

$$F_{nc}(9,i) = \left\{ 2 \frac{\bar{\ell}^3}{3} (\beta_{k0} + \beta_p) - 2 \nu \frac{\bar{\ell}^4}{4} (\theta_0 + \phi_{k0}) + \nu \frac{\bar{\ell}^3}{3} \lambda \right\} \frac{\Omega_1}{\Omega_i}$$

$$F_{nc}(10,i) = \left\{ -\nu \frac{\bar{\ell}^3}{3} \bar{b} - \frac{1}{2} \nu \frac{\bar{\ell}^3}{3} \bar{b} \cos\theta_0 \right\} \frac{\Omega_1}{\Omega_i}$$

$$F_{nc}(11,i) = \left\{ \frac{\bar{\ell}^3}{3} + \frac{1}{2} \nu \frac{\bar{\ell}^3}{3} \bar{b} \cos\theta_0 \right\} \left(\frac{\Omega_1}{\Omega_i} \right)^2$$

$$F_{nc}(12,i) = -\delta_n \frac{\bar{\ell}^3}{3} \left(\frac{\Omega_1}{\Omega_i} \right)^2$$

$$F_{nc}(13,i) = -\delta_n \nu \frac{\bar{\ell}^4}{4} \frac{\Omega_1}{\Omega_i}$$

$$F_{nc}(14,i) = \left\{ +\delta_n 2 \frac{\bar{\ell}^3}{3} + \delta_n 2 \nu \frac{\bar{\ell}^3}{3} \theta_0 \bar{h}_2 - \bar{h}_2 \nu \frac{\bar{\ell}^2}{2} \lambda \delta_n \right\} \frac{\Omega_1}{\Omega_i}$$

$$F_{nc}(15,i) = \left(-\delta_n 2 \nu \frac{\bar{\ell}^3}{3} \theta_0 + \nu \frac{\bar{\ell}^2}{2} \lambda \delta_n \right) \frac{\Omega_1}{\Omega_i}$$

$$F_{nc}(16,i) = \left(-\delta_n 2 \nu \frac{\bar{\ell}^3}{3} \theta_0 \eta_1(\ell_{Fi}) + \eta_1(\ell_{Fi}) \nu \frac{\bar{\ell}^2}{2} \lambda \delta_n \right) \frac{\Omega_1}{\Omega_i}$$

$$F_{nc}(17,i) = \left(\delta_n \, 2\nu\frac{\bar{\ell}^3}{3} \; \theta_0 \, \bar{h}_2 \, \eta_3 \, (\ell_{Fi}) - \bar{h}_2 \, \eta_3 \, (\ell_{Fi}) \, \nu \frac{\bar{\ell}^2}{2} \, \lambda \, \delta_n \right) \frac{\Omega_1}{\Omega_i}$$

where

$$\delta_n = 1 \qquad \text{when } n = 1$$

$$= 0 \qquad\quad n \neq 1$$

n-Sine Flap Equation

$$\beta^i_{ns} F_{ns}(1,i) + \beta^i_{nc} F_{ns}(2,i) + \zeta^i_{ns} F_{ns}(3,i) + \zeta^i_{nc} F_{ns}(4,i)$$

$$+ \phi^i_{ns} F_{ns}(5,i) + \phi^i_{nc} F_{ns}(6,i) + \dot{\beta}^i_{ns} F_{ns}(7,i) + \dot{\beta}^i_{nc} F_{ns}(8,i)$$

$$+ \dot{\zeta}^i_{ns} F_{ns}(9,i) + \dot{\phi}^i_{ns} F_{ns}(10,i) + \ddot{\beta}^i_{ns} F_{ns}(11,i) + \ddot{\theta}_x F_{ns}(12,i)$$

$$+ \dot{\theta}_x F_{ns}(13,i) + \dot{\theta}_y F_{ns}(14,i) + \dot{\bar{R}}_{xs} F_{ns}(15,i) + \frac{\dot{\xi}_2}{R} F_{ns}(16,i) = 0 \qquad (3.10)$$

$$F_{ns}(1,i) = \bar{\omega}_F^2 + (\bar{\omega}_L^2 - \bar{\omega}_F^2) \sin^2\theta_0 + \phi_{k0} (\bar{\omega}_L^2 - \bar{\omega}_F^2) \sin\theta_0 \cos\theta_0$$

$$+ \nu\frac{\bar{\ell}^4}{4} \zeta_{k0} + \frac{\bar{\ell}^3}{3} + \frac{\bar{\ell}^2}{2} \bar{e} - n^2 \frac{\bar{\ell}^3}{3} - \frac{1}{2} \nu \bar{b} \frac{\bar{\ell}^3}{3} n^2 \cos\theta_0$$

$$F_{ns}(2,i) = n \left\{ - \nu \frac{\bar{\ell}^4}{4} - \nu \frac{\bar{\ell}^3}{3} \bar{e} - \bar{g}_{SF} \right\}$$

$$F_{ns}(3,i) = - \phi_{k0} \left\{ \bar{\omega}_F^2 + (\bar{\omega}_L^2 - \bar{\omega}_F^2) \sin^2\theta_0 \right\} + (\bar{\omega}_L^2 - \bar{\omega}_F^2) \sin\theta_0 \cos\theta_0$$

$$+ \nu \frac{\bar{\ell}^4}{4} (\beta_p + \beta_{k0})$$

$$F_{ns}(4,i) = n \left\{ - 2 \frac{\bar{\ell}^3}{3} (\beta_{k0} + \beta_p) + 2 \nu \frac{\bar{\ell}^4}{4} (\theta_0 + \phi_{k0}) - \nu\frac{\bar{\ell}^3}{3} \lambda \right\}$$

$$F_{ns}(5,i) = - \zeta_{k0} \left\{ \bar{\omega}_F^2 + (\bar{\omega}_L^2 - \bar{\omega}_F^2) \sin^2\theta_0 \right\} + \beta_{k0} (\bar{\omega}_L^2 - \bar{\omega}_F^2) \sin\theta_0 \cos\theta_0$$

$$- \nu \frac{\bar{\ell}^4}{4} - \nu \frac{\bar{\ell}^3}{3} 2 \bar{e}$$

$$F_{ns}(6,i) = n \left\{ \nu\frac{\bar{\ell}^3}{3} \bar{b} + \frac{1}{2} \nu \bar{b} \frac{\bar{\ell}^3}{3} \cos\theta_0 \right\}$$

$$F_{ns}(7,i) = \left\{ \nu \frac{\bar{\ell}^4}{4} + \nu \frac{\bar{\ell}^3}{3} \bar{e} + \bar{g}_{SF} \right\} \frac{\Omega_1}{\Omega_i}$$

$$F_{ns}(8,i) = n\{ -2\frac{\bar{\ell}^3}{3} - \frac{1}{2}2\nu\bar{b}\frac{\bar{\ell}^3}{3}\cos\theta_0 \}\frac{\Omega_1}{\Omega_i}$$

$$F_{ns}(9,i) = \{ 2\frac{\bar{\ell}^3}{3}(\beta_{k0}+\beta_p) - 2\nu\frac{\bar{\ell}^4}{4}(\theta_0+\phi_{k0}) + \nu\frac{\bar{\ell}^3}{3}\lambda \}\frac{\Omega_1}{\Omega_i}$$

$$F_{ns}(10,i) = \{ -\nu\frac{\bar{\ell}^3}{3}\bar{b} - \frac{1}{2}\nu\bar{b}\frac{\bar{\ell}^3}{3}\cos\theta_0 \}\frac{\Omega_1}{\Omega_i}$$

$$F_{ns}(11,i) = (\frac{\bar{\ell}^3}{3} + \frac{1}{2}\nu\bar{b}\frac{\bar{\ell}^3}{3}\cos\theta_0)(\frac{\Omega_1}{\Omega_i})^2$$

$$F_{ns}(12,i) = +\delta_n\frac{\bar{\ell}^3}{3}(\frac{\Omega_1}{\Omega_i})^2$$

$$F_{ns}(13,i) = \delta_n\nu\frac{\bar{\ell}^4}{4}(\frac{\Omega_1}{\Omega_i})$$

$$F_{ns}(14,i) = \{ +\delta_n 2\frac{\bar{\ell}^3}{3} + \delta_n 2\nu\frac{\bar{\ell}^3}{3}\theta_0\bar{h}_2 - \bar{h}_2\nu\frac{\bar{\ell}^2}{2}\lambda\delta_n \}\frac{\Omega_1}{\Omega_i}$$

$$F_{ns}(15,i) = (\delta_n 2\nu\frac{\bar{\ell}^3}{3}\theta_0 - \nu\frac{\bar{\ell}^2}{2}\lambda\delta_n)\frac{\Omega_1}{\Omega_i}$$

$$F_{ns}(16,i) = R\{ -\delta_n 2\nu\frac{\bar{\ell}^3}{3}\theta_0\bar{h}_2\eta_{2,x}(\ell_{Fi}) + \bar{h}_2\eta_{2,x}(\ell_{Fi})\nu\frac{\bar{\ell}^2}{2}\lambda\delta_n \}\frac{\Omega_1}{\Omega_i}$$

Collective Lead-Lag Equation

$$\zeta_M^i L_c(1,i) + \beta_M^i L_c(2,i) + \phi_M^i L_c(3,i)$$
$$+ \dot{\zeta}_M^i L_c(4,i) + \dot{\beta}_M^i L_c(5,i) + \dot{\phi}_M^i L_c(6,i)$$
$$+ \ddot{\zeta}_M^i L_c(7,i) + \ddot{\beta}_M^i L_c(8,i) + \dot{\theta}_y L_c(9,i) + \frac{\dot{\xi}_2}{R} L_c(10,i) = 0 \qquad (3.11)$$

$$L_c(1,i) = -\bar{\omega}_L^2 + (\bar{\omega}_L^2 - \bar{\omega}_F^2)\sin^2\theta_0 + \phi_{k0}(\bar{\omega}_L^2 - \bar{\omega}_F^2)\sin\theta_0\cos\theta_0$$
$$- \frac{\bar{\ell}^2}{2}\bar{e} - \nu\frac{\bar{\ell}^4}{4}\theta_0\beta_p$$

$$L_c(2,i) = -\phi_{k0}\{ \bar{\omega}_L^2 - (\bar{\omega}_L^2 - \bar{\omega}_F^2)\sin^2\theta_0 \} - (\bar{\omega}_L^2 - \bar{\omega}_F^2)\sin\theta_0\cos\theta_0$$

$$L_c(3,i) = -\beta_{k0}\{ \bar{\omega}_L^2 - (\bar{\omega}_L^2 - \bar{\omega}_F^2)\sin^2\theta_0 \} + \zeta_{k0}(\bar{\omega}_L^2 - \bar{\omega}_F^2)\sin\theta_0\cos\theta_0$$
$$-\nu\frac{\bar{\ell}^3}{3}\lambda$$

$$L_c(4,i) = \{-2\nu\frac{c_{d0}}{a}\ \frac{\bar{\ell}^4}{4} - \nu\frac{\bar{\ell}^3}{3}\ \theta_0\lambda - \bar{g}_{SL}\}\frac{\Omega_1}{\Omega_i}$$

$$L_c(5,i) = \{2\frac{\bar{\ell}^3}{3}\ (\beta_{k0} + \beta_p) - \nu\frac{\bar{\ell}^4}{4}\ (\theta_0 + \phi_{k0}) - \nu\frac{\bar{\ell}^3}{3}\ (-2\lambda + \bar{e}\ \theta_0)\ \}\frac{\Omega_1}{\Omega_i}$$

$$L_c(6,i) = -\frac{1}{2}\nu\bar{b}\ \frac{\bar{\ell}^3}{3}\ \sin\theta_0\ \frac{\Omega_1}{\Omega_i}$$

$$L_c(7,i) = -\frac{\bar{\ell}^3}{3}\left(\frac{\Omega_1}{\Omega_i}\right)^2$$

$$L_c(8,i) = \frac{1}{2}\nu\bar{b}\ \frac{\bar{\ell}^3}{3}\ \sin\theta_0\left(\frac{\Omega_1}{\Omega_i}\right)^2$$

$$L_c(9,i) = -\bar{\ell}_{Fi}\{-\nu\frac{\bar{\ell}^3}{3}\ (\theta_0+\phi_{k0}) + \nu\frac{\bar{\ell}^2}{2}\ 2\lambda\}\frac{\Omega_1}{\Omega_i}$$

$$L_c(10,i) = \eta_2(\ell_{Fi})\{-\nu\frac{\bar{\ell}^3}{3}\ (\theta_0 + \phi_{k0}) + \nu\frac{\bar{\ell}^2}{2}\ 2\lambda\}\frac{\Omega_1}{\Omega_i}$$

Alternating Lead-Lag Equation (for even N only)

$$\zeta_{-M}^{i}\ L_A(1,i) + \beta_{-M}^{i}\ L_A(2,i) + \phi_{-M}^{i}\ L_A(3,i)$$
$$\dot{\zeta}_{-M}^{i}\ L_A(4,i) + \dot{\beta}_{-M}^{i}\ L_A(5,i) + \dot{\phi}_{-M}^{i}\ L_A(6,i)$$
$$+ \ddot{\zeta}_{-M}^{i}\ L_A(7,i) + \ddot{\beta}_{-M}^{i}\ L_A(8,i) = 0 \qquad (3.12)$$

$$L_A(1,i) = -\bar{\omega}_L^2 + (\bar{\omega}_L^2 - \bar{\omega}_F^2)\sin^2\theta_0 + \phi_{k0}(\bar{\omega}_L^2 - \bar{\omega}_F^2)\sin\theta_0\cos\theta_0$$
$$- \frac{\bar{\ell}^2}{2}\ \bar{e} - \nu\frac{\bar{\ell}^4}{4}\ \beta_p\theta_0$$

$$L_A(2,i) = -\phi_{k0}\{\bar{\omega}_L^2 - (\bar{\omega}_L^2 - \bar{\omega}_F^2)\sin^2\theta_0\} - (\bar{\omega}_L^2 - \bar{\omega}_F^2)\sin\theta_0\cos\theta_0$$

$$L_A(3,i) = -\beta_{k0}\{\bar{\omega}_L^2 - (\bar{\omega}_L^2 - \bar{\omega}_F^2)\sin^2\theta_0\} + \zeta_{k0}(\bar{\omega}_L^2 - \bar{\omega}_F^2)\sin\theta_0\cos\theta_0$$
$$- \nu\frac{\bar{\ell}^3}{3}\lambda$$

$$L_A(4,i) = \{-2\nu\frac{c_{d0}}{a}\ \frac{\bar{\ell}^4}{4} - \nu\frac{\bar{\ell}^3}{3}\ \theta_0\lambda - \bar{g}_{SL}\}\frac{\Omega_1}{\Omega_i}$$

$$L_A(5,i) = \{2\frac{\bar{\ell}^3}{3}\ (\beta_{k0} + \beta_p) - \nu\frac{\bar{\ell}^4}{4}\ (\theta_0 + \phi_{k0}) - \nu\frac{\bar{\ell}^3}{3}\ (-2\lambda+\bar{e}\theta_0)\}\frac{\Omega_1}{\Omega_i}$$

$$L_A(6,i) = -\frac{1}{2}\nu\bar{b}\ \frac{\bar{\ell}^3}{3}\ \sin\theta_0\ \frac{\Omega_1}{\Omega_i}$$

$$L_A(7,i) = -\frac{\bar{\ell}^3}{3}\left(\frac{\Omega_1}{\Omega_i}\right)^2$$

$$L_A(8,i) = \frac{1}{2}\nu\bar{b}\ \frac{\bar{\ell}^3}{3}\ \sin\theta_0\left(\frac{\Omega_1}{\Omega_i}\right)^2$$

n-Cosine Lead-Lag Equation

$$\begin{aligned}
&\zeta^i_{nc}\ L_{nc}(1,i) + \zeta^i_{ns}\ L_{nc}(2,i) + \beta^i_{nc}\ L_{nc}(3,i) + \beta^i_{ns}\ L_{nc}(4,i)\\
&+ \phi^i_{nc}\ L_{nc}(5,i) + \phi^i_{ns}\ L_{nc}(6,i) + \dot{\zeta}^i_{nc}\ L_{nc}(7,i) + \dot{\zeta}^i_{ns}\ L_{nc}(8,i)\\
&+ \dot{\beta}^i_{nc}\ L_{nc}(9,i) + \dot{\beta}^i_{ns}\ L_{nc}(10,i) + \dot{\phi}^i_{nc}\ L_{nc}(11,i) + \ddot{\zeta}^i_{nc}\ L_{nc}(12,i)\\
&+ \ddot{\beta}^i_{nc}\ L_{nc}(13,i) + \ddot{\theta}_x\ L_{nc}(14,i) + \ddot{\theta}_y\ L_{nc}(15,i) + \dot{\theta}_y\ L_{nc}(16,i)\\
&+ \ddot{\bar{R}}_{ys}\ L_{nc}(17,i) + \ddot{\bar{R}}_{xs}\ L_{nc}(18,i) + \frac{\ddot{\xi}_1}{R}\ L_{nc}(19,i) + \frac{\ddot{\xi}_2}{R}\ L_{nc}(20,i)\\
&+ \ddot{\xi}_3\ L_{nc}(21,i) = 0
\end{aligned} \tag{3.13}$$

$$L_{nc}(1,i) = -\bar{\omega}_L^2 + (\bar{\omega}_L^2 - \bar{\omega}_F^2)\sin^2\theta_0 + \phi_{k0}(\bar{\omega}_L^2 - \bar{\omega}_F^2)\sin\theta_0\cos\theta_0 - \frac{\bar{\ell}^2}{2}\bar{e} + n^2\frac{\bar{\ell}^3}{3} - \nu\frac{\bar{\ell}^4}{4}\beta_p\theta_0$$

$$L_{nc}(2,i) = -n\left\{2\nu\frac{c_{d0}}{a}\frac{\bar{\ell}^4}{4} + \nu\frac{\bar{\ell}^3}{3}\theta_0\lambda + \bar{g}_{SL}\right\}$$

$$L_{nc}(3,i) = -\phi_{k0}\left\{\bar{\omega}_L^2 - (\bar{\omega}_L^2 - \bar{\omega}_F^2)\sin^2\theta_0\right\} - (\bar{\omega}_L^2 - \bar{\omega}_F^2)\sin\theta_0\cos\theta_0 - \frac{1}{2}\nu\bar{b}\ \frac{\bar{\ell}^3}{3}\ \sin\theta_0\, n^2$$

$$L_{nc}(4,i) = n\left\{2\frac{\bar{\ell}^3}{3}(\beta_{k0} + \beta_p) - \nu\frac{\bar{\ell}^4}{4}(\theta_0 + \phi_{k0}) - \nu\frac{\bar{\ell}^3}{3}(-2\lambda + \bar{e}\ \theta_0)\right\}$$

$$L_{nc}(5,i) = -\beta_{k0}\left\{\bar{\omega}_L^2 - (\bar{\omega}_L^2 - \bar{\omega}_F^2)\sin^2\theta_0\right\} + \zeta_{k0}(\bar{\omega}_L^2 - \bar{\omega}_F^2)\sin\theta_0\cos\theta_0$$

$$- \nu \frac{\bar{\ell}^3}{3} \lambda$$

$$L_{nc}(6,i) = - \frac{1}{2} \nu \bar{b} \frac{\bar{\ell}^3}{3} \sin\theta_0 \, n$$

$$L_{nc}(7,i) = \{ - 2 \nu \frac{c_{d0}}{a} \frac{\bar{\ell}^4}{4} - \nu \frac{\bar{\ell}^3}{3} \lambda \theta_0 - \bar{g}_{SL} \} \frac{\Omega_1}{\Omega_i}$$

$$L_{nc}(8,i) = - 2 n \frac{\bar{\ell}^3}{3} \frac{\Omega_1}{\Omega_i}$$

$$L_{nc}(9,i) = \{2 \frac{\bar{\ell}^3}{3} (\beta_{k0} + \beta_p) - \nu \frac{\bar{\ell}^4}{4} (\theta_0 + \phi_{k0}) - \nu \frac{\bar{\ell}^3}{3} (-2\lambda + \bar{e} \theta_0) \} \frac{\Omega_1}{\Omega_i}$$

$$L_{nc}(10,i) = \frac{1}{2} \nu \bar{b} \frac{\bar{\ell}^3}{3} \sin\theta_0 \, 2 n \frac{\Omega_1}{\Omega_i}$$

$$L_{nc}(11,i) = - \frac{1}{2} \nu \bar{b} \frac{\bar{\ell}^3}{3} \sin\theta_0 \frac{\Omega_1}{\Omega_i}$$

$$L_{nc}(12,i) = - \frac{\bar{\ell}^3}{3} \left(\frac{\Omega_1}{\Omega_i} \right)^2$$

$$L_{nc}(13,i) = \frac{1}{2} \nu \bar{b} \frac{\bar{\ell}^3}{3} \sin\theta_0 \left(\frac{\Omega_1}{\Omega_i} \right)^2$$

$$L_{nc}(14,i) = \{ \delta_n \frac{\bar{\ell}^3}{3} (\beta_p + \beta_{k0}) + \delta_n \bar{h}_2 \frac{\bar{\ell}^2}{2} \} \left(\frac{\Omega_1}{\Omega_i} \right)^2$$

$$L_{nc}(15,i) = \delta_n \frac{\bar{\ell}^2}{2} \zeta_{k0} \bar{h}_2 \left(\frac{\Omega_1}{\Omega_i} \right)^2$$

$$L_{nc}(16,i) = \{ \delta_n \nu \frac{\bar{\ell}^4}{4} (\theta_0 + \phi_{k0}) - \delta_n \frac{\bar{\ell}^3}{3} 2 \lambda \nu \} \frac{\Omega_1}{\Omega_i}$$

$$L_{nc}(17,i) = - \delta_n \frac{\bar{\ell}^2}{2} \left(\frac{\Omega_1}{\Omega_i} \right)^2$$

$$L_{nc}(18,i) = \delta_n \frac{\bar{\ell}^2}{2} \zeta_{k0} \left(\frac{\Omega_1}{\Omega_i} \right)^2$$

$$L_{nc}(19,i) = - \delta_n \frac{\bar{\ell}^2}{2} \eta_1 (\ell_{Fi}) \left(\frac{\Omega_1}{\Omega_i} \right)^2$$

$$L_{nc}(20,i) = - \delta_n \frac{\bar{\ell}^2}{2} \zeta_{k0} \bar{h}_2 \eta_{2,x} (\ell_{Fi}) R \left(\frac{\Omega_1}{\Omega_i} \right)^2$$

$$L_{nc}(21,i) = \delta_n \frac{\bar{\ell}^2}{2} \bar{h}_2 \eta_3 (\ell_{Fi}) \left(\frac{\Omega_1}{\Omega_i} \right)^2$$

n-Sine Lead-Lag Equation

$$\zeta^i_{ns}\ L_{ns}(1,i) + \zeta^i_{nc}\ L_{ns}(2,i) + \beta^i_{ns}\ L_{ns}(3,i) + \beta^i_{nc}\ L_{ns}(4,i)$$
$$+ \phi^i_{ns}\ L_{ns}(5,i) + \phi^i_{nc}\ L_{ns}(6,i) + \dot{\zeta}^i_{ns}\ L_{ns}(7,i) + \dot{\zeta}^i_{nc}\ L_{ns}(8,i)$$
$$+ \dot{\beta}^i_{ns}\ L_{ns}(9,i) + \dot{\beta}^i_{nc}\ L_{ns}(10,i) + \dot{\phi}^i_{ns}\ L_{ns}(11,i) + \ddot{\zeta}^i_{ns}\ L_{ns}(12,i)$$
$$+ \ddot{\beta}^i_{ns}\ L_{ns}(13,i) + \ddot{\theta}_y\ L_{ns}(14,i) + \ddot{\theta}_x\ L_{ns}(15,i) + \dot{\theta}_x\ L_{ns}(16,i)$$
$$+ \ddot{\bar{R}}_{xs}\ L_{ns}(17,i) + \ddot{\bar{R}}_{ys}\ L_{ns}(18,i) + \frac{\ddot{\xi}_1}{R}\ L_{ns}(19,i) + \frac{\ddot{\xi}_2}{R}\ L_{ns}(20,i)$$
$$+ \ddot{\xi}_3\ L_{ns}(21,i) = 0 \qquad (3.14)$$

$$L_{ns}(1,i) = -\bar{\omega}_L^2 + (\bar{\omega}_L^2 - \bar{\omega}_F^2)\sin^2\theta_0 + \phi_{k0}(\bar{\omega}_L^2 - \bar{\omega}_F^2)\sin\theta_0\cos\theta_0$$
$$- \frac{\bar{\ell}^2}{2}\bar{e} + \frac{\bar{\ell}^3}{3}n^2 - \nu\frac{\bar{\ell}^4}{4}\beta_p\theta_0$$

$$L_{ns}(2,i) = n\{2\nu\frac{c_{d0}}{a}\frac{\bar{\ell}^4}{4} + \nu\frac{\bar{\ell}^3}{3}\lambda\theta_0 + \bar{g}_{SL}\}$$

$$L_{ns}(3,i) = -\phi_{k0}\{\bar{\omega}_L^2 - (\bar{\omega}_L^2 - \bar{\omega}_F^2)\sin^2\theta_0\} - (\bar{\omega}_L^2 - \bar{\omega}_F^2)\sin\theta_0\cos\theta_0$$
$$- \frac{1}{2}\nu\bar{b}\frac{\bar{\ell}^3}{3}\sin\theta_0 n^2$$

$$L_{ns}(4,i) = n\{-2\frac{\bar{\ell}^3}{3}(\beta_p + \beta_{k0}) + \nu\frac{\bar{\ell}^4}{4}(\theta_0 + \phi_{k0}) + \nu\frac{\bar{\ell}^3}{3}(-2\lambda + \bar{e}\theta_0)\}$$

$$L_{ns}(5,i) = -\beta_{k0}\{\bar{\omega}_L^2 - (\bar{\omega}_L^2 - \bar{\omega}_F^2)\sin^2\theta_0\} + \zeta_{k0}(\bar{\omega}_L^2 - \bar{\omega}_F^2)\sin\theta_0\cos\theta_0$$
$$- \nu\frac{\bar{\ell}^3}{3}\lambda$$

$$L_{ns}(6,i) = \frac{1}{2}\nu\bar{b}\frac{\bar{\ell}^3}{3}\sin\theta_0 n$$

$$L_{ns}(7,i) = \{-2\nu\frac{c_{d0}}{a}\frac{\bar{\ell}^4}{4} - \nu\frac{\bar{\ell}^3}{3}\lambda\theta_0 - \bar{g}_{SL}\}\frac{\Omega_1}{\Omega_i}$$

$$L_{ns}(8,i) = \frac{\bar{\ell}^3}{3} \; 2 \; n \; \frac{\Omega_1}{\Omega_i}$$

$$L_{ns}(9,i) = \{ \; 2 \; \frac{\bar{\ell}^3}{3} \; (\beta_p + \beta_{k0}) - \nu \; \frac{\bar{\ell}^4}{4} \; (\theta_0 + \phi_{k0}) - \nu \frac{\bar{\ell}^3}{3} \; (-2\lambda + \bar{e}\theta_0) \} \; \frac{\Omega_1}{\Omega_i}$$

$$L_{ns}(10,i) = -\frac{1}{2} \; \nu \; \bar{b} \; \frac{\bar{\ell}^3}{3} \; \sin\theta_0 \; 2 \; n \; \frac{\Omega_1}{\Omega_i}$$

$$L_{ns}(11,i) = -\frac{1}{2} \; \nu \; \bar{b} \; \frac{\bar{\ell}^3}{3} \; \sin\theta_0 \; \frac{\Omega_1}{\Omega_i}$$

$$L_{ns}(12,i) = -\frac{\bar{\ell}^3}{3} \; \left(\frac{\Omega_1}{\Omega_i} \right)^2$$

$$L_{ns}(13,i) = \frac{1}{2} \; \nu \; \bar{b} \; \frac{\bar{\ell}^3}{3} \; \sin\theta_0 \; \left(\frac{\Omega_1}{\Omega_i} \right)^2$$

$$L_{ns}(14,i) = \{ \; \delta_n \; \frac{\bar{\ell}^3}{3} \; (\beta_p + \beta_{k0}) + \delta_n \; \frac{\bar{\ell}^2}{2} \; \bar{h}_2 \; \} \; \left(\frac{\Omega_1}{\Omega_i} \right)^2$$

$$L_{ns}(15,i) = -\delta_n \; \frac{\bar{\ell}^2}{2} \; \zeta_{k0} \; \bar{h}_2 \; \left(\frac{\Omega_1}{\Omega_i} \right)^2$$

$$L_{ns}(16,i) = \{ \; -\delta_n \; \nu \; \frac{\bar{\ell}^4}{4} \; (\theta_0 + \phi_{k0}) + \delta_n \; \frac{\bar{\ell}^3}{3} \; 2 \; \lambda\nu \} \; \frac{\Omega_1}{\Omega_i}$$

$$L_{ns}(17,i) = \delta_n \; \frac{\bar{\ell}^2}{2} \; \left(\frac{\Omega_1}{\Omega_i} \right)^2$$

$$L_{ns}(18,i) = \delta_n \; \frac{\bar{\ell}^2}{2} \; \zeta_{k0} \; \left(\frac{\Omega_1}{\Omega_i} \right)^2$$

$$L_{ns}(19,i) = \delta_n \; \frac{\bar{\ell}^2}{2} \; \zeta_{k0} \; \eta_1 \; (\ell_{Fi}) \; \left(\frac{\Omega_1}{\Omega_i} \right)^2$$

$$L_{ns}(20,i) = -\delta_n \; \frac{\bar{\ell}^2}{2} \; \bar{h}_2 \; \eta_{2,x} \; (\ell_{Fi}) \; R \; \left(\frac{\Omega_1}{\Omega_i} \right)^2$$

$$L_{ns}(21,i) = -\delta_n \; \frac{\bar{\ell}^2}{2} \; \zeta_{k0} \; \bar{h}_2 \; \eta_3 \; (\ell_{Fi}) \; \left(\frac{\Omega_1}{\Omega_i} \right)^2$$

Collective Torsion Equation

$$\phi_M^i \; T_c(1,i) + \beta_M^i \; T_c(2,i) + \zeta_M^i \; T_c(3,i)$$

$$+ \dot{\phi}_M^i \; T_c(4,i) + \dot{\beta}_M^i \; T_c(5,i) + \dot{\zeta}_M^i \; T_c(6,i)$$

$$+ \ddot{\phi}_M^i \; T_c \; (7,i) + \ddot{\beta}_M^i \; T_c \; (8,i) + \ddot{\zeta}_M^i \; T_c \; (9,i)$$

$$+ \dot{\theta}_y \, T_c(10,i) + \frac{\dot{\xi}_2}{R} \, T_c(11,i) + \ddot{\theta}_y \, T_c(12,i) + \frac{\ddot{\xi}_2}{R} \, T_c(13,i) = 0 \qquad (3.15)$$

$$T_c(1,i) = T1$$

$$T_c(2,i) = T2$$

$$T_c(3,i) = T3$$

$$T_c(4,i) = T4 \; \frac{\Omega_1}{\Omega_i}$$

$$T_c(5,i) = T5 \; \frac{\Omega 1}{\Omega_i}$$

$$T_c(6,i) = T6 \; \frac{\Omega_1}{\Omega_i}$$

$$T_c(7,i) = T7 \; \left(\frac{\Omega_1}{\Omega_i} \right)^2$$

$$T_c(8,i) = T8 \; \left(\frac{\Omega_1}{\Omega_i} \right)^2$$

$$T_c(9,i) = T9 \; \left(\frac{\Omega_1}{\Omega_i} \right)^2$$

$$T_c(10,i) = - \bar{\ell}_{Fi} \; T18 \; \frac{\Omega_1}{\Omega_i}$$

$$T_c(11,i) = \eta_2 \; (\ell_{Fi}) \; T18 \; \frac{\Omega_1}{\Omega_i}$$

$$T_c(12,i) = - \bar{\ell}_{Fi} \; T21 \; \left(\frac{\Omega_1}{\Omega_i} \right)^2$$

$$T_c(13,i) = \eta_2 \; (\ell_{Fi}) \; T21 \; \left(\frac{\Omega_1}{\Omega_i} \right)^2$$

Alternating Torsion Equation (For even N only)

$$\phi^i_{-M} \; T_A(1,i) + \beta^i_{-M} \; T_A(2,i) + \zeta^i_{-M} \; T_A(3,i)$$

$$\dot{\phi}^i_{-M} \; T_A(4,i) + \dot{\beta}^i_{-M} \; T_A(5,i) + \dot{\zeta}^i_{-M} \; T_A(6,i)$$

$$\ddot{\phi}^{i}_{-M}\ T_A(7,i) + \ddot{\beta}^{i}_{-M}\ T_A(8,i) + \ddot{\zeta}^{i}_{-M}\ T_A(9,i) = 0 \qquad (3.16)$$

$$T_A(1,i) = T1$$

$$T_A(2,i) = T2$$

$$T_A(3,i) = T3$$

$$T_A(4,i) = T4\ \frac{\Omega_1}{\Omega_i}$$

$$T_A(5,i) = T5\ \frac{\Omega_1}{\Omega_i}$$

$$T_A(6,i) = T6\ \frac{\Omega_1}{\Omega_i}$$

$$T_A(7,i) = T7\ \left(\frac{\Omega_1}{\Omega_i}\right)^2$$

$$T_A(8,i) = T8\ \left(\frac{\Omega_1}{\Omega_i}\right)^2$$

$$T_A(9,i) = T9\ \left(\frac{\Omega_1}{\Omega_i}\right)^2$$

n-Cosine Torsion Equation

$$\phi^{i}_{nc}\ T_{nc}(1,i) + \phi^{i}_{ns}\ T_{nc}(2,i) + \beta^{i}_{nc}\ T_{nc}(3,i) + \beta^{i}_{ns}\ T_{nc}(4,i)$$

$$+ \zeta^{i}_{nc}\ T_{nc}(5,i) + \zeta^{i}_{ns}\ T_{nc}(6,i) + \dot{\phi}^{i}_{nc}\ T_{nc}(7,i) + \dot{\phi}^{i}_{ns}\ T_{nc}(8,i)$$

$$+ \dot{\beta}^{i}_{nc}\ T_{nc}(9,i) + \dot{\beta}^{i}_{ns}\ T_{nc}(10,i) + \dot{\zeta}^{i}_{nc}\ T_{nc}(11,i) + \dot{\zeta}^{i}_{ns}\ T_{nc}(12,i)$$

$$+ \ddot{\phi}^{i}_{nc}\ T_{nc}(13,i) + \ddot{\beta}^{i}_{nc}\ T_{nc}(14,i) + \ddot{\zeta}^{i}_{nc}\ T_{nc}(15,i) + \ddot{\theta}_x\ T_{nc}(16,i)$$

$$+ \ddot{\theta}_y\ T_{nc}(17,i) + \dot{\theta}_x\ T_{nc}(18,i) + \dot{\theta}_y\ T_{nc}(19,i) + \ddot{\bar{R}}_{xs}\ T_{nc}(20,i)$$

$$+ \ddot{\bar{R}}_{ys}\ T_{nc}(21,i) + \dot{\bar{R}}_{xs}\ T_{nc}(22,i) + \dot{\bar{R}}_{ys}\ T_{nc}(23,i)$$

$$+ \frac{\ddot{\xi}_1}{R} T_{nc}(24,i) + \frac{\ddot{\xi}_2}{R} T_{nc}(25,i) + \ddot{\xi}_3 T_{nc}(26,i)$$
$$+ \frac{\dot{\xi}_1}{R} T_{nc}(27,i) + \frac{\dot{\xi}_2}{R} T_{nc}(28,i) + \dot{\xi}_3 T_{nc}(29,i) = 0 \qquad (3.17)$$

$$T_{nc}(1,i) = T1 - n^2\, T7$$

$$T_{nc}(2,i) = n\, T4$$

$$T_{nc}(3,i) = T2 - n^2\, T8$$

$$T_{nc}(4,i) = n\, T5$$

$$T_{nc}(5,i) = T3 - n^2\, T9$$

$$T_{nc}(6,i) = n\, T6$$

$$T_{nc}(7,i) = T4\ \frac{\Omega_1}{\Omega_i}$$

$$T_{nc}(8,i) = 2\, n\, T7\ \frac{\Omega_1}{\Omega_i}$$

$$T_{nc}(9,i) = T5\ \frac{\Omega_1}{\Omega_i}$$

$$T_{nc}(10,i) = 2\, n\, T8\ \frac{\Omega_1}{\Omega_i}$$

$$T_{nc}(11,i) = T6\ \frac{\Omega_1}{\Omega_i}$$

$$T_{nc}(12,i) = 2\, n\, T9\ \frac{\Omega_1}{\Omega_i}$$

$$T_{nc}(13,i) = T7\ \left(\frac{\Omega_1}{\Omega_i}\right)^2$$

$$T_{nc}(14,i) = T8\ \left(\frac{\Omega_1}{\Omega_i}\right)^2$$

$$T_{nc}(15,i) = T9\ \left(\frac{\Omega_1}{\Omega_i}\right)^2$$

$$T_{nc}(16,i) = \{ \delta_n \; T13(1) - \bar{h}_2 \; \delta_n \; T20(1) \} \left(\frac{\Omega_1}{\Omega_i} \right)^2$$

$$T_{nc}(17,i) = \{ \delta_n \; T14(1) + \bar{h}_2 \; \delta_n \; T19(1) \} \left(\frac{\Omega_1}{\Omega_i} \right)^2$$

$$T_{nc}(18,i) = \{ \delta_n \; T10(1) - \bar{h}_2 \; \delta_n \; T17(1) \} \frac{\Omega_1}{\Omega_i}$$

$$T_{nc}(19,i) = \{ \delta_n \; T11(1) + \bar{h}_2 \; \delta_n \; T16(1) \} \frac{\Omega_1}{\Omega_i}$$

$$T_{nc}(20,i) = T19(1) \; \delta_n \left(\frac{\Omega_1}{\Omega_i} \right)^2$$

$$T_{nc}(21,i) = T20(1) \; \delta_n \left(\frac{\Omega_1}{\Omega_i} \right)^2$$

$$T_{nc}(22,i) = T16(1) \; \delta_n \left(\frac{\Omega_1}{\Omega_i} \right)$$

$$T_{nc}(23,i) = T17(1) \; \delta_n \left(\frac{\Omega_1}{\Omega_i} \right)$$

$$T_{nc}(24,i) = \eta_1(\ell_{Fi}) \; \delta_n \; T20(1) \left(\frac{\Omega_1}{\Omega_i} \right)^2$$

$$T_{nc}(25,i) = - h_2 \; \eta_{2,x} \; (\ell_{Fi}) \; T19(1) \; \delta_n \; R \left(\frac{\Omega_1}{\Omega_i} \right)^2$$

$$T_{nc}(26,i) = - \bar{h}_2 \; \eta_3 \; (\ell_{Fi}) \; T20(1) \; \delta_n \left(\frac{\Omega_1}{\Omega_i} \right)^2$$

$$T_{nc}(27,i) = \eta_1 \; (\ell_{Fi}) \; T17(1) \; \delta_n \frac{\Omega_i}{\Omega_i}$$

$$T_{nc}(28,i) = - \bar{h}_2 \; \eta_{2,x} \; (\ell_{Fi}) \; T16(1) \; \delta_n \; R \; \frac{\Omega_1}{\Omega_i}$$

$$T_{nc}(29,i) = - \bar{h}_2 \; \eta_3 \; (\ell_{Fi}) \; T17(1) \; \delta_n \; \frac{\Omega_1}{\Omega i}$$

n-Sine Torsion Equation

$$\phi^i_{ns} \; T_{ns}(1,i) + \phi^i_{nc} \; T_{ns}(2,i) + \beta^i_{ns} \; T_{ns}(3,i) + \beta^i_{nc} \; T_{ns}(4,i)$$

$$+ \zeta^i_{ns} \; T_{ns}(5,i) + \zeta^i_{nc} \; T_{ns}(6,i) + \dot{\phi}^i_{ns} \; T_{ns}(7,i) + \dot{\phi}^i_{nc} \; T_{ns}(8,i)$$

$$+ \dot{\beta}^{i}_{ns}\, T_{ns}(9,i) + \dot{\beta}^{i}_{nc}\, T_{ns}(10,i) + \dot{\zeta}^{i}_{ns}\, T_{ns}(11,i) + \dot{\zeta}^{i}_{nc}\, T_{ns}(12,i)$$

$$+ \ddot{\phi}^{i}_{ns}\, T_{ns}(13,i) + \ddot{\beta}^{i}_{ns}\, T_{ns}(14,i) + \ddot{\zeta}^{i}_{ns}\, T_{ns}(15,i) + \ddot{\theta}_{y}\, T_{ns}(16,i)$$

$$+ \ddot{\theta}_{x}\, T_{ns}(17,i) + \dot{\theta}_{y}\, T_{ns}(18,i) + \dot{\theta}_{x}\, T_{ns}(19,i) + \ddot{\bar{R}}_{ys}\, T_{ns}(20,i)$$

$$+ \ddot{\bar{R}}_{xs}\, T_{ns}(21,i) + \dot{\bar{R}}_{ys}\, T_{ns}(22,i) + \dot{\bar{R}}_{xs}\, T_{ns}(23,i)$$

$$+ \frac{\ddot{\xi}_1}{R}\, T_{ns}(24,i) + \frac{\ddot{\xi}_2}{R}\, T_{ns}(25,i) + \ddot{\xi}_3\, T_{ns}(26,i)$$

$$+ \frac{\dot{\xi}_1}{R}\, T_{ns}(27,i) + \frac{\dot{\xi}_2}{R}\, T_{ns}(28,i) + \dot{\xi}_3\, T_{ns}(29,i) = 0 \qquad (3.18)$$

$$T_{ns}(1,i) = T1 - n^2\, T7$$

$$T_{ns}(2,i) = -n\, T4$$

$$T_{ns}(3,i) = T2 - n^2\, T8$$

$$T_{ns}(4,i) = -\, n\, T5$$

$$T_{ns}(5,i) = T3 - n^2\, T9$$

$$T_{ns}(6,i) = -n\, T6$$

$$T_{ns}(7,i) = T4\ \frac{\Omega_1}{\Omega_i}$$

$$T_{ns}(8,i) = -2n\, T7\ \frac{\Omega_1}{\Omega_i}$$

$$T_{ns}(9,i) = T5\ \frac{\Omega_1}{\Omega_i}$$

$$T_{ns}(10,i) = -2n\, T8\ \frac{\Omega_1}{\Omega_i}$$

$$T_{ns}(11,i) = T6\ \frac{\Omega_1}{\Omega_i}$$

$$T_{ns}(12,i) = -\ 2\ n\ T9\ \frac{\Omega_1}{\Omega_i}$$

$$T_{ns}(13,i) = T7\ \left(\frac{\Omega_1}{\Omega_i}\right)^2$$

$$T_{ns}(14,i) = T8\ \left(\frac{\Omega_1}{\Omega_i}\right)^2$$

$$T_{ns}(15,i) = T9\ \left(\frac{\Omega_1}{\Omega_i}\right)^2$$

$$T_{ns}(16,i) = \{\delta_n\ T14(2) + \bar{h}_2\ \delta_n\ T19(2)\ \}\ \left(\frac{\Omega_1}{\Omega_i}\right)^2$$

$$T_{ns}(17,i) = \{\delta_n\ T13(2) - \bar{h}_2\ \delta_n\ T20(2)\}\ \left(\frac{\Omega_1}{\Omega_i}\right)^2$$

$$T_{ns}(18,i) = \{\delta_n\ T11(2) + \bar{h}_2\ \delta_n\ T16(2)\}\ \frac{\Omega_1}{\Omega_i}$$

$$T_{ns}(19,i) = \{\delta_n\ T10(2) - \bar{h}_2\ \delta_n\ T17(2)\}\ \frac{\Omega_1}{\Omega_i}$$

$$T_{ns}(20,i) = \delta_n\ T20(2)\ \left(\frac{\Omega_1}{\Omega_i}\right)^2$$

$$T_{ns}(21,i) = \delta_n\ T19(2)\ \left(\frac{\Omega_1}{\Omega_i}\right)^2$$

$$T_{ns}(22,i) = \delta_n\ T17(2)\ \frac{\Omega_1}{\Omega_i}$$

$$T_{ns}(23,i) = \delta_n\ T16(2)\ \frac{\Omega_1}{\Omega_i}$$

$$T_{ns}(24,i) = \eta_1(\ell_{Fi})\ T20(2)\ \delta_n\ \left(\frac{\Omega_1}{\Omega_i}\right)^2$$

$$T_{ns}(25,i) = -\ \bar{h}_2\ \eta_{2,x}(\ell_{Fi})\ T19(2)\ \delta_n\ R\ \left(\frac{\Omega_1}{\Omega_i}\right)^2$$

$$T_{ns}(26,i) = -\ \bar{h}_2\ \eta_3\ (\ell_{Fi})\ T20(2)\ \delta_n\ \left(\frac{\Omega_1}{\Omega_i}\right)^2$$

$$T_{ns}(27,i) = \eta_1\ (\ell_{Fi})\ T17(2)\ \delta_n\ \left(\frac{\Omega_1}{\Omega_i}\right)$$

$$T_{ns}(28,i) = -\ \bar{h}_2\ \eta_{2,x}(\ell_{Fi})\ T16(2)\ \delta_n\ \frac{\Omega_1}{\Omega_i}$$

$$T_{ns}(29,i) = - \bar{h}_2 \, \eta_3 \, (\ell_{Fi}) \; T17(2) \quad \delta_n \quad \frac{\Omega_1}{\Omega_i}$$

The various coefficients for the torsional equations are:

$$T1 = - \bar{\omega}_{T1}^2 - \bar{\omega}_{T2}^2 - \frac{\bar{\ell}^2}{2} \zeta_{k0} \bar{X}_I \cos\theta_0 + \frac{\bar{\ell}^2}{2} \beta_p \bar{X}_I \sin\theta_0$$
$$+ (1-\bar{e})\left[\frac{I_{MB3}}{mR^2} - \frac{I_{MB2}}{mR^2} \right] (\sin^2\theta_0 - \cos^2\theta_0)$$
$$+ \nu\zeta_{k0} \left(\frac{\bar{\ell}^4}{4} + \frac{\bar{\ell}^3}{3} \, 2\,\bar{e} \right) + \nu\beta_{k0} (1 + \zeta_{k0}^2)\left[\frac{\bar{\ell}^4}{4} \zeta_{k0} (\beta_{k0}+\beta_p) \right.$$
$$\left. + \frac{\bar{\ell}^3}{3} \lambda + \frac{\bar{\ell}^2}{2} \lambda \, \bar{e} \right]$$
$$+ \nu\bar{X}_A \left(\frac{\bar{\ell}^3}{3} + \frac{\bar{\ell}^2}{2} \, 2\,\bar{e} \right)$$

$$T2 = \bar{\omega}_{T1}^2 \zeta_{k0} - \frac{\bar{\ell}^3}{3} \zeta_{k0} + \zeta_{k0}(1-\bar{e})\left[\frac{I_{MB3}}{mR^2} \cos^2\theta_0 + \frac{I_{MB2}}{mR^2} \sin^2\theta_0 \right] - \nu \frac{\bar{\ell}^4}{4} \zeta_{k0}^2$$
$$+ \nu\beta_{k0} (1 + \zeta_{k0}^2)\left[\frac{\bar{\ell}^4}{4} \zeta_{k0} (\theta_0 + \phi_{k0}) - 2 \frac{\bar{\ell}^3}{3} \lambda\zeta_{k0} \right] - \frac{\bar{\ell}^2}{2} \bar{X}_I \cos\theta_0$$
$$- \nu(1 + \zeta_{k0}^2)\left\{ - \frac{c_{d0}}{a} \left(\frac{\bar{\ell}^4}{4} + \frac{\bar{\ell}^3}{3} 2\,\bar{e} \right) - \frac{\bar{\ell}^4}{4} \zeta_{k0} (\beta_{k0} + \beta_p)(\theta_0 + \phi_{l:0}) \right.$$
$$- \frac{\bar{\ell}^3}{3} \lambda (\theta_0 + \phi_{k0} - 2 \zeta_{k0}\beta_p - 2 \zeta_{k0}\beta_{k0})$$
$$\left. + \frac{\bar{\ell}^2}{2} \lambda \left(\lambda - \bar{e} (\theta_0 + \phi_{k0}) \right) \right\} - \nu \bar{X}_A \frac{\bar{\ell}^3}{3} \zeta_{k0}$$

$$T3 = \bar{\omega}_{T1}^2 \beta_{k0} - \beta_p\left(\frac{\bar{\ell}^3}{3} + \frac{\bar{\ell}^2}{2} \bar{e} \right) - \beta_{k0} \frac{\bar{\ell}^3}{3} - \frac{\bar{\ell}^2}{2} \phi_{k0} \bar{X}_I \cos\theta_0 - \frac{\bar{\ell}^2}{2} \bar{X}_I \sin\theta_0$$
$$+ (1-\bar{e})(\beta_p + \beta_{k0}) \left[\frac{I_{MB3}}{mR^2} \cos^2\theta_0 + \frac{I_{MB2}}{mR^2} \sin^2\theta_0 \right] - \nu \frac{\bar{\ell}^4}{4} \zeta_{k0}(\beta_p + \beta_{k0})$$
$$+ \nu\left[\frac{\bar{\ell}^4}{4} (\theta_0 + \phi_{k0} - \zeta_{k0}\beta_p - \zeta_{k0}\beta_{k0}) + \frac{\bar{\ell}^3}{3}(-\lambda+2\bar{e}\theta_0+2\bar{e}\phi_{k0}) - \frac{\bar{\ell}^2}{2} \bar{e} \, \lambda \right]$$
$$+ \nu\beta_{k0} (1 + \zeta_{k0}^2) \left[\frac{\bar{\ell}^4}{4} (\beta_{k0} + \beta_p)(\theta_0 + \phi_{k0}) - 2 \frac{\bar{\ell}^3}{3} \lambda (\beta_p + \beta_{k0}) \right]$$
$$- \nu 2\beta_{k0}\zeta_{k0} \left\{ - \frac{c_{d0}}{a} \left(\frac{\bar{\ell}^4}{4} + \frac{\bar{\ell}^3}{3} \, 2\,\bar{e} \right) - \frac{\bar{\ell}^4}{4} \zeta_{k0} (\beta_{k0} + \beta_p)(\theta_0 + \phi_{k0}) \right.$$
$$\left. - \frac{\bar{\ell}^3}{3} \lambda (\theta_0 + \phi_{k0} - 2 \zeta_{k0}\beta_p - 2\zeta_{k0}\beta_{k0}) \right.$$

$$+ \frac{\bar{\ell}^2}{2} \lambda \left(\lambda - \bar{e} \left(\theta_0 + \phi_{k0}\right)\right) \} - \nu \bar{X}_A \frac{\bar{\ell}^3}{3} \left(\beta_p + \beta_{k0}\right)$$

$$T4 = 2 \zeta_{k0} (1-\bar{e}) \left[\frac{I_{MB3}}{mR^2} \sin^2\theta_0 + \frac{I_{MB2}}{mR^2} \cos^2\theta_0 \right] + \nu \frac{\bar{\ell}^3}{3} \zeta_{k0} \bar{b}$$

$$+ \frac{1}{2} \nu \bar{b} \zeta_{k0} \frac{\bar{\ell}^3}{3} \cos\theta_0 + \nu \bar{X}_A \frac{\bar{\ell}^2}{2} \bar{b}$$

$$+ \nu \beta_{k0} \left(1 + \zeta_{k0}^2\right) \left[\frac{\bar{\ell}^2}{2} \lambda \bar{b} + \frac{1}{2} \bar{b} \frac{\bar{\ell}^3}{3} \left(\sin\theta_0 + \phi_{k0} \cos\theta_0\right) \right]$$

$$+ \frac{1}{2} \nu \bar{b} \left(\bar{X}_A - \frac{\bar{b}}{2}\right) \frac{\bar{\ell}^2}{2} - \frac{1}{2} \nu \bar{b} \frac{\bar{b}}{2} \left(\frac{\bar{\ell}^2}{2} + \bar{\ell} \bar{e} \right) - \bar{g}_{ST}$$

$$T5 = -2 \frac{\bar{\ell}^3}{3} \beta_{k0} \left(\beta_p + \beta_{k0}\right) - \bar{\ell}^2 \bar{X}_I \sin\theta_0 \left(\beta_p + \beta_{k0}\right)$$

$$- 2 (1-\bar{e}) \left[\frac{I_{MB3}}{mR^2} \sin^2\theta_0 + \frac{I_{MB2}}{mR^2} \cos^2\theta_0 \right] - \nu \zeta_{k0} \left(\frac{\bar{\ell}^4}{4} + \frac{\bar{\ell}^3}{3} \bar{e} \right)$$

$$+ \nu \beta_{k0} \left(1 + \zeta_{k0}^2\right) \left[\frac{\bar{\ell}^4}{4} \left(\theta_0 + \phi_{k0} - \zeta_{k0} \beta_p - \zeta_{k0} \beta_{k0}\right) - \frac{\bar{\ell}^4}{4} \zeta_{k0} \left(\beta_p + \beta_{k0}\right) \right.$$

$$\left. + \frac{\bar{\ell}^3}{3} \left(-2 \lambda + \bar{e} \left(\theta_0 + \phi_{k0}\right)\right) \right] - \nu \bar{X}_A \left(\frac{\bar{\ell}^3}{3} + \frac{\bar{\ell}^2}{2} \bar{e} \right)$$

$$T6 = -2 \frac{\bar{\ell}^3}{3} \zeta_{k0} \left(\beta_p + \beta_{k0}\right) - \bar{\ell}^2 \bar{X}_I \sin\theta_0 \zeta_{k0} - \beta_p \bar{\ell}^2 \bar{X}_I \cos\theta_0$$

$$+ 2 \phi_{k0} (1-\bar{e}) \left[\frac{I_{MB3}}{mR^2} \sin^2\theta_0 + \frac{I_{MB2}}{mR^2} \cos^2\theta_0 \right] + \nu \frac{\bar{\ell}^4}{4} 2 \zeta_{k0} \left(\theta_0 + \phi_{k0}\right)$$

$$- 2 \phi_{k0} (1-\bar{e}) \left[\frac{I_{MB3}}{mR^2} \cos^2\theta_0 + \frac{I_{MB2}}{mR^2} \sin^2\theta_0 \right] - \nu \frac{\bar{\ell}^3}{3} \zeta_{k0} \lambda$$

$$- 2 (1-\bar{e}) \left(\frac{I_{MB3}}{mR^2} - \frac{I_{MB2}}{mR^2} \right) \cos\theta_0 \sin\theta_0$$

$$+ \nu \beta_{k0} \left(1 + \zeta_{k0}^2\right) \left[2 \frac{c_{d0}}{a} \frac{\bar{\ell}^4}{4} + \frac{\bar{\ell}^3}{3} \left(\theta_0 + \phi_{k0}\right) \lambda \right]$$

$$+ \nu \bar{X}_A \left[2 \frac{\bar{\ell}^3}{3} \left(\theta_0 + \phi_{k0}\right) - \frac{\bar{\ell}^2}{2} \lambda \right]$$

$$T7 = - (1-\bar{e}) \left[\frac{I_{MB3}}{mR^2} + \frac{I_{MB2}}{mR^2} \right] - \frac{1}{2} \nu \bar{b} \frac{\bar{b}^2}{2} \bar{\ell}$$

$$T8 = - \zeta_{k0} \frac{\bar{\ell}^3}{3} - \frac{\bar{\ell}^2}{2} \bar{X}_I \cos\theta_0 + \frac{\bar{\ell}^2}{2} \phi_{k0} \bar{X}_I \sin\theta_0$$

$$+ (1-\bar{e})\ \zeta_{k0}\ \left[\ \frac{I_{MB3}}{mR^2}\cos^2\theta_0 + \frac{I_{MB2}}{mR^2}\sin^2\theta_o\ \right] - \frac{1}{2}\nu\ \bar{b}\ \zeta_{k0}\ \frac{\bar{\ell}^3}{3}\ \cos\theta_0$$

$$- \frac{1}{2}\nu\ \bar{b}\ \beta_{k0}\ (1 + \zeta_{k0}^2)\ \frac{\bar{\ell}^3}{3}\ (\sin\theta_0 + \phi_{k0}\cos\theta_0) - \frac{1}{2}\nu\ \bar{b}\ (\bar{X}_A - \frac{\bar{b}}{2})\ \frac{\bar{\ell}^2}{2}$$

$$T9 = \frac{\bar{\ell}^3}{3}\ \beta_{k0} + \frac{\bar{\ell}^2}{2}\ \phi_{k0}\ \bar{X}_I\ \cos\theta_0 + \frac{\bar{\ell}^2}{2}\ \bar{X}_I\ \sin\theta_0$$

$$+ (1-\bar{e})\ \beta_{k0}\ \left[\ \frac{I_{MB3}}{mR^2}\cos^2\theta_0 + \frac{I_{MB2}}{mR^2}\sin^2\theta_0\ \right] + \frac{1}{2}\nu\ \bar{b}\ \beta_{k0}(1 + \zeta_{k0}^2)\ \frac{\bar{\ell}^3}{3}\ \theta_0\sin\theta_0$$

$$T10(1) = -\ 2\ \frac{\bar{\ell}^3}{3}\ \zeta_{k0} - 2\bar{e}\ \frac{\bar{\ell}^2}{2}\ \zeta_{k0} - 2\ \frac{\bar{\ell}^2}{2}\ \bar{X}_I\ \cos\theta_0 - 2\ \bar{\ell}\ \bar{e}\ \bar{X}_I\ \cos\theta_0$$

$$+ \frac{\bar{\ell}^2}{2}\ 2\phi_{k0}\ \bar{X}_I\ \sin\theta_0 + 2\zeta_{k0}\ (1-\bar{e})\left[\ \frac{I_{MB3}}{mR^2}\cos^2\theta_0 + \frac{I_{MB2}}{mR^2}\sin^2\theta_0\ \right]$$

$$+ \nu\beta_{k0}\ (1 + \zeta_{k0}^2)\ \left[\ \frac{\bar{\ell}^4}{4}\ \zeta_{k0}\theta_0 - \frac{1}{2}\ \bar{b}\ \frac{\bar{\ell}^3}{3}\ \sin\theta_0\ \right]$$

$$T10(2) = 2\ \frac{\bar{\ell}^3}{3}\ \zeta_{k0}^2 + 2\ \frac{\bar{\ell}^2}{2}\ \zeta_{k0}\ \bar{X}_I\ \cos\theta_0$$

$$+ 2\ (1-\bar{e})\ \left[\ \frac{I_{MB3}}{mR^2}\cos^2\theta_0 + \frac{I_{MB2}}{mR^2}\sin^2\theta_0\ \right] - \nu\zeta_{k0}\ \frac{\bar{\ell}^4}{4}\ - \nu\ \bar{X}_A\ \frac{\bar{\ell}^3}{3}$$

$$+ \nu\beta_{k0}\ (1 + \zeta_{k0}^2)\ \left[\ \frac{\bar{\ell}^4}{4}\ (\theta_0 + \phi_{k0}) - 2\ \frac{\bar{\ell}^3}{3}\ (\lambda - \bar{e}\theta_0)\ \right]$$

$$T11(1) = -\ 2\ \frac{\bar{\ell}^3}{3}\ \zeta_{k0}^2\ - 2\ \frac{\bar{\ell}^2}{2}\ \zeta_{k0}\ \bar{X}_I\ \cos\theta_0$$

$$- 2\ (1-\bar{e})\ \left[\ \frac{I_{MB3}}{mR^2}\cos^2\theta_0 + \frac{I_{MB2}}{mR^2}\sin^2\theta_0\ \right] + \nu\zeta_{k0}\ \frac{\bar{\ell}^4}{4} + \nu\ \bar{X}_A\ \frac{\bar{\ell}^3}{3}$$

$$- \nu\beta_{k0}\ (1 + \zeta_{k0}^2)\ \left[\ \frac{\bar{\ell}^4}{4}\ (\theta_0 + \phi_{k0}) - 2\ \frac{\bar{\ell}^3}{3}\ (\lambda - \bar{e}\theta_0)\ \right]$$

$$T11(2) = -\ 2\ \frac{\bar{\ell}^3}{3}\ \zeta_{k0} - 2\ \bar{e}\ \frac{\bar{\ell}^2}{2}\ \zeta_{k0} - 2\ \frac{\bar{\ell}^2}{2}\ \bar{X}_I\ \cos\theta_0 - 2\ \bar{\ell}\ \bar{e}\ \bar{X}_I\ \cos\theta_0$$

$$+ \frac{\bar{\ell}^2}{2}\ 2\ \ \phi_{k0}\ \bar{X}_I\ \sin\theta_0 + 2\ \zeta_{k0}\ (1-\bar{e})\ \left[\ \frac{I_{MB3}}{mR^2}\cos^2\theta_0 + \frac{I_{MB2}}{mR^2}\sin^2\theta_0\ \right]$$

$$+ \nu\beta_{k0}\ (1 + \zeta_{k0}^2)\ \left[\ \frac{\bar{\ell}^4}{4}\ \ \theta_0\ \zeta_{k0} - \frac{1}{2}\ \bar{b}\ \ \frac{\bar{\ell}^3}{3}\ \ \sin\theta_0\ \right]$$

$$T13(1) = -\ \frac{\bar{\ell}^3}{3}\ \zeta_{k0}^2 - \beta_{k0}(\beta_p + \beta_{k0})\ \frac{\bar{\ell}^3}{3} - \frac{\bar{\ell}^2}{2}\ \zeta_{k0}\ \bar{X}_I\ \cos\theta_0 - \frac{\bar{\ell}^2}{2}\ (\beta_p + \beta_{k0})\bar{X}_I\sin\theta_0$$

$$- (1 - \bar{e}) \left[\frac{I_{MB3}}{mR^2} + \frac{I_{MB2}}{mR^2} \right]$$

$$T13(2) = - \frac{\bar{\ell}^3}{3} \zeta_{k0} - \frac{\bar{\ell}^2}{2} \bar{e} \zeta_{k0} - \frac{\bar{\ell}^2}{2} \bar{X}_I \cos\theta_0 - \bar{\ell} \bar{e} \bar{X}_I \cos\theta_0$$

$$+ \frac{\bar{\ell}^2}{2} \phi_{k0} \bar{X}_I \sin\theta_0 + (1 - \bar{e}) \zeta_{k0} \left[\frac{I_{MB3}}{mR^2} \cos^2\theta_0 + \frac{I_{MB3}}{mR^2} \sin^2\theta_0 \right]$$

$$- \frac{1}{2} \nu \bar{b} \beta_{k0} (1 + \zeta_{k0}^2) \frac{\bar{\ell}^3}{3} \sin\theta_0$$

$$T14(1) = \frac{\bar{\ell}^3}{3} \zeta_{k0} + \frac{\bar{\ell}^2}{2} \bar{e} \zeta_{k0} + \frac{\bar{\ell}^2}{2} \bar{X}_I \cos\theta_0 + \bar{\ell} \bar{e} \bar{X}_I \cos\theta_0$$

$$- \frac{\bar{\ell}^2}{2} \phi_{k0} \bar{X}_I \sin\theta_0 - (1-\bar{e}) \zeta_{k0} \left[\frac{I_{MB3}}{mR^2} \cos^2\theta_0 + \frac{I_{MB2}}{mR^2} \sin^2\theta_0 \right]$$

$$+ \frac{1}{2} \nu \bar{b} \beta_{k0} (1 + \zeta_{k0}^2) \frac{\bar{\ell}^3}{3} \sin\theta_0$$

$$T14(2) = - \frac{\bar{\ell}^3}{3} \zeta_{k0}^2 - \beta_{k0} (\beta_p + \beta_{k0}) \frac{\bar{\ell}^3}{3} - \frac{\bar{\ell}^2}{2} \zeta_{k0} \bar{X}_I \cos\theta_0 - \frac{\bar{\ell}^2}{2} \bar{X}_I (\beta_p + \beta_{k0}) \sin\theta_0$$

$$- (1-\bar{e}) \left[\frac{I_{MB3}}{mR^2} + \frac{I_{MB2}}{mR^2} \right]$$

$$T16(1) = - \nu \beta_{k0} (1 + \zeta_{k0}^2) \frac{\bar{\ell}^3}{3} \theta_0 (\beta_p + \beta_{k0})$$

$$T16(2) = - \nu \zeta_{k0} \frac{\bar{\ell}^3}{3} 2 \theta_0 - \nu \beta_{k0} (1 + \zeta_{k0}^2) \left[2 \frac{c_{d0}}{a} \frac{\bar{\ell}^3}{3} + \frac{\bar{\ell}^2}{2} \lambda \theta_0 \right] - \nu \bar{X}_A \frac{\bar{\ell}^2}{2} 2\theta_0$$

$$T17(1) = \nu \frac{\bar{\ell}^3}{3} \zeta_{k0} 2\theta_0 + \nu \beta_{k0} (1 + \zeta_{k0}^2) \left[2 \frac{c_{d0}}{a} \frac{\bar{\ell}^3}{3} + \frac{\bar{\ell}^2}{2} \lambda \theta_0 \right] + \nu \bar{X}_A \frac{\bar{\ell}^2}{2} 2\theta_0$$

$$T17(2) = - \nu \beta_{k0} (1 + \zeta_{k0}^2) \frac{\bar{\ell}^3}{3} \theta_0 (\beta_p + \beta_{k0})$$

$$T18 = - \nu \frac{\bar{\ell}^3}{3} \zeta_{k0} + \nu \beta_{k0} (1 + \zeta_{k0}^2) \left[\frac{\bar{\ell}^3}{3} (\theta_0 + \phi_{k0}) + \frac{\bar{\ell}^2}{2} (-2 \lambda + \bar{e} \theta_0) \right] - \nu \bar{X}_A \frac{\bar{\ell}^2}{2}$$

$$T19(1) = \frac{\bar{\ell}^2}{2} \beta_p \zeta_{k0} + \bar{\ell} \beta_p \bar{X}_I \cos\theta_0$$

$$T19(2) = - \frac{\bar{\ell}^2}{2} \beta_{k0} - \phi_{k0} \bar{\ell} \bar{X}_I \cos\theta_0 - \bar{\ell} \bar{X}_I \sin\theta_0$$

$$T20(1) = \beta_{k0} \frac{\bar{\ell}^2}{2} + \phi_{k0} \bar{\ell} \bar{X}_I \cos\theta_0 + \bar{\ell} \bar{X}_I \sin\theta_0$$

$$T20(2) = \frac{\bar{\ell}^2}{2} \beta_p \zeta_{k0} + \bar{\ell} \beta_p \bar{X}_I \cos\theta_0$$

$$T21 = -\zeta_{k0}\frac{\bar{\ell}^2}{2} - \bar{\ell}\,\bar{X}_I\cos\theta_0 + \bar{\ell}\,\phi_{k0}\,\bar{X}_I\sin\theta_0 - \frac{1}{2}\nu\,\bar{b}\,\beta_{k0}\,(1+\zeta_{k0}^2)\,\frac{\bar{\ell}^2}{2}\sin\theta_0$$

Rigid Body Equations

X-Translation

$$\frac{N}{2}\sum_{i=1}^{2}\{m\Omega_i^2 R^2 [\beta_{1c}^i < -\nu\frac{\bar{\ell}^3}{3}\theta_0 + \nu\frac{\bar{\ell}^2}{2}\lambda + \frac{\bar{\ell}^2}{2}\beta_p + \bar{\ell}^2\beta_{k0} - \nu\frac{\bar{\ell}^2}{2}(-2\lambda + \bar{e}\theta_0) - \nu\frac{\bar{\ell}^3}{3}(\theta_0 + \phi_{k0}) >$$

$$+ \beta_{1s}^i < \nu\frac{\bar{\ell}^3}{3}\beta_p + \nu\frac{\bar{\ell}^3}{3}\beta_{k0} + \nu\frac{\bar{\ell}^3}{3}\theta_0\zeta_{k0} + \frac{1}{2}\nu\,\bar{b}\,\frac{\bar{\ell}^2}{2}\sin\theta_0 >$$

$$+ \zeta_{1c}^i < \bar{\ell}^2\zeta_{k0} - 2\nu\frac{c_{d0}}{a}\frac{\bar{\ell}^3}{3} - \nu\frac{\bar{\ell}^2}{2}\lambda\theta_0 >$$

$$+ \zeta_{1s}^i < -\nu\frac{\bar{\ell}^3}{3}\beta_p\theta_0 + \nu\frac{\bar{\ell}^3}{3}\beta_{k0}\theta_0 >$$

$$+ \phi_{1c}^i < -\nu\beta_p\frac{\bar{\ell}^3}{3} - \frac{1}{2}\nu\,\bar{b}\,\frac{\bar{\ell}^2}{2}\sin\theta_0 >$$

$$+ \phi_{1s}^i < \nu\frac{\bar{\ell}^2}{2}\lambda >$$

$$+ \dot{\beta}_{1c}^i < \nu\beta_p\frac{\bar{\ell}^3}{3} + \nu\frac{\bar{\ell}^3}{3}\beta_{k0} + 2\,\frac{1}{2}\nu\,\bar{b}\,\frac{\bar{\ell}^2}{2}\sin\theta_0 > \frac{\Omega_1}{\Omega_i}$$

$$+ \dot{\beta}_{1s}^i < -\bar{\ell}^2\beta_{k0} + \nu\frac{\bar{\ell}^3}{3}(\theta_0 + \phi_{k0}) + \nu\frac{\bar{\ell}^2}{2}(-2\lambda + \bar{e}\theta_0) > \frac{\Omega_1}{\Omega_i}$$

$$+ \dot{\zeta}_{1c}^i < -2\nu\beta_p\frac{\bar{\ell}^3}{3}\theta_0 > \frac{\Omega_1}{\Omega_i}$$

$$+ \dot{\zeta}_{1s}^i < -\bar{\ell}^2\zeta_{k0} + 2\nu\frac{c_{d0}}{a}\frac{\bar{\ell}^3}{3} + \nu\frac{\bar{\ell}^2}{2}\lambda\theta_0 > \frac{\Omega_1}{\Omega_i}$$

$$+ \dot{\phi}_{1s}^i < \frac{1}{2}\nu\,\bar{b}\,\frac{\bar{\ell}^2}{2}\sin\theta_0 > \frac{\Omega_1}{\Omega_i}$$

$$+ \ddot{\beta}_{1c}^i < \frac{\bar{\ell}^2}{2}\beta_p > \left(\frac{\Omega_1}{\Omega_i}\right)^2$$

$$+ \ddot{\beta}_{1s}^i < -\frac{1}{2}\nu\,\bar{b}\,\frac{\bar{\ell}^2}{2}\sin\theta_0 > \left(\frac{\Omega_1}{\Omega_i}\right)^2$$

$$+ \ddot{\zeta}_{1s}^i < \frac{\bar{\ell}^2}{2} > \left(\frac{\Omega_1}{\Omega_i}\right)^2$$

$$+ \ddot{\theta}_y < -\frac{\bar{\ell}^2}{2} (2\beta_p + \beta_{k0}) - 2\,\bar{\ell}\,\bar{h}_2 > \left(\frac{\Omega_1}{\Omega_i}\right)^2$$

$$+ \dot{\theta}_x < 2\beta_p \frac{\bar{\ell}^2}{2} - 2\nu \frac{\bar{\ell}^2}{2} \lambda + \nu \frac{\bar{\ell}^3}{3} (\theta_0 + \phi_{k0}) > \frac{\Omega_1}{\Omega_i}$$

$$+ \dot{\theta}_y < -\nu\beta_p \frac{\bar{\ell}^3}{3} - \nu \frac{\bar{\ell}^3}{3} \beta_{k0} > \frac{\Omega_1}{\Omega_i}$$

$$+ \theta_y < 2\nu \frac{\bar{\ell}^3}{3} (\theta_0 + \phi_{k0}) - 2\nu \frac{\bar{\ell}^2}{2} \lambda >$$

$$+ \frac{\ddot{\xi}_2}{R} < 2\,\bar{h}_2\, \eta_{2,x}(\ell_{Fi})\, R\, \bar{\ell} > \left(\frac{\Omega_1}{\Omega_i}\right)^2$$

$$+ \ddot{\bar{R}}_{xs} < -2\,\bar{\ell} > \left(\frac{\Omega_1}{\Omega_i}\right)^2] \}_i$$

$$- \frac{W}{g}\, \Omega_1^2\, R\, \ddot{\bar{R}}_{xs} = 0 \qquad (3.19)$$

where $W = W_{F1} + W_{F2} + W_{UN} + W_{EN} + W_S$

Y-Translation

$$\frac{N}{2} \sum_{i=1}^{2} \{ m\Omega_i^2 R^2 [\beta_{1c}^i < -\nu\frac{\bar{\ell}^3}{3}\beta_p - \nu\frac{\bar{\ell}^3}{3}\beta_{k0} - \nu\frac{\bar{\ell}^3}{3}\theta_0\zeta_{k0} - \frac{1}{2}\nu\,\bar{b}\,\frac{\bar{\ell}^2}{2}\sin\theta_0 >$$

$$+ \beta_{1s}^i < -\nu\frac{\bar{\ell}^3}{3}\theta_0 + \nu\frac{\bar{\ell}^2}{2}\lambda + \frac{\bar{\ell}^2}{2}\beta_p + \bar{\ell}^2\beta_{k0} - \nu\frac{\bar{\ell}^3}{3}(\theta_0 + \phi_{k0}) - \nu\frac{\bar{\ell}^2}{2}(-2\lambda + \bar{e}\theta_0) >$$

$$+ \zeta_{1s}^i < \bar{\ell}^2\zeta_{k0} - \nu\frac{\bar{\ell}^2}{2}\lambda\theta_0 - 2\nu\frac{c_{d0}}{a}\frac{\bar{\ell}^3}{3} > + \zeta_{1c}^i < -\nu\frac{\bar{\ell}^3}{3}\beta_{k0}\theta_0 + \nu\frac{\bar{\ell}^3}{3}\beta_p\theta_0 >$$

$$+ \phi_{1c}^i < -\nu\frac{\bar{\ell}^2}{2}\lambda >$$

$$+ \phi_{1s}^i < -\nu\frac{\bar{\ell}^3}{3}\beta_p - \frac{1}{2}\nu\,\bar{b}\,\frac{\bar{\ell}^2}{2}\sin\theta_0 >$$

$$+ \dot{\beta}_{1c}^i < \bar{\ell}^2\beta_{k0} - \nu\frac{\bar{\ell}^3}{3}(\theta_0 + \phi_{k0}) - \nu\frac{\bar{\ell}^2}{2}(-2\lambda + \bar{e}\theta_0) > \frac{\Omega_1}{\Omega_i}$$

$$+ \dot{\beta}_{1s}^i < \nu\frac{\bar{\ell}^3}{3}\beta_p + \nu\frac{\bar{\ell}^3}{3}\beta_{k0} + 2\frac{1}{2}\nu\,\bar{b}\,\frac{\bar{\ell}^2}{2}\sin\theta_0 > \frac{\Omega_1}{\Omega_i}$$

$$+ \dot{\zeta}_{1c}^i < \bar{\ell}^2\zeta_{k0} - 2\nu\frac{c_{d0}}{a}\frac{\bar{\ell}^3}{3} - \nu\frac{\bar{\ell}^2}{2}\lambda\theta_0 > \frac{\Omega_1}{\Omega_i}$$

$$+ \dot{\zeta}_{1s}^i < -2\nu\frac{\bar{\ell}^3}{3}\beta_p\theta_0 > \frac{\Omega_1}{\Omega_i}$$

$$
\begin{aligned}
&+ \dot{\phi}^{i}_{ic} \quad < -\frac{1}{2}\nu\,\bar{b}\,\frac{\bar{\ell}^2}{2}\,\sin\theta_0 > \frac{\Omega_1}{\Omega_i} \\
&+ \ddot{\beta}^{i}_{1c} \quad < \frac{1}{2}\nu\,\bar{b}\,\frac{\bar{\ell}^2}{2}\,\sin\theta_0 > \left(\frac{\Omega_1}{\Omega_i}\right)^2 \\
&+ \ddot{\beta}^{i}_{1s} \quad < \frac{\bar{\ell}^2}{2}\,\beta_p > \left(\frac{\Omega_1}{\Omega_i}\right)^2 \\
&+ \ddot{\zeta}^{i}_{1c} \quad < -\frac{\bar{\ell}^2}{2} > \left(\frac{\Omega_1}{\Omega_i}\right)^2 \\
&+ \ddot{\theta}_x \quad < \frac{\bar{\ell}^2}{2}(2\beta_p + \beta_{k0}) + 2\,\bar{h}_2\,\bar{\ell} > \left(\frac{\Omega_1}{\Omega_i}\right)^2 \\
&+ \dot{\theta}_x \quad < \beta_p\,\nu\,\frac{\bar{\ell}^3}{3} + \nu\,\frac{\bar{\ell}^3}{3}\,\beta_{k0} > \frac{\Omega_1}{\Omega_i} \\
&+ \dot{\theta}_y \quad < 2\,\beta_p\,\frac{\bar{\ell}^2}{2} + \nu\,\frac{\bar{\ell}^3}{3}\,(\theta_0 + \phi_{k0}) - 2\,\nu\,\frac{\bar{\ell}^2}{2}\,\lambda > \frac{\Omega_1}{\Omega_i} \\
&+ \theta_x \quad < -2\,\nu\,\frac{\bar{\ell}^3}{3}\,(\theta_0 + \phi_{k0}) + 2\,\nu\,\frac{\bar{\ell}^2}{2}\,\lambda > \\
&+ \frac{\ddot{\xi}_1}{R} \quad < -2\,\eta_1\,(\ell_{Fi})\,\bar{\ell} > \left(\frac{\Omega_1}{\Omega_i}\right)^2 \\
&+ \ddot{\xi}_3 \quad < 2\,\bar{h}_2\,\bar{\ell}\,\eta_3\,(\ell_{Fi}) > \left(\frac{\Omega_1}{\Omega_i}\right)^2 \\
&+ \ddot{\bar{R}}_{ys} \quad < -2\,\bar{\ell} >] \}_i \\
&- \frac{W}{g}\,\Omega_1^2\,R\,\ddot{\bar{R}}_{ys} = 0
\end{aligned}
\tag{3.20}
$$

It should be noted that equations (3.7) - (3.20) are valid for both articulated and hingeless rotors.

For articulated blades, the following quantities should be set equal to zero.

$$\bar{\omega}_F = 0 \quad , \quad \bar{\omega}_L = 0 \quad , \quad \bar{\omega}_{T1} = 0$$

while for hingeless blades

$$\bar{\omega}_{T2} = 0$$

Depending on the type of rotor, articulated or hingeless, the appropriate

substitutions indicated above, have to be made in Eqs. (3.7) - (3.20) and the resulting equations represent the linearized stability equations. The equations for pitch, roll and the supporting structure elastic modes, presented in the following pages, are different for the case of articulated or the case of hingeless rotors. This difference is primarily due to the terms representing the transfer of moments at the hub due to the blades. In articulated rotors, without lag dampers or hinge springs, flap and lead-lag moments at the hinge are zero, whereas in the case of hingeless rotors, these moments are nonzero. Hence, two sets of equations have to be given. These equations are provided below and they are identified as applicable to "Hingeless Rotors" and "Articulated Rotors" respectively.

Hingeless Rotors

Roll

$$\frac{N}{2}\sum_{i=1}^{2}\{m\Omega_i^2 R^3 [\beta_{1c}^i < \nu\frac{c_{d0}}{a}\frac{\bar{\ell}^4}{4} + \nu\frac{\bar{\ell}^3}{3}\lambda\theta_0 + \bar{g}_{SF} + \nu\frac{\bar{\ell}^4}{4} + 2\nu\frac{\bar{\ell}^3}{3}\bar{e}$$

$$+ \bar{h}_2\left(\beta_p\nu\frac{\bar{\ell}^3}{3} + \nu\frac{\bar{\ell}^3}{3}\beta_{k0} + \nu\frac{\bar{\ell}^3}{3}\theta_0\zeta_{k0} + \frac{1}{2}\bar{b}\nu\frac{\bar{\ell}^2}{2}\sin\theta_0\right) >$$

$$+ \beta_{1s}^i < -2\nu\frac{\bar{\ell}^4}{4}\zeta_{k0} + \nu\frac{\bar{\ell}^4}{4}(\beta_p + \beta_{k0})\theta_0 + \frac{1}{2}\nu\bar{b}\frac{\bar{\ell}^3}{3}\cos\theta_0 + 2\nu\frac{\bar{\ell}^4}{4}\beta_{k0}\theta_0$$

$$+ \bar{h}_2\left(\nu\frac{\bar{\ell}^3}{3}(2\theta_0 + \phi_{k0}) - \frac{\bar{\ell}^2}{2}\beta_p - \bar{\ell}^2\beta_{k0} + \nu\frac{\bar{\ell}^2}{2}(-2\lambda + \bar{e}\theta_0) - \nu\frac{\bar{\ell}^2}{2}\lambda\right) >$$

$$+ \zeta_{1c}^i < -\nu\frac{\bar{\ell}^4}{4}(\theta_0 + \phi_{k0}) + \bar{h}_2\nu\frac{\bar{\ell}^3}{3}\theta_0(-\beta_p + \beta_{k0}) >$$

$$+ \zeta_{1s}^i < \nu\frac{\bar{\ell}^4}{4}\zeta_{k0}\,2\theta_0 - \nu\frac{\bar{\ell}^4}{4}(\beta_p + \beta_{k0}) + \beta_p\bar{g}_{SL}$$

$$- \bar{h}_2\left(\bar{\ell}^2\zeta_{k0} - 2\nu\frac{c_{d0}}{a}\frac{\bar{\ell}^3}{3} - \nu\frac{\bar{\ell}^2}{2}\lambda\theta_0\right) >$$

$$+ \phi_{1c}^i < \nu\frac{\bar{\ell}^4}{4}\zeta_{k0} - \nu\frac{\bar{\ell}^3}{3}\bar{b} - \frac{1}{2}\nu\bar{b}\frac{\bar{\ell}^3}{3}\cos\theta_0 + \bar{h}_2\nu\frac{\bar{\ell}^2}{2}\lambda >$$

$$+ \phi_{1s}^i < -\bar{g}_{ST} + \nu\left(\frac{\bar{\ell}^4}{4} + \frac{\bar{\ell}^3}{3}3\bar{e}\right)$$

$$+ \bar{h}_2 \left(\beta_p \nu \frac{\bar{\ell}^3}{3} + \frac{1}{2} \nu \bar{b} \frac{\bar{\ell}^2}{2} \sin\theta_0\right) >$$

$$+ \dot{\beta}^i_{1c} < - \nu \frac{\bar{\ell}^4}{4} \zeta_{k0} + \nu \frac{\bar{\ell}^4}{4} (\beta_{k0} + \beta_p)\, \theta_0 + 2 \frac{\bar{\ell}^3}{3} + 2 \frac{\bar{\ell}^2}{2} \bar{e}$$

$$+ 2 \frac{1}{2} \nu \bar{b} \frac{\bar{\ell}^3}{3} \cos\theta_0 - \bar{h}_2 \bar{\ell}^2 \beta_{k0}$$

$$+ \bar{h}_2 \nu \frac{\bar{\ell}^3}{3} (\theta_U + \phi_{k0}) + \bar{h}_2 \nu \frac{\bar{\ell}^2}{2} (- 2\lambda + \bar{e}\theta_0) > \frac{\Omega_1}{\Omega_i}$$

$$+ \dot{\beta}^i_{1s} < - 2 \frac{\bar{\ell}^3}{3} \zeta_{k0} - \bar{g}_{SF} - \nu \frac{\bar{\ell}^4}{4} - 2 \nu \frac{\bar{\ell}^3}{3} \bar{e}$$

$$- \bar{h}_2 \left(\beta_p \nu \frac{\bar{\ell}^3}{3} + \nu \frac{\bar{\ell}^3}{3} \beta_{k0} + 2 \frac{1}{2} \nu \bar{b} \frac{\bar{\ell}^2}{2} \sin\theta_0\right) > \frac{\Omega_1}{\Omega_i}$$

$$+ \dot{\zeta}^i_{1c} < \nu \frac{\bar{\ell}^4}{4} \zeta_{k0}\, 2\theta_0 + \beta_p \bar{g}_{SL} - \bar{h}_2 \bar{\ell}^2 \zeta_{k0}$$

$$+ \bar{h}_2 \left(\nu \frac{c_{d0}}{a} 2 \frac{\bar{\ell}^3}{3} + \nu \frac{\bar{\ell}^2}{2} \lambda\, \theta_0\right) > \frac{\Omega_1}{\Omega_i}$$

$$+ \dot{\zeta}^i_{1s} < 2 \nu \frac{\bar{\ell}^4}{4} (\theta_0 + \phi_{k0}) - \nu \frac{\bar{\ell}^3}{3} \lambda + \nu \frac{\bar{\ell}^3}{3} \bar{e}\, 2\theta_0 + \bar{h}_2 \nu\beta_p \frac{\bar{\ell}^3}{3} 2\theta_0 > \frac{\Omega_1}{\Omega_i}$$

$$+ \dot{\phi}^i_{1c} < - \bar{g}_{ST} + \bar{h}_2 \frac{1}{2} \nu \bar{b} \frac{\bar{\ell}^2}{2} \sin\theta_0 > \frac{\Omega_1}{\Omega_i}$$

$$+ \dot{\phi}^i_{1s} < \nu \frac{\bar{\ell}^3}{3} \bar{b} + \frac{1}{2} \nu \bar{b} \frac{\bar{\ell}^3}{3} \cos\theta_0 > \frac{\Omega_1}{\Omega_i}$$

$$+ \ddot{\beta}^i_{1c} < - \frac{\bar{\ell}^3}{3} \zeta_{k0} - \bar{h}_2 \frac{1}{2} \nu \bar{b} \frac{\bar{\ell}^2}{2} \sin\theta_0 > \left(\frac{\Omega_1}{\Omega_i}\right)^2$$

$$+ \ddot{\beta}^i_{1s} < - \frac{\bar{\ell}^3}{3} - \frac{1}{2} \nu \bar{b} \frac{\bar{\ell}^3}{3} \cos\theta_0 - \frac{\bar{\ell}^2}{2} \bar{e} - \bar{h}_2 \beta_p \frac{\bar{\ell}^2}{2} > \left(\frac{\Omega_1}{\Omega_i}\right)^2$$

$$+ \ddot{\theta}_x < - \frac{\bar{\ell}^3}{3} - \bar{e} \frac{\bar{\ell}^2}{2} - \bar{h}_2 \frac{\bar{\ell}^2}{2} (\beta_p + \beta_{k0}) - \bar{h}_2 \beta_p \frac{\bar{\ell}^2}{2}$$

$$- \bar{h}_2 \left(\frac{\bar{\ell}^2}{2} (\beta_p + \beta_{k0}) + 2 \bar{h}_2 \bar{\ell}\right) > \left(\frac{\Omega_1}{\Omega_i}\right)^2$$

$$+ \dot{\theta}_x < - \frac{\bar{\ell}^3}{3} 2\zeta_{k0} - \nu \frac{\bar{\ell}^3}{3} \bar{e} - \nu \frac{\bar{\ell}^4}{4} - \bar{h}_2 \beta_p \nu \frac{\bar{\ell}^3}{3} - \bar{h}_2 \beta_{k0} \nu \frac{\bar{\ell}^3}{3} > \left(\frac{\Omega_1}{\Omega_i}\right)$$

$$+ \ddot{\theta}_y < \frac{\bar{\ell}^3}{3} \zeta_{k0} > \left(\frac{\Omega_1}{\Omega_i}\right)^2$$

$$+ \dot{\theta}_y < \nu \frac{\bar{\ell}^4}{4} \zeta_{k0} - 2 \frac{\bar{\ell}^3}{3} - \frac{\bar{\ell}^2}{2} \; 2 \bar{e} - 2 \bar{h}_2 \beta_p \frac{\bar{\ell}^2}{2} - \bar{h}_2 \nu \frac{\bar{\ell}^3}{3} (\theta_0 + \phi_{k0})$$

$$+ \nu \frac{\bar{\ell}^2}{2} \lambda \; 2 \bar{h}_2 - \bar{h}_2 \nu \frac{\bar{\ell}^3}{3} 2\theta_0 + \bar{h}_2 \nu \frac{\bar{\ell}^2}{2} \lambda > \frac{\Omega_1}{\Omega_i}$$

$$+ \ddot{\bar{R}}_{ys} < \frac{\bar{\ell}^2}{2} (\beta_p + \beta_{k0}) + 2 \bar{h}_2 \bar{\ell} > \left(\frac{\Omega_1}{\Omega_i} \right)^2$$

$$+ \dot{\bar{R}}_{xs} < - \nu \frac{\bar{\ell}^3}{3} \; 2\theta_0 + \nu \frac{\bar{\ell}^2}{2} \lambda > \frac{\Omega_1}{\Omega_i}$$

$$+ \frac{\ddot{\xi}_1}{R} < \eta_1 (\ell_{Fi}) \left(\frac{\bar{\ell}^2}{2} (\beta_p + \beta_{k0}) + 2 \bar{h}_2 \bar{\ell} \right) > \left(\frac{\Omega_1}{\Omega_i} \right)^2$$

$$+ \ddot{\xi}_3 < - \bar{h}_2 \; \eta_3 (\ell_{Fi}) \left(\frac{\bar{\ell}^2}{2} (\beta_p + \beta_{k0}) + 2 \bar{h}_2 \bar{\ell} \right) > \left(\frac{\Omega_1}{\Omega_i} \right)^2$$

$$+ \frac{\dot{\xi}_2}{R} < \bar{h}_2 \eta_{2,x} (\ell_{Fi}) \nu \frac{\bar{\ell}^3}{3} \; 2\theta_0 \, R - \bar{h}_2 \eta_{2,x} (\ell_{Fi}) \nu \frac{\bar{\ell}^2}{2} \lambda \, R > \left(\frac{\Omega_1}{\Omega_i} \right)] \}_i$$

$$+ \theta_x < - h_3 P_Z^S + h_1 W_{UN} + h_4 W_{EN} >$$

$$- I_{xx} \; \Omega_1^2 \ddot{\theta}_x + I_{xy} \; \Omega_1^2 \; \ddot{\theta}_y = 0 \qquad (3.21)$$

Pitch

$$\frac{N}{2} \sum_{i=1}^{2} \{ m\Omega_i^2 R^3 [\beta_{1c}^i < 2 \nu \frac{\bar{\ell}^4}{4} \zeta_{k0} - \nu \frac{\bar{\ell}^4}{4} (\beta_p + \beta_{k0}) \theta_0 - \frac{1}{2} \nu \bar{b} \frac{\bar{\ell}^3}{3} \cos\theta_0 - \nu \frac{\bar{\ell}^4}{4} 2\beta_{k0} \theta_0$$

$$- \bar{h}_2 \left(\nu \frac{\bar{\ell}^3}{3} (2\theta_0 + \phi_{k0}) - \frac{\bar{\ell}^2}{2} \beta_p - \bar{\ell}^2 \beta_{k0} + \nu \frac{\bar{\ell}^2}{2} (-2\lambda + \bar{e}\theta_0) - \nu \frac{\bar{\ell}^2}{2} \lambda \right) >$$

$$+ \beta_{1s}^i < \nu \frac{c_{d0}}{a} \frac{\bar{\ell}^4}{4} + \nu \frac{\bar{\ell}^3}{3} \lambda\theta_0 + \bar{g}_{SF} + \nu \frac{\bar{\ell}^4}{4} + 2 \nu \frac{\bar{\ell}^3}{3} \bar{e}$$

$$+ \bar{h}_2 \left(\beta_p \nu \frac{\bar{\ell}^3}{3} + \beta_{k0} \nu \frac{\bar{\ell}^3}{3} + \nu \frac{\bar{\ell}^3}{3} \zeta_{k0} \theta_0 + \frac{1}{2} \nu \bar{b} \frac{\bar{\ell}^2}{2} \sin\theta_0 \right) >$$

$$+ \zeta_{1c}^i < - \nu \frac{\bar{\ell}^4}{4} \zeta_{k0} 2\theta_0 - \beta_p \bar{g}_{SL} + \nu \frac{\bar{\ell}^4}{4} (\beta_p + \beta_{k0})$$

$$+ \bar{h}_2 \left(\bar{\ell}^2 \zeta_{k0} - 2 \nu \frac{c_{d0}}{a} \frac{\bar{\ell}^3}{3} - \nu \frac{\bar{\ell}^2}{2} \lambda\theta_0 \right) >$$

$$+ \zeta_{1s}^i < - \nu \frac{\bar{\ell}^4}{4} (\theta_0 + \phi_{k0}) + \bar{h}_2 \nu \frac{\bar{\ell}^3}{3} (-\beta_p + \beta_{k0}) \theta_0 >$$

$$+ \phi^i_{1c} < \bar{g}_{ST} - \nu \frac{\bar{\ell}^4}{4} - \nu \frac{\bar{\ell}^3}{3} 3\,\bar{e} - \bar{h}_2 \beta_p \nu \frac{\bar{\ell}^3}{3} - \bar{h}_2 \frac{1}{2} \nu \bar{b} \frac{\bar{\ell}^2}{2} \sin\theta_0 >$$

$$+ \phi^i_{1s} < \nu \frac{\bar{\ell}^4}{4} \zeta_{k0} - \nu \frac{\bar{\ell}^3}{3} \bar{b} - \frac{1}{2} \nu \bar{b} \frac{\bar{\ell}^3}{3} \cos\theta_0 + \bar{h}_2 \nu \frac{\bar{\ell}^2}{2} \lambda >$$

$$+ \dot{\beta}^i_{ic} < 2 \frac{\bar{\ell}^3}{3} \zeta_{k0} + \bar{g}_{SF} + \nu \frac{\bar{\ell}^4}{4} + 2 \nu \frac{\bar{\ell}^3}{3} \bar{e}$$

$$+ \bar{h}_2 (\beta_p \nu \frac{\bar{\ell}^3}{3} + \beta_{k0} \nu \frac{\bar{\ell}^3}{3} + 2 \frac{1}{2} \nu \bar{b} \frac{\bar{\ell}^2}{2} \sin\theta_0) > \frac{\Omega_1}{\Omega_i}$$

$$+ \dot{\beta}^i_{1s} < - \nu \frac{\bar{\ell}^4}{4} \zeta_{k0} + \nu \frac{\bar{\ell}^4}{4} (\beta_p + \beta_{k0}) \theta_0 + 2 \frac{\bar{\ell}^3}{3} + 2 \frac{\bar{\ell}^2}{2} \bar{e}$$

$$+ 2 \frac{1}{2} \nu \bar{b} \frac{\bar{\ell}^3}{3} \cos\theta_0 - \bar{h}_2 \bar{\ell}^2 \beta_{k0}$$

$$+ \bar{h}_2 \nu \frac{\bar{\ell}^3}{3} (\theta_0 + \phi_{k0}) + \bar{h}_2 \nu \frac{\bar{\ell}^2}{2} (-2\lambda + \bar{e}\theta_0) > \frac{\Omega_1}{\Omega_i}$$

$$+ \dot{\zeta}^i_{1c} < - 2 \nu \frac{\bar{\ell}^4}{4} (\theta_0 + \phi_{k0}) + \nu \frac{\bar{\ell}^3}{3} \lambda - \nu \frac{\bar{\ell}^3}{3} \bar{e}\, 2\theta_0 - \bar{h}_2 \beta_p \nu \frac{\bar{\ell}^3}{3} 2\theta_0 > \frac{\Omega_1}{\Omega_i}$$

$$+ \dot{\zeta}^i_{1s} < \nu \frac{\bar{\ell}^4}{4} \zeta_{k0}\, 2\theta_0 + \beta_p \bar{g}_{SL} - \bar{h}_2 \bar{\ell}^2 \zeta_{k0}$$

$$+ \bar{h}_2 (\nu \frac{c_{d0}}{a} 2 \frac{\bar{\ell}^3}{3} + \nu \frac{\bar{\ell}^2}{2} \lambda\, \theta_0) > \frac{\Omega_1}{\Omega_i}$$

$$+ \dot{\phi}^i_{1c} < - \nu \frac{\bar{\ell}^3}{3} \bar{b} - \frac{1}{2} \nu \bar{b} \frac{\bar{\ell}^3}{3} \cos\theta_0 > \frac{\Omega_1}{\Omega_i}$$

$$+ \dot{\phi}^i_{1s} < - \bar{g}_{ST} + \bar{h}_2 \frac{1}{2} \nu \bar{b} \frac{\bar{\ell}^2}{2} \sin\theta_0 > \frac{\Omega_1}{\Omega_i}$$

$$+ \ddot{\beta}^i_{1c} < \frac{\bar{\ell}^3}{3} + \frac{1}{2} \nu \bar{b} \frac{\bar{\ell}^3}{3} \cos\theta_0 + \frac{\bar{\ell}^2}{2} \bar{e} + \bar{h}_2 \beta_p \frac{\bar{\ell}^2}{2} > (\frac{\Omega_1}{\Omega_i})^2$$

$$+ \ddot{\beta}^i_{1s} < - \frac{\bar{\ell}^3}{3} \zeta_{k0} - \bar{h}_2 \frac{1}{2} \nu \bar{b} \frac{\bar{\ell}^2}{2} \sin\theta_0 > (\frac{\Omega_1}{\Omega_i})^2$$

$$+ \ddot{\zeta}^i_{1s} < \frac{\bar{\ell}^3}{3} (\beta_p + \beta_{k0}) + \bar{h}_2 \frac{\bar{\ell}^2}{2} > (\frac{\Omega_1}{\Omega_i})^2$$

$$+ \beta^i_M < 2 \bar{\ell}_{Fi} (\nu \frac{\bar{\ell}^3}{3} \zeta_{k0} + \nu \frac{\bar{\ell}^3}{3} \beta_p \theta_0) >$$

$$+ \zeta^i_M < 2 \bar{\ell}_{Fi} \nu \frac{\bar{\ell}^3}{3} (\beta_p + \beta_{k0}) >$$

$$+ \phi^i_M < 2 \bar{\ell}_{Fi} (- \nu \frac{\bar{\ell}^3}{3} - \nu \frac{\bar{\ell}^2}{2} 2\,\bar{e}) >$$

$$+ \dot{\beta}_M^i < 2\,\bar{\ell}_{Fi}\left(\nu\frac{\bar{\ell}^3}{3} + \nu\frac{\bar{\ell}^2}{2}\,\bar{e}\right) > \left(\frac{\Omega_1}{\Omega_i}\right)$$

$$+ \dot{\zeta}_M^i < 2\,\bar{\ell}_{Fi}\left(\beta_p\frac{\bar{\ell}^2}{2} - 2\nu\frac{\bar{\ell}^3}{3}(\theta_0 + \phi_{k0}) + \nu\frac{\bar{\ell}^2}{2}\lambda - \beta_p\,\bar{\ell}^2\right) > \left(\frac{\Omega_1}{\Omega_i}\right)$$

$$+ \dot{\phi}_M^i < 2\,\bar{\ell}_{Fi}\left(-\nu\frac{\bar{\ell}^2}{2}\,\bar{b} - \frac{1}{2}\nu\,\bar{b}\,\frac{\bar{\ell}^2}{2}\cos\theta_0\right) > \left(\frac{\Omega_1}{\Omega_i}\right)$$

$$+ \ddot{\beta}_M^i < 2\,\bar{\ell}_{Fi}\left(\frac{\bar{\ell}^2}{2} + \frac{1}{2}\nu\,\bar{b}\,\frac{\bar{\ell}^2}{2}\cos\theta_0\right) > \left(\frac{\Omega_1}{\Omega_i}\right)^2$$

$$+ \ddot{\theta}_x < -\frac{\bar{\ell}^3}{3}\,\zeta_{k0} > \left(\frac{\Omega_1}{\Omega_i}\right)^2$$

$$+ \dot{\theta}_x < -\nu\frac{\bar{\ell}^4}{4}\,\zeta_{k0} + 2\frac{\bar{\ell}^3}{3} + \frac{\bar{\ell}^2}{2}\,2\,\bar{e} + 2\,\bar{h}_2\,\beta_p\frac{\bar{\ell}^2}{2} + \bar{h}_2\,\nu\frac{\bar{\ell}^3}{3}(\theta_0 + \phi_{k0})$$

$$- \nu\frac{\bar{\ell}^2}{2}\,2\lambda\,\bar{h}_2 + \bar{h}_2\,\nu\frac{\bar{\ell}^3}{3}\,2\theta_0 - \nu\frac{\bar{\ell}^2}{2}\lambda\,\bar{h}_2 > \frac{\Omega_1}{\Omega_i}$$

$$+ \ddot{\theta}_y < -\frac{\bar{\ell}^3}{3} - \frac{\bar{\ell}^2}{2}\,\bar{e} - \bar{h}_2\,\frac{\bar{\ell}^2}{2}(\beta_p + \beta_{k0}) - \bar{h}_2\beta_p\frac{\bar{\ell}^2}{2}$$

$$+ \bar{h}_2\left(-\frac{\bar{\ell}^2}{2}(\beta_p + \beta_{k0}) - 2\,\bar{\ell}\,\bar{h}_2\right) - \bar{\ell}_{Fi}\,2\,\bar{\ell}\,\bar{\ell}_{Fi} > \left(\frac{\Omega_1}{\Omega_i}\right)^2$$

$$+ \dot{\theta}_y < -\frac{\bar{\ell}^3}{3}\,2\zeta_{k0} - \nu\frac{\bar{\ell}^4}{4} - \nu\frac{\bar{\ell}^3}{3}\,\bar{e} - \nu\frac{\bar{\ell}^3}{3}\,\beta_p\bar{h}_2 - \nu\frac{\bar{\ell}^3}{3}\,\beta_{k0}\bar{h}_2 - \bar{\ell}_{Fi}2\bar{\ell}_{Fi}\,\nu\frac{\bar{\ell}^2}{2} > \frac{\Omega_1}{\Omega_i}$$

$$+ \ddot{\bar{R}}_{xs} < -\frac{\bar{\ell}^2}{2}(\beta_p + \beta_{k0}) - 2\,\bar{\ell}\;\bar{h}_2 > \left(\frac{\Omega_1}{\Omega_i}\right)^2$$

$$+ \dot{\bar{R}}_{ys} < -\nu\frac{\bar{\ell}^3}{3}\,2\theta_0 + \nu\frac{\bar{\ell}^2}{2}\lambda > \frac{\Omega_1}{\Omega_i}$$

$$+ \frac{\ddot{\xi}_2}{R} < -\bar{h}_2\,\eta_{2,x}(\bar{\ell}_{Fi})\,R\left(-\frac{\bar{\ell}^2}{2}(\beta_p + \beta_{k0}) - 2\bar{\ell}\,\bar{h}_2\right) + \eta_2(\ell_{Fi})\,2\bar{\ell}\,\bar{\ell}_{Fi} > \left(\frac{\Omega_1}{\Omega_i}\right)^2$$

$$+ \frac{\dot{\xi}_1}{R} < \eta_1(\ell_{Fi})\left(-\nu\frac{\bar{\ell}^3}{3}\,2\theta_0 + \nu\frac{\bar{\ell}^2}{2}\lambda\right) > \frac{\Omega_1}{\Omega_i}$$

$$+ \frac{\dot{\xi}_2}{R} < \eta_2(\ell_{Fi})\,2\,\bar{\ell}_{Fi}\,\nu\frac{\bar{\ell}^2}{2} > \frac{\Omega_1}{\Omega_i}$$

$$+ \dot{\xi}_3 < -\bar{h}_2\,\eta_3(\ell_{Fi})\left(-\nu\frac{\bar{\ell}^3}{3}\,2\theta_0\right) - \bar{h}_2\,\eta_3(\ell_{Fi})\,\nu\frac{\bar{\ell}^2}{2}\lambda > \frac{\Omega_1}{\Omega_i}\,]\,\}_i$$

$$+ \theta_y < -h_3\,P_Z^S + h_1\,W_{UN} + h_4\,W_{EN} + h_5\,W_S >$$

$$- I_{yy}\,\Omega_1^2\,\ddot{\theta}_y + I_{yx}\,\Omega_1^2\,\ddot{\theta}_x = 0 \qquad (3.22)$$

Elastic Mode Equations of the Supporting Structure

Symmetric Bending in X-Y plane (Horizontal)

$$\frac{N}{2}\sum_{i=1}^{2}[\eta_1(\ell_{Fi})\, m\Omega_i^2 R^2\{\beta_{1c}^i < -\nu\beta_p \frac{\bar{\ell}^3}{3} - \nu\beta_{k0}\frac{\bar{\ell}^3}{3} - \nu\frac{\bar{\ell}^3}{3}\zeta_{k0}\theta_0 - \frac{1}{2}\nu\bar{b}\frac{\bar{\ell}^2}{2}\sin\theta_0 >$$

$$+ \beta_{1s}^i < \frac{\bar{\ell}^2}{2}(\beta_p + 2\beta_{k0}) - \nu\frac{\bar{\ell}^3}{3}(2\theta_0 + \phi_{k0}) + \nu\frac{\bar{\ell}^2}{2}(2\lambda - \bar{e}\theta_0) + \nu\frac{\bar{\ell}^2}{2}\lambda >$$

$$+ \zeta_{1c}^i < \nu\frac{\bar{\ell}^3}{3}(\beta_p - \beta_{k0})\,\theta_0 >$$

$$+ \zeta_{1s}^i < \bar{\ell}^2\zeta_{k0} - 2\nu\frac{c_{d0}}{a}\frac{\bar{\ell}^3}{3} - \nu\frac{\bar{\ell}^2}{2}\lambda\theta_0 >$$

$$+ \phi_{1c}^i < -\nu\frac{\bar{\ell}^2}{2}\lambda >$$

$$+ \phi_{1s}^i < -\beta_p\nu\frac{\bar{\ell}^3}{3} - \frac{1}{2}\nu\bar{b}\frac{\bar{\ell}^2}{2}\sin\theta_0 >$$

$$+ \dot{\beta}_{1c}^i < \bar{\ell}^2\beta_{k0} - \nu\frac{\bar{\ell}^3}{3}(\theta_0 + \phi_{k0}) + \nu\frac{\bar{\ell}^2}{2}(2\lambda - \bar{e}\theta_0) > \frac{\Omega_1}{\Omega_i}$$

$$+ \dot{\beta}_{1s}^i < \beta_p\nu\frac{\bar{\ell}^3}{3} + \dot{\beta}_{k0}\nu\frac{\bar{\ell}^3}{3} + 2\frac{1}{2}\nu\bar{b}\frac{\bar{\ell}^2}{2}\sin\theta_0 > \frac{\Omega_1}{\Omega_i}$$

$$+ \dot{\zeta}_{1c}^i < \bar{\ell}^2\zeta_{k0} - 2\nu\frac{c_{d0}}{a}\frac{\bar{\ell}^3}{3} - \nu\frac{\bar{\ell}^2}{2}\lambda\,\theta_0 > \frac{\Omega_1}{\Omega_i}$$

$$+ \dot{\zeta}_{1s}^i < -\nu\frac{\bar{\ell}^3}{3}2\theta_0\beta_p > \frac{\Omega_1}{\Omega_i}$$

$$+ \dot{\phi}_{1c}^i < -\frac{1}{2}\nu\bar{b}\frac{\bar{\ell}^2}{2}\sin\theta_0 > \frac{\Omega_1}{\Omega_i}$$

$$+ \ddot{\beta}_{1c}^i < \frac{1}{2}\nu\bar{b}\frac{\bar{\ell}^2}{2}\sin\theta_0 > \left(\frac{\Omega_1}{\Omega_i}\right)^2$$

$$+ \ddot{\beta}_{1s}^i < \beta_p\frac{\bar{\ell}^2}{2} > \left(\frac{\Omega_1}{\Omega i}\right)^2$$

$$+ \ddot{\zeta}_{1c}^i < -\frac{\bar{\ell}^2}{2} > \left(\frac{\Omega_1}{\Omega_i}\right)^2$$

$$+ \ddot{\theta}_x < \beta_p\frac{\bar{\ell}^2}{2} + \frac{\bar{\ell}^2}{2}(\beta_p + \beta_{k0}) + 2\bar{h}_2\bar{\ell} > \left(\frac{\Omega_1}{\Omega i}\right)^2$$

$$+ \dot{\theta}_x < \beta_p\nu\frac{\bar{\ell}^3}{3} + \beta_{k0}\nu\frac{\bar{\ell}^3}{3} > \frac{\Omega_1}{\Omega_i}$$

$$+ \dot{\theta}_y < 2\beta_p \frac{\bar{\ell}^2}{2} + \nu \frac{\bar{\ell}^3}{3} (\theta_0 + \phi_{k0}) - \nu \frac{\bar{\ell}^2}{2} 2\lambda > \frac{\Omega_1}{\Omega_i}$$

$$+ \ddot{\bar{R}}_{ys} < -2\bar{\ell} > (\frac{\Omega_1}{\Omega_i})^2$$

$$+ \frac{\ddot{\xi}_1}{R} < -\eta_1(\ell_{Fi})\, 2\bar{\ell} > (\frac{\Omega_1}{\Omega_i})^2$$

$$+ \ddot{\xi}_3 < \bar{h}_2 \eta_3(\ell_{Fi})\, 2\bar{\ell} > (\frac{\Omega_1}{\Omega_i})^2 \}$$

$$+ 2\eta_{1,x}(\ell_{Fi})\, m\Omega_i^2 R^3 \{ \phi_M^i < -\nu \frac{\bar{\ell}^3}{3} \lambda >$$

$$+ \dot{\beta}_M^i < 2\frac{\bar{\ell}^3}{3}(\beta_p + \beta_{k0}) - \nu \frac{\bar{\ell}^4}{4}(\theta_0 + \phi_{k0}) - \nu \frac{\bar{\ell}^3}{3}(-2\lambda + 2\bar{e}\theta_0) > \frac{\Omega_1}{\Omega_i}$$

$$+ \dot{\zeta}_M^i < -2\nu \frac{c_{d0}}{a} \frac{\bar{\ell}^4}{4} - \nu \frac{\bar{\ell}^3}{3} \lambda\theta_0 - \bar{g}_{SL} > \frac{\Omega_1}{\Omega_i}$$

$$+ \dot{\phi}_M^i < -\frac{1}{2}\nu \bar{b} \frac{\bar{\ell}^3}{3} \sin\theta_0 - \beta_p \bar{g}_{ST} > \frac{\Omega_1}{\Omega_i}$$

$$+ \ddot{\beta}_M^i < \frac{1}{2}\nu \bar{b} \frac{\bar{\ell}^3}{3} \sin\theta_0 > (\frac{\Omega_1}{\Omega_i})^2$$

$$+ \ddot{\zeta}_M^i < -\frac{\bar{\ell}^3}{3} - \frac{\bar{\ell}^2}{2} \bar{e} > (\frac{\Omega_1}{\Omega_i})^2$$

$$+ \dot{\theta}_y < -\bar{\ell}_{Fi} (-\nu \frac{\bar{\ell}^3}{3}(\theta_0 + \phi_{k0}) + 2\nu \frac{\bar{\ell}^2}{2} \lambda) > \frac{\Omega_1}{\Omega_i}$$

$$+ \frac{\dot{\xi}_2}{R} < \eta_2(\ell_{Fi})(-\nu \frac{\bar{\ell}^3}{3}(\theta_0 + \phi_{k0}) + 2\nu \frac{\bar{\ell}^2}{2} \lambda) > \frac{\Omega_1}{\Omega_i} \}]_i$$

$$+ \theta_x < \eta_1(0_s) P_Z^S - \eta_1(\ell_{F1}) W_{F1} - \eta_1(\ell_{F2}) W_{F2} - \eta_1(0_s) W_{EN} - \eta_1(0_s) W_{UN}$$

$$- \int_{\ell_{F1}}^{\ell_{F2}} \eta_1(x)\, W_S(x)\, dx >$$

$$- M_{SBXY} \Omega_1^2 \ddot{\xi}_1 - K_{SBXY} \xi_1 = 0 \qquad (3.23)$$

Symmetric Bending in X-Z plane (Vertical)

$$\frac{N}{2} \sum_{i=1}^{2} [\, \eta_{2,x}(\ell_{Fi})\, m\Omega_i^2 R^3 \{ \beta_{1c}^i < 2\nu \frac{\bar{\ell}^4}{4} \zeta_{k0} - \nu \frac{\bar{\ell}^4}{4}(\beta_p + \beta_{k0})\theta_0 - \frac{1}{2}\nu \bar{b} \frac{\bar{\ell}^3}{3} \cos\theta_0$$

$$- \nu \frac{\bar{\ell}^4}{4} 2\beta_{k0}\theta_0$$

$$
\begin{aligned}
&- \bar{h}_2 \left(\nu \frac{\bar{\ell}^3}{3} (2\theta_0 + \phi_{k0}) - \frac{\bar{\ell}^2}{2} \beta_p - \bar{\ell}^2 \beta_{k0} + \nu \frac{\bar{\ell}^2}{2} (-2\lambda + \bar{e}\theta_0) - \nu \frac{\bar{\ell}^2}{2} \lambda \right. > \\
&+ \beta^i_{1s} < \nu \frac{c_{d0}}{a} \frac{\bar{\ell}^4}{4} + \nu \frac{\bar{\ell}^3}{3} \lambda\theta_0 + \bar{g}_{SF} + \nu \frac{\bar{\ell}^4}{4} + 2\nu \frac{\bar{\ell}^3}{3} \bar{e} \\
&+ \bar{h}_2 \left(\beta_p \nu \frac{\bar{\ell}^3}{3} + \beta_{k0} \nu \frac{\bar{\ell}^3}{3} + \nu \frac{\bar{\ell}^3}{3} \zeta_{k0}\theta_0 + \frac{1}{2} \nu \bar{b} \frac{\bar{\ell}^2}{2} \sin\theta_0 \right) > \\
&+ \zeta^i_{1c} < - \nu \frac{\bar{\ell}^4}{4} \zeta_{k0} 2\theta_0 - \beta_p \bar{g}_{SL} + \nu \frac{\bar{\ell}^4}{4} (\beta_p + \beta_{k0}) \\
&+ \bar{h}_2 \left(\bar{\ell}^2 \zeta_{k0} - 2\nu \frac{c_{d0}}{a} \frac{\bar{\ell}^3}{3} - \nu \frac{\bar{\ell}^2}{2} \lambda\theta_0 \right) > \\
&+ \zeta^i_{1s} < - \nu \frac{\bar{\ell}^4}{4} (\theta_0 + \phi_{k0}) + \bar{h}_2 \nu \frac{\bar{\ell}^3}{3} (-\beta_p + \beta_{k0}) \theta_0 > \\
&+ \phi^i_{1c} < \bar{g}_{ST} - \nu \frac{\bar{\ell}^4}{4} - \nu \frac{\bar{\ell}^3}{3} 3\bar{e} - \bar{h}_2 \left(\beta_p \nu \frac{\bar{\ell}^3}{3} + \frac{1}{2} \nu \bar{b} \frac{\bar{\ell}^2}{2} \sin\theta_0 \right) > \\
&+ \phi^i_{1s} < \nu \frac{\bar{\ell}^4}{4} \zeta_{k0} - \nu \frac{\bar{\ell}^3}{3} \bar{b} - \frac{1}{2} \nu \bar{b} \frac{\bar{\ell}^3}{3} \cos\theta_0 + \bar{h}_2 \nu \frac{\bar{\ell}^2}{2} \lambda > \\
&+ \dot{\beta}^i_{1c} < 2 \frac{\bar{\ell}^3}{3} \zeta_{k0} + \bar{g}_{SF} + \nu \frac{\bar{\ell}^4}{4} + 2\nu \frac{\bar{\ell}^3}{3} \bar{e} \\
&+ \bar{h}_2 \left(\beta_p \nu \frac{\bar{\ell}^3}{3} + \beta_{k0} \nu \frac{\bar{\ell}^3}{3} + 2\frac{1}{2} \nu \bar{b} \frac{\bar{\ell}^2}{2} \sin\theta_0 \right) > \frac{\Omega_1}{\Omega_i} \\
&+ \dot{\beta}^i_{1s} < - \nu \frac{\bar{\ell}^4}{4} \zeta_{k0} + \nu \frac{\bar{\ell}^4}{4} (\beta_p + \beta_{k0}) \theta_0 + 2 \frac{\bar{\ell}^3}{3} + 2 \frac{\bar{\ell}^2}{2} \bar{e} \\
&+ 2\frac{1}{2} \nu \bar{b} \frac{\bar{\ell}^3}{3} \cos\theta_0 - \bar{h}_2 \bar{\ell}^2 \beta_{k0} \\
&+ \bar{h}_2 \nu \frac{\bar{\ell}^3}{3} (\theta_0 + \phi_{k0}) + \bar{h}_2 \nu \frac{\bar{\ell}^2}{2} (-2\lambda + \bar{e}\theta_0) > \frac{\Omega_1}{\Omega_i} \\
&+ \dot{\zeta}^i_{1c} < - 2\nu \frac{\bar{\ell}^4}{4} (\theta_0 + \phi_{k0}) + \nu \frac{\bar{\ell}^3}{3} \lambda - \nu \frac{\bar{\ell}^3}{3} \bar{e} 2\theta_0 - \bar{h}_2 \beta_p \nu \frac{\bar{\ell}^3}{3} 2\theta_0 > \frac{\Omega_1}{\Omega_i} \\
&+ \dot{\zeta}^i_{1s} < \nu \frac{\bar{\ell}^4}{4} \zeta_{k0} 2\theta_0 + \beta_p \bar{g}_{SL} - \bar{h}_2 \bar{\ell}^2 \zeta_{k0} \\
&+ \bar{h}_2 \nu \frac{c_{d0}}{a} 2 \frac{\bar{\ell}^3}{3} + \bar{h}_2 \nu \frac{\bar{\ell}^2}{2} \lambda \theta_0 > \frac{\Omega_1}{\Omega_i} \\
&+ \dot{\phi}^i_{1c} < - \nu \frac{\bar{\ell}^3}{3} \bar{b} - \frac{1}{2} \nu \bar{b} \frac{\bar{\ell}^3}{3} \cos\theta_0 > \frac{\Omega_1}{\Omega_i} \\
&+ \dot{\phi}^i_{1s} < - \bar{g}_{ST} + \bar{h}_2 \frac{1}{2} \nu \bar{b} \frac{\bar{\ell}^2}{2} \sin\theta_0 > \frac{\Omega_1}{\Omega_i}
\end{aligned}
$$

$$+ \ddot{\beta}^{i}_{1c} < \frac{\bar{\ell}^3}{3} + \frac{1}{2}\nu\,\bar{b}\,\frac{\bar{\ell}^3}{3}\cos\theta_0 + \frac{\bar{\ell}^2}{2}\,\bar{e} + \bar{h}_2\,\beta_p\,\frac{\bar{\ell}^2}{2} > \left(\frac{\Omega_1}{\Omega_i}\right)^2$$

$$+ \ddot{\beta}^{i}_{1s} < -\frac{\bar{\ell}^3}{3}\,\zeta_{k0} - \bar{h}_2\,\frac{1}{2}\,\nu\,\bar{b}\,\frac{\bar{\ell}^2}{2}\,\sin\theta_0 > \left(\frac{\Omega_1}{\Omega_i}\right)^2$$

$$+ \ddot{\zeta}^{i}_{1s} < \frac{\bar{\ell}^3}{3}(\beta_p + \beta_{k0}) + \bar{h}_2\,\frac{\bar{\ell}^2}{2} > \left(\frac{\Omega_1}{\Omega_i}\right)^2$$

$$+ \ddot{\theta}_x < -\frac{\bar{\ell}^3}{3}\,\zeta_{k0} > \left(\frac{\Omega_1}{\Omega_i}\right)^2$$

$$+ \ddot{\theta}_y < -\frac{\bar{\ell}^3}{3} - \bar{e}\,\frac{\bar{\ell}^2}{2} - \bar{h}_2\,\beta_p\,\frac{\bar{\ell}^2}{2} - \bar{h}_2\,\frac{\bar{\ell}^2}{2}(\beta_p + \beta_{k0})$$

$$+ \bar{h}_2\left(-\frac{\bar{\ell}^2}{2}\,\beta_{k0} - \frac{\bar{\ell}^2}{2}\,\beta_p - 2\,\bar{h}_2\,\bar{\ell}\right) > \left(\frac{\Omega_1}{\Omega_i}\right)^2$$

$$+ \dot{\theta}_x < -\nu\frac{\bar{\ell}^4}{4}\,\zeta_{k0} + 2\,\frac{\bar{\ell}^3}{3} + \frac{\bar{\ell}^2}{2}\,2\,\bar{e} + 2\,\bar{h}_2\,\beta_p\,\frac{\bar{\ell}^2}{2}$$

$$+ \bar{h}_2\,\nu\frac{\bar{\ell}^3}{3}(\theta_0 + \phi_{k0}) - \bar{h}_2\,\nu\frac{\bar{\ell}^2}{2}\,2\lambda + \bar{h}_2\,\nu\frac{\bar{\ell}^3}{3}\,2\theta_0 - \bar{h}_2\,\nu\frac{\bar{\ell}^2}{2}\,\lambda > \frac{\Omega_1}{\Omega_i}$$

$$+ \dot{\theta}_y < -\frac{\bar{\ell}^3}{3}\,2\,\zeta_{k0} - \nu\frac{\bar{\ell}^4}{4} - \nu\frac{\bar{\ell}^3}{3}\,\bar{e} - \bar{h}_2\,\beta_p\,\nu\frac{\bar{\ell}^3}{3} - \bar{h}_2\,\beta_{k0}\,\nu\frac{\bar{\ell}^3}{3} > \frac{\Omega_1}{\Omega_i}$$

$$+ \ddot{\bar{R}}_{xs} < -\frac{\bar{\ell}^2}{2}(\beta_p + \beta_{k0}) - 2\bar{h}_2\,\bar{\ell} > \left(\frac{\Omega_1}{\Omega_i}\right)^2$$

$$+ \dot{\bar{R}}_{ys} < -\nu\frac{\bar{\ell}^3}{3}\,2\theta_0 + \nu\frac{\bar{\ell}^2}{2}\lambda > \frac{\Omega_1}{\Omega_i}$$

$$+ \frac{\ddot{\xi}_2}{R} < \bar{h}_2\,\eta_{2,x}(\ell_{Fi})\,R\left(\frac{\bar{\ell}^2}{2}(\beta_{k0} + \beta_p) + 2\,\bar{h}_2\,\bar{\ell}\right) > \left(\frac{\Omega_1}{\Omega_i}\right)^2$$

$$+ \frac{\dot{\xi}_1}{R} < -\eta_1(\ell_{Fi})\,\nu\frac{\bar{\ell}^3}{3}\,2\theta_0 + \eta_1(\ell_{Fi})\,\nu\frac{\bar{\ell}^2}{2}\,\lambda > \frac{\Omega_1}{\Omega_i}$$

$$+ \dot{\xi}_3 < \bar{h}_2\,\eta_3(\ell_{Fi})\,\nu\frac{\bar{\ell}^3}{3}\,2\theta_0 - \bar{h}_2\eta_3(\ell_{Fi})\,\nu\frac{\bar{\ell}^2}{2}\,\lambda > \frac{\Omega_1}{\Omega_i}\ \}$$

$$+ 2\eta_2(\ell_{Fi})m\Omega_i^2R^2\{\beta^{i}_{M} <- \nu\frac{\bar{\ell}^3}{3}\,\zeta_{k0} - \nu\frac{\bar{\ell}^3}{3}\,\beta_p\theta_0 >$$

$$+ \zeta^{i}_{M} < -\nu\frac{\bar{\ell}^3}{3}(\beta_p + \beta_{k0}) >$$

$$+ \phi^{i}_{M} < \nu\frac{\bar{\ell}^3}{3} + \nu\frac{\bar{\ell}^2}{2}\,2\,\bar{e} >$$

$$+ \dot{\beta}^i_M < -\nu \frac{\bar{\ell}^3}{3} - \nu \frac{\bar{\ell}^2}{2} \bar{e} > \frac{\Omega_1}{\Omega_i}$$

$$+ \dot{\zeta}^i_M < 2\nu \frac{\bar{\ell}^3}{3} (\theta_0 + \phi_{k0}) - \nu \frac{\bar{\ell}^2}{2} \lambda > \frac{\Omega_1}{\Omega_i}$$

$$+ \dot{\phi}^i_M < \nu \frac{\bar{\ell}^2}{2} \bar{b} + \frac{1}{2} \nu \bar{b} \frac{\bar{\ell}^2}{2} \cos\theta_0 > \frac{\Omega_1}{\Omega_i}$$

$$+ \ddot{\beta}^i_M < -\frac{\bar{\ell}^2}{2} - \frac{1}{2} \nu \bar{b} \frac{\bar{\ell}^2}{2} \cos\theta_0 > \left(\frac{\Omega_1}{\Omega_i}\right)^2$$

$$+ \ddot{\theta}_y < \bar{\ell} \bar{\ell}_{Fi} > \left(\frac{\Omega_1}{\Omega_i}\right)^2$$

$$+ \dot{\theta}_y < \nu \frac{\bar{\ell}^2}{2} \bar{\ell}_{Fi} > \frac{\Omega_1}{\Omega_i}$$

$$+ \frac{\ddot{\xi}_2}{R} < -\eta_2 (\ell_{Fi}) \bar{\ell} > \left(\frac{\Omega_1}{\Omega_i}\right)^2$$

$$+ \frac{\dot{\xi}_2}{R} < -\eta_2 (\ell_{Fi}) \nu \frac{\bar{\ell}^2}{2} > \frac{\Omega_1}{\Omega_i} \}]_i$$

$$+ \theta_y < -h_3 \eta_{2,x}(0_s) P^S_Z + h_1 W_{UN} \eta_{2,x}(0_s) + h_4 W_{EN} \eta_{2,x}(0_s) >$$

$$- M_{SBXZ} \Omega_1^2 \ddot{\xi}_2 - K_{SBXZ} \xi_2 = 0 \qquad (3.24)$$

Torsion

$$\frac{N}{2} \sum_{i=1}^{2} [\eta_3(\ell_{Fi}) m \Omega^2_i R^3 \{ \beta^i_{1c} < \nu \frac{c_{d0}}{a} \frac{\bar{\ell}^4}{4} + \nu \frac{\bar{\ell}^3}{3} \lambda\theta_0 + \bar{g}_{SF} + \nu \frac{\bar{\ell}^4}{4} + 2\nu \frac{\bar{\ell}^3}{3} \bar{e}$$

$$+ \bar{h}_2 (\beta_p \nu \frac{\bar{\ell}^3}{3} + \beta_{k0} \nu \frac{\bar{\ell}^3}{3} + \nu \frac{\bar{\ell}^3}{3} \theta_0 \zeta_{k0} + \frac{1}{2} \nu \bar{b} \frac{\bar{\ell}^2}{2} \sin\theta_0) >$$

$$+ \beta^i_{1s} < -2\nu \frac{\bar{\ell}^4}{4} \zeta_{k0} + \nu \frac{\bar{\ell}^4}{4} (\beta_p + \beta_{k0}) \theta_0 + \frac{1}{2} \nu \bar{b} \frac{\bar{\ell}^3}{3} \cos\theta_0 + \nu \frac{\bar{\ell}^4}{4} 2 \beta_{k0}\theta_0$$

$$+ \bar{h}_2 (\nu \frac{\bar{\ell}^3}{3} (2\theta_0 + \phi_{k0}) - \frac{\bar{\ell}^2}{2} \beta_p - \bar{\ell}^2 \beta_{k0} + \nu \frac{\bar{\ell}^2}{2} (-2\lambda + \bar{e}\theta_0) - \nu \frac{\bar{\ell}^2}{2} \lambda >$$

$$+ \zeta^i_{ic} < -\nu \frac{\bar{\ell}^4}{4} (\theta_0 + \phi_{k0}) + \bar{h}_2 \nu \frac{\bar{\ell}^3}{3} (-\beta_p + \beta_{k0}) \theta_0 >$$

$$+ \zeta^i_{1s} < \nu \frac{\bar{\ell}^4}{4} \zeta_{k0} 2\theta_0 + \beta_p \bar{g}_{SL} - \bar{h}_2 \bar{\ell}^2 \zeta_{k0} - \nu \frac{\bar{\ell}^4}{4} (\beta_p + \beta_{k0})$$

$$+ \bar{h}_2 2\nu \frac{c_{d0}}{a} \frac{\bar{\ell}^3}{3} + \bar{h}_2 \nu \frac{\bar{\ell}^2}{2} \lambda \theta_0 >$$

$$+ \phi_{1c}^{i} < \nu \frac{\bar{\ell}^4}{4} \zeta_{k0} - \nu \frac{\bar{\ell}^3}{3} \bar{b} + \bar{h}_2 \nu \frac{\bar{\ell}^2}{2} \lambda - \frac{1}{2} \nu \bar{b} \frac{\bar{\ell}^3}{3} \cos\theta_0 >$$

$$+ \phi_{1s}^{i} < - \bar{g}_{ST} + \nu \left(\frac{\bar{\ell}^4}{4} + \frac{\bar{\ell}^3}{3} 3 \bar{e} \right)$$

$$+ \bar{h}_2 \left(\beta_p \nu \frac{\bar{\ell}^3}{3} + \frac{1}{2} \nu \bar{b} \frac{\bar{\ell}^2}{2} \sin\theta_0 \right) >$$

$$+ \dot{\beta}_{1c}^{i} < - \nu \frac{\bar{\ell}^4}{4} \zeta_{k0} + \nu \frac{\bar{\ell}^4}{4} (\beta_p + \beta_{k0}) \theta_0 + 2 \frac{\bar{\ell}^3}{3} + 2 \frac{\bar{\ell}^2}{2} \bar{e}$$

$$+ 2 \frac{1}{2} \nu \bar{b} \frac{\bar{\ell}^3}{3} \cos\theta_0 - \bar{h}_2 \bar{\ell}^2 \beta_{k0}$$

$$+ \bar{h}_2 \nu \frac{\bar{\ell}^3}{3} (\theta_0 + \phi_{k0}) + \bar{h}_2 \nu \frac{\bar{\ell}^2}{2} (- 2\lambda + \bar{e}\theta_0) > \frac{\Omega_1}{\Omega_i}$$

$$+ \dot{\beta}_{1s}^{i} < - 2 \frac{\bar{\ell}^3}{3} \zeta_{k0} - \bar{g}_{SF} - \nu \frac{\bar{\ell}^4}{4} - \nu \frac{\bar{\ell}^3}{3} 2 \bar{e}$$

$$- \bar{h}_2 \left(\beta_p \nu \frac{\bar{\ell}^3}{3} + \beta_{k0} \nu \frac{\bar{\ell}^3}{3} + 2 \frac{1}{2} \nu \bar{b} \frac{\bar{\ell}^2}{2} \sin\theta_0 \right) > \frac{\Omega_1}{\Omega_i}$$

$$+ \dot{\zeta}_{1c}^{i} < \nu \frac{\bar{\ell}^4}{4} \zeta_{k0} 2\theta_0 + \beta_p \bar{g}_{SL} - \bar{h}_2 \bar{\ell}^2 \zeta_{k0}$$

$$+ \bar{h}_2 2 \nu \frac{c_{d0}}{a} \frac{\bar{\ell}^3}{3} + \bar{h}_2 \nu \frac{\bar{\ell}^2}{2} \lambda\theta_0 > \frac{\Omega_1}{\Omega_i}$$

$$+ \dot{\zeta}_{1s}^{i} < 2 \nu \frac{\bar{\ell}^4}{4} (\theta_0 + \phi_{k0}) - \nu \frac{\bar{\ell}^3}{3} \lambda + \nu \frac{\bar{\ell}^3}{3} 2 \bar{e}\theta_0 + \bar{h}_2 \beta_p \nu \frac{\bar{\ell}^3}{3} 2\theta_0 > \frac{\Omega_1}{\Omega_i}$$

$$+ \dot{\phi}_{1c}^{i} < - \bar{g}_{ST} + \bar{h}_2 \frac{1}{2} \nu \bar{b} \frac{\bar{\ell}^2}{2} \sin\theta_0 > \frac{\Omega_1}{\Omega_i}$$

$$+ \dot{\phi}_{1s}^{i} < \nu \frac{\bar{\ell}^3}{3} \bar{b} + \frac{1}{2} \nu \bar{b} \frac{\bar{\ell}^3}{3} \cos\theta_0 > \frac{\Omega_1}{\Omega_i}$$

$$+ \ddot{\beta}_{1c}^{i} < - \frac{\bar{\ell}^3}{3} \zeta_{k0} - \bar{h}_2 \frac{1}{2} \nu \bar{b} \frac{\bar{\ell}^2}{2} \sin\theta_0 > \left(\frac{\Omega_1}{\Omega_i} \right)^2$$

$$+ \ddot{\beta}_{1s}^{i} < - \frac{\bar{\ell}^3}{3} - \bar{e} \frac{\bar{\ell}^2}{2} - \frac{1}{2} \nu \bar{b} \frac{\bar{\ell}^3}{3} \cos\theta_0 - \bar{h}_2 \beta_p \frac{\bar{\ell}^2}{2} > \left(\frac{\Omega_1}{\Omega i} \right)^2$$

$$+ \ddot{\zeta}_{1c}^{i} < \frac{\bar{\ell}^3}{3} (\beta_p + \beta_{k0}) + \bar{h}_2 \frac{\bar{\ell}^2}{2} > \left(\frac{\Omega_1}{\Omega_i} \right)^2$$

$$+ \ddot{\theta}_x < - \frac{\bar{\ell}^3}{3} - \bar{e} \frac{\bar{\ell}^2}{2} - \bar{h}_2 \beta_p \frac{\bar{\ell}^2}{2} - \bar{h}_2 \frac{\bar{\ell}^2}{2} (\beta_p + \beta_{k0})$$

$$- \bar{h}_2 \left(\frac{\bar{\ell}^2}{2} (\beta_p + \beta_{k0}) + 2 \bar{h}_2 \bar{\ell} \right) > \left(\frac{\Omega_1}{\Omega_i} \right)^2$$

$$+ \ddot{\theta}_y < \zeta_{k0} \frac{\bar{\ell}^3}{3} > \left(\frac{\Omega_1}{\Omega_i} \right)^2$$

$$+ \dot{\theta}_x < - \frac{\bar{\ell}^3}{3} 2 \zeta_{k0} - \nu \frac{\bar{\ell}^3}{3} \bar{e} - \nu \frac{\bar{\ell}^4}{4} - \bar{h}_2 \beta_p \nu \frac{\bar{\ell}^3}{3} - \bar{h}_2 \beta_{k0} \nu \frac{\bar{\ell}^3}{3} > \frac{\Omega_1}{\Omega_i}$$

$$+ \dot{\theta}_y < \nu \frac{\bar{\ell}^4}{4} \zeta_{k0} - 2 \frac{\bar{\ell}^2}{2} \bar{e} - 2 \bar{h}_2 \beta_p \frac{\bar{\ell}^2}{2} - \bar{h}_2 \nu \frac{\bar{\ell}^3}{3} (\theta_0 + \phi_{k0}) - 2 \frac{\bar{\ell}^3}{3}$$

$$+ \nu \bar{h}_2 \frac{\bar{\ell}^2}{2} 2 \lambda - \bar{h}_2 \nu \frac{\bar{\ell}^3}{3} 2\theta_0 + \bar{h}_2 \nu \frac{\bar{\ell}^2}{2} \lambda > \left(\frac{\Omega_1}{\Omega_i} \right)$$

$$+ \ddot{\bar{R}}_{ys} < \frac{\bar{\ell}^2}{2} (\beta_p + \beta_{k0}) + 2 \bar{h}_2 \bar{\ell} > \left(\frac{\Omega_1}{\Omega_i} \right)^2$$

$$+ \dot{\bar{R}}_{xs} < - \nu \frac{\bar{\ell}^3}{3} 2\theta_0 + \nu \frac{\bar{\ell}^2}{2} \lambda > \frac{\Omega_1}{\Omega_i}$$

$$+ \frac{\ddot{\xi}_1}{R} < \eta_1(\ell_{Fi}) \left(\frac{\bar{\ell}^2}{2} (\beta_p + \beta_{k0}) + 2 \bar{\ell} \bar{h}_2 \right) > \left(\frac{\Omega_1}{\Omega_i} \right)^2$$

$$+ \ddot{\xi}_3 < - \bar{h}_2 \eta_3(\ell_{Fi}) \left(\frac{\bar{\ell}^2}{2} (\beta_p + \beta_{k0}) + 2 \bar{\ell} \bar{h}_2 \right) > \left(\frac{\Omega_1}{\Omega_i} \right)^2$$

$$+ \frac{\dot{\xi}_2}{R} < \bar{h}_2 \eta_{2,x} (\ell_{Fi}) R \nu \frac{\bar{\ell}^3}{3} 2\theta_0 - \bar{h}_2 \eta_{2,x} (\ell_{Fi}) R \nu \frac{\bar{\ell}^2}{2} \lambda \}]_i$$

$$+ \theta_x < - \eta_3 (0_s) h_3 P_Z^S + \eta_3(0_s) h_1 W_{UN} + \eta_3(0_s) h_4 W_{EN} >$$

$$- M_{ST} \Omega_1^2 \ddot{\xi}_3 - K_{ST} \xi_3 = 0 \qquad (3.25)$$

Articulated Rotors

Roll

$$\frac{N}{2} \sum_{i=1}^{2} \{ m\Omega_i^2 R^3 [\beta_{1c}^i < \nu \frac{c_{d0}}{a} \frac{\bar{\ell}^4}{4} + \nu \frac{\bar{\ell}^3}{3} \lambda\theta_0 + \nu \frac{\bar{\ell}^3}{3} \bar{e}$$

$$+ \bar{h}_2 (\beta_p \nu \frac{\bar{\ell}^3}{3} + \beta_{k0} \nu \frac{\bar{\ell}^3}{3} + \nu \frac{\bar{\ell}^3}{3} \theta_0 \zeta_{k0} + \frac{1}{2} \nu \bar{b} \frac{\bar{\ell}^2}{2} \sin\theta_0) >$$

$$+ \beta_{1s}^i < - \nu \frac{\bar{\ell}^4}{4} \zeta_{k0} + \nu \frac{\bar{\ell}^4}{4} \beta_{k0}\theta_0 + \frac{\bar{\ell}^2}{2} \bar{e}$$

$$+ \bar{h}_2 (\nu \frac{\bar{\ell}^3}{3} (2\theta_0 + \phi_{k0}) - \frac{\bar{\ell}^2}{2} \beta_p - \bar{\ell}^2 \beta_{k0} + \nu \frac{\bar{\ell}^2}{2} (-2\lambda + \bar{e}\theta_0) - \nu \frac{\bar{\ell}^2}{2} \lambda) >$$

$$+ \zeta_{1c}^i < \nu \frac{\bar{\ell}^4}{4} (\theta_0 + \phi_{k0}) + \nu \frac{\bar{\ell}^3}{3} (-\lambda + 2\bar{e}\theta_0) - \frac{\bar{\ell}^3}{3} (\beta_p + 2\beta_{k0})$$

$$
\begin{aligned}
&- \nu \frac{\bar{\ell}^3}{3} \bar{e}\, 2\theta_0 + \bar{h}_2 \nu \frac{\bar{\ell}^3}{3} \theta_0 (-\beta_p + \beta_{k0}) > \\
&+ \zeta^i_{1s} < \nu \frac{\bar{\ell}^4}{4} \zeta_{k0}\, 2\theta_0 + \bar{h}_2 (-\bar{\ell}^2 \zeta_{k0} + 2\nu \frac{c_{d0}}{a} \frac{\bar{\ell}^3}{3} + \nu \frac{\bar{\ell}^2}{2} \lambda\theta_0) > \\
&+ \phi^i_{1c} < \nu \frac{\bar{\ell}^4}{4} \zeta_{k0} + \bar{h}_2 \nu \frac{\bar{\ell}^2}{2} \lambda > \\
&+ \phi^i_{1s} < -\bar{g}_{ST} + \nu \frac{\bar{\ell}^3}{3} \bar{e} + \bar{h}_2 (\beta_p \nu \frac{\bar{\ell}^3}{3} + \frac{1}{2} \nu \bar{b} \frac{\bar{\ell}^2}{2} \sin\theta_0) > \\
&+ \dot{\beta}^i_{1c} < -\nu \frac{\bar{\ell}^4}{4} \zeta_{k0} + \nu \frac{\bar{\ell}^4}{4} \beta_{k0}\theta_0 + 2 \frac{\bar{\ell}^2}{2} \bar{e} \\
&+ \bar{h}_2 (-\bar{\ell}^2 \beta_{k0} + \nu \frac{\bar{\ell}^3}{3} (\theta_0 + \phi_{k0}) + \nu \frac{\bar{\ell}^2}{2} (-2\lambda + \bar{e}\theta_0) > \frac{\Omega_1}{\Omega_i} \\
&+ \dot{\beta}^i_{1s} < -2 \frac{\bar{\ell}^3}{3} \zeta_{k0} - \nu \frac{\bar{\ell}^3}{3} \bar{e} - \bar{h}_2 (\beta_p \nu \frac{\bar{\ell}^3}{3} + \beta_{k0} \nu \frac{\bar{\ell}^3}{3} + 2 \frac{1}{2} \nu \bar{b} \frac{\bar{\ell}^2}{2} \sin\theta_0) > \frac{\Omega_1}{\Omega_i} \\
&+ \dot{\zeta}^i_{1c} < \nu \frac{\bar{\ell}^4}{4} \zeta_{k0}\, 2\theta_0 + \bar{h}_2 (-\bar{\ell}^2 \zeta_{k0} + \nu \frac{c_{d0}}{a} 2 \frac{\bar{\ell}^3}{3} + \nu \frac{\bar{\ell}^2}{2} \lambda\theta_0) > \frac{\Omega_1}{\Omega_i} \\
&+ \dot{\zeta}^i_{1s} < 2 \beta_{k0} \frac{\bar{\ell}^3}{3} + \nu \frac{\bar{\ell}^3}{3} \bar{e}\, 2\theta_0 + \bar{h}_2 \beta_p \nu \frac{\bar{\ell}^3}{3} 2\theta_0 > \frac{\Omega_1}{\Omega_i} \\
&+ \dot{\phi}^i_{1c} < + \bar{h}_2 \frac{1}{2} \nu \bar{b} \frac{\bar{\ell}^2}{2} \sin\theta_0 - \bar{g}_{ST} > \frac{\Omega_1}{\Omega_i} \\
&+ \ddot{\beta}^i_{1c} < -\frac{\bar{\ell}^3}{3} \zeta_{k0} - \bar{h}_2 \frac{1}{2} \nu \bar{b} \frac{\bar{\ell}^2}{2} \sin\theta_0 > (\frac{\Omega_1}{\Omega_i})^2 \\
&+ \ddot{\beta}^i_{1s} < -\frac{\bar{\ell}^2}{2} \bar{e} - \bar{h}_2 \beta_p \frac{\bar{\ell}^2}{2} > (\frac{\Omega_1}{\Omega_i})^2 \\
&+ \ddot{\zeta}^i_{1c} < \frac{\bar{\ell}^3}{3} \beta_{k0} + \bar{h}_2 \frac{\bar{\ell}^2}{2} > (\frac{\Omega_1}{\Omega_i})^2 \\
&+ \ddot{\theta}_x < -\bar{e} \frac{\bar{\ell}^2}{2} - \bar{h}_2 \beta_p \frac{\bar{\ell}^2}{2} - (\beta_p + \beta_{k0}) \bar{h}_2 \frac{\bar{\ell}^2}{2} \\
&- \bar{h}_2 (\beta_{k0} \frac{\bar{\ell}^2}{2} + 2\bar{\ell}) > (\frac{\Omega_1}{\Omega_i})^2 \\
&+ \dot{\theta}_x < -\nu \frac{\bar{\ell}^3}{3} \bar{e} - \bar{h}_2 \beta_p \nu \frac{\bar{\ell}^3}{3} - \bar{h}_2 \beta_{k0} \nu \frac{\bar{\ell}^3}{3} - 2 \frac{\bar{\ell}^3}{3} \zeta_{k0} > \frac{\Omega_1}{\Omega_i} \\
&+ \dot{\theta}_y < -2 \frac{\bar{\ell}^2}{2} \bar{e} + \nu \frac{\bar{\ell}^2}{2} \lambda\, 2\, \bar{h}_2 - 2 \frac{\bar{\ell}^2}{2} \beta_p \bar{h}_2 + \nu \frac{\bar{\ell}^4}{4} \zeta_{k0}
\end{aligned}
$$

$$
\begin{aligned}
&-\bar{h}_2\ \nu\ \frac{\bar{\ell}^3}{3}\ (\theta_0 + \phi_{k0}) \ > \ \frac{\Omega_1}{\Omega_i} \\
&+\ \ddot{\bar{R}}_{ys} < 2\ \bar{h}_2\ \ \bar{\ell} + \frac{\bar{\ell}^2}{2}\ \beta_{k0} > \ (\frac{\Omega_1}{\Omega_i})^2 \\
&+\ \frac{\ddot{\xi}_1}{R} <\eta_1\ (\ell_{Fi})\ (2\ \bar{h}_2\ \bar{\ell} + \frac{\bar{\ell}^2}{2}\ \beta_{k0}) \ > \ (\frac{\Omega_1}{\Omega_i})^2 \\
&+\ \ddot{\xi}_3 < -\ \bar{h}_2\ \eta_3\ (\ell_{Fi})\ (2\ \bar{h}_2\ \bar{\ell} + \frac{\bar{\ell}^2}{2}\ \beta_{k0}) \ > \ (\frac{\Omega_1}{\Omega_i})^2\ ]\ \}_i \\
&+\ \theta_x < -\ h_3\ P_Z^S + h_1\ W_{UN} + h_4\ W_{EN} > \\
&-\ I_{xx}\ \Omega_1^2\ \ \ddot{\theta}_x + I_{xy}\ \Omega_1^2\ \ \ddot{\theta}_y = 0
\end{aligned}
\tag{3.26}
$$

Pitch

$$
\begin{aligned}
&\frac{N}{2}\ \sum_{i=1}^{2}\ \{\ m\ \Omega_i^2\ R^3\ [\ \beta_{ic}^i < \nu\ \frac{\bar{\ell}^4}{4}\ \ \zeta_{k0} - \nu\ \frac{\bar{\ell}^4}{4}\ \ \beta_{k0}\theta_0 - \frac{\bar{\ell}^2}{2}\ \ \bar{e} \\
&+\ \bar{h}_2\ (-\ \nu\ \frac{\bar{\ell}^3}{3}\ (2\theta_0 + \phi_{k0}) + \frac{\bar{\ell}^2}{2}\ \ \beta_p + 2\ \frac{\bar{\ell}^2}{2}\ \ \beta_{k0} - \nu\ \frac{\bar{\ell}^2}{2}\ (-2\lambda + \bar{e}\theta_0) + \nu\ \frac{\bar{\ell}^2}{2}\ \lambda) \ > \\
&+\ \beta_{1s}^i < \nu\ \frac{c_{d0}}{a}\ \ \frac{\bar{\ell}^4}{4}\ + \nu\ \frac{\bar{\ell}^3}{3}\ \lambda\theta_0\ + \nu\ \frac{\bar{\ell}^3}{3}\ \ \bar{e} \\
&+\ \bar{h}_2\ (\ \nu\ \beta_p\ \frac{\bar{\ell}^3}{3} + \nu\ \beta_{k0}\ \ \frac{\bar{\ell}^3}{3} + \nu\ \frac{\bar{\ell}^3}{3}\ \ \zeta_{k0}\ \theta_0 + \frac{1}{2}\ \nu\ \bar{b}\ \ \frac{\bar{\ell}^2}{2}\ \sin\theta_0) \ > \\
&+\ \zeta_{1c}^i < -\ \nu\ \frac{\bar{\ell}^4}{4}\ \ \zeta_{k0}\ 2\theta_0 + \bar{h}_2\ (\ \bar{\ell}^2\ \zeta_{k0} - \nu\ \frac{c_{d0}}{a}\ \ \frac{\bar{\ell}^3}{3}\ \ 2 - \nu\ \frac{\bar{\ell}^2}{2}\ \lambda\ \theta_0) > \\
&+\ \zeta_{1s}^i < \nu\ \frac{\bar{\ell}^4}{4}\ (\theta_0 + \phi_{k0}) + \nu\ \frac{\bar{\ell}^3}{3}\ (\ -\lambda + 2\bar{e}\theta_0) - \nu\ \frac{\bar{\ell}^3}{3}\ \bar{e}\ 2\theta_0 - \frac{\bar{\ell}^3}{3}\ (\beta_p + 2\beta_{k0}) \\
&+\ \bar{h}_2\ \nu\ \frac{\bar{\ell}^3}{3}\ \ \theta_0\ (-\ \beta_p + \beta_{k0}) \ > \\
&+\ \phi_{1c}^i < \bar{g}_{ST} - \nu\ \frac{\bar{\ell}^3}{3}\ \ \bar{e} - \bar{h}_2\ \beta_p\ \nu\ \frac{\bar{\ell}^3}{3}\ \ - \bar{h}_2\ \ \frac{1}{2}\ \nu\ \bar{b}\ \ \frac{\bar{\ell}^2}{2}\ \ \sin\theta_0 \ > \\
&+\ \phi_{1s}^i < \nu\ \frac{\bar{\ell}^4}{4}\ \ \zeta_{k0} + \bar{h}_2\ \nu\ \frac{\bar{\ell}^2}{2}\ \lambda \ > \\
&+\ \dot{\beta}_{1c}^i < 2\ \frac{\bar{\ell}^3}{3}\ \ \zeta_{k0} + \nu\ \frac{\bar{\ell}^3}{3}\ \bar{e} + \bar{h}_2\ \beta_p\ \nu\ \frac{\bar{\ell}^3}{3} + \bar{h}_2\ \beta_{k0}\ \nu\ \frac{\bar{\ell}^3}{3} + 2\ \bar{h}_2\ \frac{1}{2}\ \nu\ \bar{b}\ \frac{\bar{\ell}^2}{2}\ \sin\theta_0 > \frac{\Omega_1}{\Omega_i}
\end{aligned}
$$

$$+ \dot{\beta}^{i}_{1s} < -\nu \frac{\bar{\ell}^4}{4} \zeta_{k0} + \nu \frac{\bar{\ell}^4}{4} \beta_{k0}\theta_0 + 2 \frac{\bar{\ell}^2}{2} \bar{e}$$

$$+ \bar{h}_2 \left(\nu \frac{\bar{\ell}^3}{3} (\theta_0 + \phi_{k0}) + \nu \frac{\bar{\ell}^2}{2} (-2\lambda + \bar{e}\theta_0) - \bar{\ell}^2 \beta_{k0} \right) > \frac{\Omega_1}{\Omega_i}$$

$$+ \dot{\zeta}^{i}_{1c} < -2 \frac{\bar{\ell}^3}{3} \beta_{k0} - \nu \frac{\bar{\ell}^3}{3} 2 \bar{e}\theta_0 - \bar{h}_2 \beta_p \nu \frac{\bar{\ell}^3}{3} 2\theta_0 > \frac{\Omega_1}{\Omega_i}$$

$$+ \dot{\zeta}^{i}_{1s} < \nu \frac{\bar{\ell}^4}{4} \zeta_{k0} 2\theta_0 - \bar{h}_2 \left(\bar{\ell}^2 \zeta_{k0} - \nu \frac{c_{d0}}{a} \frac{\bar{\ell}^3}{3} 2 - \nu \frac{\bar{\ell}^2}{2} \lambda \theta_0 \right) > \frac{\Omega_1}{\Omega_i}$$

$$+ \dot{\phi}^{i}_{1s} < -\bar{g}_{ST} + \bar{h}_2 \frac{1}{2} \nu \bar{b} \frac{\bar{\ell}^2}{2} \sin\theta_0 > \frac{\Omega_1}{\Omega_i}$$

$$+ \ddot{\beta}^{i}_{1c} < \frac{\bar{\ell}^2}{2} \bar{e} + \bar{h}_2 \beta_p \frac{\bar{\ell}^2}{2} > \left(\frac{\Omega_1}{\Omega_i} \right)^2$$

$$+ \ddot{\beta}^{i}_{1s} < -\frac{\bar{\ell}^3}{3} \zeta_{k0} - \bar{h}_2 \frac{1}{2} \nu \bar{b} \frac{\bar{\ell}^2}{2} \sin\theta_0 > \left(\frac{\Omega_1}{\Omega_i} \right)^2$$

$$+ \ddot{\zeta}^{i}_{1s} < \frac{\bar{\ell}^3}{3} \beta_{k0} + \bar{h}_2 \frac{\bar{\ell}^2}{2} > \left(\frac{\Omega_1}{\Omega_i} \right)^2$$

$$+ \beta^{i}_{M} < 2 \bar{\ell}_{Fi} \left(\nu \frac{\bar{\ell}^3}{3} \zeta_{k0} + \nu \frac{\bar{\ell}^3}{3} \beta_p \theta_0 \right) >$$

$$+ \zeta^{i}_{M} < 2 \bar{\ell}_{Fi} \nu \frac{\bar{\ell}^3}{3} (\beta_p + \beta_{k0}) >$$

$$+ \phi^{i}_{M} < 2 \bar{\ell}_{Fi} \left(-\nu \frac{\bar{\ell}^3}{3} - \frac{\bar{\ell}^2}{2} \nu 2 \bar{e} \right) >$$

$$+ \dot{\beta}^{i}_{M} < 2 \bar{\ell}_{Fi} \left(\nu \frac{\bar{\ell}^3}{3} + \nu \frac{\bar{\ell}^2}{2} \bar{e} \right) > \frac{\Omega_1}{\Omega_i}$$

$$+ \dot{\zeta}^{i}_{M} < 2 \bar{\ell}_{Fi} \left(\frac{\bar{\ell}^2}{2} \beta_p - 2 \nu \frac{\bar{\ell}^3}{3} (\theta_0 + \phi_{k0}) + \nu \frac{\bar{\ell}^2}{2} \lambda - \beta_p \bar{\ell}^2 \right) > \frac{\Omega_1}{\Omega_i}$$

$$+ \dot{\phi}^{i}_{M} < 2 \bar{\ell}_{Fi} \left(-\nu \frac{\bar{\ell}^2}{2} \bar{b} - \frac{1}{2} \nu \bar{b} \frac{\bar{\ell}^2}{2} \cos\theta_0 \right) > \frac{\Omega_1}{\Omega_i}$$

$$+ \ddot{\beta}^{i}_{M} < 2 \bar{\ell}_{Fi} \left(\frac{\bar{\ell}^2}{2} + \frac{1}{2} \nu \bar{b} \frac{\bar{\ell}^2}{2} \cos\theta_0 \right) > \left(\frac{\Omega_1}{\Omega_i} \right)^2$$

$$+ \ddot{\theta}_x < -\frac{\bar{\ell}^3}{3} \zeta_{k0} > \left(\frac{\Omega_1}{\Omega_i} \right)^2$$

$$+ \dot{\theta}_x < -\nu \frac{\bar{\ell}^4}{4} \zeta_{k0} + \frac{\bar{\ell}^2}{2} 2 \bar{e} + \bar{h}_2 \left(\frac{\bar{\ell}^2}{2} 2\beta_p + \nu \frac{\bar{\ell}^3}{3} (\theta_0 + \phi_{k0}) - \nu \frac{\bar{\ell}^2}{2} 2\lambda \right) > \frac{\Omega_1}{\Omega_i}$$

$$+ \ddot{\theta}_y < -\frac{\bar{\ell}^2}{2}\ \bar{e} - \bar{h}_2\ \frac{\bar{\ell}^2}{2}\ (\beta_p + \beta_{k0}) - \bar{h}_2\ \frac{\bar{\ell}^2}{2}\ \beta_p$$

$$+ \bar{h}_2\ (-\frac{\bar{\ell}^2}{2}\ \beta_{k0} - 2\ \bar{\ell}\ \bar{h}_2) - \bar{\ell}_{Fi}\ 2\ \bar{\ell}\ \bar{\ell}_{Fi} > (\frac{\Omega_1}{\Omega_i})^2$$

$$+ \dot{\theta}_y < -2\ \frac{\bar{\ell}^3}{3}\ \zeta_{k0} - \nu\ \frac{\bar{\ell}^3}{3}\ \bar{e} - \bar{h}_2\ \beta_p\ \nu\ \frac{\bar{\ell}^3}{3} - \bar{\ell}_{Fi}\ \nu\ \frac{\bar{\ell}^2}{2}\ 2\ \bar{\ell}_{Fi} > \frac{\Omega_1}{\Omega_i}$$

$$+ \ddot{\bar{R}}_{xs} < -2\bar{\ell}\ \bar{h}_2 - \frac{\bar{\ell}^2}{2}\ \beta_{k0} > (\frac{\Omega_1}{\Omega_i})^2$$

$$+ \frac{\ddot{\xi}_2}{R} < -\bar{h}_2\ \eta_{2,x}\ (\ell_{Fi})\ R\ (-\frac{\bar{\ell}^2}{2}\ \beta_{k0} - 2\ \bar{\ell}\ \bar{h}_2) + \eta_2\ (\ell_{Fi})\ 2\bar{\ell}\ \bar{\ell}_{Fi} > (\frac{\Omega_1}{\Omega_i})^2$$

$$+ \frac{\dot{\xi}_2}{R} < \eta_2\ (\ell_{Fi})\ 2\ \nu\ \frac{\bar{\ell}^2}{2}\ \bar{\ell}_{Fi} > (\frac{\Omega_1}{\Omega_i})\ ]\ \}_i$$

$$+ \theta_y < -h_3\ P_Z^S + h_1\ W_{UN} + h_4\ W_{EN} + h_5\ W_S >$$

$$- I_{yy}\ \Omega_1^2\ \ddot{\theta}_y + I_{yx}\ \Omega_1^2\ \ddot{\theta}_x = 0 \qquad (3.27)$$

Elastic Mode Equations of the Supporting Structure

Symmetric Bending in X-Y plane (Horizontal)

$$\frac{N}{2}\sum_{i=1}^{2}[\ \eta_1(\ell_{Fi})\ m\ \Omega_i^2\ R^2\ \{\ \beta_{1c}^i < -\nu\beta_p\ \frac{\bar{\ell}^3}{3} - \nu\beta_{k0}\ \frac{\bar{\ell}^3}{3} - \nu\ \frac{\bar{\ell}^3}{3}\ \zeta_{k0}\theta_0 - \frac{1}{2}\ \nu\bar{b}\ \frac{\bar{\ell}^2}{2}\ \sin\theta_0 >$$

$$+ \beta_{1s}^i < \frac{\bar{\ell}^2}{2}\ (\beta_p + 2\beta_{k0}) - \nu\frac{\bar{\ell}^3}{3}\ (2\theta_0 + \phi_{k0}) + \nu\frac{\bar{\ell}^2}{2}\ (2\lambda - \bar{e}\theta_0) + \nu\ \frac{\bar{\ell}^2}{2}\ \lambda >$$

$$+ \zeta_{1c}^i < \nu\ \frac{\bar{\ell}^3}{3}\ (\beta_p - \beta_{k0})\ \theta_0 >$$

$$+ \zeta_{1s}^i < 2\ \frac{\bar{\ell}^2}{2}\ \zeta_{k0} - 2\ \nu\ \frac{c_{d0}}{a}\ \frac{\bar{\ell}^3}{3} - \nu\ \frac{\bar{\ell}^2}{2}\ \lambda\ \theta_0 >$$

$$+ \phi_{1c}^i < -\nu\ \frac{\bar{\ell}^2}{2}\ \lambda >$$

$$+ \phi_{1s}^i < -\nu\ \frac{\bar{\ell}^3}{3}\ \beta_p - \frac{1}{2}\ \nu\ \bar{b}\ \frac{\bar{\ell}^2}{2}\ \sin\theta_0 >$$

$$+ \dot{\beta}_{1c}^i < 2\ \frac{\bar{\ell}^2}{2}\ \beta_{k0} - \nu\ \frac{\bar{\ell}^3}{3}\ (\theta_0 + \phi_{k0}) + \nu\ \frac{\bar{\ell}^2}{2}\ (2\ \lambda - \bar{e}\theta_0) > \frac{\Omega_1}{\Omega_i}$$

$$+ \dot{\beta}^{i}_{1s} < \nu \frac{\bar{\ell}^3}{3} \beta_p + \nu \frac{\bar{\ell}^3}{3} \beta_{k0} + \frac{1}{2} \nu \bar{b} \frac{\bar{\ell}^2}{2} \sin\theta_0 \, 2 > \frac{\Omega_1}{\Omega_i}$$

$$+ \dot{\zeta}^{i}_{1c} < 2 \frac{\bar{\ell}^2}{2} \zeta_{k0} - 2 \nu \frac{c_{d0}}{a} \frac{\bar{\ell}^3}{3} - \nu \frac{\bar{\ell}^2}{2} \lambda \theta_0 > \frac{\Omega_1}{\Omega_i}$$

$$+ \dot{\zeta}^{i}_{1s} < - \nu \frac{\bar{\ell}^3}{3} 2 \beta_p \theta_0 > \frac{\Omega_1}{\Omega_i}$$

$$+ \dot{\phi}^{i}_{1c} < - \frac{1}{2} \nu \bar{b} \frac{\bar{\ell}^2}{2} \sin\theta_0 > \frac{\Omega_1}{\Omega_i}$$

$$+ \ddot{\beta}^{i}_{1c} < \frac{1}{2} \nu \bar{b} \frac{\bar{\ell}^2}{2} \sin\theta_0 > \left(\frac{\Omega_1}{\Omega_i} \right)^2$$

$$+ \ddot{\beta}^{i}_{1s} < \frac{\bar{\ell}^2}{2} \beta_p > \left(\frac{\Omega_1}{\Omega_i} \right)^2$$

$$+ \ddot{\zeta}^{i}_{1c} < - \frac{\bar{\ell}^2}{2} > \left(\frac{\Omega_1}{\Omega_i} \right)^2$$

$$+ \ddot{\theta}_x < \frac{\bar{\ell}^2}{2} \beta_p + \frac{\bar{\ell}^2}{2} (\beta_p + \beta_{k0}) > \left(\frac{\Omega_1}{\Omega_i} \right)^2$$

$$+ \dot{\theta}_x < \nu \frac{\bar{\ell}^3}{3} \beta_p + \nu \frac{\bar{\ell}^3}{3} \beta_{k0} > \frac{\Omega_1}{\Omega_i}$$

$$+ \dot{\theta}_y < 2 \beta_p \frac{\bar{\ell}^2}{2} + \nu \frac{\bar{\ell}^3}{3} (\theta_0 + \phi_{k0}) - \nu \frac{\bar{\ell}^2}{2} 2 \lambda > \frac{\Omega_1}{\Omega_i}$$

$$+ \ddot{\bar{R}}_{ys} < - 2 \bar{\ell} > \left(\frac{\Omega_1}{\Omega_i} \right)^2$$

$$+ \frac{\ddot{\xi}_1}{R} < - \eta_1 (\ell_{Fi}) 2 \bar{\ell} > \left(\frac{\Omega_1}{\Omega_i} \right)^2$$

$$+ \ddot{\xi}_3 < \bar{h}_2 \eta_3 (\ell_{Fi}) 2 \bar{\ell} > \left(\frac{\Omega_1}{\Omega_i} \right)^2 \}$$

$$+ 2 \eta_{1,x} (\ell_{Fi}) m \Omega_i^2 R^3 \{ \zeta^{i}_{M} < \frac{\bar{\ell}^2}{2} + \nu \frac{\bar{\ell}^4}{4} \beta_p \theta_0 >$$

$$+ \dot{\beta}^{i}_{M} < - \nu \frac{\bar{\ell}^3}{3} \theta_0 \bar{e} > \frac{\Omega_1}{\Omega_i}$$

$$+ \dot{\phi}^{i}_{M} < - \beta_p \bar{g}_{ST} > \frac{\Omega_1}{\Omega_i}$$

$$+ \ddot{\zeta}^{i}_{M} < - \frac{\bar{\ell}^2}{2} \bar{e} > \left(\frac{\Omega_1}{\Omega_i} \right)^2 \} \,]_i$$

$$+ \theta_x < \eta_1 (0_s) P^{S}_{Z} - \eta_1 (\ell_{F1}) W_{F1} - \eta_1 (\ell_{F1}) W_{F2} - \eta_1 (0_s) W_{EN} - \eta_1 (0_s) W_{UN}$$

$$- \int_{\ell_{F1}}^{\ell_{F2}} \eta_1(x)\, W_s(x)\, dx >$$

$$- M_{SBXY}\, \Omega_1^2\, \ddot{\xi}_1 - K_{SBXY}\, \xi_1 = 0 \qquad (3.28)$$

Symmetric Bending in X-Z plane (Vertical)

$$\frac{N}{2} \sum_{i=1}^{2} [\, \eta_{2,x}\, m\Omega_1^2\, R^3 \{ \beta_{1c}^i < \nu \frac{\bar{\ell}^4}{4}\, \zeta_{k0} - \nu \frac{\bar{\ell}^4}{4}\, \beta_{k0}\theta_0 - \frac{\bar{\ell}^2}{2}\, \bar{e}$$

$$- \bar{h}_2 (\nu \frac{\bar{\ell}^3}{3} (2\theta_0 + \phi_{k0}) - \frac{\bar{\ell}^2}{2} \beta_p - \bar{\ell}^2\, \beta_{k0} \cdot \frac{\bar{\ell}^2}{2} (-2\lambda + \bar{e}\theta_0) - \nu \frac{\bar{\ell}^2}{2} \lambda) >$$

$$+ \beta_{1s}^i < \nu \frac{\bar{\ell}^4}{4}\, \frac{c_{d0}}{a} + \nu \frac{\bar{\ell}^3}{3} \lambda\, \theta_0 + \nu \frac{\bar{\ell}^3}{3}\, \bar{e}$$

$$+ \bar{h}_2 (\beta_p\, \nu \frac{\bar{\ell}^3}{3} + \beta_{k0}\, \nu \frac{\bar{\ell}^3}{3} + \nu \frac{\bar{\ell}^3}{3}\, \zeta_{k0}\theta_0 + \frac{1}{2}\, \nu\, \bar{b}\, \frac{\bar{\ell}^2}{2}\, \sin\theta_0) >$$

$$+ \zeta_{1c}^i < - \nu \frac{\bar{\ell}^4}{4}\, \zeta_{k0}\, 2\theta_0 + \bar{h}_2 (\bar{\ell}^2\, \zeta_{k0} - \nu \frac{c_{d0}}{a}\, 2\, \frac{\bar{\ell}^3}{3} - \nu \frac{\bar{\ell}^2}{2} \lambda\, \theta_0) >$$

$$+ \zeta_{1s}^i < - \nu \frac{\bar{\ell}^3}{3}\, \bar{e}\, 2\theta_0 + \nu \frac{\bar{\ell}^4}{4} (\theta_0 + \phi_{k0}) + \nu \frac{\bar{\ell}^3}{3} (-\lambda + 2\, \bar{e}\theta_0)$$

$$- \frac{\bar{\ell}^3}{3}\, (\beta_p + 2\beta_{k0}) + \bar{h}_2\, \nu \frac{\bar{\ell}^3}{3}\, \theta_0\, (-\beta_p + \beta_{k0}) >$$

$$+ \phi_{1c}^i < \bar{g}_{ST} - \nu \frac{\bar{\ell}^3}{3}\, \bar{e} - \bar{h}_2 (\beta_p\, \nu \frac{\bar{\ell}^3}{3} + \frac{1}{2}\, \nu\, \bar{b}\, \frac{\bar{\ell}^2}{2} \sin\theta_0) >$$

$$+ \phi_{1s}^i < \nu \frac{\bar{\ell}^4}{4}\, \zeta_{k0} + \bar{h}_2\, \nu\, \frac{\bar{\ell}^2}{2} \lambda >$$

$$+ \dot{\beta}_{1c}^i < 2 \frac{\bar{\ell}^3}{3}\, \zeta_{k0} + \nu \frac{\bar{\ell}^3}{3}\, \bar{e} + \bar{h}_2 (\beta_p\, \nu \frac{\bar{\ell}^3}{3} + \beta_{k0}\, \nu \frac{\bar{\ell}^3}{3} + 2\, \frac{1}{2}\, \nu\, \bar{b}\, \frac{\bar{\ell}^2}{2} \sin\theta_0) > \frac{\Omega_1}{\Omega_i}$$

$$+ \dot{\beta}_{1s}^i < - \nu \frac{\bar{\ell}^4}{4}\, \zeta_{k0} + \nu \frac{\bar{\ell}^4}{4}\, \beta_{k0}\theta_0 + 2 \frac{\bar{\ell}^2}{2}\, \bar{e} - \bar{h}_2\, \bar{\ell}^2\, \beta_{k0}$$

$$+ \bar{h}_2\, \nu \frac{\bar{\ell}^3}{3} (\theta_0 + \phi_{k0}) + \bar{h}_2\, \nu \frac{\bar{\ell}^2}{2} (-2\lambda + \bar{e}\theta_0) > \frac{\Omega_1}{\Omega_i}$$

$$+ \dot{\zeta}_{1c}^i < - 2 \frac{\bar{\ell}^3}{3}\, \beta_{k0} - \nu \frac{\bar{\ell}^3}{3}\, \bar{e}\, 2\theta_0 - \bar{h}_2\, \beta_p\, \nu \frac{\bar{\ell}^3}{3}\, 2\theta_0 > \frac{\Omega_1}{\Omega_i}$$

$$+ \dot{\phi}_{1s}^i < - \bar{g}_{ST} + \bar{h}_2\, \frac{1}{2}\, \nu\, \bar{b}\, \frac{\bar{\ell}^2}{2}\, \sin\theta_0 > \frac{\Omega_1}{\Omega_i}$$

$$+ \ddot{\beta}^{i}_{1c} < \frac{\bar{\ell}^2}{2}\bar{e} + \bar{h}_2\,\beta_p\,\frac{\bar{\ell}^2}{2} > \left(\frac{\Omega_1}{\Omega_i}\right)^2$$

$$+ \ddot{\beta}^{i}_{1s} < -\bar{h}_2\,\frac{1}{2}\,\nu\,\bar{b}\,\frac{\bar{\ell}^2}{2}\,\sin\theta_0 - \frac{\bar{\ell}^3}{3}\,\zeta_{k0} > \left(\frac{\Omega_1}{\Omega_i}\right)^2$$

$$+ \ddot{\zeta}^{i}_{1s} < \frac{\bar{\ell}^3}{3}\,\beta_{k0} + \bar{h}_2\,\frac{\bar{\ell}^2}{2} > \left(\frac{\Omega_1}{\Omega_i}\right)^2$$

$$+ \ddot{\theta}_x < -\frac{\bar{\ell}^3}{3}\,\zeta_{k0} > \left(\frac{\Omega_1}{\Omega_i}\right)^2$$

$$+ \dot{\theta}_x < -\nu\frac{\bar{\ell}^4}{4}\,\zeta_{k0} + 2\,\frac{\bar{\ell}^2}{2}\,\bar{e} + \bar{h}_2\left(2\,\frac{\bar{\ell}^2}{2}\,\beta_p + \nu\,\frac{\bar{\ell}^3}{3}\,(\theta_0 + \phi_{k0}) - 2\,\nu\,\frac{\bar{\ell}^2}{2}\,\lambda\right) > \frac{\Omega_1}{\Omega_i}$$

$$+ \ddot{\theta}_y < -\frac{\bar{\ell}^2}{2}\,\bar{e} - \bar{h}_2\,\beta_p\,\frac{\bar{\ell}^2}{2} - \bar{h}_2\,\frac{\bar{\ell}^2}{2}\,(\beta_p + \beta_{k0})$$

$$+ \bar{h}_2\left(-\frac{\bar{\ell}^2}{2}\,\beta_{k0} - 2\,\bar{\ell}\,\bar{h}_2\right) > \left(\frac{\Omega_1}{\Omega_i}\right)^2$$

$$+ \dot{\theta}_y < -2\,\frac{\bar{\ell}^3}{3}\,\zeta_{k0} - \nu\,\frac{\bar{\ell}^3}{3}\,\bar{e} - \bar{h}_2\,\beta_p\,\nu\,\frac{\bar{\ell}^3}{3} - \bar{h}_2\,\beta_{k0}\,\nu\,\frac{\bar{\ell}^3}{3} > \frac{\Omega_1}{\Omega_i}$$

$$+ \ddot{\bar{R}}_{xs} < -\frac{\bar{\ell}^2}{2}\,\beta_{k0} - 2\,\bar{h}_2\,\bar{\ell} > \left(\frac{\Omega_1}{\Omega_i}\right)^2$$

$$+ \frac{\ddot{\xi}_2}{R} < \bar{h}_2\;\eta_{2,x}\,(\ell_{Fi})\,R\left(\frac{\bar{\ell}^2}{2}\,\beta_{k0} + 2\,\bar{h}_2\,\bar{\ell}\right) > \left(\frac{\Omega_1}{\Omega_i}\right)^2 \}$$

$$+ 2\,\eta_2\,(\ell_{Fi})\,m\Omega_i^2R^2\;\{\,\beta^{i}_{M} < -\nu\,\frac{\bar{\ell}^3}{3}\,\zeta_{k0} - \nu\,\frac{\bar{\ell}^3}{3}\,\beta_p\theta_0 >$$

$$+ \zeta^{i}_{M} < -\nu\,\frac{\bar{\ell}^3}{3}\,(\beta_p + \beta_{k0}) >$$

$$+ \phi^{i}_{M} < +\nu\,\frac{\bar{\ell}^3}{3} + \nu\,\frac{\bar{\ell}^2}{2}\;2\,\bar{e} >$$

$$+ \dot{\beta}^{i}_{M} < -\nu\,\frac{\bar{\ell}^3}{3} - \nu\,\frac{\bar{\ell}^2}{2}\,\bar{e} > \frac{\Omega_1}{\Omega_i}$$

$$+ \dot{\zeta}^{i}_{M} < 2\,\nu\,\frac{\bar{\ell}^3}{3}\,(\theta_0 + \phi_{k0}) - \nu\,\frac{\bar{\ell}^2}{2}\,\lambda > \frac{\Omega_1}{\Omega_i}$$

$$+ \dot{\phi}^{i}_{M} < \nu\,\frac{\bar{\ell}^2}{2}\,\bar{b} + \frac{1}{2}\,\nu\,\bar{b}\,\frac{\bar{\ell}^2}{2}\,\cos\theta_0 > \frac{\Omega_1}{\Omega_i}$$

$$+ \ddot{\beta}^{i}_{M} < -\frac{\bar{\ell}^2}{2} - \frac{1}{2}\,\nu\,\bar{b}\,\frac{\bar{\ell}^2}{2}\,\cos\theta_0 > \left(\frac{\Omega_1}{\Omega_1}\right)^2$$

$$+ \ddot{\theta}_y < \bar{\ell}\ \bar{\ell}_{Fi} > \left(\frac{\Omega_1}{\Omega_i}\right)^2$$

$$+ \dot{\theta}_y < \nu\frac{\bar{\ell}^2}{2}\ \bar{\ell}_{Fi} > \frac{\Omega_1}{\Omega_i}$$

$$+ \frac{\ddot{\xi}_2}{R} < -\eta_2\ (\ell_{Fi})\ \bar{\ell}\ > \left(\frac{\Omega_1}{\Omega_i}\right)^2$$

$$+ \frac{\dot{\xi}_2}{R} < -\eta_2\ (\ell_{Fi})\ \nu\frac{\bar{\ell}^2}{2} > \frac{\Omega_1}{\Omega_i}\ \}\ ]_i$$

$$+ \theta_y < (-h_3 P_Z^S + h_1 W_{UN} + h_4 W_{EN})\ \eta_{2,x}\ (0_s)$$

$$- M_{SBXZ}\Omega_1^2\ \ddot{\xi}_2 - K_{SBXZ}\xi_2 = 0 \qquad (3.29)$$

Torsion

$$\frac{N}{2}\sum_{i=1}^{2}[\ \eta_3(\ell_{Fi})\ m\Omega_i^2R^3\ \{\ \beta_{1c}^i < \nu\frac{\bar{\ell}^4}{4}\ \frac{c_{d0}}{a} + \nu\frac{\bar{\ell}^3}{3}\lambda\ \theta_0 + \nu\frac{\bar{\ell}^3}{3}\ \bar{e}$$

$$+ \bar{h}_2\ (\beta_p\ \nu\frac{\bar{\ell}^3}{3} + \beta_{k0}\ \nu\frac{\bar{\ell}^3}{3} + \nu\frac{\bar{\ell}^3}{3}\ \theta_0\zeta_{k0} + \frac{1}{2}\nu\ \bar{b}\ \frac{\bar{\ell}^2}{2}\ \sin\theta_0) >$$

$$+ \beta_{1s}^i < -\nu\frac{\bar{\ell}^4}{4}\ \zeta_{k0} + \nu\frac{\bar{\ell}^4}{4}\ \beta_{k0}\theta_0 + \frac{\bar{\ell}^2}{2}\ \bar{e}$$

$$+ \bar{h}_2\ (\nu\frac{\bar{\ell}^3}{3}(2\theta_0 + \phi_{k0}) + \nu\frac{\bar{\ell}^2}{2}(-2\lambda + \bar{e}\theta_0) - \nu\frac{\bar{\ell}^2}{2}\lambda - \bar{\ell}^2\ \beta_{k0} - \frac{\bar{\ell}^2}{2}\ \beta_p) >$$

$$+ \zeta_{1c}^i < \nu\frac{\bar{\ell}^4}{4}(\theta_0 + \phi_{k0}) + \nu\frac{\bar{\ell}^3}{3}(-\lambda + 2\ \bar{e}\theta_0) - \frac{\bar{\ell}^3}{3}(2\beta_{k0} + \beta_p)$$

$$- \nu\frac{\bar{\ell}^3}{3}\ 2\ \bar{e}\theta_0 + \bar{h}_2\ \nu\frac{\bar{\ell}^3}{3}\ \theta_0\ (\beta_{k0} - \beta_p) >$$

$$+ \zeta_{1s}^i < \nu\frac{\bar{\ell}^4}{4}\ \zeta_{k0}\ 2\theta_0 - \bar{h}_2\ (\bar{\ell}^2\ \zeta_{k0} - \nu\frac{c_{d0}}{a}\ \frac{\bar{\ell}^3}{3}\ 2 - \nu\frac{\bar{\ell}^2}{2}\lambda\ \theta_0) >$$

$$+ \phi_{1c}^i < \nu\frac{\bar{\ell}^4}{4}\ \zeta_{k0} + \bar{h}_2\ \nu\frac{\bar{\ell}^2}{2}\lambda >$$

$$+ \phi_{1s}^i < -\bar{g}_{ST} + \nu\frac{\bar{\ell}^3}{3}\bar{e} + \bar{h}_2\ (\beta_p\ \nu\frac{\bar{\ell}^3}{3} + \frac{1}{2}\nu\ \bar{b}\ \frac{\bar{\ell}^2}{2}\ \sin\theta_0) >$$

$$+ \dot{\beta}_{1c}^i < -\nu\frac{\bar{\ell}^4}{4}\ \beta_{k0} + \nu\frac{\bar{\ell}^4}{4}\ \beta_{k0}\theta_0 + 2\frac{\bar{\ell}^2}{2}\ \bar{e}$$

$$+ \bar{h}_2 \left(- \bar{\ell}^2 \beta_{k0} + \nu \frac{\bar{\ell}^3}{3} (\theta_0 + \phi_{k0}) + \nu \frac{\bar{\ell}^2}{2} (- 2\lambda + \bar{e}\theta_0)\right) > \frac{\Omega_1}{\Omega_i}$$

$$+ \dot{\beta}^i_{1s} < - 2 \frac{\bar{\ell}^3}{3} \zeta_{k0} - \nu \bar{e} \frac{\bar{\ell}^3}{3} - \bar{h}_2 \left(\beta_p \nu \frac{\bar{\ell}^3}{3} + \beta_{k0} \nu \frac{\bar{\ell}^3}{3} + 2 \frac{1}{2} \nu \bar{b} \frac{\bar{\ell}^2}{2} \sin\theta_0\right) > \frac{\Omega_1}{\Omega_i}$$

$$+ \dot{\zeta}^i_{1c} < \nu \frac{\bar{\ell}^4}{4} 2\zeta_{k0}\theta_0 - \bar{h}_2 \left(\bar{\ell}^2 \zeta_{k0} - \nu \frac{c_{d0}}{a} \frac{\bar{\ell}^3}{3} 2 - \nu \frac{\bar{\ell}^2}{2} \lambda \theta_0\right) > \frac{\Omega_1}{\Omega_i}$$

$$+ \dot{\zeta}^i_{1s} < 2 \frac{\bar{\ell}^3}{3} \beta_{k0} + \nu \frac{\bar{\ell}^3}{3} 2 \bar{e}\theta_0 + \bar{h}_2 \beta_p \nu \frac{\bar{\ell}^3}{3} 2\theta_0 > \frac{\Omega_1}{\Omega_i}$$

$$+ \dot{\phi}^i_{1c} < - \bar{g}_{ST} + \bar{h}_2 \frac{1}{2} \nu \bar{b} \frac{\bar{\ell}^2}{2} \sin\theta_0 > \frac{\Omega_1}{\Omega_i}$$

$$+ \ddot{\beta}^i_{1c} < - \frac{\bar{\ell}^3}{3} \zeta_{k0} - \bar{h}_2 \frac{1}{2} \nu \bar{b} \frac{\bar{\ell}^2}{2} \sin\theta_0 > \left(\frac{\Omega_1}{\Omega_i}\right)^2$$

$$+ \ddot{\beta}^i_{1s} < - \frac{\bar{\ell}^2}{2} \bar{e} - \bar{h}_2 \beta_p \frac{\bar{\ell}^2}{2} > \left(\frac{\Omega_1}{\Omega_i}\right)^2$$

$$+ \ddot{\zeta}^i_{1c} < \frac{\bar{\ell}^3}{3} \beta_{k0} + \bar{h}_2 \frac{\bar{\ell}^2}{2} > \left(\frac{\Omega_1}{\Omega_i}\right)^2$$

$$+ \ddot{\theta}_x < - \frac{\bar{\ell}^2}{2} \bar{e} - \bar{h}_2 \frac{\bar{\ell}^2}{2} \beta_p - \bar{h}_2 \frac{\bar{\ell}^2}{2} (\beta_p + \beta_{k0})$$

$$- \bar{h}_2 \left(\frac{\bar{\ell}^2}{2} \beta_{k0} + 2 \bar{h}_2 \bar{\ell}\right) > \left(\frac{\Omega_1}{\Omega_i}\right)^2$$

$$+ \dot{\theta}_x < - 2 \frac{\bar{\ell}^3}{3} \zeta_{k0} - \nu \frac{\bar{\ell}^3}{3} \bar{e} - \bar{h}_2 \nu \frac{\bar{\ell}^3}{3} \beta_p - \bar{h}_2 \nu \frac{\bar{\ell}^3}{3} \beta_{k0} > \frac{\Omega_1}{\Omega_i}$$

$$+ \ddot{\theta}_y < \frac{\bar{\ell}^3}{3} \zeta_{k0} > \left(\frac{\Omega_1}{\Omega_i}\right)^2$$

$$+ \dot{\theta}_y < \nu \frac{\bar{\ell}^4}{4} \zeta_{k0} - \frac{\bar{\ell}^2}{2} 2 \bar{e} - \bar{h}_2 \left(\frac{\bar{\ell}^2}{2} 2\beta_p + \nu \frac{\bar{\ell}^3}{3} (\theta_0 + \phi_{k0}) - \nu \frac{\bar{\ell}^2}{2} 2\lambda\right) > \frac{\Omega_1}{\Omega_i}$$

$$+ \ddot{\bar{R}}_{ys} < \frac{\bar{\ell}^2}{2} \beta_{k0} + 2 \bar{h}_2 \bar{\ell} > \left(\frac{\Omega_1}{\Omega_i}\right)^2$$

$$+ \frac{\ddot{\xi}_1}{R} < \eta_1 (\ell_{Fi}) \left(\frac{\bar{\ell}^2}{2} \beta_{k0} + 2 \bar{h}_2 \bar{\ell}\right) > \left(\frac{\Omega_1}{\Omega_i}\right)^2$$

$$+ \ddot{\xi}_3 < - \bar{h}_2 \eta_3 (\ell_{Fi}) \left(\frac{\bar{\ell}^2}{2} \beta_{k0} + 2 \bar{h}_2 \bar{\ell}\right) > \left(\frac{\Omega_1}{\Omega_i}\right)^2 \}]_i$$

$$+ \theta_x < \left(- h_3 P^S_Z + h_1 W_{UN} + h_4 W_{EN}\right) \eta_3 (0_s) >$$

$$- M_{ST} \Omega_1^2 \ddot{\xi}_3 - K_{ST} \xi_3 = 0 \qquad (3.30)$$

In the relatively long set of equations presented in the preceding pages, Eqs. (3.1) - (3.6) represent the equilibrium position or trim equations, while Eqs. (3.7) - (3.30) are the linearized stability equations written in the rotor-plane or multiblade coordinates. The trim equations are the same for both articulated and hingeless rotors. For the case of hingeless rotors, the stability equations are given by Eqs. (3.7) - (3.25) and for the case of articulated rotors, the stability equations are given by Eqs. (3.7) - (3.20) and (3.26) - (3.30). These equations can be used to analyze the aeroelastic and aeromechanical stability of a twin rotor system, with a buoyant envelope (Fig. 2), in hover.

The stability equations can be written more compactly by using a matrix representation

$$[M]\{\ddot{q}\} + [C]\{\dot{q}\} + [K]\{q\} = 0 \qquad (3.31)$$

where [M], [C], [K] are constant coefficient matrices in which the elements are dependent on the equilibrium quantities, and {q} is the generalized coordinate vector, which can be written as

$$\{q\} = \begin{Bmatrix} \tilde{q}_1 \\ \tilde{q}_2 \\ \tilde{q}_3 \\ \tilde{q}_4 \\ \tilde{q}_5 \\ \tilde{q}_6 \end{Bmatrix}$$

For a four bladed rotor, the value of n, in the blade equations, is 1. The corresponding generalized coordinates are

$$\{\tilde{q}_1\} = \begin{Bmatrix} \beta_M^1 \\ \beta_{1c}^1 \\ \beta_{1s}^1 \\ \zeta_M^1 \\ \zeta_{1c}^1 \\ \zeta_{1s}^1 \\ \phi_M^1 \\ \phi_{1c}^1 \\ \phi_{1s}^1 \end{Bmatrix} \qquad \{\tilde{q}_2\} = \begin{Bmatrix} \beta_M^2 \\ \beta_{1c}^2 \\ \beta_{1s}^2 \\ \zeta_M^2 \\ \zeta_{1c}^2 \\ \zeta_{1s}^2 \\ \phi_M^2 \\ \phi_{1c}^2 \\ \phi_{1s}^2 \end{Bmatrix}$$

$$\{\tilde{q}_3\} = \begin{Bmatrix} \bar{R}_{xs} \\ \bar{R}_{ys} \\ \theta_x \\ \theta_y \end{Bmatrix} \qquad \{\tilde{q}_4\} = \begin{Bmatrix} \zeta_{1/R} \\ \zeta_{2/R} \\ \zeta_3 \end{Bmatrix}$$

$$\{\tilde{q}_5\} = \begin{Bmatrix} \beta_{-M}^1 \\ \zeta_{-M}^1 \\ \phi_{-M}^1 \end{Bmatrix} \qquad \{\tilde{q}_6\} = \begin{Bmatrix} \beta_{-M}^2 \\ \zeta_{-M}^2 \\ \phi_{-M}^2 \end{Bmatrix}$$

It can be seen from the equations associated with alternating modes, Eq. (3.8), (3.12) and (3.16), that these equations are decoupled from other degrees of freedom. Similarly, the equations corresponding to the other degrees of freedom do not depend on the alternating modes. Hence, Eqs. (3.8), (3.12) and (3.16) can be solved independently, thereby reducing the size of the matrices [M], [C] and [K]. Based on this property of the alternating modes, Eq. (3.31) can be split into three groups of equations, namely:

$$[M_1] \begin{Bmatrix} \ddot{\tilde{q}}_1 \\ \ddot{\tilde{q}}_2 \\ \ddot{\tilde{q}}_3 \\ \ddot{\tilde{q}}_4 \end{Bmatrix} + [C_1] \begin{Bmatrix} \dot{\tilde{q}}_1 \\ \dot{\tilde{q}}_2 \\ \dot{\tilde{q}}_3 \\ \dot{\tilde{q}}_4 \end{Bmatrix} + [K_1] \begin{Bmatrix} \tilde{q}_1 \\ \tilde{q}_2 \\ \tilde{q}_3 \\ \tilde{q}_4 \end{Bmatrix} = 0 \qquad (3.32)$$

$$[M_2] \{\ddot{\tilde{q}}_5\} + [C_2] \{\dot{\tilde{q}}_5\} + [K_2] \{\tilde{q}_5\} = 0 \qquad (3.33)$$

$$[M_3] \{\ddot{\tilde{q}}_6\} + [C_3] \{\dot{\tilde{q}}_6\} + [K_3] \{\tilde{q}_6\} = 0 \qquad (3.34)$$

The order of the various matrices is given below

$[M_1]$, $[C_1]$, $[K_1]$ 25 x 25

$[M_2]$, $[C_2]$, $[K_2]$ 3 x 3

$[M_3]$, $[C_3]$, $[K_3]$ 3 x 3

After obtaining the equilibrium state, the three groups of Equations (3.32) - (3.34) can be solved separately for the stability analysis. The information about system stability is obtained from an eigenanalysis of Equations (3.32) - (3.34). The various results obtained together with the physical interpretation of these results are presented in the next chapter.

3.2 Equations for Single Coupled Rotor/Body Model

It is evident from the preceding discussion that the mathematical model of a multiple rotor system, coupled with a supporting structure, is algebraically complicated. To develop confidence in this model it seemed prudent to use it first for simulating the behavior of a single rotor system coupled with a fuselage. For a coupled rotor/body system, in ground resonance, including the effect of the aerodynamic loads, high quality experimental data has been published by Bousman in Ref. 6. A comparison of the results obtained from the analytical model developed in this report, with experimental data [Ref. 6] is a reasonable approach for validating the equations. In this section, the equations of motion for the multirotor model, derived in the

previous sections are modified to study the aeromechanical stability of a single rotor/body model of a helicopter in ground resonance. The modifications introduced consist of deleting a number of degrees of freedom so as to simulate the particular configuration tested by Bousman [Ref. 6]. A brief description of this test is provided below.

Bousman [Ref. 6] has obtained excellent experimental data for the aeromechanical stability of a hingeless rotor on a special gimbaled support, simulating body pitch and roll degrees of freedom. The rotor consisted of three blades and five different configurations were tested. The different configurations represent different blade parameters characterized by the nonrotating natural frequencies of the blade in flap and lag, pitch-lag coupling and flap-lag coupling. The rotor was designed such that most of the blade flexibility was concentrated at the root by building in root flexures. The rotor assembly was supported on gimbal which had pitch and roll degrees of freedom. In this report, the analytical results obtained are compared with the experimental results, presented by Bousman, for rotor configuration 1, where the designation of this configuration is consistent with that in Bousman's paper [Ref. 6]. Configuration 1 had different stiffnesses in flap and lag respectively, the corresponding non-rotating flap frequency was 3.13 Hz and that for lead-lag was 6.70 Hz. The airfoil cross-section of the blade was cambered and has a zero lift angle of attack equal to -1.5 degrees. A substantial part of the experimental data was obtained for zero pitch setting, however, due to the presence of camber the rotor produces a small amount of thrust at this pitch setting. The rotor blades were rigid outboard of the flap and lag flexures which were located at a radial station 0.105R. There was no flap-pitch or pitch-lag couplings for this configuration. Furthermore, the blade was very stiff in torsion. In the case of the experiments

conducted for pitch angles other than zero, the experimental set up was so designed as to introduce the changes in pitch angle outboard of the flexures and hence there was no flap-lag structural coupling for these cases. The structural damping in body roll was very small in comparison with that for body pitch. The body pitch and roll frequencies were controlled by cantilever springs on which the gimbal was mounted. It was stated in Ref. 6 that the body pitch spring was selected to provide a dimensionless body pitch frequency of about 0.12 at a nominal rotor speed of 720 R.P.M. and the roll spring was selected to give a dimensionless roll frequency of about 0.28. (The frequencies are nondimensionalized by dividing by rotor speed.) As indicated in a letter by Bousman to the authors the design objectives for the model were dimensional frequencies of 1.44 Hz in pitch and 3.36 Hz in roll. However the actual measured frequencies were 2 Hz in pitch and 4 Hz in roll. From the experimental results presented in Ref. 6 it is evident that over a wide range of Ω(200~1000 R.M.) the pitch and roll frequencies are very close to 2 Hz and 4 Hz respectively. Hence, for the present study, the pitch and roll frequencies are chosen to be 2 Hz and 4 Hz. With this combination of frequencies, at a rotor speed of 750 R.P.M., the lead-lag regressing mode frequency coalesces with the body roll frequency causing an aeromechanical instability.

The degrees of freedom required to study this aeromechanical stability problem are: the fundamental flap and lag modes for each blade and the pitch and roll degrees of freedom of the body. In this class of problems, it has been established that the collective flap and lag modes do not couple with the body motion and thus, these modes are not considered. Therefore, the number of degrees of freedom for the aeromechanical problem are six. These consist of: cyclic flap (β_{1c}, β_{1s}), cyclic lead-lag (ζ_{1c}, ζ_{1s}), body pitch (θ) and body roll (ϕ). The relevant equilibrium and stability equations, for this problem are given in the following sections.

3.2.1 Static Equilibrium Equations

Flap:

$$\beta_0 \{\bar{\omega}_F^2 + (\bar{\omega}_L^2 - \bar{\omega}_F^2) \sin^2\theta_c + \frac{\bar{\ell}^3}{3} + \frac{\bar{\ell}^2}{2} \bar{e}\}$$

$$+ \zeta_0 \{(\bar{\omega}_L^2 - \bar{\omega}_F^2) \sin\theta_c \cos\theta_c + \nu \frac{\bar{\ell}^4}{4} \beta_p\}$$

$$+ \beta_0\zeta_0 \{\nu \frac{\bar{\ell}^4}{4}\}$$

$$+ \beta_p \{ \frac{\bar{\ell}^3}{3} + \frac{\bar{\ell}^2}{2} \bar{e} \} - \nu\{\frac{\bar{\ell}^4}{4} \theta_0 + \frac{\bar{\ell}^3}{3} (-\lambda+2\bar{e}\theta_0) - \frac{\bar{\ell}^2}{2} \bar{e}\lambda\} = 0 \quad (3.35)$$

Lead-Lag

$$\beta_0 \{ - (\bar{\omega}_L^2 - \bar{\omega}_F^2) \sin\theta_c \cos\theta_c \}$$

$$+ \zeta_0 \{ - \bar{\omega}_L^2 + (\bar{\omega}_L^2 - \bar{\omega}_F^2) \sin^2\theta_c - \frac{\bar{\ell}^2}{2} \bar{e} + \nu(- \frac{\bar{\ell}^4}{4} \beta_p\theta_0 - \frac{\bar{\ell}^3}{3} 2\lambda\beta_p)\}$$

$$+ \beta_0\zeta_0 \{\nu \frac{\bar{\ell}^3}{3} \lambda\}$$

$$+ \nu\{- \frac{c_{d0}}{a} (\frac{\bar{\ell}^4}{4} + 2\frac{\bar{\ell}^3}{3} \bar{e}) - \frac{\bar{\ell}^3}{3} \lambda\theta_0 + \frac{\bar{\ell}^2}{2} \lambda (\lambda- \bar{e}\theta_0)\} = 0 \quad (3.36)$$

where $\bar{\omega}_F^2 = \dfrac{K_\beta}{m\Omega^2R^3}$

$\bar{\omega}_L^2 = \dfrac{K_\zeta}{m\Omega^2R^3}$

$\nu = \dfrac{\rho_A abR}{m}$; $\bar{e} = \dfrac{e}{R}$; $\bar{\ell} = 1 - \bar{e}$

When there is no structural flap-lag coupling, the terms containing $\sin\theta_c$

and cos $_c$ must be deleted from the above equations as well as in the stability equations given below.

$$\theta_0 = \theta_c - \theta_{ZL}$$

where θ_0 is the effective angle of attack

θ_c is the collective pitch setting of the blade

θ_{ZL} is the zero lift angle of attack

3.2.2 Stability Equations

n-cosine Flap

$$\beta_{nc} F_{nc}(1) + \beta_{ns} F_{nc}(2) + \zeta_{nc} F_{nc}(3) + \zeta_{ns} F_{nc}(4)$$
$$+ \dot{\beta}_{nc} F_{nc}(5) + \dot{\beta}_{ns} F_{nc}(6) + \dot{\zeta}_{nc} F_{nc}(7) + \ddot{\beta}_{nc} F_{nc}(8)$$
$$+ \ddot{\theta} F_{nc}(9) + \dot{\theta} F_{nc}(10) + \dot{\phi} F_{nc}(11) = 0 \qquad (3.37)$$

where

$$F_{nc}(1) = \bar{\omega}_F^2 + (\bar{\omega}_L^2 - \bar{\omega}_F^2) \sin^2\theta_c + \nu\frac{\bar{\ell}^4}{4} \zeta_0 + \frac{\bar{\ell}^3}{3} + \frac{\bar{\ell}^2}{2} \bar{e} - n^2 \frac{\bar{\ell}^3}{3}$$
$$- n^2 \frac{1}{2} \nu\bar{b} \frac{\bar{\ell}^3}{3} \cos\theta_0$$

$$F_{nc}(2) = n(\nu\frac{\bar{\ell}^4}{4} + \nu\frac{\bar{\ell}^3}{3} \bar{e} + \bar{g}_{SF})$$

$$F_{nc}(3) = (\bar{\omega}_L^2 - \bar{\omega}_F^2) \sin\theta_c \cos\theta_c + \nu\frac{\bar{\ell}^4}{4} (\beta_p + \beta_0)$$

$$F_{nc}(4) = n(2 \frac{\bar{\ell}^3}{3} (\beta_0 + \beta_p) - 2\nu\frac{\bar{\ell}^4}{4} \theta_0 + \nu\frac{\bar{\ell}^3}{3} \lambda)$$

$$F_{nc}(5) = \nu \frac{\bar{\ell}^4}{4} + \nu \frac{\bar{\ell}^3}{3} \bar{e} + \bar{g}_{SF}$$

$$F_{nc}(6) = n\{ 2 \frac{\bar{\ell}^3}{3} + 2 \frac{1}{2} \nu \frac{\bar{\ell}^3}{3} \bar{b} \cos\theta_0 \}$$

$$F_{nc}(7) = 2 \frac{\bar{\ell}^3}{3} (\beta_0 + \beta_p) - 2\nu \frac{\bar{\ell}^4}{4} \theta_0 + \nu \frac{\bar{\ell}^3}{3} \lambda$$

$$F_{nc}(8) = \frac{\bar{\ell}^3}{3} + \frac{1}{2} \nu \bar{b} \frac{\bar{\ell}^3}{3} \cos\theta_0$$

$$F_{nc}(9) = - \frac{\bar{\ell}^3}{3} \delta_n$$

$$F_{nc}(10) = - \delta_n \nu \frac{\bar{\ell}^4}{4}$$

$$F_{nc}(11) = \delta_n \{ 2 \frac{\bar{\ell}^3}{3} + \bar{h}_2 (2\nu \frac{\bar{\ell}^3}{3} \theta_0 - \nu \frac{\bar{\ell}^2}{2} \lambda) \}$$

where $\delta_n = 1$ when $n = 1$

$= 0$ $\quad n \neq 1$

$$\bar{g}_{SF} = \frac{g_{SF}}{m\Omega R^3}$$

n-Sine Flap

$$\beta_{ns} F_{ns}(1) + \beta_{nc} F_{ns}(2) + \zeta_{ns} F_{ns}(3) + \zeta_{nc} F_{ns}(4)$$

$$+ \dot{\beta}_{ns} F_{ns}(5) + \dot{\beta}_{nc} F_{ns}(6) + \dot{\zeta}_{ns} F_{ns}(7) + \ddot{\beta}_{ns} F_{ns}(8)$$

$$+ \ddot{\phi} F_{ns}(9) + \dot{\phi} F_{ns}(10) + \dot{\theta} F_{ns}(11) = 0 \qquad (3.38)$$

where

$$F_{ns}(1) = \bar{\omega}_F^2 + (\bar{\omega}_L^2 - \bar{\omega}_F^2) \sin^2\theta_c + \nu \frac{\bar{\ell}^4}{4} \zeta_0 + \frac{\bar{\ell}^3}{3} + \frac{\bar{\ell}^2}{2} \bar{e} - n^2 \frac{\bar{\ell}^3}{3}$$

$$- \frac{1}{2} \nu \bar{b} \frac{\bar{\ell}^3}{3} n^2 \cos\theta_0$$

$$F_{ns}(2) = n\{-\nu\frac{\bar{\ell}^4}{4} - \nu\frac{\bar{\ell}^3}{3}\bar{e} - \bar{g}_{SF}\}$$

$$F_{ns}(3) = (\bar{\omega}_L^2 - \bar{\omega}_F^2)\sin\theta_c\cos\theta_c + \nu\frac{\bar{\ell}^4}{4}(\beta_0 + \beta_p)$$

$$F_{ns}(4) = n\{-2\frac{\bar{\ell}^3}{3}(\beta_0 + \beta_p) + 2\nu\frac{\bar{\ell}^4}{4}\theta_0 - \nu\frac{\bar{\ell}^3}{3}\lambda\}$$

$$F_{ns}(5) = \nu\frac{\bar{\ell}^4}{4} + \nu\frac{\bar{\ell}^3}{3}\bar{e} + \bar{g}_{SF}$$

$$F_{ns}(6) = n\{-2\frac{\bar{\ell}^3}{3} - 2\frac{1}{2}\nu\frac{\bar{\ell}^3}{3}\bar{b}\cos\theta_0\}$$

$$F_{ns}(7) = 2\frac{\bar{\ell}^3}{3}(\beta_0 + \beta_p) - 2\nu\frac{\bar{\ell}^4}{4}\theta_0 + \nu\frac{\bar{\ell}^3}{3}\lambda$$

$$F_{ns}(8) = \frac{\bar{\ell}^3}{3} + \frac{1}{2}\nu\bar{b}\frac{\bar{\ell}^3}{3}\cos\theta_0$$

$$F_{ns}(9) = \delta_n\frac{\bar{\ell}^3}{3}$$

$$F_{ns}(10) = \delta_n\nu\frac{\bar{\ell}^4}{4}$$

$$F_{ns}(11) = \delta_n\{2\frac{\bar{\ell}^3}{3} + 2\nu\frac{\bar{\ell}^3}{3}\theta_0\bar{h}_2 - \bar{h}_2\nu\frac{\bar{\ell}^2}{2}\lambda\}$$

n - Cosine lead-lag

$$\zeta_{nc}L_{nc}(1) + \zeta_{ns}L_{nc}(2) + \beta_{nc}L_{nc}(3) + \beta_{ns}L_{nc}(4)$$

$$+ \dot{\zeta}_{nc}L_{nc}(5) + \dot{\zeta}_{ns}L_{nc}(6) + \dot{\beta}_{nc}L_{nc}(7) + \dot{\beta}_{ns}L_{nc}(8)$$

$$+ \ddot{\zeta}_{nc}L_{nc}(9) + \ddot{\beta}_{nc}L_{nc}(10) + \ddot{\phi}L_{nc}(11) + \ddot{\theta}L_{nc}(12) + \dot{\theta}L_{nc}(13) = 0 \qquad (3.39)$$

where

$$L_{nc}(1) = -\bar{\omega}_L^2 + (\bar{\omega}_L^2 - \bar{\omega}_F^2)\sin^2\theta_c - \frac{\bar{\ell}^2}{2}\bar{e} + n^2\frac{\bar{\ell}^3}{3} - \nu\frac{\bar{\ell}^4}{4}\beta_p\theta_0$$

$$L_{nc}(2) = -n\left\{2\nu\frac{c_{d0}}{a}\frac{\bar{\ell}^4}{4} + \nu\frac{\bar{\ell}^3}{3}\theta_0\lambda + \bar{g}_{SL}\right\}$$

$$L_{nc}(3) = -(\bar{\omega}_L^2 - \bar{\omega}_F^2)\sin\theta_c\cos\theta_c - n^2\frac{1}{2}\nu\bar{b}\frac{\bar{\ell}^3}{3}\sin\theta_0$$

$$L_{nc}(4) = n\left\{2\frac{\bar{\ell}^3}{3}(\beta_0 + \beta_p) - \nu\frac{\bar{\ell}^4}{4}\theta_0 - \nu\frac{\bar{\ell}^3}{3}(-2\lambda + \bar{e}\theta_0)\right\}$$

$$L_{nc}(5) = -2\nu\frac{c_{d0}}{a}\frac{\bar{\ell}^4}{4} - \nu\frac{\bar{\ell}^3}{3}\theta_0\lambda - \bar{g}_{SL}$$

$$L_{nc}(6) = -n\,2\frac{\bar{\ell}^3}{3}$$

$$L_{nc}(7) = 2\frac{\bar{\ell}^3}{3}(\beta_0 + \beta_p) - \nu\frac{\bar{\ell}^4}{4}\theta_0 - \nu\frac{\bar{\ell}^3}{3}(-2\lambda + \bar{e}\theta_0)$$

$$L_{nc}(8) = 2n\frac{1}{2}\nu\bar{b}\frac{\bar{\ell}^3}{3}\sin\theta_0$$

$$L_{nc}(9) = -\frac{\bar{\ell}^3}{3}$$

$$L_{nc}(10) = \frac{1}{2}\nu\bar{b}\frac{\bar{\ell}^3}{3}\sin\theta_0$$

$$L_{nc}(11) = \delta_n\left\{\frac{\bar{\ell}^3}{3}(\beta_p + \beta_0) + \bar{h}_2\frac{\bar{\ell}^2}{2}\right\}$$

$$L_{nc}(12) = \delta_n\bar{h}_2\frac{\bar{\ell}^2}{2}\zeta_0$$

$$L_{nc}(13) = \delta_n\left\{\nu\frac{\bar{\ell}^4}{4}\theta_0 - \frac{\bar{\ell}^3}{3}2\lambda\nu\right\}$$

where $\bar{g}_{SL} = g_{SL}/m\Omega R^3$

n-Sine lead-lag

$$\zeta_{ns}\, L_{ns}(1) + \zeta_{nc}\, L_{ns}(2) + \beta_{ns}\, L_{ns}(3) + \beta_{nc}\, L_{ns}(4)$$

$$+ \dot{\zeta}_{ns}\, L_{ns}(5) + \dot{\zeta}_{nc}\, L_{ns}(6) + \dot{\beta}_{ns}\, L_{ns}(7) + \dot{\beta}_{nc}\, L_{ns}(8)$$

$$+ \ddot{\zeta}_{ns}\, L_{ns}(9) + \ddot{\beta}_{ns}\, L_{ns}(10) + \ddot{\theta}\, L_{ns}(11) + \ddot{\phi}\, L_{ns}(12) + \dot{\phi}\, L_{ns}(13) = 0 \tag{3.40}$$

where

$$L_{ns}(1) = -\bar{\omega}_L^2 + (\bar{\omega}_L^2 - \bar{\omega}_F^2)\sin^2\theta_c - \frac{\bar{\ell}^2}{2}\bar{e} + n^2\frac{\bar{\ell}^3}{3} - \nu\frac{\bar{\ell}^4}{4}\beta_p\theta_0$$

$$L_{ns}(2) = n\{2\nu\frac{c_{d0}}{a}\frac{\bar{\ell}^4}{4} + \nu\frac{\bar{\ell}^3}{3}\lambda\theta_0 + \bar{g}_{SL}\}$$

$$L_{ns}(3) = -(\bar{\omega}_L^2 - \bar{\omega}_F^2)\sin\theta_c\cos\theta_c - n^2\frac{1}{2}\nu\bar{b}\frac{\bar{\ell}^3}{3}\sin\theta_0$$

$$L_{ns}(4) = n\{-2\frac{\bar{\ell}^3}{3}(\beta_0 + \beta_p) + \nu\frac{\bar{\ell}^4}{4}\theta_0 + \nu\frac{\bar{\ell}^3}{3}(-2\lambda + \bar{e}\theta_0)\}$$

$$L_{ns}(5) = -2\nu\frac{c_{d0}}{a}\frac{\bar{\ell}^4}{4} - \nu\frac{\bar{\ell}^3}{3}\lambda\theta_0 - \bar{g}_{SL}$$

$$L_{ns}(6) = 2n\frac{\bar{\ell}^3}{3}$$

$$L_{ns}(7) = 2\frac{\bar{\ell}^3}{3}(\beta_p + \beta_0) - \nu\frac{\bar{\ell}^4}{4}\theta_0 - \nu\frac{\bar{\ell}^3}{3}(-2\lambda + \bar{e}\theta_0)$$

$$L_{ns}(8) = -2n\frac{1}{2}\nu\bar{b}\frac{\bar{\ell}^3}{3}\sin\theta_0$$

$$L_{ns}(9) = -\frac{\bar{\ell}^3}{3}$$

$$L_{ns}(10) = \frac{1}{2}\nu\bar{b}\frac{\bar{\ell}^3}{3}\sin\theta_0$$

$$L_{ns}(11) = \delta_n\{\frac{\bar{\ell}^3}{3}(\beta_p + \beta_0) + \frac{\bar{\ell}^2}{2}\bar{h}_2\}$$

$$L_{ns}(12) = - \delta_n \bar{h}_2 \frac{\bar{\ell}^2}{2} \zeta_0$$

$$L_{ns}(13) = \delta_n \{ - \nu \frac{\bar{\ell}^4}{4} \theta_0 + \frac{\bar{\ell}^3}{3} 2\lambda\nu \}$$

Roll

$$\frac{N}{2} m\Omega^2 R^3 \{ \beta_{1c} < \nu \frac{c_{d0}}{a} \frac{\bar{\ell}^4}{4} + \nu \frac{\bar{\ell}^3}{3} \lambda\theta_0 + \bar{g}_{SF} + \nu \frac{\bar{\ell}^4}{4} + 2 \nu \frac{\bar{\ell}^3}{3} \bar{e}$$

$$+ \bar{h}_2 (\nu \frac{\bar{\ell}^3}{3} (\beta_p + \beta_0) + \nu \frac{\bar{\ell}^3}{3} \theta_0 \zeta_0 + \frac{1}{2} \nu \bar{b} \frac{\bar{\ell}^2}{2} \sin\theta_0) >$$

$$+ \beta_{1s} < - 2 \nu \frac{\bar{\ell}^4}{4} \zeta_0 + \nu \frac{\bar{\ell}^4}{4} (\beta_p + 3\beta_0) \theta_0 + \frac{1}{2} \nu \bar{b} \frac{\bar{\ell}^3}{3} \cos\theta_0$$

$$+ \bar{h}_2 (2 \nu \frac{\bar{\ell}^3}{3} \theta_0 - \frac{\bar{\ell}^2}{2} \beta_p - \bar{\ell}^2 \beta_0 + \nu \frac{\bar{\ell}^2}{2} (- 3\lambda + \bar{e} \theta_0)) >$$

$$+ \zeta_{1c} < - \nu \frac{\bar{\ell}^4}{4} \theta_0 + \bar{h}_2 \nu \frac{\bar{\ell}^3}{3} \theta_0 (- \beta_p + \beta_0) >$$

$$+ \zeta_{1s} < \nu \frac{\bar{\ell}^4}{4} \zeta_0 2\theta_0 - \nu \frac{\bar{\ell}^4}{4} (\beta_p + \beta_0) + \beta_p \bar{g}_{SL}$$

$$- \bar{h}_2 (\bar{\ell}^2 \zeta_0 - 2 \nu \frac{c_{d0}}{a} \frac{\bar{\ell}^3}{3} - \nu \frac{\bar{\ell}^2}{2} \lambda\theta_0) >$$

$$+ \dot{\beta}_{1c} < - \nu \frac{\bar{\ell}^4}{4} \zeta_0 + \nu \frac{\bar{\ell}^4}{4} (\beta_0 + \beta_p) \theta_0 + 2 \frac{\bar{\ell}^3}{3} + 2 \frac{\bar{\ell}^2}{2} \bar{e} + 2 \frac{1}{2} \nu \bar{b} \frac{\bar{\ell}^3}{3} \cos\theta_0$$

$$- \bar{h}_2 (\bar{\ell}^2 \beta_0 - \nu \frac{\bar{\ell}^3}{3} \theta_0 - \nu \frac{\bar{\ell}^2}{2} (- 2\lambda + \bar{e} \theta_0)) >$$

$$+ \dot{\beta}_{1s} < - 2 \frac{\bar{\ell}^3}{3} \zeta_0 - \bar{g}_{SF} - \nu \frac{\bar{\ell}^4}{4} - 2 \nu \frac{\bar{\ell}^3}{3} \bar{e}$$

$$- \bar{h}_2 (\nu \frac{\bar{\ell}^3}{3} (\beta_p + \beta_0) + 2 \frac{1}{2} \nu \bar{b} \frac{\bar{\ell}^2}{2} \sin\theta_0) >$$

$$+ \dot{\zeta}_{1c} < \nu \frac{\bar{\ell}^4}{4} \zeta_0 \, 2\theta_0 + \beta_p \bar{g}_{SL}$$

$$- \bar{h}_2 \left(\bar{\ell}^2 \zeta_0 - 2 \nu \frac{c_{d0}}{a} \frac{\bar{\ell}^3}{3} - \nu \frac{\bar{\ell}^2}{2} \lambda\theta_0\right)>$$

$$+ \dot{\zeta}_{1s} < 2 \nu \frac{\bar{\ell}^4}{4} \theta_0 - \nu \frac{\bar{\ell}^3}{3} \lambda + 2 \nu \frac{\bar{\ell}^3}{3} \bar{e} \, \theta_0 + \bar{h}_2 \nu\beta_p \frac{\bar{\ell}^3}{3} 2 \theta_0 >$$

$$+ \ddot{\beta}_{1c} < - \frac{\bar{\ell}^3}{3} \zeta_0 - \bar{h}_2 \frac{1}{2} \nu \bar{b} \frac{\bar{\ell}^2}{2} \sin\theta_0 >$$

$$+ \ddot{\beta}_{1s} < - \frac{\bar{\ell}^3}{3} - \frac{1}{2} \nu \bar{b} \frac{\bar{\ell}^3}{3} \cos\theta_0 - \frac{\bar{\ell}^2}{2} \bar{e} - \bar{h}_2 \beta_p \frac{\bar{\ell}^2}{2} >$$

$$+ \ddot{\zeta}_{1c} < \frac{\bar{\ell}^3}{3} (\beta_p + \beta_0) + \bar{h}_2 \frac{\bar{\ell}^2}{2} >$$

$$+ \ddot{\phi} < - \frac{\bar{\ell}^3}{3} - \frac{\bar{\ell}^2}{2} \bar{e} - \bar{h}_2 \beta_p \frac{\bar{\ell}^2}{2} - \bar{h}_2 \frac{\bar{\ell}^2}{2} (\beta_p + \beta_0)$$

$$- \bar{h}_2 \left(\frac{\bar{\ell}^2}{2} (\beta_p + \beta_0) + 2 \bar{h}_2 \bar{\ell}\right) >$$

$$+ \dot{\phi} < - \frac{\bar{\ell}^3}{3} 2 \zeta_0 - \nu \frac{\bar{\ell}^3}{3} \bar{e} - \nu \frac{\bar{\ell}^4}{4} - \bar{h}_2 \beta_p \nu \frac{\bar{\ell}^3}{3} - \bar{h}_2 \beta_0 \nu \frac{\bar{\ell}^3}{3} >$$

$$+ \ddot{\theta} < \frac{\bar{\ell}^3}{3} \zeta_0 >$$

$$+ \dot{\theta} < \nu \frac{\bar{\ell}^4}{4} \zeta_0 - 2 \frac{\bar{\ell}^3}{3} - \frac{\bar{\ell}^2}{2} 2 \bar{e} - 2 \bar{h}_2 \beta_p \frac{\bar{\ell}^2}{2} - \bar{h}_2 \nu \frac{\bar{\ell}^3}{3} \theta_0 + \nu \frac{\bar{\ell}^2}{2} \lambda 2 \bar{h}_2$$

$$+ \bar{h}_2 \nu \frac{\bar{\ell}^2}{2} \lambda - \bar{h}_2 \nu \frac{\bar{\ell}^3}{3} 2\theta_0 > \}$$

$$- I_{xx} \Omega^2 \ddot{\phi} + I_{xy} \Omega^2 \ddot{\theta} = 0 \qquad (3.41)$$

Pitch

$$\frac{N}{2} m\Omega^2 R^3 \{ \beta_{1c} < 2 \nu \frac{\bar{\ell}^4}{4} \zeta_0 - \nu \frac{\bar{\ell}^4}{4} (\beta_p + 3\beta_0) \theta_0 - \frac{1}{2} \nu \bar{b} \frac{\bar{\ell}^3}{3} \cos\theta_0$$

$$- \bar{h}_2 \left(\nu \frac{\bar{\ell}^3}{3} 2\theta_0 - \frac{\bar{\ell}^2}{2} \beta_p - \bar{\ell}^2 \beta_0 + \nu \frac{\bar{\ell}^2}{2} (-3\lambda + \bar{e}\theta_0) \right) >$$

$$+ \beta_{1s} < \nu \frac{c_{d0}}{a} \frac{\bar{\ell}^4}{4} + \nu \frac{\bar{\ell}^3}{3} \lambda\theta_0 + \bar{g}_{SF} + \nu \frac{\bar{\ell}^4}{4} + 2 \nu \frac{\bar{\ell}^3}{3} \bar{e}$$

$$+ \bar{h}_2 \left(\beta_p \nu \frac{\bar{\ell}^3}{3} + \beta_0 \nu \frac{\bar{\ell}^3}{3} + \nu \frac{\bar{\ell}^3}{3} \zeta_0\theta_0 + \frac{1}{2} \nu \bar{b} \frac{\bar{\ell}^2}{2} \sin\theta_0 \right) >$$

$$+ \zeta_{1c} < - \nu \frac{\bar{\ell}^4}{4} \zeta_0 2\theta_0 - \beta_p \bar{g}_{SL} + \nu \frac{\bar{\ell}^4}{4} (\beta_p + \beta_0)$$

$$+ \bar{h}_2 \left(\bar{\ell}^2 \zeta_0 - 2 \nu \frac{c_{d0}}{a} \frac{\bar{\ell}^3}{3} - \nu \frac{\bar{\ell}^2}{2} \lambda\theta_0 \right) >$$

$$+ \zeta_{1s} < - \nu \frac{\bar{\ell}^4}{4} \theta_0 + \bar{h}_2 \nu \frac{\bar{\ell}^3}{3} (-\beta_p + \beta_0) \theta_0 >$$

$$+ \dot{\beta}_{1c} < 2 \frac{\bar{\ell}^3}{3} \zeta_0 + \bar{g}_{SF} + \nu \frac{\bar{\ell}^4}{4} + 2 \nu \frac{\bar{\ell}^3}{3} \bar{e}$$

$$+ \bar{h}_2 \left(\nu \frac{\bar{\ell}^3}{3} (\beta_p + \beta_0) + 2 \frac{1}{2} \nu \bar{b} \frac{\bar{\ell}^2}{2} \sin\theta_0 \right)$$

$$+ \dot{\beta}_{1s} < - \nu \frac{\bar{\ell}^4}{4} \zeta_0 + \nu \frac{\bar{\ell}^4}{4} \theta_0 (\beta_p + \beta_0) + 2 \frac{\bar{\ell}^3}{3} + 2 \frac{\bar{\ell}^2}{2} \bar{e} + 2 \frac{1}{2} \nu \bar{b} \frac{\bar{\ell}^3}{3} \cos\theta_0$$

$$- \bar{h}_2 \left(\bar{\ell}^2 \beta_0 - \nu \frac{\bar{\ell}^3}{3} \theta_0 - \nu \frac{\bar{\ell}^2}{2} (-2\lambda + \bar{e}\theta_0) \right) >$$

$$+ \dot{\zeta}_{1c} < - 2 \nu \frac{\bar{\ell}^4}{4} \theta_0 + \nu \frac{\bar{\ell}^3}{3} \lambda - \nu \frac{\bar{\ell}^3}{3} \bar{e} 2\theta_0 - \bar{h}_2 \beta_p \nu \frac{\bar{\ell}^3}{3} 2\theta_0 >$$

$$+ \dot{\zeta}_{1s} < \nu \frac{\bar{\ell}^4}{4} \zeta_0 2\theta_0 + \beta_p \bar{g}_{SL} - \bar{h}_2 \bar{\ell}^2 \zeta_0 + \bar{h}_2 \nu \frac{c_{d0}}{a} 2 \frac{\bar{\ell}^3}{3} + \bar{h}_2 \nu \frac{\bar{\ell}^2}{2} \lambda\theta_0 >$$

$$+ \ddot{\beta}_{1c} < \frac{\bar{\ell}^3}{3} + \frac{1}{2} \nu \bar{b} \frac{\bar{\ell}^3}{3} \cos\theta_0 + \frac{\bar{\ell}^2}{2} \bar{e} + \bar{h}_2 \beta_p \frac{\bar{\ell}^2}{2} >$$

$$+ \ddot{\beta}_{1s} < - \frac{\bar{\ell}^3}{3} \zeta_0 - \bar{h}_2 \frac{1}{2} \nu \bar{b} \frac{\bar{\ell}^2}{2} \sin\theta_0 >$$

$$+ \ddot{\zeta}_{1s} < \frac{\bar{\ell}^3}{3} (\beta_0 + \beta_p) + \bar{h}_2 \frac{\bar{\ell}^2}{2} >$$

$$+ \ddot{\phi} < - \frac{\bar{\ell}^3}{3} \zeta_0 >$$

$$+ \dot{\phi} < - \nu \frac{\bar{\ell}^4}{4} \zeta_0 + 2 \frac{\bar{\ell}^3}{3} + \frac{\bar{\ell}^2}{2} 2 \bar{e} + 2 \bar{h}_2 \beta_p \frac{\bar{\ell}^2}{2} + \bar{h}_2 \nu \frac{\bar{\ell}^3}{3} \theta_0$$

$$- \nu \frac{\bar{\ell}^2}{2} 2 \lambda \bar{h}_2 + \bar{h}_2 \nu \frac{\bar{\ell}^3}{3} 2\theta_0 - \bar{h}_2 \nu \frac{\bar{\ell}^2}{2} \lambda >$$

$$+ \ddot{\theta} < - \frac{\bar{\ell}^3}{3} - \frac{\bar{\ell}^2}{2} \bar{e} - \bar{h}_2 \frac{\bar{\ell}^2}{2} (\beta_p + \beta_0) - \bar{h}_2 \beta_p \frac{\bar{\ell}^2}{2}$$

$$+ \bar{h}_2 \left(- \frac{\bar{\ell}^2}{2} (\beta_p + \beta_0) - 2 \bar{\ell} \bar{h}_2 \right) >$$

$$+ \dot{\theta} < - \frac{\bar{\ell}^3}{3} 2\zeta_0 - \nu \frac{\bar{\ell}^4}{4} - \nu \frac{\bar{\ell}^3}{3} \bar{e} - \nu \frac{\bar{\ell}^3}{3} \beta_p \bar{h}_2 - \nu \frac{\bar{\ell}^3}{3} \beta_0 \bar{h}_2 > \}$$

$$- I_{yy} \Omega^2 \ddot{\theta} + I_{yx} \Omega^2 \ddot{\phi} = 0 \qquad (3.42)$$

For a three bladed rotor, the value of n, in the above equations is 1.

The inflow ratio, λ, used in the calculation of the aerodynamic loads is taken from [Ref. 3]

$$\lambda = \left\{ \frac{\sigma a}{16} \left[- 1 + \sqrt{1 + \frac{24 |\theta_0|}{\sigma a}} \right] \right\} \operatorname{sgn} \theta_0 \qquad (3.43)$$

In the last equation θ_0 is the effective angle of attack of the blade.

As indicated in Ref. 6, a cambered airfoil was used in the model rotor tested, thus

$$\theta_0 = \theta_c - \theta_{ZL} \qquad (3.44)$$

where θ_c is the collective pitch setting of the blade and θ_{ZL} is the zero lift angle of attack. The static equilibrium equations, Eqs. (3.35) and (3.36), are used to evaluate the blade equilibrium positions and Eqs. (3.37)-(3.42) are solved t

determine the aeromechanical stability of a single rotor helicopter, in ground resonance.

The procedure followed in this analysis is slightly different from the procedure used to analyze the stability of a vehicle in hover, presented in Chapter 2. During hovering flight, the vehicle equilibrium conditions have to be satisfied. Whereas for ground resonance problems, the equilibrium condition of the vehicle do not have to be satisfied. Hence, the collective pitch angle of the blade, θ_c, is not an independent variable to be evaluated from the equilibrium conditions of the vehicle, and it becomes a prescribed quantity. The procedure for the analysis of ground resonance problem is as follows. For a given value of the collective pitch setting of the rotor, under the prescribed conditions of operation, the equilibrium deflections of the blade have to be evaluated from the equilibrium equations of the blade, Eqs. (3.35)-(3.36). Then, these quantities are substituted in the linearized stability equations, Eqs. (3.37) - (3.42), to analyze the stability of the vehicle.

The results of this analysis together with the results obtained for the stability of the complete HHLA model are presented in the next chapter.

4. RESULTS

Based on the equations presented in the previous chapter, two types of problems were solved. First, the aeromechanical stability of a single rotor helicopter, in ground resonance, is analyzed and the analytical results are compared with the experimental results available in the literature [Ref. 6]. Next a detailed stability analysis of a multirotor vehicle, representing an HHLA (Fig. 2), in hover, was carried out. The results are presented in two separate sections.

4.1 Results for the Ground Resonance Problem and Comparison with Experimental Data

In this analysis, aimed at predicting the aeromechanical stability of a single rotor helicopter, the behavior of the model was studied at various values of the rotor speed Ω. The results of this aeromechanical problem are presented in Figs. 4-8 together with the experimental results. Also presented in these figures are the results obtained by Johnson [Ref. 7]. The aerodynamic model used by Johnson was based on a dynamic inflow model, whereas a quasisteady aerodynamic model is used in this report. The data used for this analysis is presented in Appendix C.

The variation modal frequencies with Ω are presented in Fig. 4, together with the experimental data obtained in Ref. 6. The progressing flap (β_p) and the progressing lead-lag (ζ_p) frequencies increase very rapidly with Ω. The lead-lag regressing mode (ζ_R) frequency evaluated from our analytical model is in excellent agreement with the experimental results. The body pitch (θ) and roll (ϕ) frequencies have slightly higher values than the experimental results. The damping in pitch as a function of Ω is shown in Fig. 5. The analytical results are in good agreement with the experimental data. The variation of damping in roll as a function of Ω is shown in Fig. 6. It is evident that for this case the analytical results yield values which are somewhat higher than the experimental data. The differences observed between our analytical results

and the experimental points, for the frequency and damping in body modes, could be explained as follows. In our calculations, the numerical values used for the stiffness and structural damping in body pitch and roll modes are evaluated based on pitch frequency equal to 2 Hz and roll frequency equal to 4 Hz.

Fig. 7 presents the variation of damping in lead-lag regressing mode with Ω. The results of the present analysis show slightly better agreement than the results obtained in Ref. 7 with inflow dynamics. It is also important to note that in the region, beyond 800 R.P.M., our results are in excellent agreement with the experimental results, while the theory with inflow dynamics predicts higher values.

Changes in damping of the lead-lag regressing mode as a function of the collective pitch setting of the blade are presented in Fig. 8. At Ω = 650 R.P.M., the results shown in Fig. 8a indicate that the theoretical analysis used by Bousman [Ref. 6] predicts a much lower value for the damping than the experimental results. The present analysis shows considerably better agreement. At Ω = 900 R.P.M., the experimental results indicate a lead-lag regressing mode which is always stable, but the theoretical results shown by Bousman [Ref. 6] imply an instability which becomes stronger beyond a collective pitch setting of 2 degrees. As evident from Fig. 7b, the results of our analysis predict the correct trend and the predicted damping levels are much closer to the experimental results. An item to be noted in these figures (8a, 8b) is that the curve representing our analytical results starts from an angle θ_c = - 1.5 degrees. Although Fig. 8 contains an experimental data point corresponding to θ_c = - 3 degrees, we have not computed the results for this pitch setting.

C-2

The above comparison shows good agreement between our analytical results and the experimental results for the aeromechanical stability of a helicopter in ground resonance. Therefore, it can be concluded that our analytical model for the dynamics of the coupled rotor/vehicle system and the method of solution for the stability analysis are valid.

Finally it should be noted that more comprehensive results comparing the experimental data [Ref. 6] with the results from the mathematical model developed in this report, using a quasisteady aerodynamic model, can be found in Ref. 8. Additional results showing the sensitivity of the results to unsteady aerodynamic effects was presented in Ref. 9.

4.2 Results for Multirotor Model of an HHLA

Based on the equations presented in Chapter 3, two computer programs were developed to analyze the trim and stability of the twin rotor vehicle with a buoyant envelope shown in Fig. 2. The results are presented in three main sections. The first section gives the data and certain preliminary calculations for various frequencies. The second section presents the results of a parametric study in which certain relevant physical parameters of the system are varied so as to determine their effect on the stability of the vehicle. This parameter variation was also utilized for identifying the physical meaning of the various eigenvalues obtained in the analysis. The last section presents the physical interpretations of the results. These calculations were done on a vehicle without a sling load.

4.2.1 Data for the Multirotor Model

The data used for the calculation of equilibrium or trim state and stability of the vehicle are given on the next two pages.

Blade data

The HHLA model (Fig. 2) has identical rotors.

Type of rotor: Articulated rotor

Number of blades N		4
Blade chord	c = 2b	41.654 cm (1.3666 ft.)
Hinge offset	e	30.48 cm (1 ft.)
Rotor radius	R	8.6868 m (28.5 ft.)
Blade precone	β_p	0
Distance between elastic center and aerodynamic center	X_A	0
Distance between elastic center and mass center	X_I	0
Mass/unit length of the blade m		7.9529 kg/m (0.1661 slug/ft)

Principal mass moment of inertia of the blade/unit length

I_{MB3}	1.1503×10^{-1} kg.m	$(2.586 \times 10^{-2}$ slug ft)
I_{MB2}	6.6723×10^{-3} kg.m	$(1.5 \times 10^{-3}$ slug ft)

Aerodynamic data

Blade airfoil		NACA 0012
Lift curve slope	a	2π
Density of air	ρ_A	1.2256 kg/m^3 $(0.2378 \times 10^{-2}$ slug/ft^3)
Blade profile drag coefficient	c_{d0}	0.01
Rotor R.P.M.	Ω	217.79 R.P.M.
Solidity ratio	σ	0.0622
Lock number	γ	10.9

Nonrotating blade frequency parameters (Articulated blade)

Flap frequency parameter	$\omega_F = \left(\frac{K_{\beta_B}}{mR^3}\right)^{\frac{1}{2}}$	0
Lead-lag frequency parameter	$\omega_L = \left(\frac{K_{\zeta_B}}{mR^3}\right)^{\frac{1}{2}}$	0

Torsional frequency parameter (articulated)	$\omega_{T1} = \left(\frac{K_\phi}{mR^3}\right)^{\frac{1}{2}}$		0
Torsional frequency parameter (hingeless)	$\omega_{T2} = \left(\frac{K_\phi}{mR^3}\right)^{\frac{1}{2}}$	(Assumed)	1.895 rad/sec
Damping in flap	g_{SF}		0
Damping in lead-lag	g_{SL}		0
Damping in torsion	g_{ST}		0

Vehicle data

Weight of fuselage F_1	W_{F1}	3.5919×10^4N(8075 lb)
Weight of fuselage F_2	W_{F2}	3.5919×10^4N(8075 lb)
Weight of underslung load	W_{UN}	6.6723×10^4N(1.5×10^4lb)
Weight of envelope	W_{EN}	8.5539×10^4N(1.923×10^4lb)
Weight of supporting structure	W_S	9.4302×10^3N(2120 lb)
Weight of passenger compartment (Treated as a lumped structural load attached at the point O_s on the structure (Fig. 2)	W_S'	6.6723×10^3N(1500 lb)
Buoyancy on the envelope		1.3748×10^5N(30907 lb)

Geometric data

Distance between origin O_s and F_1	ℓ_{F1}	-21.946m (-72 ft)
Distance between origin O_s and F_2	ℓ_{F2}	21.946m (72 ft)
Distance between origin O_s and underslung load (Assumed)	h_1	-15.24m (-50 ft)
Distance between centerline and rotor hub	h_2	2.591m (8.5 ft)
Distance between centerline and center of volume of envelope	h_3	14.64m (48.03 ft)

Distance between center line and

C.G. of the envelope h_4 8.544m (28.03 ft)

Structural Dynamic Properties of the Supporting Structure

The supporting structure is modelled as an elastic structure with three normal modes of vibration: two normal modes for bending in vertical and in horizontal plane and one mode for torsion. The two bending modes are symmetric modes and the torsion is an anti-symmetric mode. It was assumed that the envelope and the underslung load are attached to the supporting structure at the origin 0_s. The data given above shows that the vehicle is symmetric about Y-Z plane. Furthermore due to the presence of a heavy mass attached at the center (0_s) of the supporting structure, the mode shapes in bending and torsion for each half of the model are assumed to be the modes of a cantilever with a tip mass.

Modal Displacement at F_1, F_2 and 0_s

The symmetric mode shape in bending for each half of the supporting structure can be written as [Ref. 11, Page 140]

$$\eta_1 \left(\frac{X}{L}\right) = 6\left(\frac{X}{L}\right)^2 - 4\left(\frac{X}{L}\right)^3 + \left(\frac{X}{L}\right)^4 \quad \text{(Bending in X-Y plane)} \quad (4.1a)$$

and

$$\eta_2 \left(\frac{X}{L}\right) = 6\left(\frac{X}{L}\right)^2 - 4\left(\frac{X}{L}\right)^3 + \left(\frac{X}{L}\right)^4 \quad \text{(Bending in X-Z plane)} \quad (4.1b)$$

where X is the coordinate of any section of the supporting structure from origin 0_s and L is the length of the supporting structure, L = 21.946m (72 ft).

Bending in X-Y plane

The modal displacement at any location on the supporting structure during the symmetric bending in X-Y plane can be obtained from Eq. (4.1a). The modal displacement

at location F_1	$\eta_1(\ell_{F1})$	3.0
at location F_2	$\eta_1(\ell_{F2})$	3.0

at origin 0_s $\eta_1(0_s)$ 0

The slope due to the modal displacement, at any section, can be obtained by differentiating Eq. (4.1) with respect to $(\frac{X}{L})$. The slopes due to the modal displacement

at location F_1 : $\eta_{1,x}(\ell_{F1}) = \frac{1}{L} \left.\frac{d\eta_1}{d(\frac{X}{L})}\right|_{\ell_{F1}}$ -0.1823

at location F_2 : $\eta_{1,x}(\ell_{F2}) = \frac{1}{L} \left.\frac{d\eta_1}{d(\frac{X}{L})}\right|_{\ell_{F2}}$ 0.1823

at location 0_s : $\eta_{1,x}(0_s) = \frac{1}{L} \left.\frac{d\eta_1}{d(\frac{X}{L})}\right|_{0_s}$ 0

Bending in X-Z plane

The modal displacement and slopes due to the modal displacement at any location on the supporting structure, during symmetric bending in X-Z plane can be obtained from Eq. (4.1b).

The modal displacement

at location F_1 : $\eta_2(\ell_{F1})$ 3.0

at location F_2 : $\eta_2(\ell F_2)$ 3.0

at location 0_s : $\eta_2(0_s)$ 0

The slopes due to modal displacement

at location F_1 : $\eta_{2,x}(\ell_{F1}) = \frac{1}{L} \left.\frac{d\eta_2}{d(\frac{X}{L})}\right|_{\ell_{F1}}$ -0.1823

at location F_2 : $\eta_{2,x}(\ell_{F2}) = \frac{1}{L} \left.\frac{d\eta_2}{d(\frac{X}{L})}\right|_{\ell_{F2}}$ 0.1823

at location 0_s : $\eta_{2,x}(0_s) = \frac{1}{L} \left.\frac{d\eta_2}{d(\frac{X}{L})}\right|_{0_s}$ 0

Torsion

The mode shape for torsion, for each half of the supporting structure is [Ref.10, Page 99]

$$\eta_3 \left(\frac{X}{L} \right) = \sin \frac{\pi}{2} \left(\frac{X}{L} \right) \qquad (4.2)$$

The modal displacement due to torsion

at location F_1 :	$\eta_3(\ell_{F1})$	-1.0
at location F_2 :	$\eta_3(\ell_{F2})$	1.0
at location 0_s :	$\eta_3(0_s)$	0

Generalized mass and stiffness data

Generalized mass (M) and generalized stiffness (K) for the i^{th} mode of vibration of the supporting structure is defined as

$$M = \int_{\ell_{F1}}^{\ell_{F2}} m \, \eta_i^2 \, dx$$

and $$K = \omega_i^2 \, M$$

where ω_i is the i^{th} modal frequency

η_i is the i^{th} mode shape

and m is the mass/unit length (for bending modes), or m is the mass moment of inertia/unit length (for torsion modes)

Bending in X-Y plane (horizontal)

generalized mass	M_{SBXY}	6.801×10^4 kg (4.66×10^3 slug)
generalized stiffness	K_{SBXY}	7.96×10^7 kg/sec^2 (5.454×10^6 slug/sec^2)

Bending in X-Z plane (vertical)

generalized mass	M_{SBXZ}	6.801×10^4 kg (4.66×10^3 slug)
generalized stiffness	K_{SBXZ}	7.96×10^7 kg/sec^2 (5.454×10^6 slug/sec^2)

Torsion

generalized mass	M_{ST}	1.936×10^4 kg.m^2 (1.428×10^4 slug ft^2)
generalized stiffness	K_{ST}	7.202×10^6 kg.m^2/sec^2 (5.312×10^6 slug ft^2/sec^2)

Rotary inertia data for the vehicle

The rotary inertia tensor of the various masses of the system are added together to obtain the rotary inertia of the complete vehicle about X-Y-Z axes. The inertia tensor is an assumed quantity

$$I_{XX} = 6.44 \times 10^5 \text{ kg.m}^2 \ (4.75 \times 10^5 \text{ slug.ft}^2)$$

$$I_{YY} = 2.59 \times 10^6 \text{ kg.m}^2 \ (1.91 \times 10^6 \text{ slug.ft}^2)$$

$$I_{YX} = I_{XY} = 0$$

To facilitate distinction between data which was available and data which had to be assumed, the list of assumed data is provided below:

(1) Torsional frequency of the blade

(2) Principal moments of inertia of the blade

(3) The mode shapes of the supporting structure and hence the generalized masses and stiffnesses

(4) Inertia tensor of the vehicle

4.2.2 Preliminary Calculations

In the preliminary calculations, the frequencies of various modes are calculated using elementary structural dynamics. These calculated frequencies are useful in identifying the various eigenvalues obtained in the stability analysis.

Supporting structure frequencies

Bending: If the supporting structure is considered to be a free-free beam (Fig. 9a) with uniform properties, the first elastic mode frequency in bending is [Ref. 10, page 80].

$$\omega = \left(\frac{1.51\pi}{L}\right)^2 \left(\frac{EI}{m}\right)^{\frac{1}{2}}$$

where L is the length of the beam

EI is the stiffness of the beam

m is the mass/unit length of the beam

In the present analysis

m = 21.908 kg/m (0.4576 slug/ft)

$EI = 1.471 \times 10^{10}$ N.m^2 (3.56×10^{10} lb ft^2)

L = 43.891 m (144 ft)

thus

$$\omega = \left(\frac{1.51\pi}{43.891}\right)^2 \left(\frac{1.471\times10^{10}}{21.908}\right)^{\frac{1}{2}} = 302.7 \text{ rad/sec}$$

For the case of the vehicle being considered, a heavy mass is attached at the center of the beam. This heavy mass is due to the envelope and underslung weight. Therefore, the model for the supporting structure becomes a beam with a heavy mass in the center (Fig. 9b). It is shown in Ref.10 that if the ratio between the mass fixed at the center of the beam to the mass of the beam is greater than 3, then frequency of the beam in the symmetric modes becomes close to the natural frequency of a cantilever beam with length equal to half the length of the free-free beam. In the present case, even with the envelope mass alone, the ratio is $\frac{8.5539\times10^4}{9.4302\times10^3} = 9.07$. Hence the first symmetric mode for one half of the structure can be assumed to be the fundamental mode of a cantilever. The natural frequency of a cantilever in fundamental mode is [Ref.10, page 77]

$$\omega_c = \left(\frac{0.597\pi}{L}\right)^2 \left(\frac{EI}{m}\right)^{\frac{1}{2}}$$

where L = 21.946m (72 ft)

Therefore, the natural frequency is ω_c = 189.27 rad/sec (4.3)

In addition to the heavy mass attached to the center, there are also two masses, representing the helicopter, attached at the two ends of the beam. Thus an

equivalent approximate model would consist of two cantilevers with tip mass (Fig. 9c). The natural frequency for this approximate model is calculated using Rayleigh's quotient. Since the model is symmetric about the center, only one half should be considered for the frequency evaluation in fundamental mode.

The fundamental mode shape for a cantilever is [Ref. 9, page 140]

$$\eta \left(\frac{X}{L} \right) = 6 \left(\frac{X}{L} \right)^2 - 4 \left(\frac{X}{L} \right)^3 + \left(\frac{X}{L} \right)^4 \qquad (4.4)$$

The generalized mass for the fundamental mode is

$$M = \int_0^L m dx \eta^2 + \frac{W_{F1}}{g} \eta^2 \left(\frac{L}{L} \right)$$

$$= 2.311 \text{ mL} + 9 \frac{W_{F1}}{g}$$

where m is the mass/unit length of the beam

L is the length of the cantilever

W_{F1} is the weight of the tip mass

The corresponding generalized stiffness in fundamental mode is

$$K = 2.311 \omega_c^2 \text{ mL}$$

where ω_c is the fundamental frequency of the cantilever without tip mass, which in the present case 189.27 rad/sec (Eq. 4.3). Thus the fundamental frequency of a cantilever with tip mass is

$$\omega_B = \left[\frac{2.311 \text{ mL } \omega_c^2}{2.311 \text{ mL} + 9 \frac{W_{F1}}{g}} \right]^{\frac{1}{2}}$$

where

$$m = 21.908 \text{ kg/m}$$

$$L = 21.946 \text{ m}$$

$$\omega_c = 189.27 \text{ rad/sec}$$

$$W_{F1} = 3.5919 \times 10^4 \text{ N}$$

Therefore $\omega_B = 0.180\ \omega_c = 34.18$ rad/sec (4.6)

This is the bending frequency of the supporting structure in both X-Y and X-Z planes in fundamental symmetric mode. The mode shape is given in Eq. 4.4 for one half of the structure.

Torsion:

If the supporting structure is considered as a uniform beam (Fig. 10a) then the fundamental torsional frequency of the beam is given by [Ref. 11, page 193]

$$\omega = \frac{\pi}{L} \left(\frac{GJ}{I} \right)^{\frac{1}{2}}$$

where L is the length of the beam

GJ is the torsional rigidity of the beam

I is the moment of inertia/unit length about center of twist

In the present case

$$L = 43.891 \text{ m } (144 \text{ ft})$$

$$GJ = 6.4054 \times 10^7 \text{ N m}^2 \ (1.55 \times 10^8 \text{ lb ft}^2)$$

$$I = 140.972 \text{ kg m } (31.706 \text{ slug ft})$$

So $\omega = \frac{\pi}{43.891} \left(\frac{6.4054 \times 10^7}{140.972} \right)^{\frac{1}{2}} = 48.25$ rad/sec (4.7)

Because of a large mass attached at the center of the beam (due to envelope and underslung load), the model in Fig. 10a can be modified as shown in Fig. 10b. In this model, the beam is assumed to be clamped at the center. The natural frequency for the fundamental mode in torsion is [Ref. 10, page 99]

$$\omega = \frac{\pi}{2L} \left(\frac{GJ}{I} \right)^{\frac{1}{2}}$$

In this case L = 21.946 m (length of the cantilever beam)

Thus $$\omega = \frac{\pi}{2 \times 21.946} \left(\frac{6.4054 \times 10^7}{140.972} \right)^{\frac{1}{2}} = 48.25 \text{ rad/sec} \qquad (4.8)$$

Actually, this value is the same as that obtained in Eq. (4.7) because the torsional frequency of a beam with length ℓ with one end fixed and the other end free is the same as that of a beam with length 2ℓ with both ends free, this is due to the fact that when vibrating in its fundamental mode the center of the free-free beam is a nodal point.

In the vehicle model shown in Fig. 2, there are two helicopters attached to the end of the supporting structure. They can be idealized to two tip masses having rotary inertia which are attached to the beam (Fig. 10c). Due to symmetry only one half of the model has to be considered when evaluating the natural frequency. Assuming the mode shape to be [Ref.10, page 99]

$$\eta\left(\frac{X}{L}\right) = \sin\frac{\pi}{2}\left(\frac{X}{L}\right) \qquad (4.9)$$

the generalized mass is

$$M = \int_0^L I\eta^2 \left(\frac{X}{L}\right) dx + I_H \eta^2 \left(\frac{L}{L}\right)$$

$$= IL/2 + I_{F1}$$

where I_{F1} is the inertia of the helicopter attached at the end of the beam. The generalized stiffness is

$$K = \frac{IL}{2} \omega_{NT}^2$$

where ω_{NT} is the natural frequency in fundamental mode without tip mass. In the present case, ω_{NT} = 48.25 rad/sec, and thus the fundamental frequency of the beam in torsion including the effect of tip mass is

$$\omega_T = \left[\frac{\frac{IL}{2} \omega_{NT}^2}{\frac{IL}{2} + I_{F1}} \right]^{\frac{1}{2}}$$

where I = 140.972 Kg m

I_{F1} = 8.135 x 10^3 Kg m^2 (6000 slug ft^2)

L = 21.946 m

and

$$\omega_T = \frac{\omega_{NT}}{\left(1 + \frac{2 \times 8.135 \times 10^3}{140.972 \times 21.946}\right)^{\frac{1}{2}}}$$

$$= .3997\ \omega_{NT} = 19.29 \text{ rad/sec} \qquad (4.10)$$

The fundamental mode shape and the corresponding natural frequency in torsion are given by Eq. (4.9) and (4.10).

Assumption regarding the torsional frequency of the blade

The following calculation shows why the nonrotating torsional frequency parameter of the blade is assumed to be ω_{T2} = 1.895 rad/sec.

Torsional frequency of a blade with root spring K_ϕ is

$$\omega_\phi^2 = \frac{K_\phi}{I_{MB3}R}$$

where I_{MB3} is the mass moment of inertia/unit length of the blade. Assuming $\omega_\phi = 6\Omega$ where Ω is the angular speed in R.P.M.

$$K_\phi = 36\ \Omega^2\ I_{MB3}R$$

Using the values

$$I_{MB3} = 1.1503 \times 10^{-1} \text{ Kg m}$$

and

$$R = 8.6868 \text{ m}$$

ω_{T2} becomes

$$\omega_{T2} = \left(\frac{K_\phi}{mR^3} \right)^{\frac{1}{2}}$$

$$= \left(\frac{36\Omega^2 \, I_{MB3} R}{mR^3} \right)^{\frac{1}{2}}$$

where m = 7.9529 Kg/m

Ω = 22.807 rad/sec

Thus

$$\omega_{T2} = \left(\frac{36 \times 22.807 \times .11503 \times 8.6868}{7.9529 \times 8.6868^3} \right)^{\frac{1}{2}}$$

$$= 1.895 \text{ rad/sec}$$

This value of ω_{T2} provides a torsional frequency 6Ω for the blade.

Roll Frequency of the Vehicle

The roll frequency of the vehicle is evaluated based on the simple model (Fig. 11) where the force due to buoyancy is assumed to act above the C.G.. From Fig. 11, the equation of roll motion can be written as

$$I_{xx} \ddot{\theta}_x + (P_Z^S h_3 - W_{EN} h_4) \theta = 0 \qquad (4.11)$$

Thus

$$\omega_{roll} = \left(\frac{P_Z^S h_3 - W_{EN} h_4}{I_{xx}} \right)^{\frac{1}{2}}$$

Using the values

$$P_Z^S = 1.3748 \times 10^5 \text{ N}$$

$$W_{EN} = 8.5539 \times 10^4 \text{ N}$$

$$h_3 = 14.640 \text{ m}$$

$$h_4 = 8.544 \text{ m}$$

$$I_{xx} = 6.44 \times 10^5 \text{ Kg m}^2$$

$$\omega_{roll} = \left(\frac{1.3748 \times 10^5 \times 14.640 - 8.5539 \times 10^4 \times 8.544}{6.4401 \times 10^5} \right)^{\frac{1}{2}} \qquad (4.12)$$

$$= 1.4108 \text{ rad/sec}$$

Pitch Frequency of the Vehicle

The pitch frequency of the vehicle, is evaluated using the same assumption used in determining the roll frequency, thus

$$\omega_{pitch} = \left(\frac{P_Z S h_3 - W_{EN} h_4}{I_{yy}} \right)^{\frac{1}{2}}$$

where $I_{yy} = 2.59 \times 10^6$ Kg m^2

and $\omega_{pitch} = 0.7036$ rad/sec (4.13)

4.2.3 Summary of the Various Frequencies

For the sake of convenience, the various frequencies, needed during the analysis of the vehicle, are summarized below. These frequencies are nondimensionalized with respect to rotor speed Ω, which is equal to $\Omega = 22.807$ rad/sec.

Rotor Blade: (In uncoupled modes)

Rotating flap frequency for an articulated blade is

$$\bar{\omega}_\beta^2 = 1 + \frac{3}{2} \frac{e}{R-e}$$

where $e = 0.3048$ m

$R = 8.6868$ m

Thus

$$\bar{\omega}_\beta^2 = 1.0545$$

and

$$\bar{\omega}_\beta = 1.027 \quad (4.14)$$

Nondimensional rotating lead-lag frequency is

$$\bar{\omega}_\zeta^2 = \frac{3}{2} \frac{e}{R-e}$$

$$= 0.0545$$

Thus

$$\bar{\omega}_\zeta = 0.233 \quad (4.15)$$

Nondimensional rotating torsional frequency is

$$\bar{\omega}_{\phi}^2 = \frac{K_{\phi}}{I_{MB3}R\Omega^2} + 1$$

$$= 37$$

Thus

$$\bar{\omega}_{\phi} = 6.08 \tag{4.16}$$

Vehicle:

Rigid body translation $\bar{\omega}_{RX} = 0$

$\bar{\omega}_{RY} = 0$

Rigid body rotation Pitch $\bar{\omega}_{pitch} = \frac{0.7036}{22.807} = .3085 \times 10^{-1}$ (4.17)

Roll $\bar{\omega}_{roll} = \frac{1.4108}{22.807} = .6185 \times 10^{-1}$ (4.18)

Supporting structure flexible modes

Bending in X-Y plane $\bar{\omega}_{S_{BXY}} = \frac{34.18}{22.807} = 1.499$ (4.19)

Bending in X-Z plane $\bar{\omega}_{S_{BXZ}} = \frac{34.18}{22.807} = 1.499$ (4.20)

Torsion $\bar{\omega}_{ST} = \frac{19.29}{22.807} = 0.846$ (4.21)

4.2.4 Equilibrium (Trim) Results without Sling Loads

An equilibrium analysis for the vehicle in hover is performed using the data given in the previous sections and assuming that the magnitude of the underslung load is zero.

Total weight of the vehicle $W = W_{EN} + W_S + W_H + W_{S'}$

$$= 8.5539 \times 10^4 + 9.4302 \times 10^3 + 2 \times 3.5919 \times 10^4 + 6.6723 \times 10^3$$

$$= 1.7348 \times 10^5 \text{ N (39000 lb)}$$

Buoyancy of the envelope

$$= 1.3748 \times 10^5 \text{ N (30907 lb)}$$

Weight to be supported by the two rotors

$$= 0.36 \times 10^5 \text{ N (8093 lb)}$$

Thus each rotor has to develop a thrust = 0.18×10^5 N (4046.5 lb)

The various equilibrium values for these conditions are:

Equilibrium flap angle of the blade $\beta_{k0} = 2.302$ degrees

lead-lag angle $\zeta_{k0} = -3.963$ degrees

torsion angle $\phi_{k0} = -0.115$ degrees

Collective pitch angle $\theta_0 = 4.206$ degrees

Inflow ratio $\lambda = 0.03272$

Thrust developed by each rotor $= 0.1797 \times 10^5$ N (4040 lb)

Thrust coefficient $C_T = 0.00158$

Buoyancy ratio $BR = \dfrac{1.3748 \times 10^5}{1.7348 \times 10^5} = 0.792$

As indicated previously the equilibrium values are evaluated using an iterative procedure. Therefore, the difference in thrust equal to 30 N is a very small quantity which is assumed to represent a converged value. This quantity will change the equilibrium angles only in 4th or 5th decimal point.

4.2.5 Stability Results

Using the equilibrium values from Section 4.2.4, a stability analysis was performed. From the stability analysis, the eigenvalues of the linearized system of equations are obtained. Since the present model consists of 31 degrees of freedom, one obtains 62 eigenvalues. Before proceeding to obtain

the stability boundaries, the eigenvalues have to be identified. To identify these eigenvalues, a parametric study was performed, in which the stiffness of the supporting structure and the rotary inertia of the vehicle were varied. The various other input quantities were kept fixed. Nine cases, listed below, were studied. It should be noted that for all these cases, the trim quantities are the same because the trim quantities are independent of the parameters modified in the parametric study.

Case 1: Data as presented in the previous section.

Case 2: The generalized stiffness in torsion, K_{ST}, is increased from 7.202×10^6 Kg $\frac{m^2}{sec^2}$ to 1.21×10^7 Kg $\frac{m^2}{sec^2}$. This increases the torsional frequency of the supporting structure, ω_{ST} from 19.29 rad/sec to 25 rad/sec. In nondimensional form, the increased torsional frequency is $\bar{\omega}_{ST} = \frac{25}{\Omega} = 1.096$.

Case 3: Torsional frequency of the supporting structure is $\bar{\omega}_T = 1.096$. Rotary inertia of the vehicle is increased in pitch and roll I_{xx} is increased from 6.44×10^5 Kg m^2 to 2.0×10^6 Kg m^2. I_{yy} is increased from 2.59×10^6 Kg m^2 to 4.7454×10^6 Kg m^2.

Case 4: Bending stiffness of the supporting structure is increased in both directions. The generalized stiffnesses K_{SBXY} and K_{SBXZ} are increased from 7.96×10^7 Kg/sec^2 to 1.7×10^8 Kg/sec^2. This increases the bending frequency of the supporting structure in both directions from 34.18 rad/sec to 50 rad/sec. In nondimensional form, $\bar{\omega}_{SBXY} = \bar{\omega}_{SBXZ} = \frac{50}{22.807} = 2.192$.

Case 5: Torsional frequency of the supporting structure is increased to 40 rad/sec. The generalized stiffness K_{ST} corresponding to this frequency is 3.098×10^7 Kg m^2/sec^2. In nondimensional form

$\bar{\omega}_{ST} = \frac{40}{22.807} = 1.754$. The bending frequencies are $\bar{\omega}_{SBXY} = \bar{\omega}_{SBXZ} = 2.192$.

Case 6: Rotary inertia in roll is increased from 6.44×10^5 Kg m^2 to 2.0×10^6 Kg m^2, $\bar{\omega}_{ST} = 1.754$, $\bar{\omega}_{SBXY} = \bar{\omega}_{SBXZ} = 2.192$.

Case 7: Rotary inertia in pitch and roll are increased

$I_{xx} = 2.0 \times 10^6$ Kg m^2, $I_{yy} = 4.7454 \times 10^6$ Kg m^2

$\bar{\omega}_{ST} = 1.754$, $\bar{\omega}_{SBXY} = \bar{\omega}_{SBXZ} = 2.192$

Case 8: A spring is introduced in the X-direction of the translational motion such that the nondimensional X-translational frequency is $\bar{\omega}_{Rx} = 0.01$. Also $I_{xx} = 2.0 \times 10^6$ Kg m^2, $I_{yy} = 4.7454 \times 10^6$ Kg m^2, $\bar{\omega}_{ST} = 1.754$, $\bar{\omega}_{SBXY}$, $= \bar{\omega}_{SBXZ} = 2.192$

Case 9: A spring is introduced in the Y-direction of the translational motion such that the nondimensional Y-translational frequency is $\bar{\omega}_{Ry} = 0.01$. $I_{xx} = 2.0 \times 10^6$ Kg m^2, $I_{yy} = 4.7454 \times 10^6$ Kg m^2, $\bar{\omega}_{ST} = 1.754$, $\bar{\omega}_{SBXY} = \bar{\omega}_{SBXZ} = 2.192$.

The results of the stability analysis for these nine cases are presented in Tables I, II and III, each column representing one case. For convenience a row number is also used on the left hand side of the Tables I, II and III. Thus (I,J) refers to the eigenvalue in I^{th} column and J^{th} row.

It has been previously noted that the alternating mode of the blade is independent of the other degrees of freedom. Thus there are two sets of identical eigenvalues (presented from rows 28 - 33) one for each rotor. These are

$$-0.5200 \pm i\, 0.5845 \times 10^1$$

$$-0.6562 \pm i\, 0.7265$$

$$-0.6522 \times 10^{-2} \pm i\, 0.2346$$

Since it was assumed that the torsional frequency of the rotating blade was

$\bar{\omega}_\phi$ = 6.08 (Eq. 4.16), the eigenvalue - 0.5200 ± i 0.5845 x 10^1 should correspond to alternative torsion mode. The second eigenvalue - 0.6562 ± i 0.7265 corresponds to alternating flap mode. This mode has a high damping and the damped flap frequency is 0.7265. The other eigenvalue -0.6522 x 10 ± i 0.2346 corresponds to the alternating lead-lag mode. This mode has a low damping. These three modes are all damped modes. These alternating modes have the same values for all the nine cases. Since the alternating modes are stable and remain unchanged for all cases, no further discussion of these modes is presented.

It can be seen from the results in column 1, there are 5 eigenvalues with frequencies close to 0.7 (1, 15 - 1, 19) of which one eigenvalue has a positive real part (1, 17). The eigenvalue is 0.1024 ± i 0.7428. This eigenvalue can correspond either to the torsional frequency of the structure or low frequency progressive lead-lag mode or collective flap mode. Because the torsional frequency of the structure (shown in preliminary calculations) is $\bar{\omega}_{ST}$ = 0.846 (Eq. 4.21) and the collective lead-lag frequency is 0.233 (Eq. 4.15), the progressive low frequency lead-lag mode could be close to the torsional frequency of the supporting structure. Hence there can be coupling between these modes. In order to identify the various eigenvalues, the parametric study was performed with an aim to decouple various blade and vehicle modes.

Consider the results for case 7 (column 7 in Table II). First all the eigenvalues will be identified as shown on pp. 107-108 and subsequently discussions of each mode are given in Section 4.2.6. Since the HHLA model (Fig. 2) consists of two rotor systems, the stability analysis will provide a pair of eigenvalues for each rotor degree of freedom.

It is easy to identify the blade torsional, flap and lead-lag frequencies. From the preliminary calculations, the torsional frequency is $\bar{\omega}_\phi$=6.08 (Eq. 4.18), the flap frequency is $\bar{\omega}_\beta$=1.027 (Eq. 4.14) and the lead lag frequency is $\bar{\omega}_\zeta$=0.233 (Eq. 4.15).

Torsional Frequency of the Blade

Collective	$-0.5198 \pm i\ 0.5845 \times 10^{1}$	(7,5)
	$-0.5199 \pm i\ 0.5845 \times 10^{1}$	(7,6)
High Frequency or Progressing	$-0.5207 \pm i\ 0.6846 \times 10^{1}$	(7,3)
	$-0.5202 \pm i\ 0.6845 \times 10^{1}$	(7,4)
Low Frequency or Regressing	$-0.5207 \pm i\ 0.4845 \times 10^{1}$	(7,7)
	$-0.5202 \pm i\ 0.4845 \times 10^{1}$	(7,8)

Flap Frequency of the Blade

Collective	$-0.6341 \pm i\ 0.7361$	(7,15)
	$-0.6534 \pm i\ 0.7210$	(7,16)
High Frequency or Progressing	$-0.6555 \pm i\ 0.1726 \times 10^{1}$	(7,9)
	$-0.6558 \pm i\ 0.1727 \times 10^{1}$	(7,10)
Low Frequency or Progressing	$-0.6565 \pm i\ 0.2737$	(7,20)
	$-0.6562 \pm i\ 0.2737$	(7,21)

Lead-lag Frequency of the Blade

Collective	$-0.6210 \times 10^{-2} \pm i\ 0.2337$	(7,22)
	$-0.6524 \times 10^{-2} \pm i\ 0.2346$	(7,23)
High Frequency or Progressing	$-0.1676 \times 10^{-3} \pm i\ 0.1136 \times 10^{1}$	(7,13)
	$-0.6923 \times 10^{-2} \pm i\ 0.1252 \times 10^{1}$	(7,14)
Low Frequency or Progressing	$-0.4893 \times 10^{-2} \pm i\ 0.7536$	(7,18)
	$-0.8424 \times 10^{-2} \pm i\ 0.7772$	(7,19)

Rigid Body Modes

Rigid body translation in X and Y directions

	0.0	(7,1)
	0.0	(7,2)
	$0.9833 \times 10^{-5} \pm i\ 0.2333 \times 10^{-4}$	(7,27)

Rigid body rotation

pitch	-0.3621×10^{-1}	(7,24)
	-0.1446×10^{-1}	(7,26)
roll	$-0.5947 \times 10^{-4} \pm i\ 0.3510 \times 10^{-1}$	(7,25)

Elastic Modes of the Supporting Structure

Bending in X-Y plane (Horizontal)

$-0.1029 \times 10^{-2} \pm i\ 0.217\supset \times 10^{1}$	(7,11)

Bending in X-Z plane (Vertical)

$-0.6136 \times 10^{-2} \pm i\ 0.2188 \times 10^{1}$	(7,12)
$-0.6372 \times 10^{-2} \pm i\ 0.1782 \times 10^{1}$	(7,17)

Torsion

4.2.6 Interpretation of the Physical Meaning of the Eigenvalues

Blade Torsion Modes

It is assumed that the uncoupled torsional rotating natural frequency of the blade is $\bar{\omega}_\phi = 6.08$ (Eq. 4.16). Thus the eigenvalues corresponding to this frequency must represent the collective torsional mode frequency. Frequencies corresponding to $\bar{\omega}_\phi \pm 1$ represent the cyclic mode frequencies. The cyclic modes are ϕ_{1c} and ϕ_{1s}. The progressing mode has a higher frequency and the regressing mode is the lower frequency. All these modes have negative real part indicating a positive damping and hence these modes are stable.

Blade Flap Modes

The uncoupled rotating natural frequency in flap is shown to be $\bar{\omega}_\beta = 1.027$ Eq. (4.14). In the presence of aerodynamics, the flap mode is heavily damped. Thus the damped natural frequency in flap should be less than 1.027. In the present case, the damped flap frequencies $\bar{\omega}_\beta$ are 0.7361 and 0.7210. These frequencies correspond to the collective flap modes. Frequencies corresponding to $\bar{\omega}_\beta \pm 1$ are the cyclic flap modes. These modes are also heavily damped. In this case, both cyclic modes are progressing modes, one with higher frequency and the other with a lower frequency. (When the collective mode frequency is less than 1, then both cyclic mode frequencies are progressing modes, Ref. 3.)

Blade Lead-Lag Modes

The uncoupled rotating natural frequency in lag is $\bar{\omega}_\zeta = 0.233$, Eq. (4.15). This particular frequency will appear in the eigenvalues as a collective lead-lag frequency. Another typical property of lead-lag mode is that these modes are very lightly damped. Since the collective lead-lag frequency is less than 1, both the cyclic mode frequencies are progressing. All these three modes are lightly damped.

Inspection of the eigenvalues reveals that all the blade modes are associated with two sets of eigenvalues. This is caused by the presence of the two rotors each with its own set of blade modes.

Rigid Body Translation Modes

There are four eigenvalues corresponding to the rigid body translation in X and Y directions. Two of them having zero real and zero imaginary parts. The other eigenvalue set has a very small positive real part and a very small imaginary

part. $(0.9833 \times 10^{-5} \pm i\ 0.2333 \times 10^{-4})$. The reason for choosing this eigenvalue as one corresponding to the rigid body translation is given below.

Comparing the results given in columns 7 and 8, it can be seen that all the eigenvalues except a few remain the same. The results of column 8 are obtained by introducing a translational spring in the X-direction. The spring constant is prescribed to yield a natural frequency of oscillation $\bar{\omega}_{RX} = 0.01$. From the results of column 8, it can be seen that the second eigenvalue corresponds to this frequency having a value of $0.5621 \times 10^{-5} \pm i\ .1172 \times 10^{-1}$.

The eigenvalues corresponding to R_y motion must be $0.0 + i\ 0.0$, $(8,1)^*$, and $0.9762 \times 10^{-5} + i\ 0.0$, which is assumed to be equivalent to zero. Then R_y motion results in a pure translatory motion. A similar observation can be made when a translational spring is introduced in the Y-direction (results of column 9) leaving the translational motion in X-direction free. It is seen from the results that there is an eigenvalue corresponding to a frequency $\bar{\omega}_{Ry} = 0.01$ which is $0.3349 \times 10^{-5} \pm i\ 0.1171 \times 10^{-1}$ (9,2). The eigenvalues corresponding to translational motion in the X-direction becomes $0.0 + i\ 0.0$ (9,1) and $0.9784 \times 10^{-5} + i\ 0.0$ (9,27). Then R_x motion becomes a pure translational motion.

The previous statements also imply that when the R_x motion is oscillatory, R_y motion becomes pure translational motion and vice versa. However, when both R_x and R_y are free (results of column 7) the combined R_x, R_y motions have eigenvalues which are complex conjugates. This oscillatory mode is a divergent mode, but the frequency and damping are very small. This indicates that R_x and R_y motions cannot be separated.

---

*Recall, as indicated on P. 105 (I,J) stands for the I^{th} column and J^{th} row.

Rigid Body Rotation Modes

There are four eigenvalues corresponding to pitch and roll motions. These are

$$-0.5947 \times 10^{-4} \pm i\, 0.3510 \times 10^{-1} \qquad (7,25)$$

$$-0.3621 \times 10^{-1} \pm i\, 0.0 \qquad (7,24)$$

$$-0.1446 \times 10^{-1} \pm i\, 0.0 \qquad (7,26)$$

The oscillatory mode corresponds to the roll mode and the other two pure damped modes correspond to pitch mode. These statements are further clarified by discussion presented below. Using Eq. (4.11), the roll frequency of the vehicle is

$$\bar{\omega}_{roll} = \left(\frac{P_Z^S h_3 - W_{EN} h_4}{I_{xx}} \right)^{\frac{1}{2}} \frac{1}{\Omega}$$

Substituting the various quantities

$$\bar{\omega}_{roll} = \left(\frac{1.3748 \times 10^5 \times 14.64 - 8.5539 \times 10^4 \times 8.544}{2.0 \times 10^6} \right) \frac{1}{22.807}$$

Thus

$$\bar{\omega}_{roll} = \frac{0.8006}{22.807} = 0.3510 \times 10^{-1}$$

This calculation shows that the eigenvalue $-0.5945 \times 10^{-4} \pm i\, 0.3510 \times 10^{-1}$ (7,25) corresponds to the roll mode.

Using the same elementary Eq.(4.11), the pitch frequency is

$$\bar{\omega}_{pitch} = \left(\frac{1.3748 \times 10^5 \times 14.64 - 8.5539 \times 10^4 \times 8.544}{4.7454 \times 10^6} \right)^{\frac{1}{2}} \frac{1}{22.807}$$

$$= \frac{0.5197}{22.807} = 0.2279 \times 10^{-1}$$

But this frequency is not evident in the eigenvalues. Note that for a tandem rotor system, the pitch mode is a heavily damped mode. When the damping

is in excess of the critical damping, the pitch motion becomes a pure damped motion. However when the inertia in pitch is increased, this mode will also become a oscillatory mode [Ref. 3]. The reason for the presence of a relatively high damping in pitch can be explained using Fig. 2. For positive pitching motion of the vehicle, rotor system R_1 moves up and rotor R_2 moves down. If $\dot{\theta}_y$ is the pitch rate, then the rotor R_1 has an upward velocity of $\ell_{F1}\dot{\theta}_y$, is experienced by rotor R_1. This increases the net inflow velocity sensed by rotor R_1. If the net inflow is increased, the effective angle of attack experienced by a typical blade section decreases. This in effect decreases the thrust developed by the rotor R_1. Similarly for rotor system R_2, the net inflow velocity decreases which in effect increases the angle of attack and hence the thrust. The combined effect of the increase in thrust for rotor system R_2 and decrease in thrust for R_1 due to a positive pitch rate $\dot{\theta}_y$, tends to restore the vehicle to its equilibrium position. This restoring force depends on $\dot{\theta}_y$ and produces damping in pitch. When this damping is high, the pitch motion becomes a pure damped motion. In the present case, the damping in pitch is sufficiently high so that the eigenvalues have only negative real part.

It is well known that for second order system with damping above the critical damping, an increase in inertia will bring the two eigenvalues closer provided that this increase in inertia is such that even with the increased inertia the system is still overdamped. A further increase inertia will make the eigenvalues to become complex conjugates. This effect is evident from the results by comparing the columns 6 and 7.

From column 6, the eigenvalues corresponding to pitch are

$$-0.8143 \times 10^{-1} \pm i\ 0.0 \qquad (6,24)$$

$$-0.1183 \times 10^{-1} \pm i\ 0.0 \qquad (6,26)$$

The rotary inertia in pitch for this case (case 6) is $I_{yy} = 2.59 \times 10^6$ Kg m^2. When the rotary inertia is increased to 4.7454×10^6 Kg m^2, keeping the other parameters the same, the eigenvalues corresponding to pitch motion become (column 7)

$$-0.3621 \times 10^{-1} + i\ 0.0 \quad (7,24)$$

$$-0.1446 \times 10^{-1} + i\ 0.0 \quad (7,26)$$

This shows that the eigenvalues have approached each other. This validates the statement that the pitch mode, in this case, is a overdamped mode.

Elastic Modes of the Supporting Structure

In the present analysis, the supporting structure is modelled by three normal modes: two for bending and one for torsion. The two bending modes correspond to bending in X-Z plane (Vertical) and bending in X-Y plane (Horizontal). The bending mode in X-Z plane has higher damping than that corresponding to the horizontal bending mode. The explanation is the same as that given for pitch motion, in previous section.

The eigenvalues for

bending in X-Z direction is $-0.6136 \times 10^{-2} \pm i\ 0.2188 \times 10^{1}$ (7,12)

bending in X-Y direction is $-0.1029 \times 10^{-2} \pm i\ 0.2175 \times 10^{1}$ (7,11)

torsion is $-0.6372 \times 10^{-2} \pm i\ 0.1782 \times 10^{1}$ (7,17)

The identification of these modes is based on the frequencies assumed in obtaining the results presented in column 7

$$\bar{\omega}_{SBXY} = \bar{\omega}_{SBXZ} = 2.192$$

and

$$\bar{\omega}_{ST} = 1.754$$

4.2.7 Coupling of Various Modes

The coupling between various blade modes and body modes are shown in Figs. 12-16. Since the HHLA model vehicle (Fig. 2) consists of two rotor systems coupled by the supporting structure, it was shown in Section 4.2.5 that the stability analysis provides a pair of eigenvalues for each rotor degree of freedom. Hence for the purpose of identification, in the presentation of the results shown in Figs. 12-16, the rotor modes will be referred to as mode 1 and mode 2, such as collective flap mode 1, collective flap mode 2 and high frequency flap mode 1 and high frequency flap mode 2, etc.

Figure 12 illustrates the variation of the eigenvalues of blade lead-lag modes and the supporting structure bending modes as a result of an increase in the bending stiffness (K_{SBXY}) of the supporting structure in X-Y (horizontal) plane. The bending stiffness K_{SBXY} was increased in increments from 5.09×10^7 N/m to 1.74×10^8 N/m, such that the corresponding uncoupled nondimensional bending frequency in X-Y plane ($\bar{\omega}_{SBXY}$) assumed the values $\bar{\omega}_{SBXY} = 1.2, 1.499, 1.754, 2.192$, where the frequencies are nondimensionalized with respect to the rotor speed of rotation Ω, where $\Omega = 217.79$ R.P.M. The arrows in the figure indicate the direction along which the eigenvalues of the modes change due to an increase in K_{SBXY}. The eigenvalues of the other modes, which are not shown in the figure, remain unaffected by the variation in K_{SBXY}. It can be seen from Fig. 12 that the bending mode, in X-Y plane, of the supporting structure is strongly couple with the high frequency lag mode 2. The high frequency lag mode 2 which was initially unstable becomes more stable as K_{SBXY} is increased. The damping in the bending mode in X-Y plane decreases asympototically with an increase in frequency and this mode is always stable. The low frequency lead-lag mode 2 shows a slight

decrease in damping as K_{SBXY} is increased. The eigenvalues corresponding to the bending mode in X-Z plane and the high frequency lag mode 1 are not affected by the changes in K_{SBXY}. However, since these two modes have nearly equal frequencies it can be seen that the high frequency lag mode 1 is unstable.

Figure 13 presents the variation of eigenvalues of the blade lead-lag modes and the supporting structure bending modes as a result of an increase in the bending stiffness (K_{SBXZ}) of the supporting structure in X-Z (vertical) plane. The bending stiffness K_{SBXZ} was increased in increments from 7.96×10^6 N/m to 1.74×10^8 N/m and the corresponding nondimensional uncoupled bending frequency in X-Z plane ($\bar{\omega}_{SBXZ}$) assumed the values $\bar{\omega}_{SBXZ}$ = 1.499, 1.754, 2.192. It can be seen from Fig. 13 that the bending mode in X-Z plane is strongly coupled with high frequency lag mode 1. The high frequency lag mode 1 which was initially unstable becomes a stable mode as K_{SBXZ} is increased from 7.96×10^7 N/m ($\bar{\omega}_{SBXZ}$ = 1.499) to 1.09×10^8 N/m ($\bar{\omega}_{SBXZ}$ = 1.754). But a further increase in K_{SBXZ} to 1.74×10^8 N/m does not affect the eigenvalue corresponding to the high frequency lag mode 1, indicating that these two modes are decoupled. Damping in the bending mode in X-Z plane decreases drastically at tne beginning and once the bending mode and the high frequency lag mode 1 are decoupled, the decrease in damping of the bending mode in X-Z plane is very small. Damping in the torsion mode of the supporting structure and low frequency lag mode 1 are slightly affected as K_{SBXZ} is increased. Since the torsion mode and the low frequency lag mode 1 have frequencies which are close to each other, the figure clearly indicates that the lag mode 1 is unstable. The eigenvalues corresponding to the rest of the modes are unaffected.

Figure 14 shows the eigenvalue variation in the rotor lead-lag modes and the torsion mode of the supporting structure as a result of an increase in the torsional stiffness (K_{ST}) of the supporting structure. The torsional stiffness, K_{ST}, was increased in increments from $K_{ST} = 1.59 \times 10^6$ N.m to 3.99×10^7 N.m and the corresponding uncoupled nondimensional torsional frequency ($\bar{\omega}_{ST}$) of the supporting structure are $\bar{\omega}_{ST} = 0.4, 0.55, 0.846, 1.096, 1.2, 1.3, 1.4, 1.5, 1.754, 2.0$. It is evident from the figure that the low frequency lag mode 2 and high frequency lag mode 2 remain unaffected during the variations in K_{ST} and these modes qre stable. In Fig. 14, the different curves are divided into three segments represented by points A, B, C and D. The curves between points A to B refer to the range of $K_{ST} = 3.01 \times 10^6$ N.m to 7.20×10^6 N.m ($\omega_{ST} = 0.55$ to 0.846); the curves between points B to C refer to the range $K_{ST} = 7.20 \times 10^6$ N.m to 1.685×10^7 N.m ($\bar{\omega}_{ST} = 0.846$ to 1.3); and th rves between points C to D refer to the range $K_{ST} = 1.685 \times 10^7$ N.m to 3.1×10^7 N.m ($\bar{\omega}_{ST} = 1.3$ to 1.754).

It is evident from Fig. 14 that in the range A to B, as the torsion stiffness K_{ST} is increased, the torsion mode of the supporting structure becomes increasingly stable and its frequency is increasing; the low frequency lag mode 1 becomes increasingly unstable with its frequency slightly increased. This clearl indicates that the torsion mode is strongly coupled with the low frequency lag mode 1. The high frequency lag mode 1 experiences a slight increase in frequency but its damping remains almost the same. In this range, A to B, the eigenvalues of these three modes have been distinctly identified based on their uncoupled nondimensional frequencies. In the range B to C, as the torsional stiffness K_{ST} is increased, the damping in the low frequency lag mode 1 decreases and its frequency tends to increase towards 1.0. At the same time, the damping in torsiona

mode of the supporting structure decreases drastically and a slight change in the frequency is observed (i.e. the frequency initially increases and then decreases). The high frequency lag mode 1 shows an increase in frequency with no appreciable change in damping. In this range B to C, the eigenvalues of these three modes do not exhibit a direct one to one correspondence to the uncoupled nondimensional frequencies, implying that all these modes are coupled. Hence in this range, B to C, the reference to the various modes, as torsion mode, low frequency lag mode 1 and high frequency lag mode 1, is only for the convenience of explaining the variation of the eigenvalues. When the torsional stiffness K_{ST} was increased still further, i.e. the range C to D, the eigenvalues start exhibiting a correspondence to the nondimensional uncoupled frequencies indicating that these three modes are slowly getting decoupled. In this range, C to D, the torsional mode of the supporting structure has low damping and it tends to decrease asymptotically while the frequency increases from 1.5 to 1.75. The high frequency lag mode 1 shows an increase in the frequency and the mode becomes stable at the point D. The damping in the low frequency lag mode 1 decreases while the frequency undergoes a slight reduction. Beyond the point D i.e. for $K_{ST} \geq 3.1 \times 10^7$ N.m the eigenvalues of low frequency lag mode 1 and high frequency lag mode 1 show negligible change and the damping in torsion mode remains the same but its frequency increases. Beyond point D all the three modes are stable.

Another interesting observation which can be made from Fig. 14 is associated with the effect due to the increase in torsional stiffness K_{ST}. When K_{ST} is increased from 1.685×10^7 N.m to 3.99×10^7 N.m (curve in the range C to D and beyond), the eigenvalues corresponding to the high frequency lag mode 1 tend to approach the eigenvalue corresponding to the high frequency lag mode 2 (which

remains unaffected during the variation in K_{ST}) and similarly the low frequency lag mode 1 approach to the low frequency lag mode 2. This behavior seems to indicate that as the torsional stiffness of the supporting structure is increased the coupling between the rwo rotors due to the torsional deformation of the supporting structure is eliminated. As a result of this lack of coupling, the eigenvalues corresponding to the high frequency lag modes 1 and 2 and low frequency lag modes 1 and 2 approach each other. It should be noted that elimination of the coupling of the rwo rotors, due to the torsional deformation of the supporting structure, does not imply that the two rotors are totally decoupled. The rotors are still coupled through the bending deformation of the supporting structure and rigid body pitch motion of the vehicle. The presence of this coupling causes the eigenvalues of the low frequency and high frequency lag modes to approach each other rather than coalescing.

The last observation which can be made using Fig. 14 is that the high frequency lag mode 1, low frequency lag mode 1 and torsion mode of the supporting structure undergo a reversal in their characteristics as K_{ST} is increased from 1.59×10^6 N.m. Thus, the mode which was initially a distinct torsion mode becomes a low frequency lag mode 1; the low frequency lag mode 1 becomes a high frequency lag mode 1 and the high frequency lag mode 1 becomes a torsion mode. For low and high values of the torsional stiffness (i.e., $K_{ST} \leq 1.59 \times 10^6$ N,m ($\bar{\omega}_{ST} \leq 0.4$) and $K_{ST} \geq 3.10 \times 10^7$ N.m ($\bar{\omega}_{ST} \geq 1.754$)) the torsional mode of the supporting structure, the low frequency by mode 1 and high frequency by mode 1 are all stable. For intermediate values of the torsional stiffness of the supporting one of the lag modes is unstable.

The variation of the eigenvalues of the collective flap modes and body pitch mode due to increase in body inertia in pitch is presented in Fig. 15. It is evident from the figure that the pitch mode is a pure damped mode. An increase in pitch inertia causes the eigenvalues, corresponding to the pitch mode, to approach each other. The eigenvalues of the collective flap mode 2 tend to approach the eigenvalue of the collective flap mode 1. The pure damped nature of the pitch mode is associated with the presence of two rotors. During pitch motion the net inflow in the two rotor system changes. If in one rotor system the net inflow increases, then in the other one the inflow decreases and vice versa. These changes in inflow results in changes in the thrust in the two rotor systems. The rotor system which moves up, during pitch motion, experiences a reduction in thrust due to the increased inflow and the rotor system which moves down produces more thrust due to the decreased inflow. These changes in the thrust tend to restore the vehicle to its equilibrium position. Since this restoring force is proportional to the pitch rate, this mechanism produces a damping in pitch. In the present case, the pitch motion is overdamped. Hence an increase in inertia causes the eigenvalues, corresponding to the pitch mode to approach each other, as shown in Fig. 15.

Figure 16 illustrates the variation of eigenvalues corresponding to the low frequency lag mode 2 and body roll mode as a result of an increase in inertia in roll. An increase in roll inertia tends to decrease the damping in roll, furthermore its frequency is also reduced. The low frequency lag mode 2 tends to become more stable. The roll mode, for the model vehicle, is a damped oscillatory mode. This is different from the pure damped mode normally observed in a conventional tandem rotor helicopter. The reason for this oscillatory nature of the roll mode is due to the presence of the buoyancy of the envelope.

For all the cases analyzed, it was found that the flap and torsional modes of the rotor are always stable. The eigenvalues corresponding to the cyclic flap modes and all the torsion modes are not affected by the variation in the quantities used in this parametric study. The alternating modes of the rotor were also found to be stable. The degree of coupling, as well as the relative strength of the coupling, between the various blade modes and the body modes is presented in a qualitative manner in Table IV. It is evident from this table that the supporting structure elastic modes are strongly coupled with the low frequency and high frequency lead-lag modes.

4.2.8 Effects of Buoyancy on the Stability of the Vehicle

The effects of varying the buoyancy ratio on the stability of the vehicle were also studied, by performing the stability analysis at different buoyancy ratios. During this analysis, only the buoyancy ratio was varied while the rest of the blade and vehicle parameters were kept fixed. The vehicle parameters are the same as those used in Case 7, presented in Section 4.2.5. The results of these analyses for different buoyancy ratios are presented in Tables V and VI.

Table V presents the results of the equilibrium (trim) analysis for various buoyancy ratios. It can be seen that as the buoyancy ratio is decreased, the thrust coefficient of the rotors (C_T) increases. The equilibrium angles of the blade in flap, lead-lag and torsion, the inflow ratio and the collective pitch angle, also increase with decrease in buoyancy ratios. Table V also presents the nondimensional roll frequency of the vehicle ($\bar{\omega}_{roll}$) at different buoyancy ratios. These roll frequencies are calculated using Eq. (4.11). These frequencies will be helpful in identifying the roll mode in the stability analysis.

Table VI presents the results of the stability analysis at different buoyancy ratios. The results of the stability analysis, presented in Table VI, are also shown in a graphical manner in Figs. 17 and 18. Figure 17 depicts the variation of eigenvalues of the supporting structure elastic modes with decrease in buoyancy ratio. The direction of arrows in the figure indicates the variation of the eigenvalues as a result of the decrease in buoyancy ratio. The frequencies corresponding to the supporting structure elastic modes are not affected by the variation in buoyancy ratio. However, the damping in bending in X-Y plane increases, the damping in X-Z plane decreases, while the damping in torsion mode increases.

Figure 18 presents the variation of eigenvalues of pitch and roll modes with buoyancy ratio. As the buoyancy ratio is decreased, one of the eigenvalues corresponding to the pitch mode decreases while the other eigenvalues increases. The pitch mode remains a pure damped mode. The roll mode which was initially a stable mode becomes unstable for buoyancy ratios BR $\leq$ 0.6. The results shown in Table VI also indicate that when the buoyancy ratio is decreased, the damping in the lead-lag modes of the rotors increases while the damping in flap and torsion modes of the rotoes decreases. However changes in the buoyancy ratio have only a minor effect on the frequencies of the rotor modes. From the results shown in Table VI, it can be seen that for a 40% reduction in buoyancy ratio, the damping in torsion modes decreases by 12%; the damping in flap modes decreases by 12% and the damping in lag modes increases by 200%.

The rigid body translation mode is stabilized as the buoyancy ratio is decreased.

The most important observation from these results is that for buoyancy ratio BR = 0.7, all the eigenvalues have negative real parts indicating that the vehicle is stable at this buoyancy ratio.

5. CONCLUDING REMARKS

This report presents the equilibrium (trim) equations and linearized stability equations for the dynamics of the coupled rotor/vehicle system in hovering flight. The stability equations are written in multiblade (or rotor plane) coordinate system. Two types of problems are solved. First, the aeromechanical stability of a helicopter in ground resonance is analyzed, and the analytical results are compared with the experimental results available in literature. It was found that the results of the present analysis compare very well with the experimental results. This indicates that the theoretical model for the coupled rotor/body dynamics appears to be accurate.

Next, the aeromechanical stability of an HHLA type vehicle in hover was analyzed. The vehicle consisted of two rotors, a buoyant envelope and an underslung load attached to a flexible supporting structure. For this vehicle, the total number of degrees of freedom is 31 and there are 31 coupled equations representing the dynamics of the system. Two computer programs were developed to analyze the trim and stability of the vehicle. The restuls of a sample problem are also presented in this report.

Before describing the conclusions obtained from the stability analysis of the HHLA type vehicle conducted in this study, it is important to emphasize that the vehicle model used in this study has only two rotors and not four rotors, which are present in the HHLA type vehicle under construction. Furthermore, no lead lag dampers were included in the treatment of the blade lead-lag dynamics Incorporation of such dampers would have probably stabilized any instability observed in the lead-lag degrees of freedom of the vehicle.

The stability analysis yields 62 eigenvalues, corresponding to the 31 degrees of freedom. The primary aim was to identify the 62 eigenvalues and relate them to the various modes of the rotor/vehicle assembly. This identification was accomplished by performing a parametric study in which the primary parameters allowed to vary were the bending and torsional stiffness of the supporting structure combined with the rotary inertia of the vehicle in pitch and roll. This parametric variation was done in order to decouple the blade modes from the vehicle and the supporting structure modes. In total, nine cases were analyzed. In these cases, the underslung load was not included. Based on the results obtained for these cases, the various eigenvalues and the coupling among different modes were identified and physical insight on the dynamics of the vehicle was developed. The most important results of this study are summarized below.

Cyclic lead-lag modes of the rotors couple strongly with the pitch, roll and bending in two orthogonal plane and torsion of the flexible supporting structure. This shows that the frequencies of vibrations of the supporting structure must be separated from the frequencies of the rotor lead-lag modes. This also implies the importance of modeling the supporting structure with an adequate number of elastic modes.

The stability analysis of the coupled rotor/vehicle dynamics illustrates the aeroelastic stability of the rotor, coupled rotor/vehicle aeromechanical stability such as air resonance and the vehicle stability in the longitudinal and lateral planes. Complete information of these ingredients are all captured by the analytical model representing the coupled rotor/vehicle dynamics.

In the discussion of the results it has been noted that the pitch mode of the vehicle is a pure damped mode while the roll mode is a stable oscillatory mode. The oscillatory nature of the roll mode can be attributed to the presence of the buoyant envelope.

The present analysis yields a divergent mode which corresponds to a pure translational mode. It is also found that when the vehicle is free in longitudinal and lateral translational motions, the results indicate a oscillatory mode for the rigid body translation. However, when the translational motion in one direction is restrained, the translational motion in the other direction becomes a pure divergent motion. This indicates that the longitudinal and lateral dynamics cannot be separated in the analysis of coupled rotors/vehicle dynamics for vehicles of the type considered in this study.

The stability of the vehicle was also studied at various buoyancy ratios and it was found that at a particular buoyancy ratio, the eigenvalues corresponding to all the modes have negative real part indicating that the vehicle is stable at this buoyancy ratio.

Based on the numerical studies conducted in this report it appears that the consistent analytical model, for the dynamics of coupled rotor/vehicle system, developed in this study is a valid mathematical model. The stability analysis of coupled rotor/vehicle dynamics yields useful information on both the aeroelastic stability, aeromechanical stability and also the vehicle dynamic stability.

6. REFERENCES

1. Venkatesan, C. and Friedmann, P.P., "Aeroelastic Effects in Multi-Rotor Vehicles with Application to a Hybrid Heavy Lift System, Part I: Formulation of Equations of Motion", NASA CR 3822, August 1984.

2. Friedmann, P.P., "Formulation and Solution of Rotary-Wing Aeroelastic Stability and Response Problems", Presented at the Eighth European Rotorcraft Forum at Aix-En-Provence, France, Aug. 31-Sept. 3, 1982.

3. Johnson, W., Helicopter Theory, Princeton University Press, Princeton, New Jersey, 1980.

4. Friedmann, P.P. and Kottapalli, S.B.R., "Coupled Flap-Lag-Torsional Dynamics of Hingeless Rotor Blades in Forward Flight", Journal of the American Helicopter Society, Vol. 27, No. 4, Oct. 1982, pp. 28-36.

5. Levin, J., "Formulation of Helicopter Air-Resonance Problem in Hover with Active Controls", M.Sc. Thesis, Mechanics and Structures Department, University of Californa, Los Angeles, Sept. 1980.

6. Bousman, W.G., "An Experimental Investigation of the Effects of Aeroelastic Couplings on Aeromechanical Stability of a Hingeless Rotor Helicopter", Journal of the American Helicopter Society, Vol. 26, No. 1, Jan. 1981, pp. 46-54.

7. Johnson W., "Influence of Unsteady Aerodynamics on Hingeless Rotor Ground Resonance", Journal of Aircraft, Vol. 19, No. 8, Aug. 1982, pp. 668-673.

8. Friedmann, P.P., and Venkatesan, C., "Coupled Helicopter Rotor/Body Aeromechanical Stability - Comparison of Theoretical and Experimental Results", Journal of Aircraft, February, 1985.

9. Friedmann, P.P., and Venkatesan, C., "Influence of Various Unsteady Aerodynamic Models on the Aeromechanical Stability of a Helicopter in Ground Resonance", Proceedings of the 2nd Decennial Specialists' Meeting on Rotorcraft Dynamics, Nov. 7-9, 1984, NASA Ames Research Center, Moffett Field, California.

10. Bisplinghoff, R.L., Ashley, H. and Halfman, R.L., "Aeroelasticity", Addison-Wesley, 1955.

11. Blevins, R.D.,"Formulas for Natural Frequency and Mode Shape", Van Nostrand Reinhold Co., 1979.

	Case 1 $\bar{\omega}_{SBXY}=\bar{\omega}_{SBXZ}=1.499, \bar{\omega}_{ST}=0.846$ $I_{xx} = 6.44 \times 10^5$ Kg m^2 $I_{yy} = 2.59 \times 10^6$ Kg m^2	Case 2 $\bar{\omega}_{SBXY}=\bar{\omega}_{SBXZ}=1.499, \bar{\omega}_{ST}=1.096$ $I_{xx} = 6.44 \times 10^5$ Kg m^2 $I_{yy} = 2.59 \times 10^6$ Kg m^2	Case 3 $\bar{\omega}_{SBXY}=\bar{\omega}_{SBXZ}=1.499, \bar{\omega}_{ST}=1.096$ $I_{xx} = 2.0 \times 10^6$ Kg m^2 $I_{yy} = 4.7454 \times 10^6$ Kg m^2	Case 4 $\bar{\omega}_{SBXY}=\bar{\omega}_{SBXZ}=2.192, \bar{\omega}_{ST}=1.096$ $I_{xx} = 6.44 \times 10^5$ Kg m^2 $I_{yy} = 2.59 \times 10^6$ Kg m^2
1	0.0 0.0	0.0 0.0	0.0 0.0	0.0 0.0
2	0.0 0.0	0.0 0.0	0.0 0.0	0.0 0.0
3	$-.5206 \pm i\ .6846 \times 10^1$	$-.5206 \pm i\ .6846 \times 10^1$	$-.5206 \pm i\ .6846 \times 10^1$	$-.5206 \pm i\ .6846 \times 10^1$
4	$-.5203 \pm i\ .6845 \times 10^1$	$-.5203 \pm i\ .6845 \times 10^1$	$-.5202 \pm i\ .6845 \times 10^1$	$-.5203 \pm i\ .6845 \times 10^1$
5	$-.5198 \pm i\ .5845 \times 10^1$	$-.5198 \pm i\ .5845 \times 10^1$	$-.5198 \pm i\ .5845 \times 10^1$	$-.5198 \pm i\ .5845 \times 10^1$
6	$-.5198 \pm i\ .5844 \times 10^1$	$-.5198 \pm i\ .5844 \times 10^1$	$-.5199 \pm i\ .5845 \times 10^1$	$-.5198 \pm i\ .5844 \times 10^1$
7	$-.5207 \pm i\ .4845 \times 10^1$	$-.5207 \pm i\ .4845 \times 10^1$	$-.5207 \pm i\ .4845 \times 10^1$	$-.5207 \pm i\ .4845 \times 10^1$
8	$-.5203 \pm i\ .4845 \times 10^1$	$-.5203 \pm i\ .4845 \times 10^1$	$-.5202 \pm i\ .4845 \times 10^1$	$-.5203 \pm i\ .4845 \times 10^1$
9	$-.6556 \pm i\ .1727 \times 10^1$	$-.6556 \pm i\ .1727 \times 10^1$	$-.6556 \pm i\ .1727 \times 10^1$	$-.6555 \pm i\ .1727 \times 10^1$
10	$-.6556 \pm i\ .1727 \times 10^1$	$-.6556 \pm i\ .1727 \times 10^1$	$-.6556 \pm i\ .1727 \times 10^1$	$-.6558 \pm i\ .1727 \times 10^1$
11	$-.4722 \times 10^{-2} \pm i.1555 \times 10^1$	$-.4722 \times 10^{-2} \pm i.1555 \times 10^1$	$-.4693 \times 10^{-2} \pm i.1555 \times 10^1$	$-.1030 \times 10^{-2} \pm i.2175 \times 10^1$
12	$-.8915 \times 10^{-2} \pm i.1474 \times 10^1$	$.2525 \times 10^{-1} \pm i.1467 \times 10^1$	$.2525 \times 10^{-1} \pm i.1467 \times 10^1$	$-.6269 \times 10^{-2} \pm i.2189 \times 10^1$
13	$-.1395 \times 10^{-1} \pm i.1408 \times 10^1$	$-.4803 \times 10^{-1} \pm i.1462 \times 10^1$	$-.4803 \times 10^{-1} \pm i.1462 \times 10^1$	$-.1143 \times 10^{-1} \pm i.1424 \times 10^1$
14	$-.3021 \times 10^{-2} \pm i.1195 \times 10^1$	$-.3021 \times 10^{-2} \pm i.1195 \times 10^1$	$-.2948 \times 10^{-2} \pm i.1193 \times 10^1$	$-.7002 \times 10^{-2} \pm i.1254 \times 10^1$
15	$-.6157 \pm i\ .7452$	$-.6157 \pm i\ .7452$	$-.6341 \pm i\ .7361$	$-.6157 \pm i\ .7452$
16	$-.6483 \pm i\ .7167$	$-.6483 \pm i\ .7167$	$-.6483 \pm i\ .7167$	$-.6534 \pm i\ .7210$
17	$.1024 \pm i\ .7428$	$.7266 \times 10^{-1} \pm i\ .8399$	$.7266 \times 10^{-1} \pm i\ .8399$	$.7352 \times 10^{-1} \pm i\ .8396$
18	$-.5095 \times 10^{-2} \pm i\ .7555$	$-.5095 \times 10^{-2} \pm i\ .7555$	$-.5375 \times 10^{-2} \pm i\ .7566$	$-.4631 \times 10^{-2} \pm i\ .7525$
19	$-.1057 \pm i\ .7306$	$-.7611 \times 10^{-1} \pm i\ .8151$	$-.7611 \times 10^{-1} \pm i\ .8151$	$-.7701 \times 10^{-1} \pm i\ .8150$
20	$-.6565 \pm i\ .2739$	$-.6565 \pm i\ .2739$	$-.6565 \pm i\ .2737$	$-.6565 \pm i\ .2739$
21	$-.6562 \pm i\ .2739$	$-.6562 \pm i\ .2738$	$-.6562 \pm i\ .2738$	$-.6562 \pm i\ .2738$
22	$-.5697 \times 10^{-2} \pm i\ .2331$	$-.5697 \times 10^{-2} \pm i\ .2331$	$-.6210 \times 10^{-2} \pm i\ .2337$	$-.5697 \times 10^{-2} \pm i\ .2331$
23	$-.6527 \times 10^{-2} \pm i\ .2346$	$-.6527 \times 10^{-2} \pm i\ .2346$	$-.6527 \times 10^{-2} \pm i\ .2346$	$-.6524 \times 10^{-2} \pm i\ .2346$
24	$-.8143 \times 10^{-1}$ 0.0	$-.8143 \times 10^{-1}$ 0.0	$-.3621 \times 10^{-1}$ 0.0	$-.8143 \times 10^{-1}$ 0.0
25	$-.2106 \times 10^{-3} \pm i.6174 \times 10^{-1}$	$-.2106 \times 10^{-3} \pm i.6147 \times 10^{-1}$	$-.5949 \times 10^{-4} \pm i.3510 \times 10^{-1}$	$-.2105 \times 10^{-3} \pm i.6174 \times 10^{-1}$
26	$-.1183 \times 10^{-1}$ 0.0	$-.1183 \times 10^{-1}$ 0.0	$-.1446 \times 10^{-1}$ 0.0	$-.1183 \times 10^{-1}$ 0.0
27	$.9833 \times 10^{-5} \pm i.2333 \times 10^{-4}$	$.9833 \times 10^{-5} \pm i.2333 \times 10^{-4}$	$.9833 \times 10^{-5} \pm i.2333 \times 10^{-4}$	$.9833 \times 10^{-5} \pm i.2333 \times 10^{-4}$
28	$-.5200 \pm i\ .5845 \times 10^1$	$-.5200 \pm i\ .5845 \times 10^1$	$-.5200 \pm i\ .5845 \times 10^1$	$-.5200 \pm i\ .5845 \times 10^1$
29	$-.6562 \pm i\ .7265$	$-.6562 \pm i\ .7265$	$-.6562 \pm i\ .7265$	$-.6562 \pm i\ .7265$
30	$-.6522 \times 10^{-2} \pm i\ .2346$	$-.6522 \times 10^{-2} \pm i\ .2346$	$-.6522 \times 10^{-2} \pm i\ .2346$	$-.6522 \times 10^{-2} \pm i\ .2346$
31	$-.5200 \pm i\ .5845 \times 10^1$	$-.5200 \pm i\ .5845 \times 10^1$	$-.5200 \pm i\ .5845 \times 10^1$	$-.5200 \pm i\ .5845 \times 10^1$
32	$-.6562 \pm i\ .7265$	$-.6562 \pm i\ .7265$	$-.6562 \pm i\ .7265$	$-.6562 \pm i\ .7265$
33	$-.6522 \times 10^{-2} \pm i\ .2346$	$-.6522 \times 10^{-2} \pm i\ .2346$	$-.6522 \times 10^{-2} \pm i\ .2346$	$-.6522 \times 10^{-2} \pm i\ .2346$

Table I Results of Stability Analysis for Various Configuration Parameters

BR = 0.792, C_T = 0.00158

	Case 5 $\bar{\omega}_{SBXY}=\bar{\omega}_{SBXZ}=2.192, \bar{\omega}_{ST}=1.754$ $I_{xx} = 6.44 \times 10^5$ Kg m^2 $I_{yy} = 2.59 \times 10^6$ Kg m^2	Case 6 $\bar{\omega}_{SBXY}=\bar{\omega}_{SBXZ}=2.192, \bar{\omega}_{ST}=1.754$ $I_{xx} = 2.0 \times 10^6$ Kg m^2 $I_{yy} = 2.59 \times 10^6$ Kg m^2	Case 7 $\bar{\omega}_{SBXY}=\bar{\omega}_{SBXZ}=2.192, \bar{\omega}_{ST}=1.754$ $I_{xx} = 2.0 \times 10^6$ Kg m^2 $I_{yy} = 4.7454 \times 10^6$ Kg m^2	Case 8 $\bar{\omega}_{SBXY}=\bar{\omega}_{SBXZ}=2.192, \bar{\omega}_{ST}=1.754, \bar{\omega}_{RX}=0.01$ $I_{xx} = 2.0 \times 10^6$ Kg m^2 $I_{yy} = 4.7454 \times 10^6$ Kg m^2
1	0.0 0.0	0.0 0.0	0.0 0.0	0.0 0.0
2	0.0 0.0	0.0 0.0	0.0 0.0	$.5621\times10^{-5} \pm i.1172\times10^{-1}$
3	$-.5207 \pm i\ .6846 \times 10^1$	$-.5207 \pm i\ .6846 \times 10^1$	$-.5207 \pm i\ .6846 \times 10^1$	$-.5207 \pm i\ .6846 \times 10^1$
4	$-.5203 \pm i\ .6845 \times 10^1$	$-.5202 \pm i\ .6845 \times 10^1$	$-.5202 \pm i\ .6845 \times 10^1$	$-.5202 \pm i\ .6845 \times 10^1$
5	$-.5198 \pm i\ .5845 \times 10^1$	$-.5198 \pm i\ .5845 \times 10^1$	$-.5198 \pm i\ .5845 \times 10^1$	$-.5198 \pm i\ .5845 \times 10^1$
6	$-.5198 \pm i\ .5844 \times 10^1$	$-.5198 \pm i\ .5844 \times 10^1$	$-.5199 \pm i\ .5845 \times 10^1$	$-.5199 \pm i\ .5845 \times 10^1$
7	$-.5207 \pm i\ .4845 \times 10^1$	$-.5207 \pm i\ .4845 \times 10^1$	$-.5207 \pm i\ .4845 \times 10^1$	$-.5207 \pm i\ .4845 \times 10^1$
8	$-.5203 \pm i\ .4845 \times 10^1$	$-.5202 \pm i\ .4845 \times 10^1$	$-.5202 \pm i\ .4845 \times 10^1$	$-.5202 \pm i\ .4845 \times 10^1$
9	$-.6555 \pm i\ .1726 \times 10^1$	$-.6555 \pm i\ .1726 \times 10^1$	$-.6555 \pm i\ .1726 \times 10^1$	$-.6555 \pm i\ .1726 \times 10^1$
10	$-.6558 \pm i\ .1727 \times 10^1$	$-.6558 \pm i\ .1727 \times 10^1$	$-.6558 \pm i\ .1727 \times 10^1$	$-.6558 \pm i\ .1727 \times 10^1$
11	$-.1030\times10^{-2} \pm i.2175\times10^1$	$-.1032\times10^{-2} \pm i.2175\times10^1$	$-.1029\times10^{-2} \pm i.2175\times10^1$	$-.1029\times10^{-2} \pm i.2175\times10^1$
12	$-.6136\times10^{-2} \pm i.2188\times10^1$	$-.6136\times10^{-2} \pm i.2188\times10^1$	$-.6136\times10^{-2} \pm i.2188\times10^1$	$-.6136\times10^{-2} \pm i.2188\times10^1$
13	$-.1676\times10^{-3} \pm i.1136\times10^1$	$-.1676\times10^{-3} \pm i.1136\times10^1$	$-.1676\times10^{-3} \pm i.1136\times10^1$	$-.1676\times10^{-3} \pm i.1136\times10^1$
14	$-.7002\times10^{-2} \pm i.1254\times10^1$	$-6951\times10^{-2} \pm i.1252\times10^1$	$-.6923\times10^{-2} \pm i.1252\times10^1$	$-.6923\times10^{-2} \pm i.1252\times10^1$
15	$-.6157 \pm i\ .7452$	$-.6157 \pm i\ .7452$	$-.6341 \pm i\ .7361$	$-.6341 \pm i\ .7361$
16	$-.6534 \pm i\ .7210$	$-.6534 \pm i\ .7210$	$-.6534 \pm i\ .7210$	$-.6534 \pm i\ .7210$
17	$-.6372\times10^{-2} \pm i.1782\times10^1$	$-.6372\times10^{-2} \pm i.1782\times10^1$	$-.6372\times10^{-2} \pm i.1782\times10^1$	$-.6372\times10^{-2} \pm i.1782\times10^1$
18	$-.4631 \times 10^{-2} \pm i.7525$	$-.4830 \times 10^{-2} \pm i.7534$	$-.4893 \times 10^{-2} \pm i.7536$	$-.4893 \times 10^{-2} \pm i.7536$
19	$-.8424 \times 10^{-2} \pm i.7772$	$-.8424 \times 10^{-2} \pm i.7772$	$-.8424 \times 10^{-2} \pm i.7772$	$-.8424 \times 10^{-2} \pm i.7772$
20	$-.6565 \pm i\ .2739$	$-.6565 \pm i\ .2737$	$-.6565 \pm i\ .2737$	$-.6565 \pm i\ .2737$
21	$-.6562 \pm i\ .2737$	$-.6562 \pm i\ .2737$	$-.6562 \pm i\ .2737$	$-.6562 \pm i\ .2737$
22	$-.5697 \times 10^{-2} \pm i.2331$	$-.5697 \times 10^{-2} \pm i.2331$	$-.6210 \times 10^{-2} \pm i.2337$	$-.6210 \times 10^{-2} \pm i.2337$
23	$-.6524 \times 10^{-2} \pm i.2346$	$-.6524 \times 10^{-2} \pm i.2346$	$-.6524 \times 10^{-2} \pm i.2346$	$-.6524 \times 10^{-2} \pm i.2346$
24	$-.8143 \times 10^{-1}$ 0.0	$-.8143 \times 10^{-1}$ 0.0	$-.3621 \times 10^{-1}$ 0.0	$-.3621 \times 10^{-1}$ 0.0
25	$-.2105\times10^{-3} \pm i.6174\times10^{-1}$	$-.5947\times10^{-4} \pm i.3510\times10^{-1}$	$-.5947\times10^{-4} \pm i.3510\times10^{-1}$	$-.5947\times10^{-4} \pm i.3510\times10^{-1}$
26	$-.1183 \times 10^{-1}$ 0.0	$-.1183 \times 10^{-1}$ 0.0	$-.1446 \times 10^{-1}$ 0.0	$-.1446 \times 10^{-1}$ 0.0
27	$.9833\times10^{-5} \pm i.2333\times10^{-4}$	$.9833\times10^{-5} \pm i.2333\times10^{-4}$	$.9833\times10^{-5} \pm i.2333\times10^{-4}$	$.9762 \times 10^{-5}$ 0.0
28	$-.5200 \pm i\ .5845 \times 10^1$	$-5200 \pm i\ .5845 \times 10^1$	$-.5200 \pm i\ .5845 \times 10^1$	$-.5200 \pm i\ .5845 \times 10^1$
29	$-.6562 \pm i\ .7265$	$-.6562 \pm i\ .7265$	$-.6562 \pm i\ .7265$	$-.6562 \pm i\ .7265$
30	$-.6522 \times 10^{-2} \pm i.2346$	$-.6522 \times 10^{-2} \pm i.2346$	$-.6522 \times 10^{-2} \pm i.2346$	$-.6522 \times 10^{-2} \pm i.2346$
31	$-.5200 \pm i\ .5845 \times 10^1$	$-.5200 \pm i\ .5845 \times 10^1$	$-.5200 \pm i\ .5845 \times 10^1$	$-.5200 \pm i\ .5845 \times 10^1$
32	$-.6562 \pm i\ .7265$	$-.6562 \pm i\ .7265$	$-.6562 \pm i\ .7265$	$-.6562 \pm i\ .7265$
33	$-.6522 \times 10^{-2} \pm i\ .2346$	$-.6522 \times 10^{-2} \pm i\ .2346$	$-.6522 \times 10^{-2} \pm i\ .2346$	$-.6522 \times 10^{-2} \pm i\ .2346$

Table II Results of Stability Analysis for Various Configurations

Parameters

BR = 0.792, C_T = 0.00158

	Case 9 $\bar{\omega}_{SBXY}=\bar{\omega}_{SBXZ}=2.192, \bar{\omega}_{ST}=1.754,$ $\bar{\omega}_{Ry}=0.01$ $I_{xx} = 2.0 \times 10^{6}$ Kg m^2 $I_{yy} = 4.7454 \times 10^{6}$ Kg m^2
1	0.0 0.0
2	$.3349\times10^{-5} \pm i.1171\times10^{-1}$
3	$-.5207 \pm i\ .6846 \times 10^{1}$
4	$-.5202 \pm i\ .6845 \times 10^{1}$
5	$-.5198 \pm i\ .5845 \times 10^{1}$
6	$-.5198 \pm i\ .5845 \times 10^{1}$
7	$-.5207 \pm i\ .4845 \times 10^{1}$
8	$-.5202 \pm i\ .4845 \times 10^{1}$
9	$-.6555 \pm i\ .1726 \times 10^{1}$
10	$-.6558 \pm i\ .1727 \times 10^{1}$
11	$-.1029\times10^{-2} \pm i.2175\times10^{1}$
12	$-.6136\times10^{-2} \pm i.2188\times10^{1}$
13	$-.1676\times10^{-3} \pm i.1136\times10^{1}$
14	$-.6923\times10^{-2} \pm i.1252\times10^{1}$
15	$-.6341 \pm i\ .7361$
16	$-.6534 \pm i\ .7210$
17	$-.6372\times10^{-2} \pm i.1782\times10^{1}$
18	$-.4893\times10^{-2} \pm i.7536$
19	$-.8424 \times 10^{-2} \pm i.7772$
20	$-.6565 \pm i\ .2737$
21	$-.6562 \pm i\ .2737$
22	$-.6210 \times 10^{-2} \pm i\ .2337$
23	$-.6524 \times 10^{-2} \pm i.2346$
24	$-.3621 \times 10^{-1}$ 0.0
25	$-.5947\times10^{-4} \pm i.3510\times10^{-1}$
26	$-.1446 \times 10^{-1}$ 0.0
27	$.9784 \times 10^{-5}$ 0.0
28	$-.5200 \pm i\ .5845 \times 10^{1}$
29	$-.6562 \pm i\ .7265$
30	$-.6522 \times 10^{-2} \pm i\ .2346$
31	$-.5200 \pm i\ 5845 \times 10^{-1}$
32	$-.6522 \pm i\ .7265$
33	$-.6522 \times 10^{-2} \pm i\ .2346$

Table III Results of Stability Analysis for Various Configuration Parameters

BR = 0.792, C_T = 0.00158

MODES	Lead-lag Modes						Flap Modes					
	High freq.		collective freq.		Low freq.		High freq.		collective freq.		Low freq.	
	1	2	1	2	1	2	1	2	1	2	1	2
Supporting structure symmetric bending in x-y (horizontal) plane		XXX				XX						
Supporting structure symmetric bending in x-z (vertical) plane	XXX		X		XX				X			
Supporting structure torsion(antisymmetric)	XXX				XXX							
Body pitch		X		X		X				X		
Body roll		X				XX						

Legend: XXX = Strongly coupled, XX = Moderately coupled, X = Weakly coupled

Table IV Coupling Between Various Body Modes and Blade Modes

Buoyancy Ratio BR	θ_0	β_{k0}	ζ_{k0}	ϕ_{k0}	λ	C_T	$\bar{\omega}_{roll}$
0.792	4.206°	2.302°	-3.963°	-0.115°	0.03272	.00158	$.3510\times10^{-1}$
0.7	5.243°	3.209°	-5.074°	-0.161°	0.03820	.00228	$.3173\times10^{-1}$
0.6	6.259°	4.179°	-6.453°	-0.236°	0.04313	.00304	$.2761\times10^{-1}$
0.5	7.207°	5.142°	-7.994°	-0.352°	0.04743	.00380	$.2276\times10^{-1}$

Table V Equilibrium Values at Different Buoyancy Ratios

$\bar{\omega}_{ST}=1.754$, $\bar{\omega}_{SBXY}=\bar{\omega}_{SBXZ}=2.192$, $I_{yy}=4.7454\times10^{6}\,kg.m^2$

$I_{xx}=2.0\times10^{6}\,kg.m^2$

$\bar{\omega}_{ST} = 1.754$, $\bar{\omega}_{SBXY} = \bar{\omega}_{SBXZ} = 2.192$

$I_{yy} = 4.7454 \times 10^6$ Kg m^2, $I_{xx} = 2.0 \times 10^6$ Kg m^2

		BR = 0.792	0.7	0.6	0.5
	Blade Torsion	$-.5207 \pm i\ .6846 \times 10^1$	$-.4954 \pm i\ .6861 \times 10^1$	$-.4727 \pm i\ .6892 \times 10^1$	$-.4589 \pm i\ .6945 \times 10^1$
		$-.5202 \pm i\ .6845 \times 10^1$	$-.4946 \pm i\ .6859 \times 10^1$	$-.4715 \pm i\ .6889 \times 10^1$	$-.4572 \pm i\ .6940 \times 10^1$
		$-.5198 \pm i\ .5845 \times 10^1$	$-.4940 \pm i\ .5858 \times 10^1$	$-.4707 \pm i\ .5888 \times 10^1$	$-.4560 \pm i\ .5939 \times 10^1$
		$-.5199 \pm i\ .5845 \times 10^1$	$-.4940 \pm i\ .5859 \times 10^1$	$-.4706 \pm i\ .5888 \times 10^1$	$-.4559 \pm i\ .5939 \times 10^1$
		$-.5202 \pm i\ .4845 \times 10^1$	$-.4945 \pm i\ .4859 \times 10^1$	$-.4731 \pm i\ .4887 \times 10^1$	$-.4570 \pm i\ .4939 \times 10^1$
		$-.5207 \pm i\ .4845 \times 10^1$	$-.4956 \pm i\ .4858 \times 10^1$	$-.4713 \pm i\ .4889 \times 10^1$	$-.4598 \pm i\ .4936 \times 10^1$
	Blade Flap	$-.6558 \pm i\ .1727 \times 10^1$	$-6411 \pm i\ .1721 \times 10^1$	$-.6118 \pm i\ .1724 \times 10^1$	$-.5670 \pm i\ .1740 \times 10^1$
		$-.6555 \pm i\ .1726 \times 10^1$	$-.6402 \pm i\ .1721 \times 10^1$	$-.6143 \pm i\ .1725 \times 10^1$	$-.5725 \pm i\ .1742 \times 10^1$
		$-.6341 \pm i\ .7361$	$-.6192 \pm i\ .7313$	$-.5925 \pm i\ .7362$	$-.5514 \pm i\ .7547$
		$-.6534 \pm i\ .7210$	$-.6393 \pm i\ .7158$	$-.6136 \pm i\ .7196$	$-.5736 \pm i\ .7364$
		$-.6565 \pm i\ .2737$	$-.6426 \pm i\ .2788$	$-.6162 \pm i\ .2750$	$-.5773 \pm i\ .2577$
		$-.6562 \pm i\ .2737$	$-.6420 \pm i\ .2789$	$-.6172 \pm i\ .2748$	$-.5758 \pm i\ .2580$
	Blade Lead-Lag	$-.6923 \times 10^{-2} \pm i.1252 \times 10^1$	$-.1006 \times 10^{-1} \pm i.1252 \times 10^1$	$-.1428 \times 10^{-1} \pm i.1252 \times 10^1$	$-.1957 \times 10^{-1} \pm i.1253 \times 10^1$
		$-.1676 \times 10^{-3} \pm i.1136 \times 10^1$	$-.1496 \times 10^{-2} \pm i.1136 \times 10^1$	$-.3490 \times 10^{-2} \pm i.1136 \times 10^1$	$-.6190 \times 10^{-2} \pm i.1136 \times 10^1$
		$-.6210 \times 10^{-2} \pm i.2337$	$-.9320 \times 10^{-2} \pm i.2337$	$-.1363 \times 10^{-1} \pm i.2335$	$-.1905 \times 10^{-1} \pm i.2328$
		$-.6524 \times 10^{-2} \pm i.2346$	$-.9659 \times 10^{-2} \pm i.2352$	$-.1389 \times 10^{-1} \pm i.2359$	$-.1920 \times 10^{-1} \pm i.2363$
		$-.8424 \times 10^{-2} \pm i.7772$	$-.1211 \times 10^{-1} \pm i.7769$	$-.1703 \times 10^{-1} \pm i.7768$	$-.2313 \times 10^{-1} \pm i.7772$
		$-.4893 \times 10^{-2} \pm i.7536$	$-.7608 \times 10^{-2} \pm i.7529$	$-.1136 \times 10^{-1} \pm i.7521$	$-.1617 \times 10^{-1} \pm i.7514$
	Rigid Body Translation	0.0 0.0	0.0 0.0	0.0 0.0	0.0 0.0
		0.0 0.0	0.0 0.0	0.0 0.0	0.0 0.0
		$.9833 \times 10^{-5} \pm i\ .2334 \times 10^{-4}$	$-.5716 \times 10^{-5} \pm i.5015 \times 10^{-4}$	$-.6929 \times 10^{-4} \pm i.1058 \times 10^{-3}$	$-.2814 \times 10^{-3} \pm i.2372 \times 10^{-3}$
	Pitch	$-.3621 \times 10^{-1}$ 0.0	$-.4181 \times 10^{-1}$ 0.0	$-.4640 \times 10^{-1}$ 0.0	$-.5012 \times 10^{-1}$ 0.0
		$-.1446 \times 10^{-1}$ 0.0	$-.1025 \times 10^{-1}$ 0.0	$-.6918 \times 10^{-2}$ 0.0	$-.4048 \times 10^{-2}$ 0.0
	Roll	$-.5947 \times 10^{-4} \pm i.3510 \times 10^{-1}$	$-.3602 \times 10^{-4} \pm i.3174 \times 10^{-1}$	$.1155 \times 10^{-5} \pm i.2765 \times 10^{-1}$	$.8069 \times 10^{-4} \pm i.2285 \times 10^{-1}$
Supporting Structure	Bending in X-Y	$-.1029 \times 10^{-2} \pm i.2175 \times 10^1$	$-.1394 \times 10^{-2} \pm i.2175 \times 10^1$	$-.1952 \times 10^{-2} \pm i.2176 \times 10^1$	$-.2762 \times 10^{-2} \pm i.2177 \times 10^1$
	Bending in X-Z	$-.6136 \times 10^{-2} \pm i.2188 \times 10^1$	$-.5773 \times 10^{-2} \pm i.2188 \times 10^1$	$-.5152 \times 10^{-2} \pm i.2188 \times 10^1$	$-.4165 \times 10^{-2} \pm i.2189 \times 10^1$
	Torsion	$-.6372 \times 10^{-2} \pm i.1782 \times 10^1$	$-.9268 \times 10^{-2} \pm i.1783 \times 10^1$	$-.1388 \times 10^{-1} \pm i.1783 \times 10^1$	$-.2100 \times 10^{-1} \pm i.1785 \times 10^1$
Alternating Modes	Torsion	$-.5200 \pm i\ .5845 \times 10^1$	$-.4941 \pm i\ .5859 \times 10^1$	$-.4706 \pm i\ .5889 \times 10^1$	$-.4557 \pm i\ .5940 \times 10^1$
	Flap	$-.6562 \pm i\ .7265$	$-.6421 \pm i\ .7213$	$-.6162 \pm i\ .7254$	$-.5759 \pm i\ .7426$
	Lead-Lag	$-.6522 \times 10^{-2} \pm i.2346$	$-.9658 \times 10^{-2} \pm i.2352$	$-.1389 \times 10^{-1} \pm i.2358$	$-.1921 \times 10^{-1} \pm i.2363$
	Torsion	$-.5200 \pm i\ .5845 \times 10^1$	$-.4941 \pm i\ .5859 \times 10^1$	$-.4706 \pm i\ .5889 \times 10^1$	$-.4557 \pm i\ .5940 \times 10^1$
	Flap	$-.6562 \pm i\ .7265$	$-.6421 \pm i\ .7213$	$-.6162 \pm i\ .7254$	$-.5759 \pm i\ .7426$
	Lead-Lag	$-.6522 \times 10^{-2} \pm i.2346$	$-.9658 \times 10^{-2} \pm i.2352$	$-.1389 \times 10^{-1} \pm i.2358$	$-.1921 \times 10^{-1} \pm i.2363$

Table VI Results of Stability Analysis at Different Buoyancy Ratios

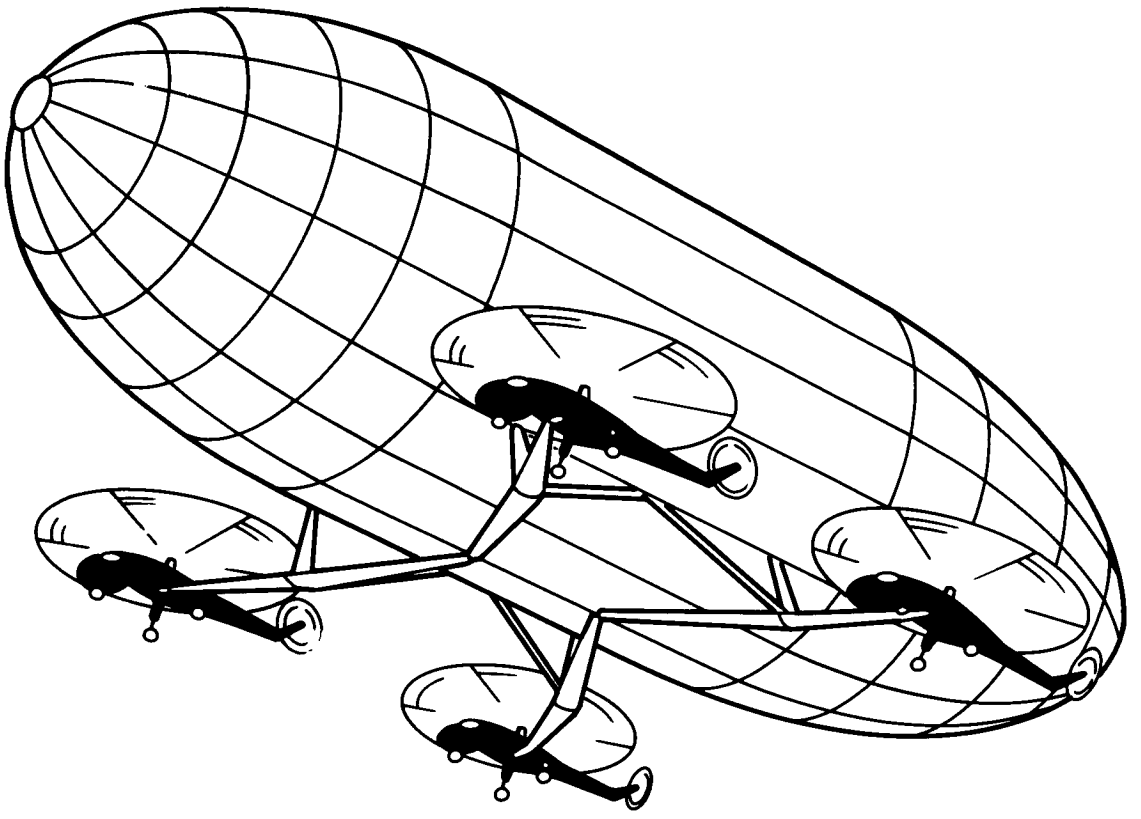

Figure 1 Hybrid Heavy Lift Airship - Approximate Configuration

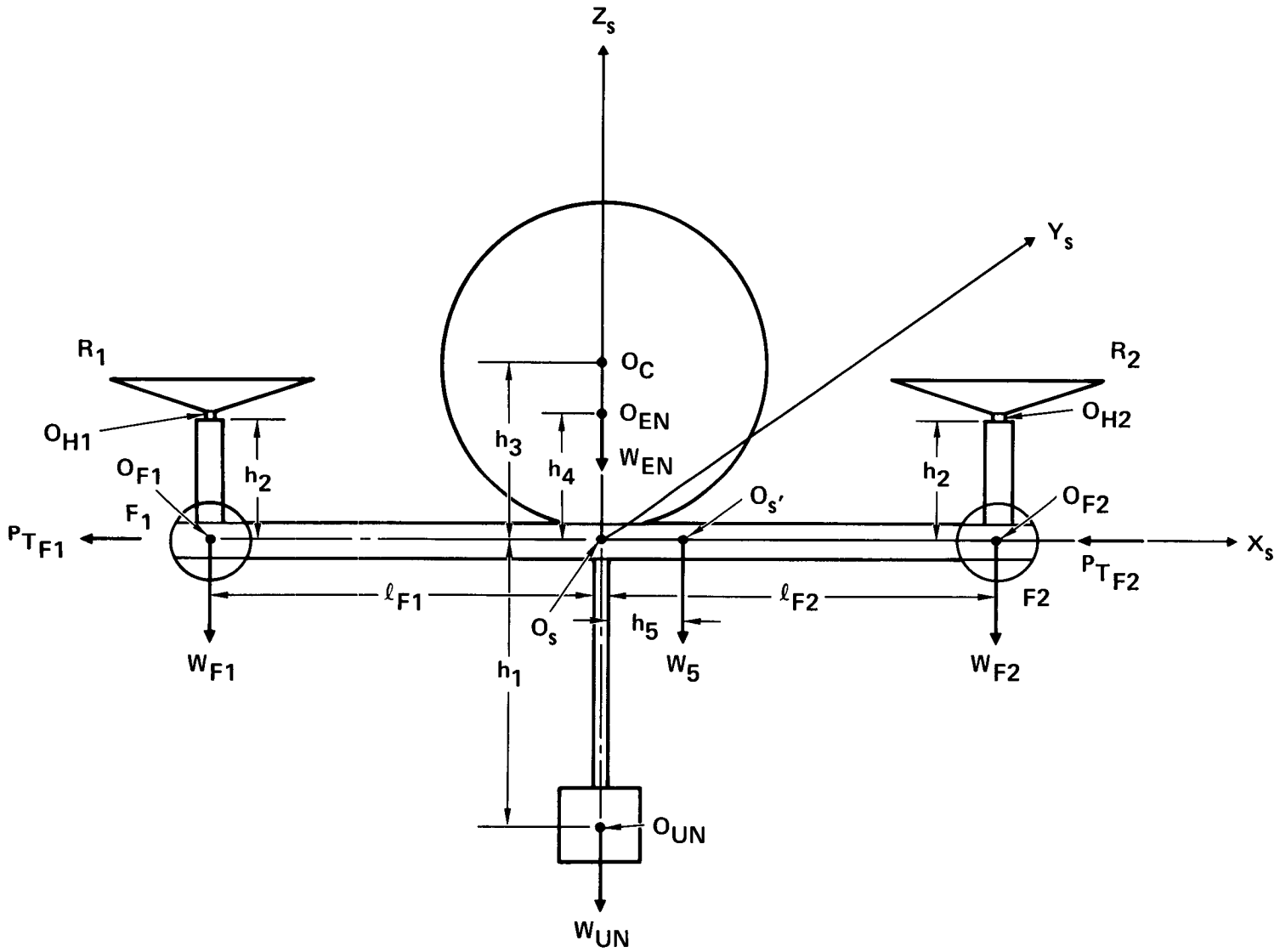

Figure 2 Twin Rotor Model of an HHLA

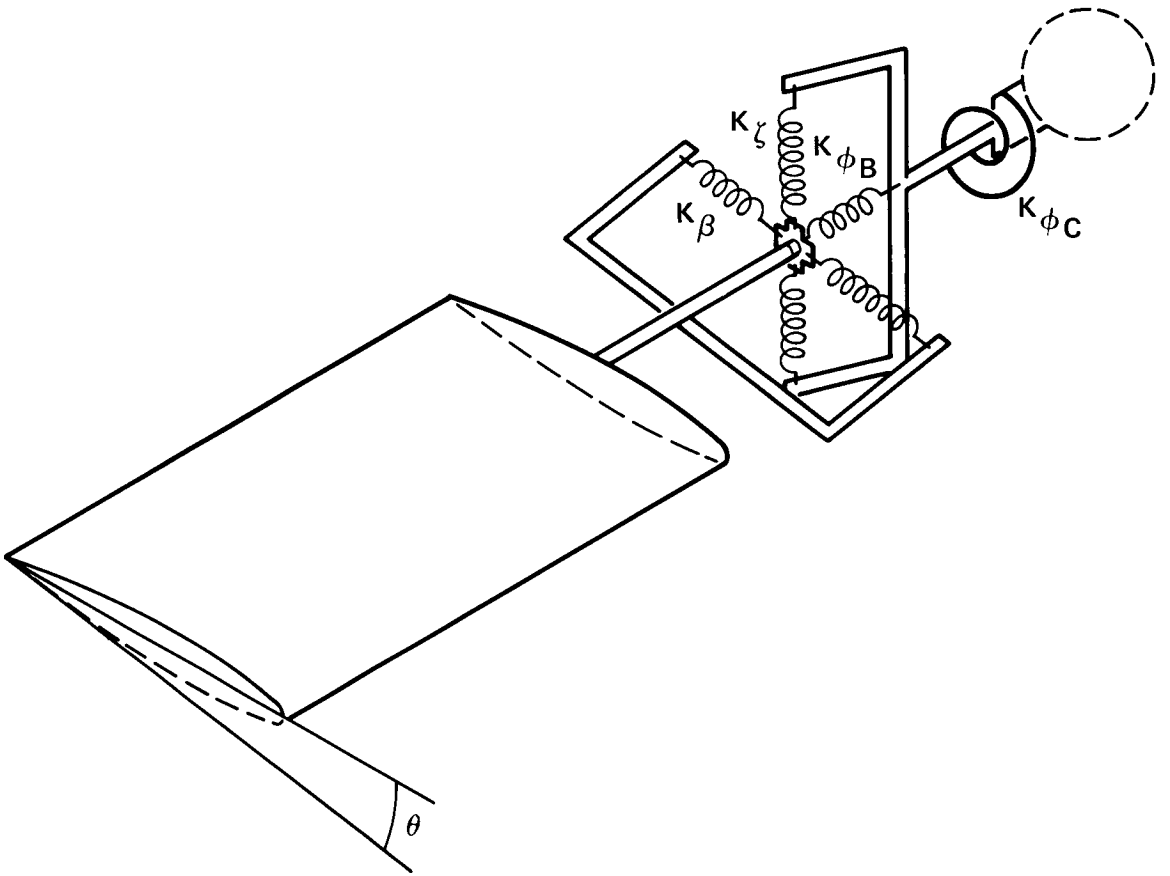

Figure 3 Equivalent Spring Restrained Blade Model

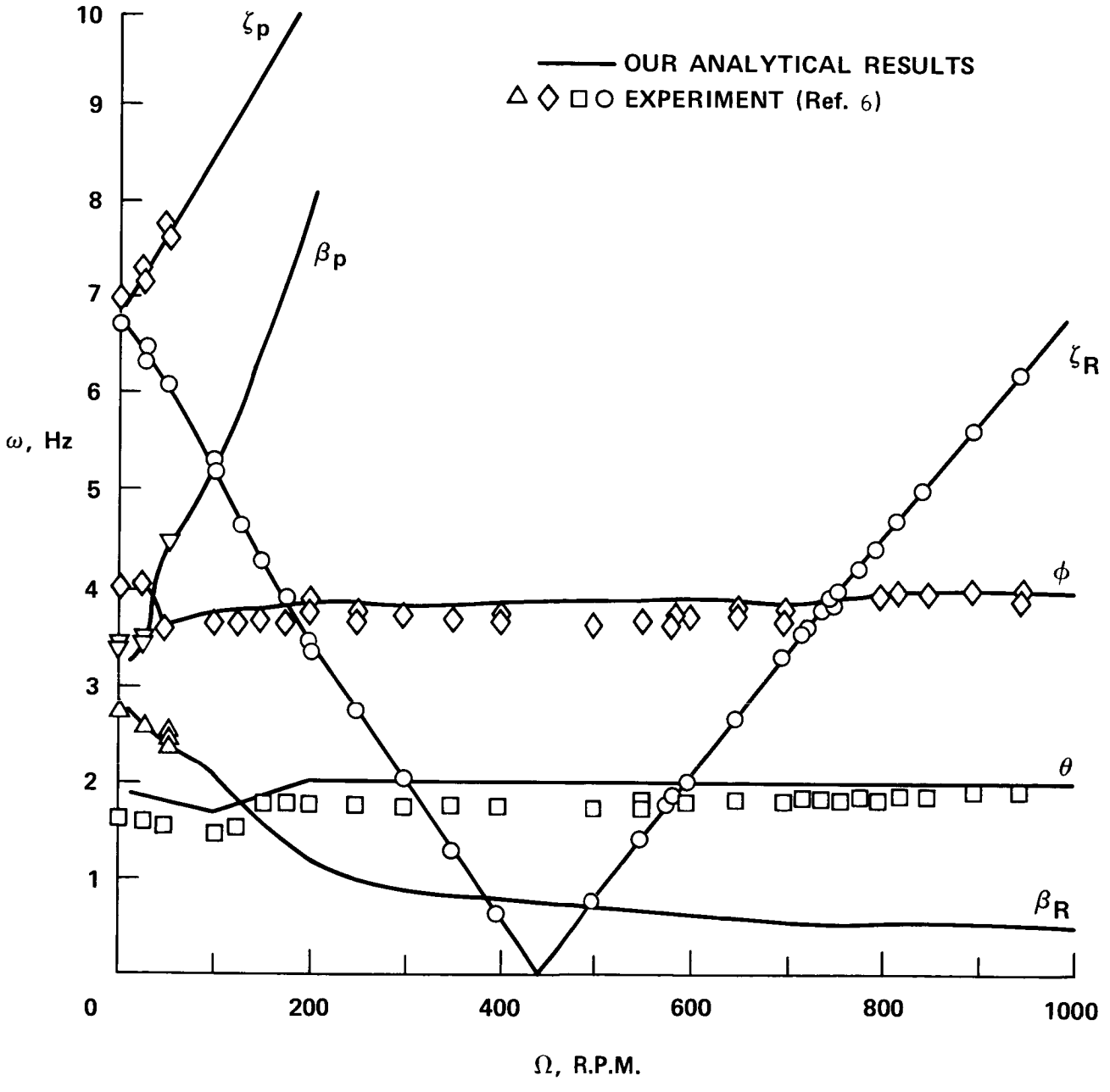

Figure 4 Model Frequencies as a Function of Ω, $\theta_c = 0$ (Configuration 1)

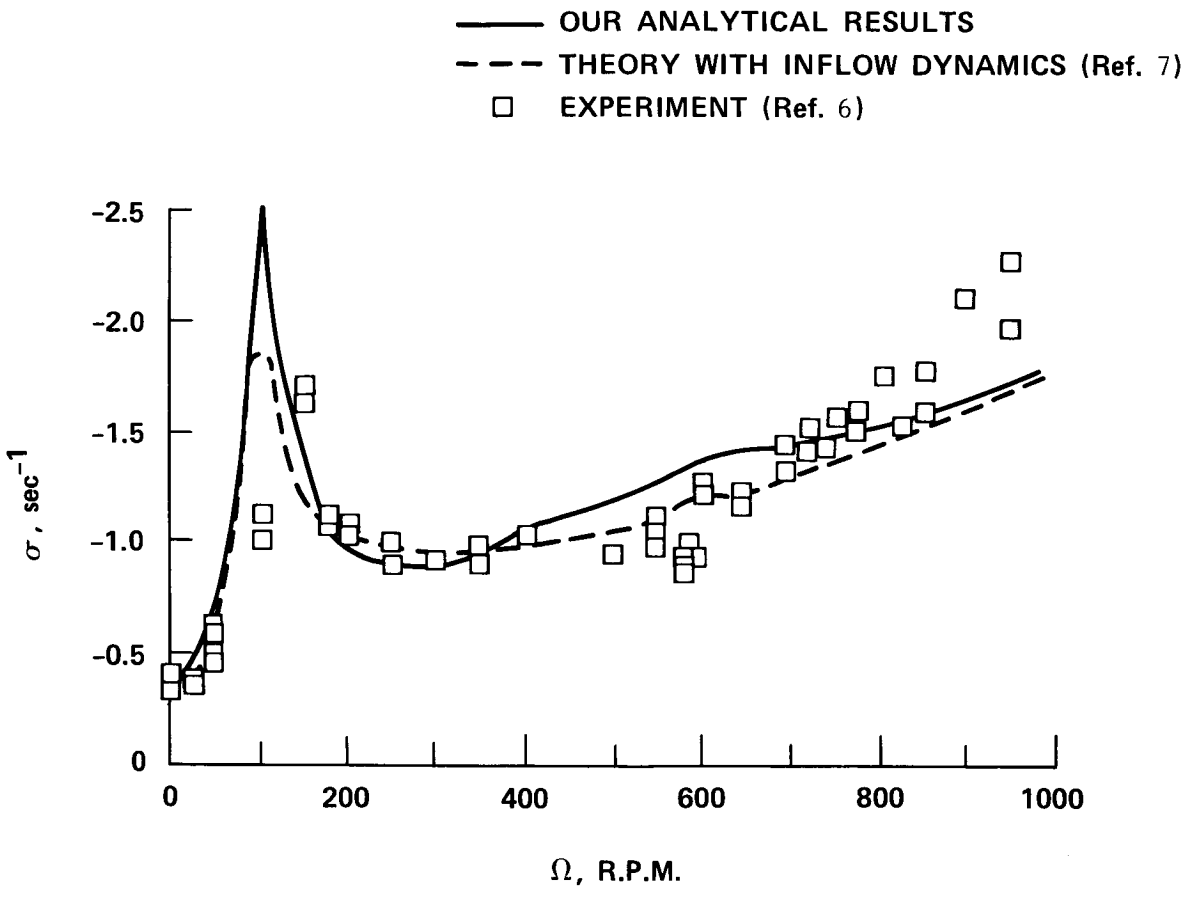

Figure 5 Body Pitch Mode Damping as a Function of Ω, $\theta_c = 0$ (Configuration 1)

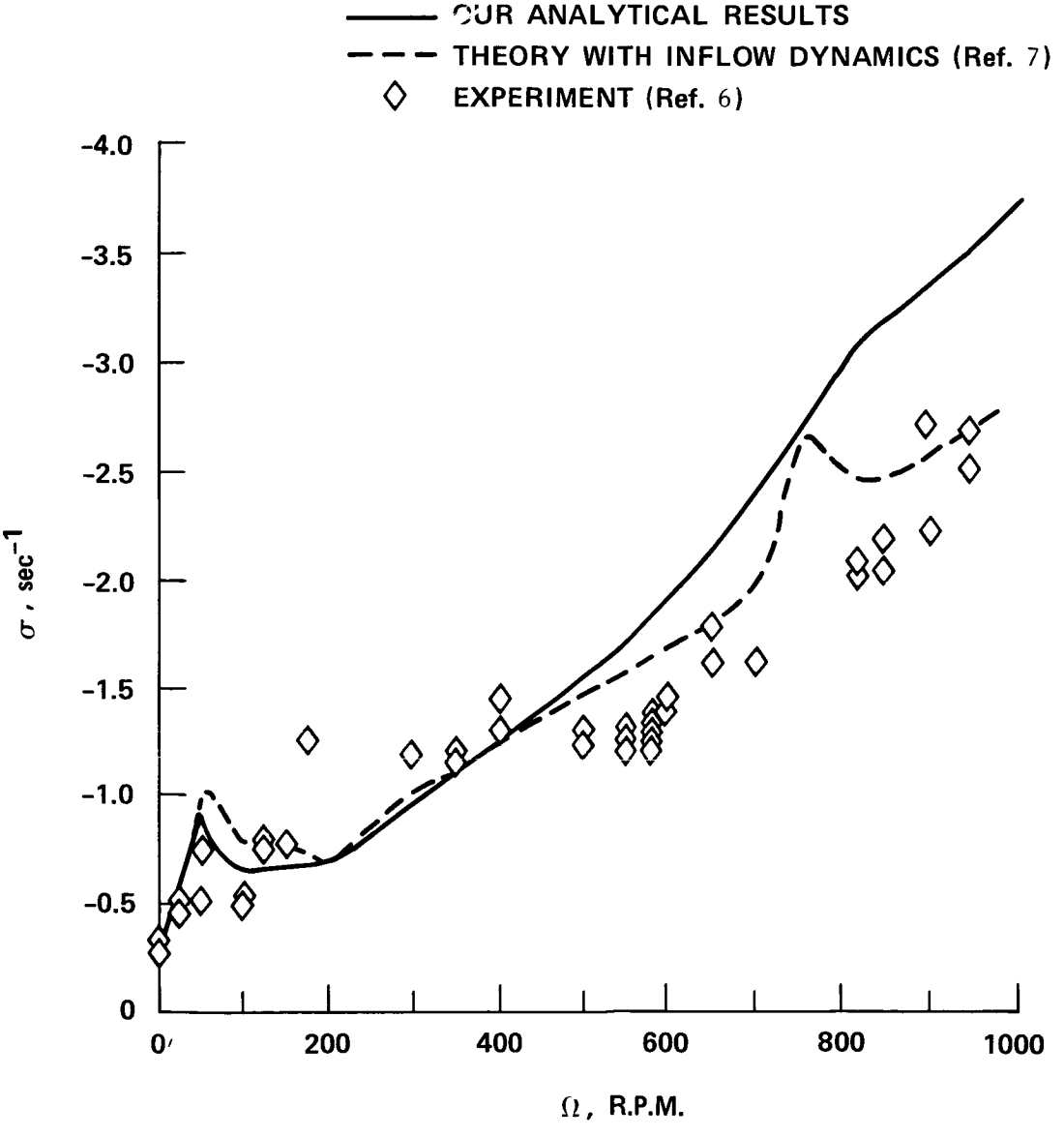

Figure 6 Body Roll Mode Damping as a Function of Ω, $\theta_c = 0$ (Configuration 1)

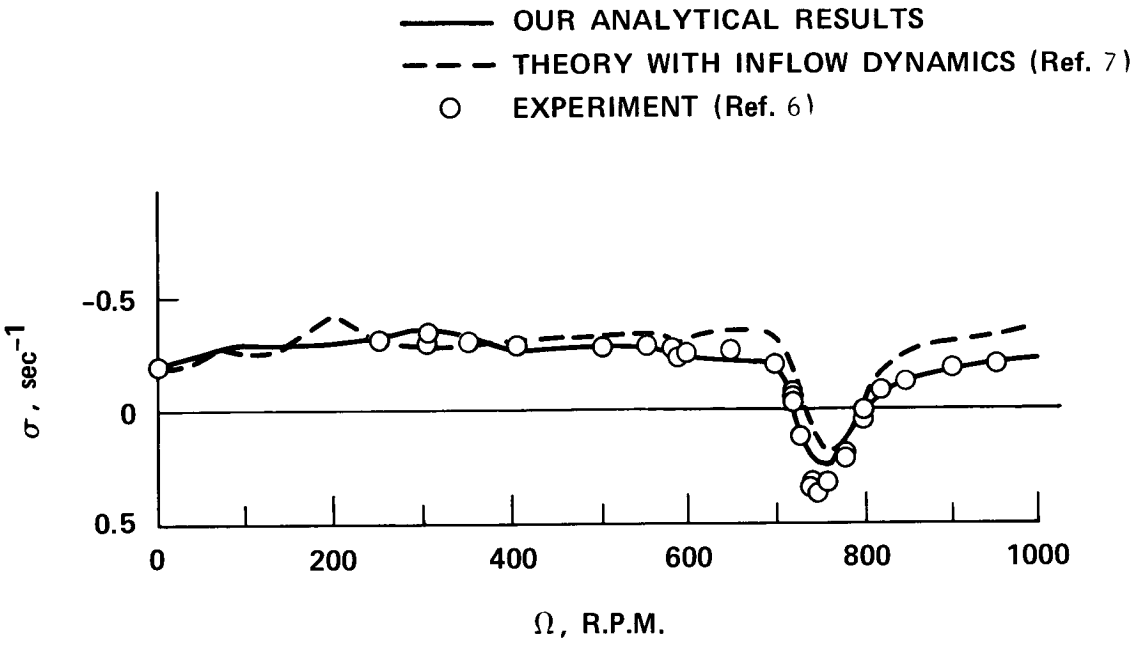

Figure 7 Regressing Lag Mode Damping as a Function of Ω, $\theta_c = 0$ (Configuration 1)

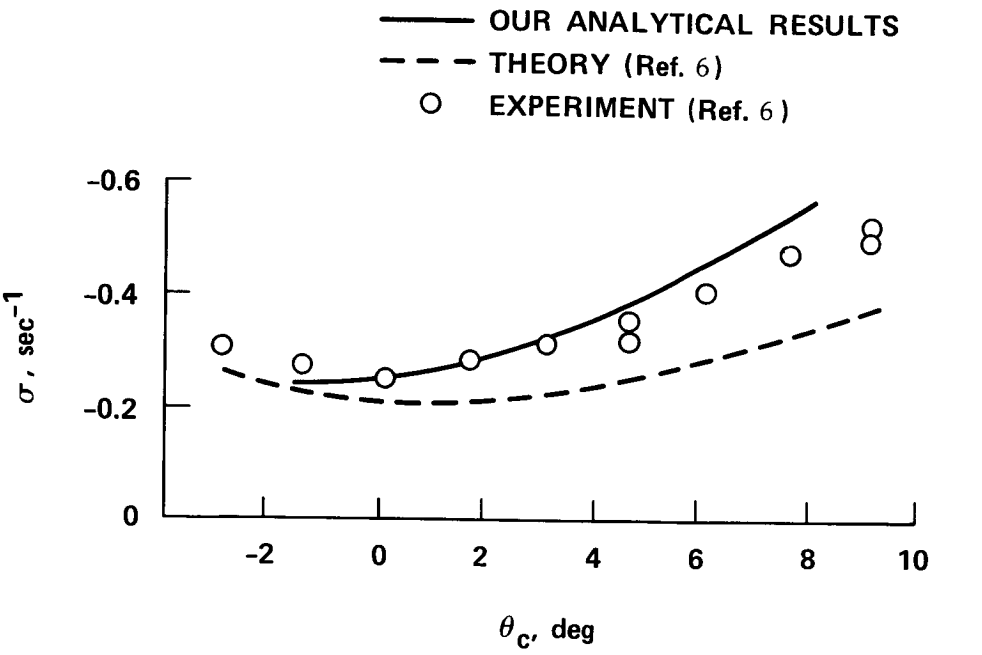

(a) Ω = 650 R.P.M.

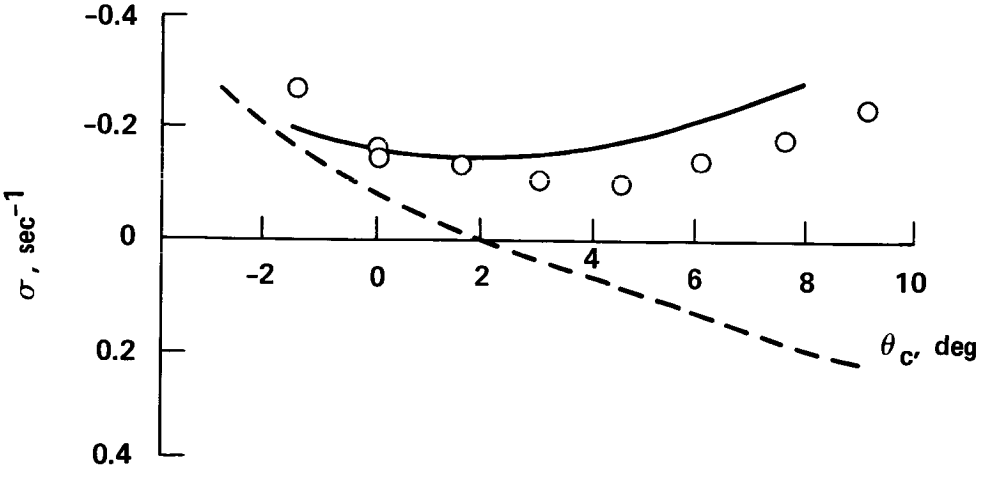

(b) Ω = 900 R.P.M.

Figure 8 Lead-Lag Regressing Mode Damping as a Function of θ_c at (a) 650 R.P.M. and (b) 900 R.P.M. (Configuration 1)

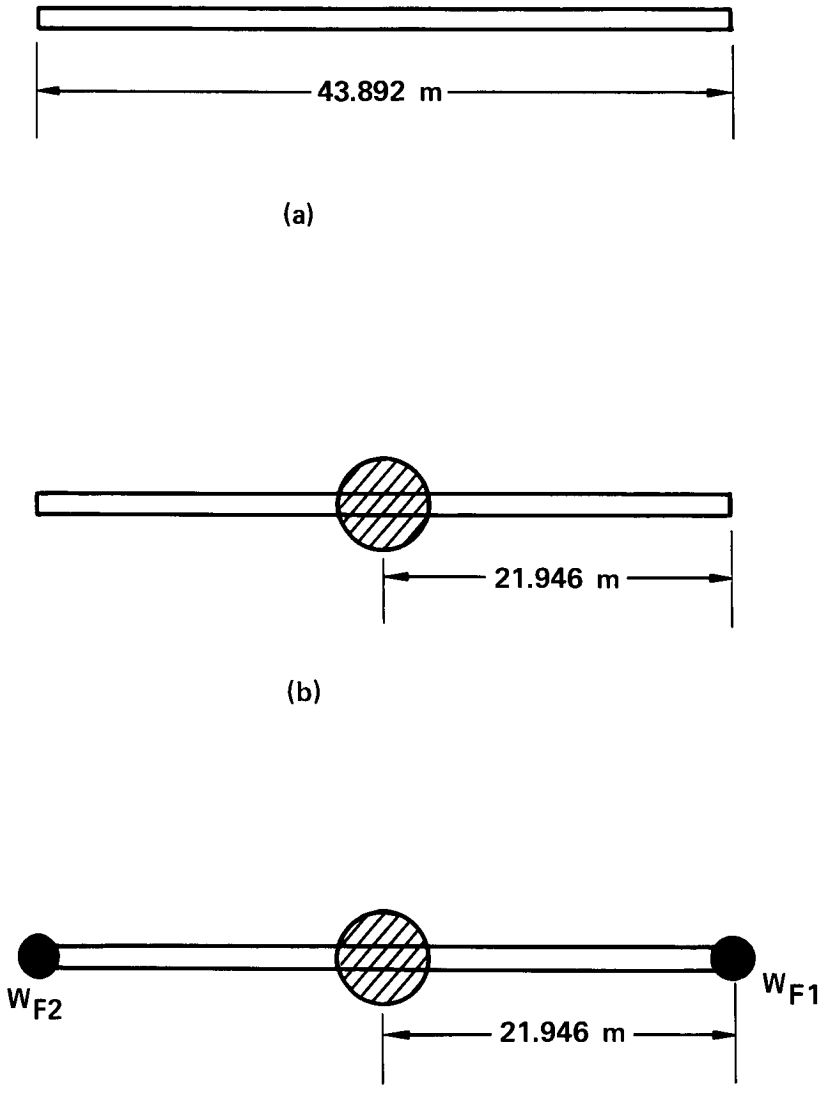

Figure 9 Idealization of Supporting Structure for Bending Type Deformations
(a) Free-Free Beam, (b) Free-Free Beam with Heavy Mass at the Center and (c) Free-Free Beam with Masses at the Center and at the Tips

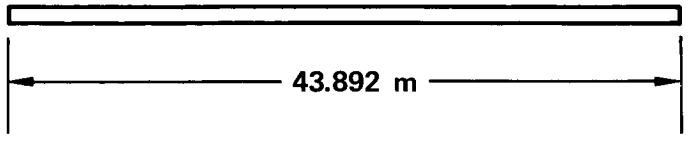

(a)

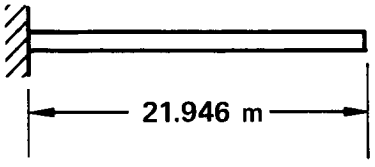

(b) EACH HALF

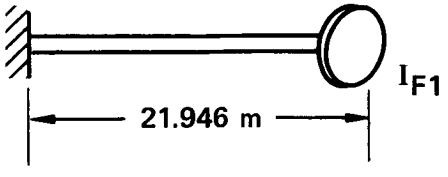

(c) EACH HALF

Figure 10 Idealization of Supporting Structure for Torsion Type Deformations
(a) Free-Free Beam, (b) Cantilevered Beam and
(c) Cantilevered Beam with Inertia at the Tip

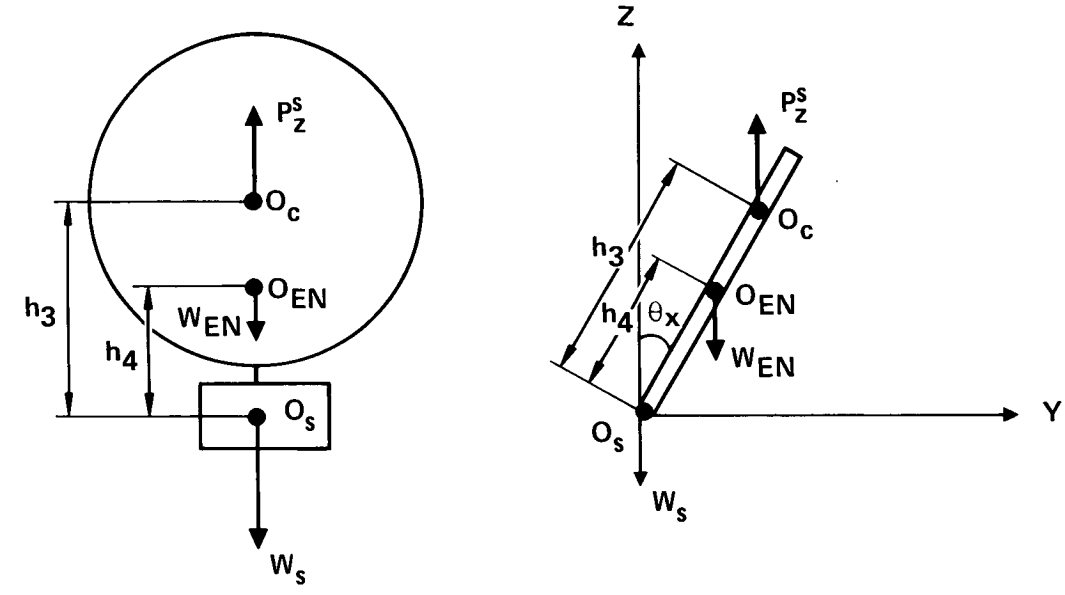

(a) ROLL

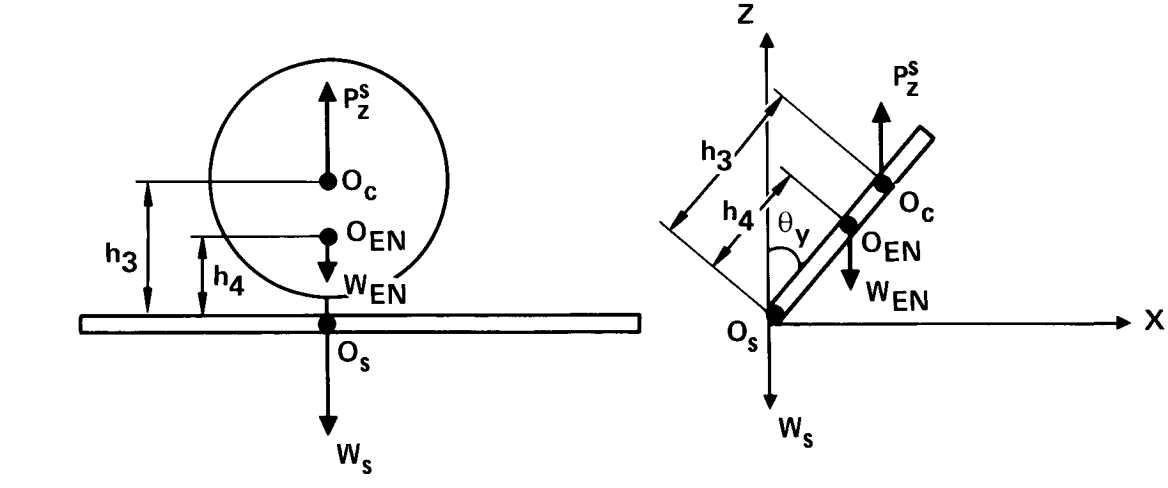

(b) PITCH

Figure 11 Elementary Model of the Vehicle for Frequency Evaluation in (a) Roll and (b) Pitch

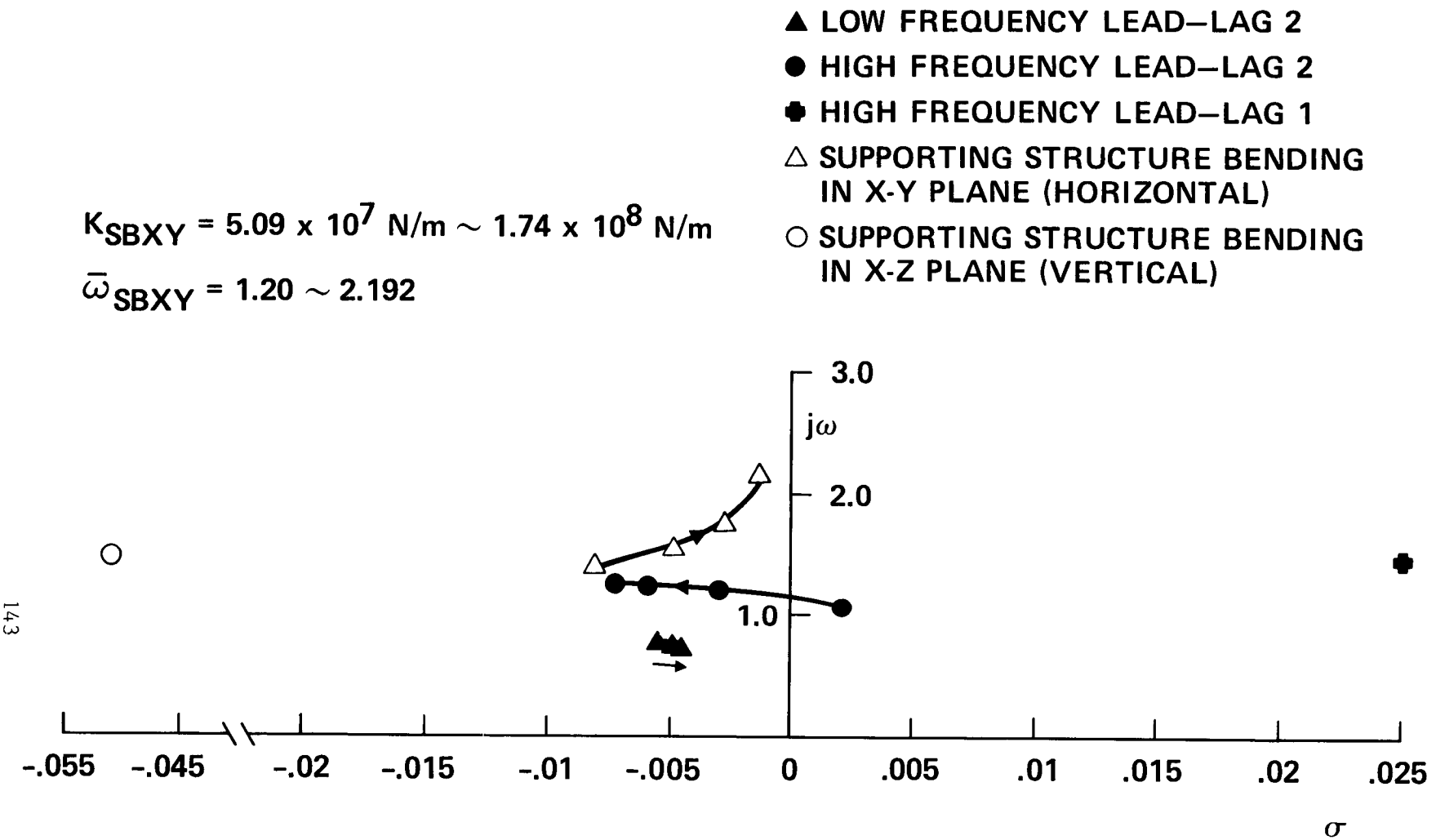

Figure 12 Variation of Nondimensional Eigenvalues of Blade Lead-Lag Modes and Supporting Structure Bending Modes with Increase in Supporting Structure Bending Stiffness in X-Y Plane (Horizontal)

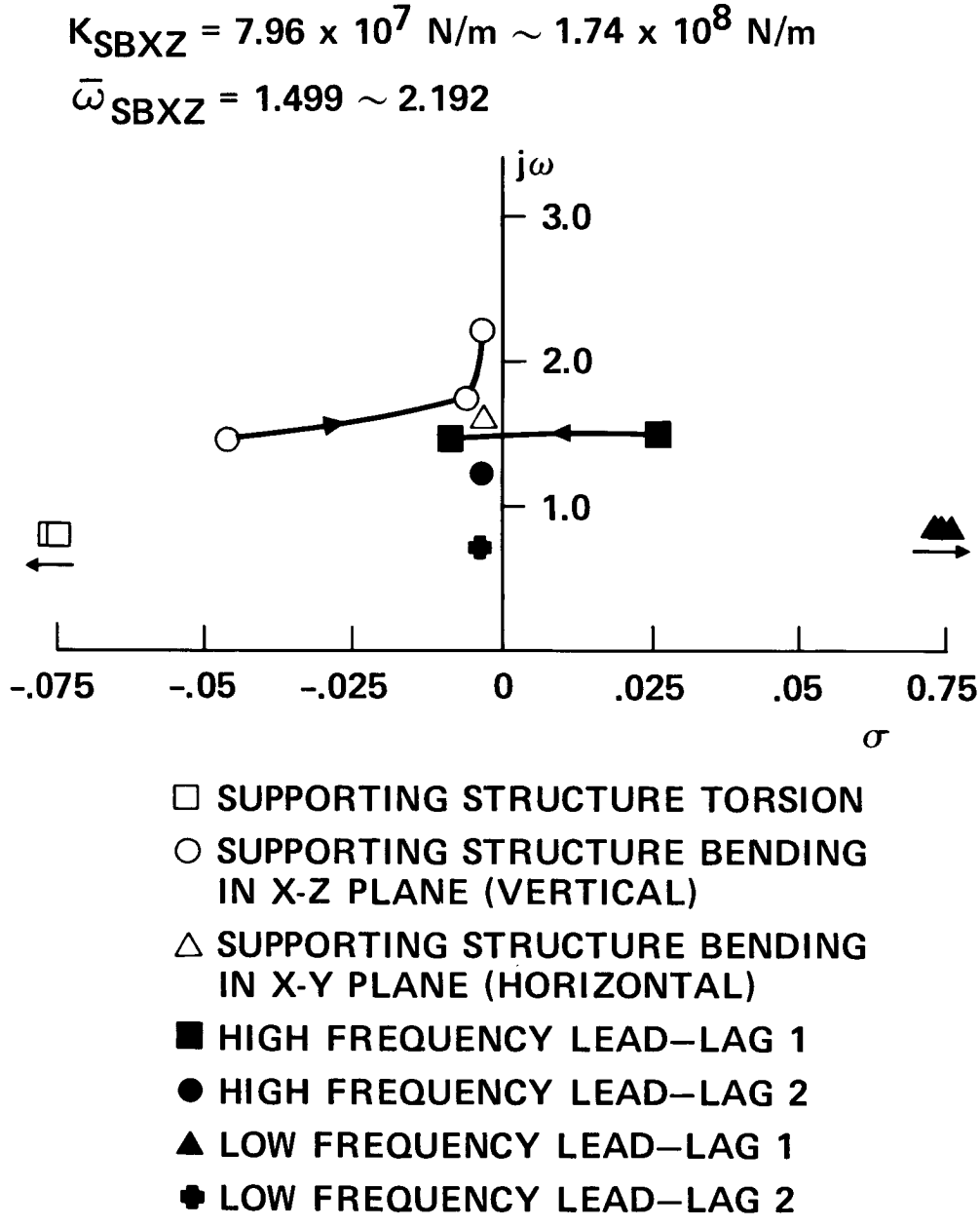

Figure 13 Variation of Nondimensional Eigenvalues of Blade Lead-Lag Modes and Supporting Structure Bending Modes with Increase in Supporting Structure Bending Stiffness in X-Z Plane (Vertical)

■ COLLECTIVE LEAD–LAG 1, 2
● SUPPORTING STRUCTURE TORSION
○ LOW FREQUENCY LEAD–LAG 1
✤ LOW FREQUENCY LEAD–LAG 2
△ HIGH FREQUENCY LEAD–LAG 1
✻ HIGH FREQUENCY LEAD–LAG 2

$K_{ST} = 1.59 \times 10^6$ N.m $\sim 3.99 \times 10^7$ N.m

$\bar{\omega}_{ST} = 0.4 \sim 2.0$

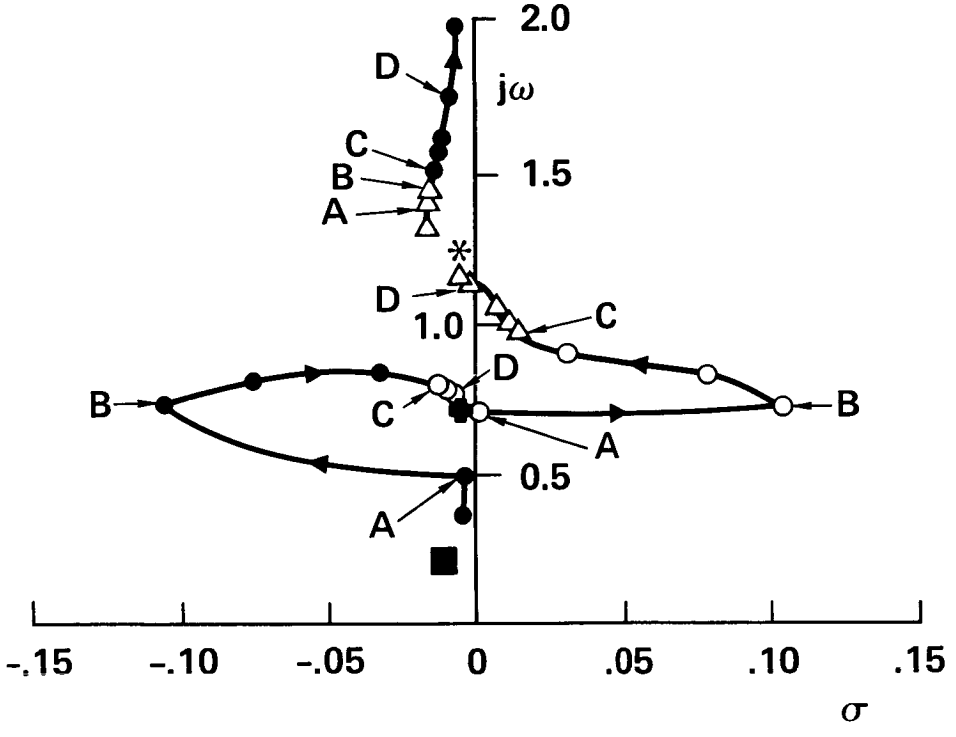

A – B $K_{ST} = 3.01 \times 10^6 \sim 7.20 \times 10^6$ N.m

B – C $K_{ST} = 7.20 \times 10^6 \sim 1.685 \times 10^7$ N.m

C – D $K_{ST} = 1.685 \times 10^7 \sim 3.10 \times 10^7$ N.m

Figure 14 Variation of Nondimensional Eigenvalues of Blade Lead-Lag Modes and Supporting Structure Torsion Mode with Increase in Supporting Structure Stiffness in Torsion

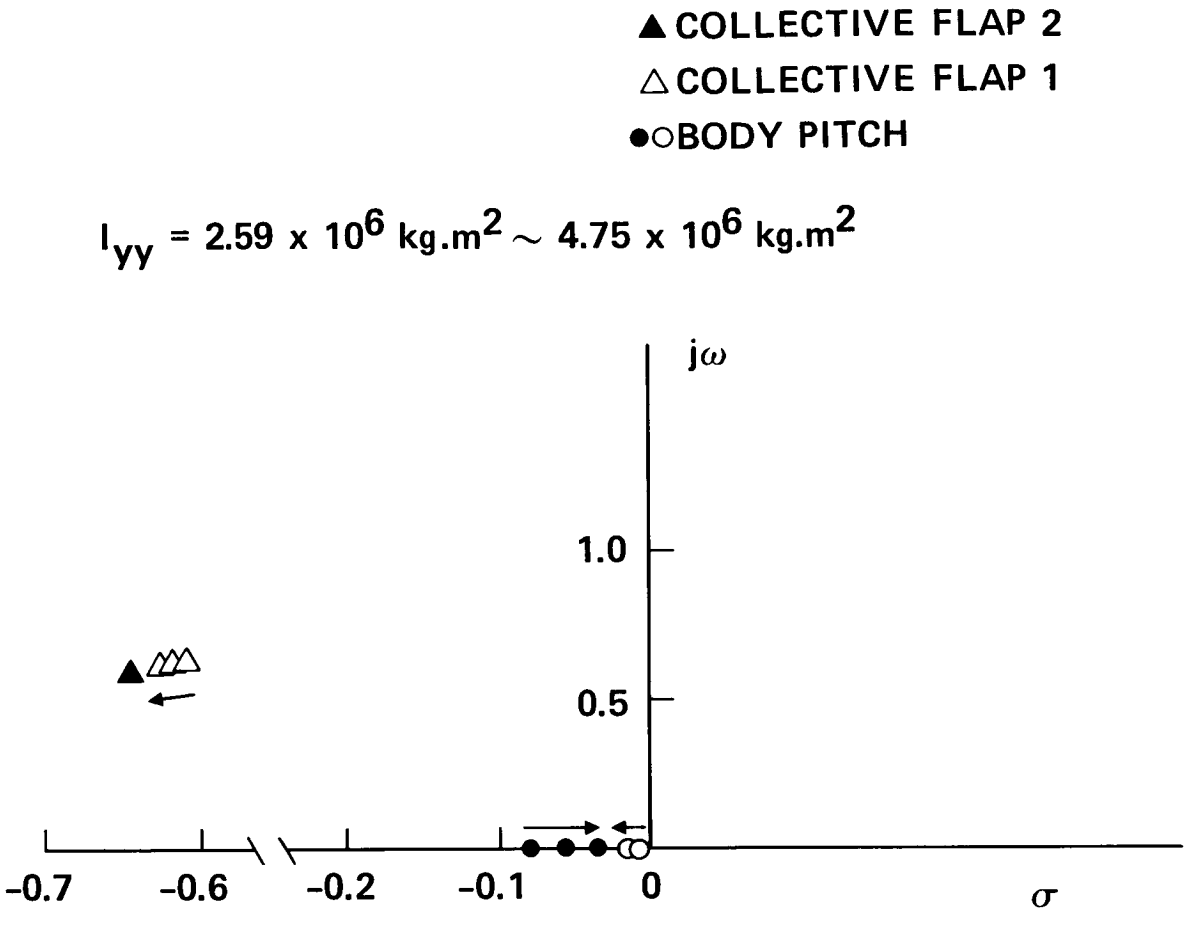

Figure 15 Variation of Nondimensional Eigenvalues of Collective Flap Modes and Body Pitch Mode with Increase in Body Inertia in Pitch

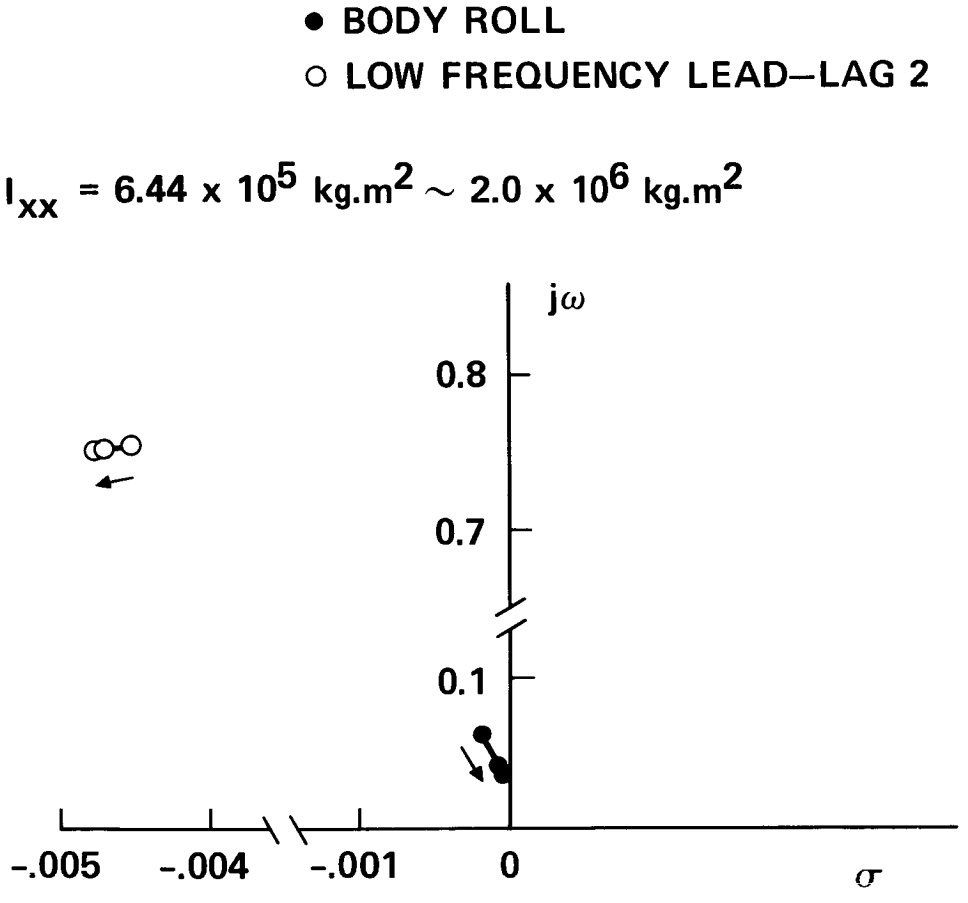

Figure 16 Variation of Nondimensional Eigenvalues of Low Frequency Lead-Lag Mode and Body Roll Mode with Increase in Body Inertia in Roll

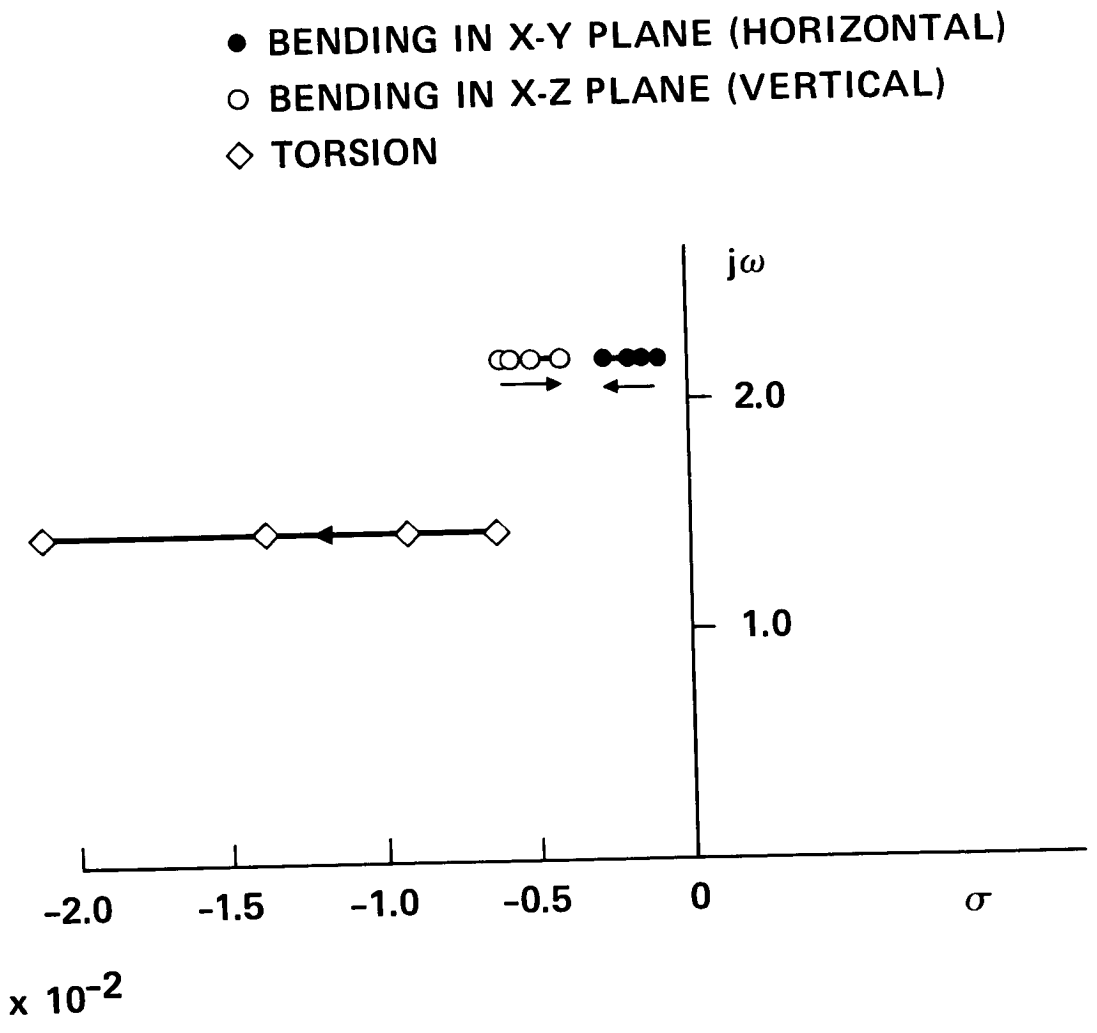

Figure 17 Variation of Nondimensional Eigenvalues of the Supporting Structure Elastic Modes with Decrease in Buoyancy Ratio

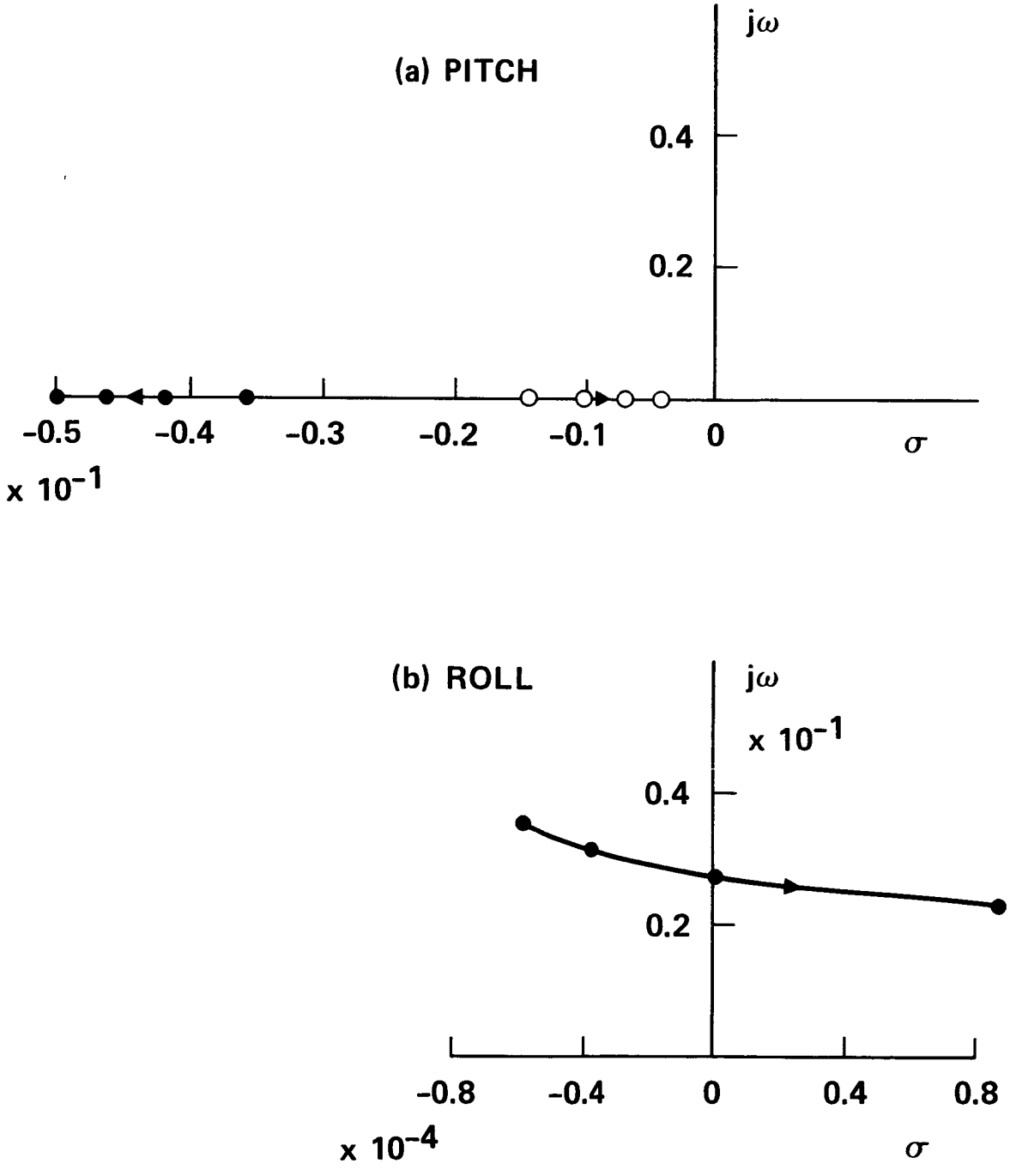

Figure 18 Variation of Nondimensional Eigenvalues in (a) Pitch and (b) Roll Modes with Decrease in Buoyancy Ratio

APPENDIX A

Transformation to Multiblade Coordinates

For an N-bladed rotor with blades evenly spaced around, the azimuth angle for the k^{th} blade, at any instant, can be written as

$$\psi_k = \psi + 2\pi \frac{K}{N} \qquad K = 1,....N \tag{A.1}$$

where $\psi = \Omega t$, the nondimensional time variable.

Let α_k be a generalized coordinate associated with any degree of freedom of the k^{th} blade, flap or lead-lag or torsion. Since this α_k is associated with the blade which is rotating, it is called a rotating coordinate. If there are N blades, the behavior of all the blade in that particular degree of freedom can be represented by N rotating coordinates $\alpha_1 \ldots \alpha_N$. By suitably choosing a transformation, these N rotating coordinates can be transformed to another set of N coordinates, each of which is associated with a specific variation of all the α_k's (rotating coordinates) when combined, as viewed from a nonrotating frame. This type of transformation is called the multiblade coordinate transformation. Basically, this transformation transforms the rotating coordinates into a nonrotating frame. Usually, the physical explanation about this transformation is given only with reference to flap motion of the blade [Ref. 3].

The transformation from the rotating to the nonrotating coordinate is obtained from the following operations

$$\alpha_M = \frac{1}{N} \sum_{k=1}^{N} \alpha_k$$

$$\alpha_{-M} = \frac{1}{N} \sum_{k=1}^{N} (-1)^k \alpha_k \qquad \text{(for even N only)}$$

$$\alpha_{nc} = \frac{1}{N} \sum_{k=1}^{N} \cos(n\psi_k)\ \alpha_k$$

$$\alpha_{ns} = \frac{1}{N} \sum_{k=1}^{N} \sin(n\psi_k)\ \alpha_k \qquad \text{(A.2)}$$

where $n = 1,....L$ and $L = \frac{N-1}{2}$ for odd N

$L = \frac{N-2}{2}$ for even N

The inverse transformation is

$$\alpha_k = \alpha_M + \sum_{n=1}^{L} (\alpha_{nc} \cos n\psi_k + \alpha_{ns} \sin n\psi_k) + (-1)^k \alpha_{-M} \qquad \text{(A.3)}$$

Last term will appear only even N. The proof for this transformation can be found in Ref. 3.

This transformation, given in Eq. (A.1), looks like a truncated Fourier series, except for the last term. The major difference between this transformation and the usual Fourier transformation is that here the coefficients α_M, α_{nc}, α_{ns}, α_{-M} are all functions of time, whereas in the Fourier series the coefficients are constants. That is why sometimes these multiblade coordinates are also referred to as Fourier coordinates.

Differentiating Eq. (A.2) with respect to time $\psi = \Omega t$ (Ω is a constant)

$$\dot{\alpha}_M = \frac{1}{N} \sum_{k=1}^{N} \dot{\alpha}_k$$

$$\dot{\alpha}_{-M} = \frac{1}{N} \sum_{k=1}^{N} (-1)^k\ \dot{\alpha}_k \qquad \text{(A.4)}$$

$$\dot{\alpha}_{nc} + n\,\alpha_{ns} = \frac{2}{N} \sum_{k=1}^{N} \cos(n\psi_k)\ \dot{\alpha}_k$$

$$\dot{\alpha}_{ns} - n\,\alpha_{nc} = \frac{2}{N} \sum_{k=1}^{N} \sin(n\psi_k)\ \dot{\alpha}_k$$

Differentiating again with respect to ψ

$$\ddot{\alpha}_M = \frac{1}{N} \sum_{k=1}^{N} \ddot{\alpha}_k$$

$$\ddot{\alpha}_{-M} = \frac{1}{N} \sum_{k=1}^{N} (1)^k \ddot{\alpha}_k$$

$$\ddot{\alpha}_{nc} + 2n \dot{\alpha}_{ns} - n^2 \alpha_{nc} = \frac{2}{N} \sum_{k=1}^{N} \cos(n\psi_k) \ddot{\alpha}_k$$

$$\ddot{\alpha}_{ns} - 2n \dot{\alpha}_{nc} - n^2 \alpha_{ns} = \frac{2}{N} \sum_{k=1}^{N} \sin(n\psi_k) \ddot{\alpha}_k \qquad \text{(A.5)}$$

It can be seen that the transformation of acceleration terms from the rotating frame introduces coriolis and centrifugal terms in the nonrotating frame. So, the transformation from the rotating frame to the nonrotating frame is accomplished by applying the following N operators to the complete set of linear equations, for the rotating blade, in the rotating frame. They are

$\frac{1}{N} \sum_{k=1}^{N} (\ldots)$	collective operator
$\frac{1}{N} \sum_{k=1}^{N} (-1)^k (\ldots)$	alternating operator
$\frac{1}{N} \sum_{k=1}^{N} \cos n\psi_k (\ldots)$	n-cosine operator
$\frac{1}{N} \sum_{k=1}^{N} \sin n\psi_k (\ldots)$	n-sine operator (A.6)

These four operators are applied to each equation representing the blade degree of freedom and the blade degrees of freedom are replaced by the multiblade coordinates using Equations (A.2), (A.4) and (A.5). The resulting equations will have the multiblade coordinates as the generalized coordinates. These equations represent the dynamics of the rotor as a whole as viewed from a non-rotating frame.

APPENDIX B

Application of Multiblade Coordinate Transformation To Multi-Rotor System

In Ref. 1, the blade loads are derived, in a general form for a typical rotor with a moving hub and the rotor is assumed to operate at a specified constant value of Ω. When using these expressions for the calculation of blade loads, for two different rotor systems operating at different values of Ω, a number of special provisions described below have to be introduced.

First note that in the general expressions for the blade loads, various time derivative terms are nondimensionalized with respect to a nondimensional time $\psi = \Omega t$, where Ω is the angular speed of the rotor. In a multirotor system, if the rotors operate at different values of Ω, the nondimensional time ψ is different for different rotors, which leads to inconsistency. This problem can be resolved using the angular speed of one rotor, say Ω_1 of the rotor R_1, as the reference Ω. Then all the time derivative terms, that appear in the blade load expressions for different rotors, can be suitably modified such that the nondimensional time is the same for the complete set of equations. The nondimensional time will be $\psi_1 = \Omega_1 t$.

The second important item is encountered while applying the multiblade coordinate transformation to a multirotor system. In the n-cosine and n-sine transformation, the following operators are applied to the blade equations:

$$\frac{2}{N}\sum_{k=1}^{N} \cos n\psi_k\,(\ldots) \qquad \text{n-cosine}$$

$$\frac{2}{N}\sum_{k=1}^{N} \sin n\psi_k\,(\ldots) \qquad \text{n-sine} \qquad \text{(B.1)}$$

where $\psi_k = \psi + 2\frac{\pi K}{N}$

and $\psi = \Omega t$

In a multirotor system, these operators are different for the blade equations in different rotors. In general, for the i^{th} rotor, these can be written as

$$\frac{2}{N} \sum_{k=1}^{N} \cos n\psi_k^i \,(\ldots) \qquad \text{n-cosine}$$

$$\frac{2}{N} \sum_{k=1}^{N} \sin n\psi_k^i \,(\ldots) \qquad \text{n-sine} \qquad \text{(B.2)}$$

where $\psi_k^i = \psi_i + 2\pi \frac{K}{N}$

$\psi_i = \Omega_i t$

Note that ψ_k^i contains the angular speed Ω_i of the i^{th} rotor. These operators have to be applied to the blade equations in the i^{th} rotor system to transform the blade equations to the nonrotating frame. When applying Eqs. (B.2) to the time derivative terms for the blade degrees of freedom, the transformation given in Eq. (A.4) and (A.5) should not be used directly because the time derivative is taken with respect to a reference nondimensional time, say ψ_1.

The derivation given below shows the modifications which have to be incorporated, in the blade equations, both for nondimensionalization and for the application multiblade coordinate transformation when dealing with a multirotor system in which each rotor is operating at a different value of Ω.

Let Ω_1 be the reference angular speed which represent rotor system R_1 and let β_k^1 be the flap degree of freedom of the k^{th} blade in the rotor system R_1. Furthermore let Ω_i be the angular speed of the i^{th} rotor system and denote by β_k^i the flap degree of freedom of the k^{th} blade in rotor system R_i. The time derivatives of these degrees of freedom can be written in the nondimensional form as,

$$\frac{d\beta_k^1}{dt} = \Omega_1 \frac{d\beta_k^1}{d(\Omega_1 t)} = \Omega_1 \frac{d\beta_k^1}{d\psi^1} = \Omega_1 \left(\frac{\Omega_1}{\Omega_1}\right) \frac{d\beta_k^1}{d\psi^1} \qquad \text{(B.3)}$$

$$\frac{d\beta_k^i}{dt} = \Omega_i \frac{d\beta_k^i}{d(\Omega_i t)} = \Omega_i \frac{d\beta_k^i}{d\psi^i} = \underline{\Omega_i \left(\frac{\Omega_1}{\Omega_i}\right) \frac{d\beta_k^i}{d\psi^1}} \qquad \text{(B.4)}$$

If the general load expressions, derived for typical rotor blade, are used for all the rotor systems in a vehicle, then the first time derivative terms in the load expressions for the rotor R_1 will be with respect to ψ^1 and that for the rotor R_i will be with respect to ψ^i. If the angular speeds in the rotor systems are different, then the nondimensional time will be different for the rotors. For consistency, the underlined expression should be used for all the first derivative terms appearing in the i^{th} rotor load expressions. Hence, the general blade load expressions can be used for different rotors after multiplying the first time derivative terms by $\left(\frac{\Omega_1}{\Omega_i}\right)$ and the second time derivative terms by $\left(\frac{\Omega_1}{\Omega_i}\right)^2$. The nondimensional time, in this case, is $\psi^1 = \Omega_1 t$. (Note: All the Ω's are constants). The following derivation shows how this nondimensionalization affects the multi-blade coordinate transformation. Let α_{nc}^i and α_{ns}^i be the transformed n-cosine and n-sine degrees of freedom in the nonrotating frame and let the corresponding rotating blade degree of freedom be α_k^i, for rotor system R_i. Thus

$$\alpha_{nc}^i = \frac{2}{N} \sum_{k=1}^{N} \cos n\psi_k^i \, \alpha_k^i \qquad \text{(B.5)}$$

$$\alpha_{ns}^i = \frac{2}{N} \sum_{k=1}^{N} \sin n\psi_k^i \, \alpha_k^i \qquad \text{(B.6)}$$

where $\psi_k^i = \psi^i + \frac{2\pi k}{N}$

and $\psi^i = \Omega_i t$, Ω_i is the i^{th} rotor angular speed

Differentiating Eq. (B.5) with respect to t

$$\dot{\alpha}_{nc}^i = \frac{2}{N} \sum_{k=1}^{N} - \sin n\psi_k^i \cdot n\Omega_i \, \alpha_k^i + \cos n\psi_k^i \, \dot{\alpha}_k^i \qquad \text{(B.7)}$$

where $(\dot{}) = \frac{d}{dt}(\ )$

Equations (B.7) can be written as

$$\dot{\alpha}^i_{nc} + n\Omega_i\, \alpha^i_{ns} = \frac{2}{N} \sum_{k=1}^{N} \cos n\psi^i_k\ \dot{\alpha}^i_k \tag{B.8}$$

Nondimensionalizing the time derivative with respect to $\psi^1 = \Omega_1 t$, where Ω_1 is the reference angular speed, Eq. (B.8) becomes

$$\Omega_1\ \overset{*i}{\alpha}_{nc} + n\Omega_i\ \alpha^i_{ns} = \frac{2}{N} \sum_{k=1}^{N} \cos n\psi^i_k\ \Omega_1\ \overset{*i}{\alpha}_k \tag{B.9}$$

Where $(*) = \frac{d}{d\psi^1}$

Multiplying both sides of Eq. (B.8) by $\left(\frac{\Omega_i}{\Omega_i}\right)$

$$\Omega_i \left[\left(\frac{\Omega_1}{\Omega_i}\right)\ \overset{*i}{\alpha}_{nc} + n\ \alpha^i_{ns} \right] = \frac{2}{N} \sum_{k=1}^{N} \cos n\psi^i_k\ \underline{\Omega_i \left(\frac{\Omega_1}{\Omega_i}\right) \overset{*i}{\alpha}_k} \tag{B.10}$$

The underlined term is the same as that in equation (B.4)

Cancelling Ω_i on both sides, Eq. (B.10) yields

$$\left(\frac{\Omega_1}{\Omega_i}\right)\ \overset{*i}{\alpha}_{nc} + n\alpha^i_{ns} = \frac{2}{N} \sum_{k=1}^{N} \cos n\psi^i_k\ \left(\frac{\Omega_1}{\Omega_i}\right)\ \overset{*i}{\alpha}_k \tag{B.11}$$

Equation (B.10) shows how the first time derivative term in the rotor system R_i transforms into the multiblade coordinate system. It turns out that in the transformed multiblade coordinate system, the first time derivative term is to be multiplied by $\left(\frac{\Omega_1}{\Omega_i}\right)$. It can also be shown that the second time derivative term is to be multiplied by $\left(\frac{\Omega_1}{\Omega_i}\right)^2$. These multiplication factors take care of both consistency in nondimensionalization and proper multiblade coordinate transformation.

A closer look at the equation (B.11) shows that $\left(\frac{\Omega_1}{\Omega_i}\right) \overset{*i}{\alpha}_k$ transforms into $\overset{*i}{\alpha}_{nc} \left(\frac{\Omega_1}{\Omega_i}\right) + n\alpha^i_{ns}$ and not $(\overset{*i}{\alpha}_{nc} + n\alpha^i_{ns}) \left(\frac{\Omega_1}{\Omega_i}\right)$ eventhough $\left(\frac{\Omega_1}{\Omega_i}\right)$ term is

independent of the summation. This term does not act as a common multiplier for both sides. This term is multiplied only to the first derivative term on the left hand side. For the case when $\Omega_1 = \Omega_i$, equation (B.11) reverts to the original equation given in equation (A.4).

Thus, in blade load expressions derived in nondimensional form for a typical rotor, the time derivative terms have to be multiplied by a factor $(\frac{\Omega_1}{\Omega_i})^p$ (power of this factor depends on the order of differentiation) and the same factor has to be introduced also in the time derivative terms which appear in the transformed multiblade coordinate.

APPENDIX C

Rotor, Blade and Body Properties

The data provided below describes the rotor tested in Ref. [6].

Rotor Geometry

Number of blades	3
Radius, cm	81.1
Chord, cm	4.19
Hinge offset, cm	8.51
Blade airfoil	NACA 23012
Profile drag coefficient	0.0079
Lock number	7.73
Solidity ratio	0.0494
Lift curve slope	2π
Height of rotor hub above gimbal, cm	24.1

Blade Mass Properties

Blade mass (to flap flexure), gram	209
Blade mass centroid (Ref. flexure centerline), cm	18.6
Blade flap inertia (Ref. flexure centerline), gram	17.3

Blade Frequency and Damping

	Configuration 1
Nonrotating flap frequency Hz	3.13
Nonrotating lead-lag frequency Hz	6.70
Damping in lead-lag (% critical)	0.52%

Body Mass Properties

Rotary inertia in pitch, gram m^2	633
Rotary inertia in roll, gram m^2	183

Body Frequency and Damping

Pitch frequency, Hz	2
Roll frequency, Hz	4
Damping in roll (% critical)	0.929%
Damping in pitch (% critical)	3.20%

1. Report No.	2. Government Accession No.	3. Recipient's Catalog No.
NASA CR-4009		

4. Title and Subtitle	5. Report Date
Aeroelastic Effects in Multirotor Vehicles - Part II: Methods of Solution and Results Illustrating Coupled Rotor/Body Aeromechanical Stability	February 1987
	6. Performing Organization Code
7. Author(s)	8. Performing Organization Report No.
C. Venkatesan and P. P. Friedmann	
	10. Work Unit No. T3516Y
9. Performing Organization Name and Address	11. Contract or Grant No.
University of California Mechanical, Aerospace and Nuclear Engineering Dept. Los Angeles, CA 90024	NAG2-116
	13. Type of Report and Period Covered
12. Sponsoring Agency Name and Address	Contractor Report
National Aeronautics and Space Administration Washington, DC 20546	14. Sponsoring Agency Code 532-06-11

15. Supplementary Notes

Technical Monitor: Dr. H. Miura, M/S 237-11
NASA Ames Research Center, Moffett Field, CA 94035
Topical Report

16. Abstract

This report is a sequel to the earlier report titled "Aeroelastic Effects in Multi-Rotor Vehicles with Application to Hybrid Heavy Lift System, Part I: Formulation of Equations of Motion" (NASA CR-3822). The trim and stability equations are presented for a twin rotor system with a buoyant envelope and an underslung load attached to a flexible supporting structure. These equations are specialized for the case of hovering flight. A stability analysis, for such a vehicle with 31 degrees of freedom, yields a total of 62 eigenvalues. A careful parametric study is performed to identify the various blade and vehicle modes, as well as the coupling between various modes. Finally, it is shown that the coupled rotor/vehicle stability analysis provides information on both the aeroelastic stability as well as complete vehicle dynamic stability. Also presented, in this report, are the results of an analytical study aimed at predicting the aeromechanical stability of a single rotor helicopter in ground resonance. The theoretical results are found to be in good agreement with the experimental results, thereby validating the analytical model for the dynamics of the coupled rotor/support system.

17. Key Words (Suggested by Author(s))	18. Distribution Statement
Rotary wing aeroelasticity Rotor dynamics Multirotor systems Aeromechanical stability	Unclassified - Unlimited Subject Category 08

19. Security Classif. (of this report)	20. Security Classif. (of this page)	21. No. of Pages	22. Price*
Unclassified	Unclassified	172	A08

For sale by the National Technical Information Service, Springfield, Virginia 22161 NASA-Langley, 1987